

**TISSUE AND PLASMA METABOLOMICS IN OESOPHAGO-GASTRIC
CARCINOGENESIS**

A thesis submitted for the degree of Doctor of Medicine at the University of
Birmingham

June 2013

Rishi Singhal MBBS, MRCS (Eng.), FRCS (Gen. Surg.)

Henry Wellcome Building for biomolecular NMR spectroscopy

School of Cancer Sciences

University of Birmingham

UNIVERSITY OF
BIRMINGHAM

University of Birmingham Research Archive

e-theses repository

This unpublished thesis/dissertation is copyright of the author and/or third parties. The intellectual property rights of the author or third parties in respect of this work are as defined by The Copyright Designs and Patents Act 1988 or as modified by any successor legislation.

Any use made of information contained in this thesis/dissertation must be in accordance with that legislation and must be properly acknowledged. Further distribution or reproduction in any format is prohibited without the permission of the copyright holder.

ABSTRACT

Introduction

Oesophageal cancer has a poor prognosis. Early diagnosis and the use of chemotherapy and surgery for local disease are key to improving survival. This study was designed to see if plasma and tissue metabolic profiles could be used to identify oesophago-gastric malignancy, indicate the presence of unstable pre-malignant (Barrett's) epithelium or predict response to chemotherapy.

Methods

Patients were recruited from University Hospitals Birmingham between May 2009 and March 2010. Nuclear Magnetic Resonance (NMR) metabolomics was performed on filtered plasma and extracted tissue samples.

Results

Some 258 participants were recruited. NMR metabolomics discriminated between normal, Barrett's and neoplastic epithelium. Tissue levels of hypoxanthine were highest in oesophageal adenocarcinoma compared to adjacent normal mucosa. Levels in Barrett's mucosa in the presence of cancer fell between normal and neoplastic mucosa. 3-hydroxybutyrate levels were elevated both in cancer tissues and plasma compared to controls. Plasma levels of 3-hydroxybutyrate were higher in patients with node positive and full thickness tumours compared to those who were node negative with early local disease.

Conclusion

NMR metabolomics identified metabolic profiles that characterized different histologic tissue types. Metabolites involved in oesophageal carcinogenesis might influence diagnostic and management strategies in these patients.

ACKNOWLEDGEMENTS

Through the past two years while working on this thesis, I had the privilege and pleasure of working with the very best and they continue to be a constant source of inspiration.

I would like to begin by thanking Christian Ludwig, Scientific Officer at HWB-NMR, University of Birmingham. Coming from a surgical background, understanding NMR was more than a task. Chris was always very patient in teaching me the various fundamentals of NMR time and time again. His supervision of the NMR data acquisition and provision of scripts for data analysis were of paramount importance to the success of this project.

John Carrigan, post doctoral fellow at the HWB-NMR, University of Birmingham helped with MS data acquisition and analysis. He was very instrumental in my understanding of metabolism and statistical analysis of data.

Doug Ward, Senior Research Fellow (Translational Medicine) at the University of Birmingham provided insight into a systems based approach and his help with proteomics experiments is greatly appreciated.

I would like to thank Olga Tucker, Senior Lecturer and Consultant Upper GI Surgeons for her constant encouragement and support during this time.

I would like to thank Janet Taylor (research phlebotomist at the University of Birmingham), Clare Box and Jonathan James (research technicians at the University of Birmingham) for their help at various stages of this project.

I would like to thank all the patients who consented to take part in this study and also thank Mike Hallissey, David Gourevitch and John Whiting, Consultant Upper GI Surgeons, who supported the recruitment of patients into the study.

I would like to thank my laboratory supervisor Ulrich Gunther, for his support with the initiation and successful conclusion of this project. His innovative ideas were one of the cornerstones of this project. I thank him for encouraging and supporting me.

Above all, I feel the greatest appreciation and gratitude towards my clinical supervisor Professor Derek Alderson. His unshaken belief in my abilities over the last five years and constant encouragement was of paramount importance to the success of this project. Without his help none of this would be possible.

DECLARATION

Patient recruitment and sample collection:

All patients were recruited by Rishi Singhal and Janet Taylor (research phlebotomist at the University of Birmingham). All blood and tissue samples were collected by Rishi Singhal and Janet Taylor.

Sample processing:

All blood samples were processed for analysis by Rishi Singhal. Methanol chloroform extraction of tissue samples was performed by Jonathan James (research technician at the University of Birmingham).

Data acquisition and analysis (NMR):

Samples were prepared for analysis by Rishi Singhal. All data acquisition and analysis was performed by Rishi Singhal under supervision from Christian Ludwig (Experimental Officer at HWB-NMR, University of Birmingham) and Ulrich Gunther. Customised scripts for data analysis were written by Christian Ludwig.

Data acquisition and analysis (MS):

Samples for MS were prepared by Rishi Singhal and John Carrigan. All data acquisition and analysis was performed by John Carrigan under supervision from Christian Ludwig. Customised scripts for data analysis were written by Christian Ludwig.

Data acquisition and analysis (transcriptomics):

Samples for transcriptomics were prepared by Sim Sahota (research technician at the University of Birmingham). Data analysis was performed by John Arrand and Wenbin Wei (Senior Bioinformatician at the University of Birmingham).

This work has not been accepted for any degree, and is not being concurrently submitted in candidature for any other degree.

Table of Contents

INTRODUCTION	19
1.1 Epidemiology	19
1.1.1 Squamous cell carcinoma	19
1.1.2 Adenocarcinoma	20
1.2 Pathogenesis of oesophageal adenocarcinoma	22
1.3 Adenocarcinoma at the oesophago-gastric junction	26
1.3.1 Pattern of spread of oesophageal carcinoma	28
1.4 Staging for oesophageal cancer	29
1.5 Treatments for oesophageal cancer	32
1.5.1. Neo adjuvant treatments for oesophageal cancer	33
1.5.2. Adjuvant therapy for oesophageal cancer	35
1.5.3 Current neo adjuvant trials in the UK	35
1.6 Prediction of response to neoadjuvant chemotherapy	35
1.6.1 Molecular techniques:	36
1.6.1.1 5-Fluorouracil	36
1.6.1.2 Cisplatin	38
1.6.1.3 Other molecular markers for prediction of response	40
1.6.2 Drawback of genomics and transcriptomics	43
1.6.3 Functional imaging:	44
1.6.4 Non-Functional imaging:	45
1.6.5 Clinicopathological factors:	45
1.7.1 Nuclear Magnetic Resonance Spectroscopy	47
1.7.2 Basics of NMR	49
1.7.3 Cancer metabolism	51
1.7.3.1 The Warburg effect	51
1.7.3.2 The role of cancer genes in metabolic regulation	52
1.7.3.3 The role of metabolic reprogramming in promoting tumorigenesis	52
1.7.4 The role of metabolomics in the study of tumour metabolism	53
1.7.4.1 Common NMR detectable changes associated with malignancy	54
1.7.4.3 Metabolomics in oesophageal cancer	56
AIMS	59
METHODS	60
2.1 Ethical considerations	60
2.1.1 Ethical approval	60
2.1.2 University Hospital Birmingham sponsorship	60
2.2 Patient Recruitment	60
2.2.1 Study duration	60
2.2.2 Inclusion criteria	61
2.2.3 Exclusion Criteria	61
2.3 Sample collection for blood	61
2.3.1. Time Intervals	61
2.3.1.1. Patients	61
2.3.1.2. Controls and patients with non-dysplastic Barrett's	62
2.3.2. Pre-processing	63
2.3.3. Processing for NMR analysis	63
2.3.3.1 Experiments to ascertain wash cycles	64

2.3.3.2 Experiments to ascertain filtration times and volumes for plasma	65
2.3.3.3 Experiments to ascertain buffer and TMSP concentration	67
2.3.3.4 Experiments to ascertain tube diameters.....	68
2.4 Sample collection for tissue	70
2.4.1. Time intervals	70
2.4.1.1. Patients with oesophago-gastric malignancies.....	70
2.4.1.2. Patients with non-dysplastic Barrett's	71
2.4.1.3. Patients with known high grade dysplastic Barrett's.....	72
2.4.1.4. Other patients	72
2.4.1.5. Controls.....	72
2.4.2. Sample aliquots	72
2.4.3. Sample transport and storage	73
2.4.4. Measures to create comparable samples.....	73
2.4.5. Experiments to optimize a protocol for tissue freezing	74
2.4.6. Extraction of tissue	74
2.4.7 Reconstitution of the polar extracts for NMR analysis.....	76
2.5 NMR data acquisition	76
2.6 Data processing.....	77
2.7 Statistical analysis	78
2.7.1 PCA.....	79
2.7.2 PLS-DA.....	80
2.7.3 OPLS-DA.....	81
2.7.4 Cross Validation.....	81
2.7.4.1 Venetian Blind algorithm.....	82
2.7.4.2 Leave one out algorithm	82
2.7.5 ROC curve	82
2.8 Assignment of peaks	83
2.9 Statistical total correlation spectroscopy (STOCSY)	84
2.10 Assessment of response to chemotherapy.....	85
2.10.1 Histopathological assessment	85
2.10.2 Radiological assessment	86
2.10.3 Calculation of overall response.....	87
2.11 Statistical modelling.....	88
2.11.1 Plasma modelling.....	88
2.11.2 Tissue modelling.....	91
RESULTS	94
3.1 Demographics	94
3.1.1 Patients with oesophago-gastric malignancy	94
3.1.2 Patients with Non dysplastic Barrett's oesophagus	96
3.1.3 Patients with high grade dysplasia of the oesophagus	97
3.1.4 Controls patients with GORD symptoms or dyspepsia	97
3.1.5 Comparison of patients with oesophago-gastric malignancy vs. controls.....	97
3.2 Quality control	98
3.2.1 Plasma samples	98
3.2.2 Endoscopic biopsies.....	99
3.2.3 Resectional tissue.....	99
3.3 NMR plasma results.....	100
Model 1. Controls vs. gastro-oesophageal adenocarcinoma.....	100
Model 2. Non-dysplastic Barrett's vs. oesophageal adenocarcinoma type 1,2	104

Model 3. Overall response	106
Model 4. Stage on N	108
Model 5. Stage on T	111
Model 6. 'Bacon and egg' model.....	114
3.4 NMR tissue results.....	116
Model 1. Normal squamous mucosa vs. normal gastric columnar mucosa.....	116
Model 2. Normal squamous mucosa vs. oesophageal adenocarcinoma type 1,2	120
Model 3. Normal squamous mucosa vs. Barrett's mucosa in the presence of a cancer vs. oesophageal adenocarcinoma type 1,2.....	122
Model 4. Non dysplastic Barrett's vs. Barrett's mucosa in the presence of a cancer	126
Model 5. Overall response	128
3.5 Univariate analysis of metabolites.....	131
3.5.1 Results of univariate analysis in plasma (tabulated results in appendix).....	132
3.5.2 Results from tissue (tabulated results in appendix)	132
3.6 Selection of metabolites of interest.....	133
3.7 Differences in metabolite levels for plasma and tissue.....	134
3.7.1 Hypoxanthine.....	134
3.7.1.1 Hypoxanthine levels in tissue (MS metabolomics)	137
3.7.1.2 Hypoxanthine phosphoribosyl transferase activity.....	140
3.7.2 3-hydroxybutyrate.....	142
3.7.3 Succinate and fumarate	149
3.7.4 Resonance at 2.737 ppm (Metabolite X)	154
3.7.5 Unassigned resonance at 3.72 ppm (Metabolite Y).....	158
DISCUSSION.....	163
4.1 Hypoxanthine.....	166
4.1.1 Hypoxanthine and its role in purine salvage.....	166
4.1.2 Activity of enzymes and metabolites of the salvage pathway in various cancers	169
4.1.3 Cancer drugs acting on purine metabolism.....	171
4.2 Succinate and fumarate	173
4.2.1 Succinate and its role in carcinogenesis.....	174
4.2.2 Succinate and fumarate in the Tricarboxylic acid cycle (TCA)	176
4.2.3 Further research into SDH	176
4.3 3-hydroxybutyrate.....	176
4.3.1 Metabolism of 3-hydroxybutyrate	177
4.3.2 Role of 3-HB and ketone bodies in carcinogenesis	179
4.4 Comparison of results to proteomic data [242].....	180
4.5 NMR metabolomics in biomarker discovery.....	182
4.5.1 Strengths of the study.....	182
4.5.2 Advantages and disadvantages of using NMR for metabolomics	183
4.5.3 Advantages and disadvantages of using metabolomics for tissue profiling	184
4.6 Future studies.....	185
CONCLUSION.....	187
APPENDIX.....	202
Metabolite integrations for plasma and tissue	202
Ethical approval	202
Substantial amendment to ethical approval	202
UHB sponsorship letter.....	202
Protocol.....	202
Patient information sheet	202

Patient consent form	202
Data collection proforma – patients	202
Volunteer control information sheet	202
Volunteer control consent form	202
Data collection proforma – controls	202
Manuscript: MALDI profiles of proteins and lipids for the rapid characterisation of upper GI-tract cancers	202

Table of figures

Figure 1 Oesophageal Cancer (C15), European Age-Standardised Incidence Rates, Great Britain, 1975-2008 [12]	21
Figure 2 Siewert classification of adenocarcinomas of the oesophago-gastric junction (AEG) [35].....	27
Figure 3 Stage II TNM subgroup survival [41]	31
Figure 4 Survival by nodal status. Forty-four node-negative (N0) and 67 node-positive (N1) patients [42]	31
Figure 5 600 MHz UltraShield plus Bruker magnet.....	49
Figure 6 NMR spectra after various wash cycles	65
Figure 7 NMR spectra from varying tube diameters and probes.....	70
Figure 8 PLS-DA Model 1 plasma	101
Figure 9 OPLS-DA Model 1 Plasma	102
Figure 10 Loadings plot for LV1 Model 1 Plasma obtained from OPLS-DA.....	103
Figure 11 OPLS-DA Model 2 Plasma	105
Figure 12 PLS-DA Model 3 Plasma	107
Figure 13 Loadings plot for LV1 Model 3 Plasma.....	108
Figure 14 PLS-DA Model 4 Plasma	110
Figure 15 Loadings plot for LV1 Model 4 Plasma.....	111
Figure 16 PLS-DA Model 5 Plasma	113
Figure 17 Loadings plot for LV1 Model 5 Plasma.....	114
Figure 18 PLS-DA Model 6 Plasma (LV1 vs. LV2 vs. LV3).	115
Figure 19 PLS-DA Model 1 Tissue (LV1 vs. LV2)	117
Figure 20 OPLS-DA Model 1 Tissue	118
Figure 21 Levels of alanine in normal squamous tissue and normal columnar tissue on Model 1 Tissue.....	119
Figure 22 Level of lactate in normal squamous tissue and normal columnar tissue on Model 1 Tissue	119
Figure 23 PLS-DA Model 2 Tissue	121
Figure 24 Loadings plot for LV1 Model 2 Tissue	122
Figure 25 PLS-DA Model 3 Tissue (LV1 vs. LV2)	125
Figure 26 PLS-DA Model 4 Tissue (LV1 vs. LV2)	127
Figure 27 Loadings plot for LV1 Model 4 Tissue	128
Figure 28 PLS-DA Model 5 Tissue	130
Figure 29 Loadings plot for LV1 Model 5 Tissue	131
Figure 30 NMR spectra of a tissue homogenate with and without a hypoxanthine spike (100 mM).....	135
Figure 31 Level of hypoxanthine in normal squamous tissue and paired cancer mucosa (model 2).....	135
Figure 32 Levels of hypoxanthine in normal squamous tissue, paired Barrett's and cancer mucosa (model 3).....	136
Figure 33 Level of hypoxanthine in pre chemotherapy cancer mucosa from responders and non responders (model 5).....	137
Figure 34 Level of hypoxanthine in normal squamous tissue and paired cancer mucosa (model 2) on MS metabolomics.....	139
Figure 35 Levels of hypoxanthine in normal squamous tissue, paired Barrett's and cancer mucosa (model 3) on MS metabolomics	140

Figure 36 Hx-PRTase activity as indicated by gene expression analysis (Affymetrix) for normal squamous mucosa and paired cancer mucosa. Patient number represents the anonimsed biopsy tag.....	141
Figure 37 Hx-PRTase activity as indicated by gene expression analysis (Affymetrix) for normal squamous mucosa, and paired Barrett's and cancer mucosa.....	142
Figure 38 2D Hadamard ^1H , ^1H -TOCSY-NMR spectrum on a tissue homogenate with suspected high level of 3-hydroxybutyrate	143
Figure 39 NMR spectra of a tissue homogenate with and without a 3-hydroxybutyrate spike (500 μM).....	144
Figure 40 NMR spectra of a tissue homogenate with and without a 3-hydroxybutyrate spike (500 μM).....	144
Figure 41 Level of 3-hydroxybutyrate in normal squamous tissue and paired cancer mucosa on Model 2 Tissue.....	145
Figure 42 Level of 3-hydroxybutyrate in plasma from control patients and pre treatment plasma from patients with cancer Model 1 Plasma	146
Figure 43 Level of 3-hydroxybutyrate in plasma from control patients and pre treatment plasma from patients with cancer Model 1 Plasma	146
Figure 44 Level of 3-hydroxybutyrate in pre treatment plasma samples from responders and non-responders Model 3 Plasma.....	147
Figure 45 Level of 3-hydroxybutyrate in pre surgery plasma samples from patients not receiving neoadjuvant chemotherapy and plasma samples from patients undergoing palliative treatment without chemotherapy on Model 4 Plasma.....	148
Figure 46 Level of 3-hydroxybutyrate in pre surgery plasma samples from patients not receiving neoadjuvant chemotherapy and plasma samples from patients undergoing palliative treatment without chemotherapy on Model 5 Plasma.....	148
Figure 47 NMR spectra of a tissue homogenate with and without a fumarate spike (500 μM).....	149
Figure 48 NMR spectra of a tissue homogenate with and without a succinate spike (500 μM).....	150
Figure 49 STOCSY on non dysplastic Barrett's tissue samples on Model 4 Tissue.....	151
Figure 50 STOCSY on dysplastic Barrett's tissue samples on Model 4 Tissue.....	151
Figure 51 STOCSY on Normal squamous mucosa on Model 3 Tissue	152
Figure 52 STOCSY on dysplastic Barrett's tissue samples on Model 3 Tissue.....	153
Figure 53 STOCSY on cancer tissue samples on Model 3 Tissue	153
Figure 54 Level of Metabolite X in normal squamous tissue, paired Barrett's and cancer mucosa on Model 3 Tissue	154
Figure 55 Level of Metabolite X in non dysplastic and dysplastic Barrett's mucosa on Model 4 Tissue.....	155
Figure 56 2D ^{13}C -HSQC on a tissue sample with high concentration of Metabolite X.....	156
Figure 57 Homonuclear 2D- ^1H , ^1H -TOCSY NMR spectrum with high concentration of Metabolite X	157
Figure 58 Level of Metabolite X in all plasma samples	158
Figure 59 Level of Metabolite Y in non dysplastic and dysplastic Barrett's mucosa on Model 4 Tissue.....	159
Figure 60 2D ^1H , ^{13}C -HSQC NMR of a tissue sample with high concentration of Metabolite Y	160
Figure 61 Homonuclear 2D- ^1H , ^1H -TOCSY NMR spectrum with high concentration of Metabolite Y	161
Figure 62 Overlay 2D ^1H , ^{13}C -HSQC.....	162

Figure 63 The purine Salvage pathway of purine synthesis	168
Figure 64 Metabolism of 3-hydroxybutyrate	178

List of tables

Table 1 TNM staging for oesophageal carcinoma	30
Table 2 Recent metabolic studies in oesophageal carcinoma	57
Table 3 Distribution of participants recruited for the study	94
Table 4 Distribution of patients according to type of cancer	95
Table 5 Stage specific breakdown of patients	95
Table 6 Breakdown of patients according to type of chemotherapy received	96

LIST OF ABBREVIATIONS (alphabetical)

3-Hydroxybutyrate	3-HB
5-Fluorouracil	5-FU
Adenocarcinoma	AC
Adenosine Tri Phosphate	ATP
Breakpoint Cluster Region	BCR-ABL
Cisplatinum, 5-Fluorouracil	CF
Contrast Enhanced Computed Tomography	CECT
Difference Gel Electrophoresis	DIGE
Electrospray Mass Spectrometry	ESI-MS
Epidermal Growth Factor Receptor	EGFR
Epidermal Growth Factor Receptor	EGFR
Epirubicin, Cisplatinum, 5-Fluorouracil	ECF
Epirubicin, Cisplatinum, Xeloda (Capecitabine)	ECX
Epirubicin, Oxaliplatin, Xeloda (Capecitabine)	EOX
Ethylenediaminetetraacetic Acid	EDTA
European Organization For Research And Treatment Of Cancer	EORTC
Flavin Adenine Dinucleotide	FAD
Free Induction Decay	FID
Gas Chromatography Mass Spectrometry	GC-MS
Gastro Oesophageal Reflux Disease	GORD
Heteronuclear Single-Quantum Correlation Spectroscopy	HSQC
High Grade Dysplasia	HGD

Human Epidermal Growth Factor Receptor 2	HER-2
Human Metabolome Database	HMDB
Human Paraganglioma	HPGL
Hypoxanthine-Guanine Phosphoribosyl Transferase	Hx-PRTase
Hypoxia Inducible Factor	HIF
Inosine 5'-Monophosphate	IMP
Intravenous	IV
Low Grade Dysplasia	LGD
Magnetic Resonance Imaging	MRI
Mass Spectrometry	MS
Mitomycin, Ifosfamide And Cisplatinum	MIC
Monocarboxylate Transporters	MCTs
Multi-Disciplinary Team	MDT
Nuclear Magnetic Resonance	NMR
Nuclear Overhauser Effect Spectroscopy	NOESY
Orthogonal Partial Least Squares - Discriminant Analysis	OPLS-DA
Partial Least Squares	PLS
Partial Least Squares - Discriminant Analysis	PLS-DA
Positron Emission Tomography	PET
Principal Component Analysis	PCA
Radiofrequency	RF
Receiver Operating Characteristic	ROC
Response Evaluation Criteria In Solid Tumors	RECIST
Rna Integrity Number	RIN

Squamous Cell Carcinoma	SCC
Statistical Total Correlation Spectroscopy	STOCSY
Succinate Dehydrogenase	SDH
Succinate-Ubiquinone Oxidoreductase Subunit B	SDHB,C or D
Thymidylate Synthetase	TS
Total Correlation Spectroscopy	TOCSY
Tricarboxylic Acid Cycle	TCA
Trimethylsilyl propanoic acid	TMSP
Tumour Regression Grade	TRG

Units of Concentration

M Molar

mM Millimolar

μ M Micromolar

nM Nanomolar

Units of Length, Area, Volume, Mass, Time

Mm Millimetre

L Litre

ml Millilitre

μ l Microlitre

Min Minutes

Physical and Chemical Units

RCF relative centrifugal force

$^{\circ}$ C degree Celcius (Centigrade)

ppm part per milliom

rpm revolutions per minute

INTRODUCTION

1.1 Epidemiology

Oesophageal cancer is the sixth most common cause of cancer-related death worldwide [1]. It is a highly aggressive malignancy with approximately 8,000 new cases diagnosed in United Kingdom every year [2]. It is the ninth leading cause of cancer and fifth leading cause of death due to cancer in the United Kingdom [2].

Oesophageal cancer was first described in the ancient Chinese medical literature. It was said to be caused by 'heavy indulgence in heated liquors' and was considered to be 'commonly seen in the elderly and rarely developing in young people' [3]. Squamous cell carcinoma (SCC) and adenocarcinoma (AC) are the most common type of oesophageal cancer. Rare histologic types of oesophageal cancer include leiomyosarcoma, malignant melanoma, rhabdomyosarcoma and lymphoma.

1.1.1 Squamous cell carcinoma

Squamous cell cancer of the oesophagus has particularly high incidences in the Transkei region of South Africa [4] and across the Central Asian 'cancer belt' that extends from the shores of the Caspian Sea in northern Iran to China. The highest incidence areas in the world are in Linxian in Henan province in China [5], where it is the most common single cause of death, with more than 100 cases per 100,000 of population per annum and in Iran on the south-eastern shores of the Caspian Sea [6]. In Europe, the Normandy region of France has been identified as an area of high incidence of oesophageal SCC. Considerable research in these high incidence areas has focused on environmental and particularly dietary factors as causal agents. In Normandy, for instance, high incidence has been attributed to the

consumption of alcohol and tobacco [7] although a recent study has shown a high frequency of biallelic p53 mutations in this population [8].

1.1.2 Adenocarcinoma

In most western countries, the incidence of squamous cell cancer has fallen or remained relatively static, while the incidence of adenocarcinoma has increased dramatically since the mid-1970s by 5-10% per annum [9]. This change is greater than that of any other neoplasm in this time. In the United States, the average yearly increase in incidence is approximately 20%. However, amongst white men, the incidence has increased >800% since the mid 1970s in some areas [10]. Europe has the highest incidence of AC compared to the other continents and the country with the highest incidence in Europe is the United Kingdom [11].

The male European age-standardised incidence rate of oesophageal carcinoma in the UK has risen from 8.8 per 100,000 population in 1975-1977 to 14.5 in 2006-2008 (Figure 1). This was accompanied with a relatively lower increase in female rates, rising from 4.8 to 5.6 [12].

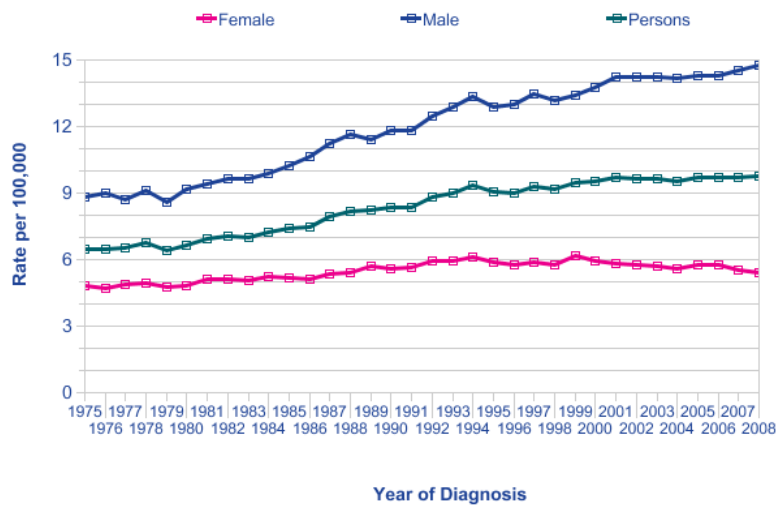


Figure 1 Oesophageal Cancer (C15), European Age-Standardised Incidence Rates, Great Britain, 1975-2008 [12]

Prepared by Cancer Research UK

Original data sources:

1. Office for National Statistics. Cancer Statistics: Registrations Series MB1. <http://www.statistics.gov.uk/statbase/Product.asp?vlnk=8843>.
2. Welsh Cancer Intelligence and Surveillance Unit. <http://www.wcisu.wales.nhs.uk>.
3. Information Services Division Scotland. Cancer Information Programme. www.isdscotland.org/cancer.
4. N. Ireland Cancer Registry. www.qub.ac.uk/nicr.

Adenocarcinoma now accounts for 60-75% of all oesophageal cancers in most western countries. It is strongly linked to the rising incidence of gastro-oesophageal reflux disease (GORD) and specifically within that condition, to the development of Barrett's oesophagus which is considered the precursor lesion for most oesophageal adenocarcinomas. Barrett's oesophagus was first described in 1950 as a condition in which the lower oesophagus is lined

by columnar epithelium [13]. Barrett originally believed that this situation resulted from a congenitally short oesophagus that pulled the proximal stomach upwards, but later accepted that it was an acquired condition secondary to gastro-oesophageal reflux. The association of adenocarcinoma of the oesophagus with Barrett's oesophagus was first described by Carrie [14]. Since then, this association has become well established.

1.2 Pathogenesis of oesophageal adenocarcinoma

The progression from Barrett's metaplasia through dysplasia to carcinoma has been extensively investigated, although the key genetic events are less well understood compared to the polyp-cancer sequence in colorectal cancer [15]. In the oesophagus, the first step is damage to the squamous epithelium secondary to gastro-oesophageal reflux. The increased cell loss leads to an increase of the proliferative zone height to maintain or increase epithelial thickness by trophic stimulation of locally produced epidermal growth factor [16]. During this process the functional stem cells in the basal zone at the tip of the papillae remain in a relatively superficial position making them more accessible and susceptible to refluxed or ingested chemical mutagens [17]. This leads to a mucosal adaptive response to the chronic inflammation secondary to reflux. When this initial increase in cell proliferation fails to compensate for the cell loss, these mucosal breaches in the absence of treatment of reflux become replaced by *de novo* Barrett's metaplasia [18]; a composite glandular epithelium characterised by incomplete intestinal metaplasia that includes mucus secreting goblet cells [19]. The degree of differentiation within this metaplastic epithelium varies considerably although most researchers see this as an adaptive response to severe reflux [20]. The protective effect of a mucus layer may account for the relative paucity of symptoms among these patients even when 24h pH testing confirms prolonged oesophageal acidification. In

turn, this is thought to explain why so many patients present when they have symptoms from their cancer (usually dysphagia) rather than those from reflux (heartburn, regurgitation and epigastric pain).

There are numerous features that are histologically specific to Barrett's oesophagus. One of the main findings is the heterogeneous nature of the metaplastic columnar mucosa. A single type of epithelium is present in less than half of the patients, but the presence of an intestinal rather than simple columnar epithelium seems important in carcinogenesis [21]. There are, however, a number of definitions for Barrett's oesophagus that in turn lead to different concepts of its frequency and cancer risk. Classic long segment Barrett's is essentially an endoscopic diagnosis where the red Barrett's lining is visibly different from the paler oesophageal squamous mucosa. Biopsy showing columnar epithelium is considered confirmatory. Short segment Barrett's refers to visible lengths of Barrett's oesophagus of less than 2cm. In order not to confuse these with the columnar mucosa of the stomach and in particular a small tubular hiatus hernia, confirmatory biopsy is generally considered essential to make a diagnosis of short segment Barrett's oesophagus. The problem is complicated though by having variable histopathologic features that are considered confirmatory. Some groups have accepted this as a simple columnar epithelium while others have accepted the diagnosis only when there are features of intestinalisation. Other confounders, such as the number of biopsies taken and consequent risks of sampling error undoubtedly contribute to variations in both incidence of Barrett's oesophagus and the risk of progression. Some of these points are expanded upon below.

To quantify the risk of developing cancer, the various stages of this sequence have been graded histologically. Theisen et al. defined low-grade dysplasia (LGD) as the presence of

nuclear enlargement, hyperchromasia and sparse mitotic figures. High-grade dysplasia (HGD) was defined by the presence of marked nuclear enlargement, pleomorphism, hyperchromasia and the presence of mitosis including atypical mitotic figures [20]. Progressive loss of normal architecture with distorted glands and an irregular surface epithelium as proper maturation fails, also characterise this change.

Numerous attempts have been made to identify the cohort of patients who are at risk of progression to adenocarcinoma. It is known that p53 protein expression localised to low-grade dysplasia confers an increased risk of progression to multifocal high-grade dysplasia or adenocarcinoma [5, 22]. Cyclin D1 polymorphism has also been associated with an increased risk of progression to adenocarcinoma [23]. Aneuploid DNA content as detected by flow cytometry has also been described as a tissue biomarker associated with progression to dysplasia [24, 25]. None of these markers, however, have yet become firmly established in routine clinical practice

Although it is known that patients with Barrett's oesophagus have severe GORD as judged by duration of oesophageal acidification [26], it is still not clear why some patients develop this condition and others do not. Thus it is imperative to identify the cohort of patients who are more likely to develop this condition. The risk that this epithelium will become dysplastic and the speed with which this can progress to HGD and on to carcinoma also show wide variations between series. Many of these differences are probably due to methodologic limitations and imprecise definitions, and further work is required to accurately quantify these risks.

Only a minority of patients with gastroesophageal reflux disease go on to develop the histological changes of Barrett's oesophagus. It has been estimated that about 15% of patients with GORD will eventually develop a classic long segment Barrett's [27], although the number of patients with Barrett's who will develop dysplasia and further progression is not accurately known. Sontag et al. in a 19-year prospective study of 848 patients with LGD, found that 3.9% of patients progressed to HGD and 2.1% of all patients progressed oesophageal adenocarcinoma [28].

Hameeteman et al. concluded that it took between one and a half and four years for patients to progress from low grade dysplasia to cancer. They also concluded that high grade dysplasia could be present for as long as three and a half years before it progressed to cancer [29]. Theisen et al. in their study concluded that in the subset of patients with Barrett's oesophagus who developed cancer, the time between diagnosis of Barrett's oesophagus and that of oesophageal adenocarcinoma was within three years [20]. Schnell et al. found a mean 7.3-year surveillance period before cancer was detected. However, when they considered patients with early visible lesions, this time decreased to about four years for the development of cancer [30].

According to the guidelines for the diagnosis and management of Barrett's columnar-lined oesophagus published by the British Society of Gastroenterology based on pooled data from many studies, it is estimated that dysplasia develops in around 5% of patients with columnar-lined oesophagus. In those developing low-grade dysplasia, 10–50% may progress to high-grade dysplasia and adenocarcinoma over 2–5 years [31]. These figures were prepared by a close examination of the data pooled from various studies and may as such differ from individual studies even if they included large numbers.

Endoscopic surveillance programmes with quadrantic biopsies (i.e. one biopsy per quadrant) every 2 cm in the columnar segment every two years can detect HGD and oesophageal adenocarcinoma at an early stage when the depth of the tumour is limited to the muscularis mucosa [31]. Current evidence suggests that a metaplasia/dysplasia/ carcinoma sequence occurs in 0.5% of patients with Barrett's oesophagus / annum [32]. A UK wide study is currently being conducted to examine the role of endoscopic surveillance in these patients. The BOSS study (Barrett's Oesophagus Surveillance Study) compares endoscopic surveillance vs. no endoscopic surveillance for the prevention of early mortality in patients diagnosed with Barrett's oesophagus. In this study patients have been randomized to receive endoscopy with biopsy every two years for 10 years or endoscopy at the time of need. Furthermore, all of these patients receive a bi-annual postal questionnaire to record their symptoms and other health related data.

1.3 Adenocarcinoma at the oesophago-gastric junction

The increasing incidence of adenocarcinoma of the oesophagus has been accompanied with a similar increase in the incidence of carcinoma of the cardia of the stomach. This suggests that they may share a common aetiology or may be the same disease [33]. One of the problems is that distal oesophageal tumours may grow downward and involve the cardia, and, vice versa. To clarify this situation, Siewert et al. divided adencarcinomas in this region into three types based on the anatomical location of the tumour centre [34] and concluded that there were marked differences in sex distribution, associated intestinal metaplasia in the oesophagus, tumour grading, tumour growth pattern, and stage distribution between the three tumour types.

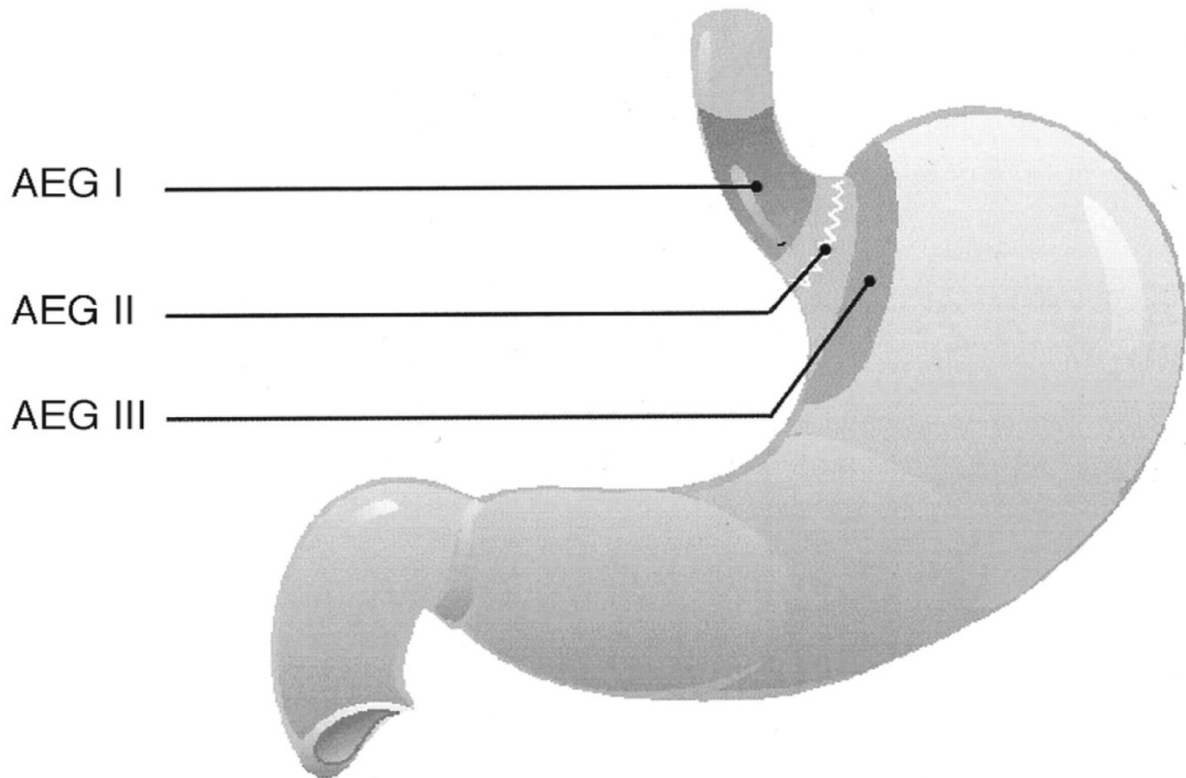


Figure 2 Siewert classification of adenocarcinomas of the oesophago-gastric junction (AEG) [35]

The Siewert classification is widely used (Figure 2). Type I tumours are considered to arise from areas of intestinal metaplasia in the distal oesophagus. Type III tumours are similar to proximal gastric cancers and are treated according to gastric cancer guidelines. Type II tumours straddle the oesophago-gastric junction. They tend to resemble proximal gastric cancer more closely than distal oesophageal adenocarcinoma. The authors found a significantly higher proportion of an intestinal-type growth pattern in type I tumours compared to type II and III tumours. Due to a difference in the anatomical location of the tumours, the pattern of lymph nodal metastasis was also different. Lymphographic studies have confirmed that the main lymphatic pathways originating from the lower oesophagus advance both up into the mediastinum and down towards the coeliac axis, whereas those from the gastric cardia and subcardial region preferentially make their way to the coeliac axis [36].

In practice, tumour location using this system influences the choice of operation. Type I tumours clearly require oesophagectomy and Type III tumours a gastrectomy. The debate centres around the appropriate operation for Type II tumours where both stomach and oesophagus are involved, albeit in variable proportions. Patients with Type I and Type II tumours whose samples were analysed in the current thesis, were both treated by oesophagectomy. This last term is often used interchangeably with oesophago-gastrectomy to denote that most of the intra-thoracic oesophagus is removed along with the lesser curvature of the upper stomach.

1.3.1 Pattern of spread of oesophageal carcinoma

The pattern of local spread of oesophageal carcinoma depends on the site of the tumour. The predominant site for both the tumour types i.e. SCC and AC is different. SCC is usually found in the upper one third or upper half of the oesophagus, whereas AC is more common in the lower half or close to the OG junction, strengthening the hypothesis that this cancer arises from Barrett's oesophagus.

SCC usually begins as a flat tumour with central ulceration. Extensive submucosal infiltration is common, with satellite tumours appearing at some distance from the main lesion. Proximal extension is more common than distal, and these tumours rarely extend downwards into the stomach.

AC usually begins in an area of intestinal metaplasia (Barrett's oesophagus) of the oesophagus. Tumours at the oesophago-gastric junction frequently spread upwards into the oesophagus.

Both cancer types exhibit similar behaviour with local invasion through the wall into adjacent structures along with lymph node spread, vascular invasion and haematogenous metastasis. Trans-peritoneal and trans-pleural metastases also occur depending on tumour site. Submucosal lymphatics of the oesophagus run for considerable distances before penetrating the oesophageal wall to connect with paraoesophageal lymphatics and adjacent lymph nodes. Thus, deep cervical nodes, peri-gastric and splenic artery nodes are easily involved by a lesion in the mid oesophagus [3]. Obstruction of lymphatics by tumour cells may alter lymphatic flow and produce skip metastases in apparently remote lymph nodes [37].

Since only a minority of patients with oesophageal carcinoma present with potentially resectable disease, the five- year survival for these patients is quite poor. The last population-based five-year relative survival rates for all patients diagnosed with oesophageal cancer in 2000-01 in England and Wales were 8% for both men and women (30% for men and 27% for women at one year after diagnosis) [38].

1.4 Staging for oesophageal cancer

Both the American Joint Committee on Cancer [39] (AJCC) and Union for International Cancer Control[40] (UICC) use systems based on staging the primary tumour (T), nodal spread (N) and distant organ involvement (M) to staging oesophageal cancer. At the time of the present study, both organisations considered SCC and AC together. It is this classification that has been used in the current work.

T stage	Description
TX	Primary tumour cannot be assessed
T0	No evidence of primary tumour
Tis	Carcinoma in situ
T1	Tumour invades lamina propria or submucosa
T2	Tumour invades muscularis propria
T3	Tumour invades adventitia
T4	Tumour invades adjacent structures

N stage	Description
NX	Regional lymph nodes cannot be assessed
N0	No regional lymph node metastasis
N1	Regional lymph node metastasis

M stage	Description
MX	Distant metastasis cannot be assessed
M0	No distant metastasis
M1	Distant metastasis

Table 1 TNM staging for oesophageal carcinoma.

This classification is linked to prognosis and overall survival. Survival of patients with T1 disease is better than for other T stages and similarly for patients with N0 disease compared to those with N1 disease (Figure 3, Figure 4) [41].

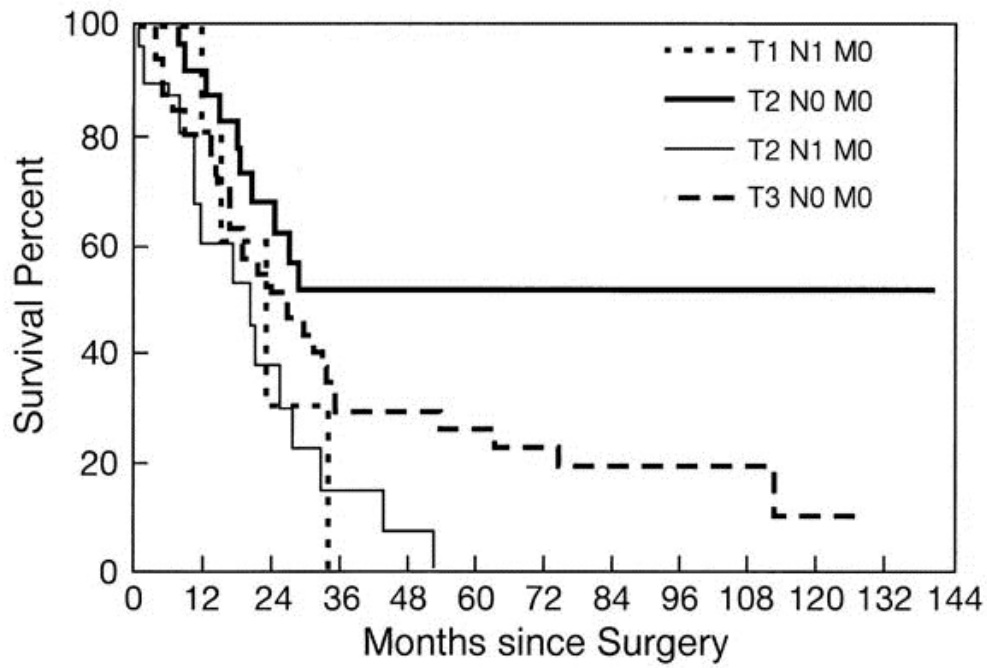


Figure 3 Stage II TNM subgroup survival [41]

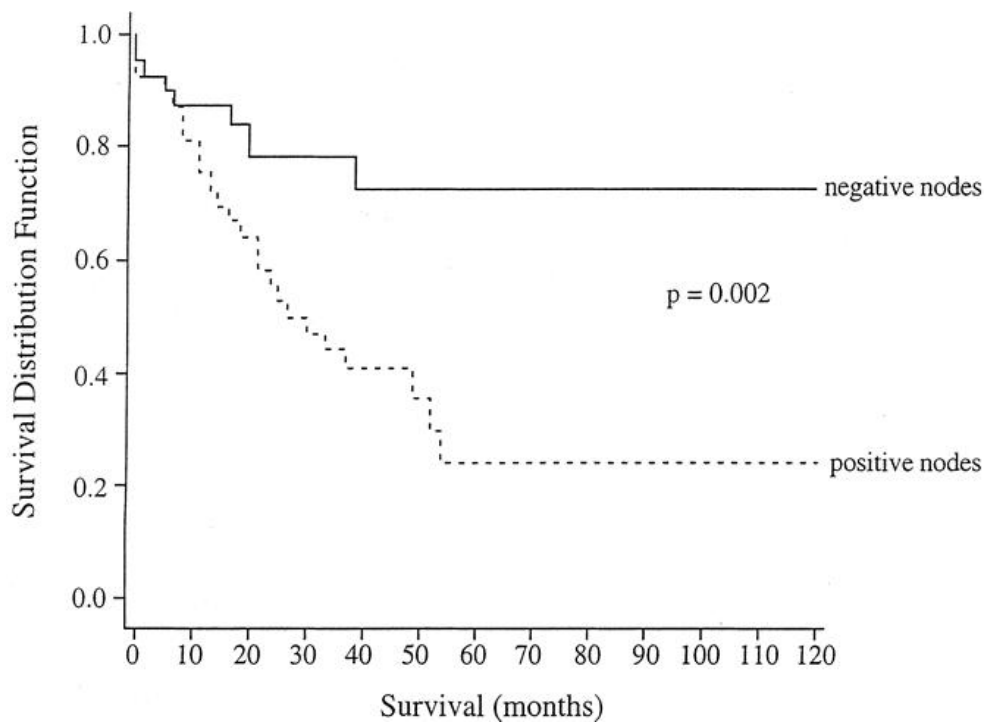


Figure 4 Survival by nodal status. Forty-four node-negative (N0) and 67 node-positive (N1) patients [42]

1.5 Treatments for oesophageal cancer

Treatment options for oesophageal cancer can be considered attempted curative or palliative. Patients with haematogenous or peritoneal metastases are considered incurable. Small proportions of patients have early mucosal disease and can be cured by endoscopic mucosal resection. For the remainder, careful pre-operative staging is used to identify patients with unresectable disease such as airway involvement and those with lymphatic dissemination outside the proposed field of surgery that makes most of these patients incurable. The mainstays of curative treatment are oesophagectomy alone, neo-adjuvant chemotherapy or chemoradiotherapy followed by oesophagectomy or definitive chemoradiotherapy. Neo-adjuvant radiotherapy before surgery has been abandoned. A small proportion of patients deemed incurable on their initial staging can go on to surgery after 'successful' neo-adjuvant treatment and similarly there are 'non-responders' whose disease progresses and become candidates for palliative treatment. Because AC characteristically affects the lower oesophagus and oesophago-gastric junction, with downward nodal spread, definitive chemoradiotherapy is used much more extensively for SCC, where a smaller volume field can be successfully irradiated.

Oesophagectomy with lymphadenectomy via the abdomen and right chest is the most widely used operation for AC. The more proximal location of SCC in the oesophagus may necessitate an additional incision in the neck to obtain an adequate proximal resection margin. The primary aim of surgery is to achieve a complete resection of the tumour (R0) and surrounding lymph nodes to maximise the opportunity for cure, obtain the maximum amount of information for prognostic purposes and minimise the risk of local recurrence. Complete

surgical resection is the most important prerequisite for long-term survival in patients with localised oesophageal cancer [34, 42-44].

1.5.1. Neo adjuvant treatments for oesophageal cancer

Neo adjuvant chemotherapy followed by surgery

A Cochrane review in 2006 analysed the role of preoperative chemotherapy in oesophageal cancer [45]. This review was based on 11 randomised trials out of 18 randomised controlled trials and two meta-analyses that were potentially eligible for the review. The authors found some evidence to suggest that preoperative chemotherapy improved survival (HR 0.88; 95% CI 0.75 to 1.04). The largest trial on this subject was from the UK (the OE02 trial). This compared two cycles of pre-operative chemotherapy with cisplatin and 5-fluorouracil followed by surgery against surgery alone [46]. OE02 demonstrated a significant benefit in survival for the chemotherapy arm (hazard ratio of 0.79; 95% CI 0.67-0.93; $p = 0.004$). The survival rate at 2 years was 43% (chemotherapy + surgery) compared with 34% (surgery alone).

Similar results were also obtained for resectable gastro-oesophageal cancer in the MAGIC trial [47]. MAGIC randomised 503 patients with adenocarcinoma of the stomach and lower third oesophagus to receive peri-operative ECF (epirubicin, cisplatin, 5-fluorouracil) chemotherapy and surgery or surgery alone. In the ECF arm, 3 cycles were given pre-operatively and 3 post-operatively. The final analysis demonstrated smaller tumours and increased resection rates in the patients treated with chemotherapy, as well as significantly improved progression-free and overall survival (hazard ratio of 0.66 (95%CI: 0.53 - 0.81),

p=0.0001 for progression-free survival and hazard ratio of 0.75 (95% CI: 0.60 - 0.93), p=0.009 for overall survival both in favour of the combined arm).

Neo adjuvant radiotherapy followed by surgery

A meta-analysis of all trials on neoadjuvant radiotherapy concluded that neo adjuvant radiotherapy did not improve survival and was not recommended [48]. This quantitative meta-analysis included updated individual patient data (1147 patients) from five randomized trials. The authors concluded that there was no clear evidence that preoperative radiotherapy improved the survival of patients with potentially resectable oesophageal cancer. They postulated that if radiotherapy regimens did improve survival, then the effect was likely to be modest with an absolute improvement in survival no more than 3 to 4%.

Neo adjuvant chemoradiotherapy followed by surgery

Of all the trials published on neo adjuvant chemoradiotherapy, only a few have reported survival benefit. The first study to show a survival advantage was published in 1996 [49]. Fiorica et al. subsequently performed a meta-analysis of the published randomised trials [50]. They concluded in favour of neo adjuvant chemoradiotherapy followed by surgery for overall survival, but they conceded that exclusion of the single study above led to a loss of a statistically significance survival advantage.

The largest single study to date to look at the effects of preoperative chemoradiotherapy in locally advanced oesophageal cancer, involved 364 patients in the Netherlands in a phase III multicentre (CROSS) trial. This study found that a combination of chemotherapy and radiation before resection was superior to surgery alone. Median survival of patients who

received chemoradiation (CRT) and surgery was 49 months, compared to 26 months for those who received surgery alone [51].

1.5.2. Adjuvant therapy for oesophageal cancer

Randomized trials comparing surgery alone against surgery with adjuvant chemotherapy, radiotherapy, or chemoradiotherapy, have not found any survival differences [52-56].

1.5.3 Current neo adjuvant trials in the UK

There are two trials that are currently being conducted in the United Kingdom to compare the efficacy of various chemotherapeutic regimes. OE05 is a randomised controlled trial comparing standard chemotherapy (OE02) followed by resection versus ECX (epirubicin, cisplatin, capecitabine) chemotherapy followed by resection in patients with resectable adenocarcinoma of the oesophagus. This trial has now completed recruitment and the results are expected in the near future. ST03 is a randomised Phase II/III study of peri-operative chemotherapy (using ECX) with or without bevacizumab in operable adenocarcinoma of the stomach and gastro-oesophageal Junction. Patients included in this thesis were offered access to these trials as appropriate.

1.6 Prediction of response to neoadjuvant chemotherapy

The findings from these trials tend to obscure the observation that pathological responders to neoadjuvant treatment have a significantly better survival than both pathological non-responders and patients treated by primary surgery alone [57]. Several analyses suggest that it is the response to preoperative therapy (particularly the absence of residual disease in the

surgical specimen) that best predicts disease-free and overall survival [58]. Distinguishing between responders and non responders would therefore seem highly desirable either before, or at least at any early stage during, treatment. For non-responders, avoidance of potential severe side effects from chemotherapy and the risk of progression to an incurable stage while awaiting surgery are also important considerations.

Factors that can influence tumour response to neoadjuvant chemotherapy include age, sex, ethnicity, comorbid conditions, drug interactions, and genetic factors [59]. Numerous studies have attempted to predict the response to neoadjuvant chemotherapy based on molecular techniques or functional and non-functional imaging.

1.6.1 Molecular techniques:

To understand the molecular techniques in the prediction of response to neoadjuvant chemotherapy, it is important to understand the mechanism of action for the main drugs (5-FU, Cisplatin) used in the treatment of oesophageal adenocarcinoma.

1.6.1.1 5-Fluorouracil

5-fluorouracil (5-FU) was designed, synthesized and patented by Charles Heidelberger in 1957 [60]. It is an analogue of uracil with a fluorine atom in place of hydrogen. 5-FU is an antimetabolite that exerts its anticancer effects through inhibition of thymidylate synthase (TS) and incorporation of its metabolites into RNA and DNA. It utilises the same cellular mechanisms as uracil and rapidly enters the cell where it is converted into several active metabolites – fluorodeoxyuridinemonophosphate (FdUMP), fluorodeoxyuridine triphosphate (FdUTP) and fluorouridine triphosphate (FUTP). These metabolites disrupt RNA synthesis

and the action of TS. Thymidylate synthase methylates deoxyuridine monophosphate (dUMP) into thymidine monophosphate (dTMP). Following scarcity of dTMP, rapidly dividing cancerous cells undergo cell death via 'thymineless' death.

Capecitabine (Xeloda) is an antimetabolite belonging to the fluoropyrimidine class of drugs. It is an orally administered precursor of 5-FU and is converted to 5-FU by carboxyesterase, cytidine deaminase and thymidine phosphorylase.

Molecular techniques for response prediction to the fluoropyrimidine class of drugs can be further subdivided into the following:

Genomics: Numerous studies have concentrated on the influence of genetic factors on the drug action pathways [61], that may contribute to resistance. Work has been performed on the genetic polymorphisms of the enzyme systems involved in folate metabolism and thus potentially in sensitivity to 5-FU-based chemotherapy to improve understanding of the variation in response to chemotherapy [62]. The methodology of these studies has been based on genomic typing utilising tumour tissue samples [61-63], peripheral blood samples [64] or immunohistochemical staining [65, 66] of paraffin embedded tumour tissue blocks.

Thymidylate synthase (TS) methylates dUMP into dTMP which is subsequently phosphorylated to thymidine triphosphate for use in DNA synthesis and repair. Genetic polymorphisms that alter the activity of TS could impact on the therapeutic activity of 5-FU. Liao et al. reported a study on 146 Caucasian patients with oesophageal adenocarcinoma treated with preoperative 5-fluorouracil-based chemoradiation [67]. They focussed on the 3' untranslated region of the TS gene. There was a trend of association between 6bp/6bp

genotype and a decreased risk of local regional recurrence and a higher three year probability of locoregional control compared to patients with other genotypes. Similar studies focusing on these genetic polymorphisms in patients with gastric cancer have been published [68, 69]. None of these studies have been able to adequately differentiate between responders and non responders with sufficient accuracy to influence management.

Transcriptomics: Studies of mRNA expression levels of TS have been published both for oesophageal adenocarcinoma and gastric carcinoma. Langer et al. examined expression of genes associated with metabolism of chemotherapeutic drugs in 21 patients with locally advanced oesophageal adenocarcinomas [70]. They noted a significant post-therapeutic reduction in the expression levels of TS and multidrug resistance-associated protein 1 (MRP1) and thus concluded that downregulation of TS and MRP1 mRNA expression levels after chemotherapy was associated with tumour response. Amplification of thymidylate synthetase has been proposed as a mechanism for poor response to 5- Fluorouracil [63]. Similar studies reporting the association of high TS mRNA expression and poor response to chemotherapy have been published for gastric carcinoma [71-73]. High TS protein expression considered indicative of resistance to 5-FU has also been associated with poorer survival in gastric cancers [74]. Conversely, low expression levels of DPD, ERCC1, GSTPi, ERB2/neu and EGFR have been reported to be associated with tumour response to chemotherapy [74].

1.6.1.2 Cisplatin

Cisplatin or cis-diamminedichloroplatinum [75] was first described by Peyrone in 1844 [76] and approved for use in testicular and ovarian cancers by the U.S. Food and Drug

Administration in 1978. The therapeutic effects of cisplatin are due to its ability to bind to DNA and produce cross-linkages [77] along with the generation of free radicals [78].

The nucleotide excision repair (NER) pathway is a DNA repair mechanism. It is an important method by which the cell can prevent unwanted mutations by removing the vast majority of damaged DNA; for instance damaged DNA in skin cells as a result of UV light exposure. Several human diseases can result from in-born genetic mutations of NER proteins including Xeroderma pigmentosum and Cockayne's syndrome. NER is the predominant DNA repair pathway involved in the repair of bulky DNA-damaging lesions caused by platinating agents [79, 80].

The base excision repair machinery (BER) is involved in the repair of oxidative DNA base damage that is a result of free radical generation by platinating agents. XRCC1 is a DNA repair protein. The protein encoded by this gene is involved in the repair of DNA breaks and forms one of the main mechanisms for base excision repair pathway [81, 82]. Glutathione S-transferases are enzymes involved in the detoxification of platinating agents.

Molecular techniques for response prediction to platinating agents can be further subdivided into the following:

Genomics: In a study by Wu et al. on 210 oesophageal carcinoma patients, polymorphisms of XRCC1 Arg399Gln were significantly associated with the absence of pathologic complete response [61]. The role of ERCC2 in response prediction to chemotherapy with platinating agents has also been evaluated [83].

Transcriptomics: The role of mRNA expression of ERCC1 has been investigated for prediction of response to platinum based chemotherapy. Although the mRNA expression levels of ERCC1 in oesophageal carcinoma are not so convincing [84, 85], the results for advanced gastric cancer indicated that the survival in patients with low ERCC1 levels was significantly longer than in patients with high levels [86].

1.6.1.3 Other molecular markers for prediction of response

Survivin: Survivin is a member of the inhibitor of apoptosis family. Survivin protein inhibits caspase activation, thereby leading to negative regulation of apoptosis or programmed cell death. In one study, nuclear expression of survivin was also detected in 80% of SCC [87]. Expression of this protein has also been documented in gastric cancer [88]. Its role has also been explored as a potential biomarker in the development of Barrett's adenocarcinoma [89]. High levels of survivin expression have been related to reduced overall survival [75] and lack of response or progressive disease [75].

Bax: The Bcl-2 associated X protein, or Bax is a protein of the Bcl-2 gene family. It promotes apoptosis by competing with Bcl-2. Bax protein is found in all cell layers of the normal oesophageal squamous epithelium [90]. Kang et al. reported that low expression of Bax was significantly associated with the poor survival of patients with locally advanced oesophageal cancer [91]. They further recommended that immunohistochemical staining for Bax with a pre-treatment biopsy specimen might be useful to select the optimal treatment options for these patients

Cyclooxygenase-2: Over-expression of cyclooxygenase-2 may be associated with resistance to apoptosis [80]. Cyclooxygenase-2 expression has been reported in up to 78% of the AC's [92]. High Cyclooxygenase-2 protein expression levels have been linked with poor prognosis and histopathological response [93].

p53: p53 is a tumour suppressor protein encoded by the TP53 gene. It regulates the cell cycle and functions as a tumour suppressor. TP53 is frequently mutated in cancer. Mutant p53 tends to be resistant to degradation and hence p53 protein expression in tumours is considered a surrogate marker of p53 mutation and hence may correlate with tumour resistance.

p53 negativity has been associated with good tumour response in gastric cancer [53, 93-95]. However, the results for oesophageal carcinoma are conflicting [96-98]. Only one study has reported that p53 negativity may correlate with increased tumour responsiveness [96].

Nuclear factor Kappa B: Activated nuclear factor kappa B is a transcriptional factor and has been reported to be identifiable in 79% of patients with oesophageal cancers [99]. Activated nuclear factor kappa B protein expression is positively associated with aggressive clinical biology and poor treatment outcome [99]. It has also been correlated with lack of tumour response to neo adjuvant therapy.

Hypoxia inducible transcription factor-1: Hypoxia inducible transcription factor-1 mediated pathway is involved in tumour angiogenesis. HIF-1 transcription factors induce the expression of several genes that regulate various biological processes critical for tumour formation, such as cell proliferation, apoptosis, immortalisation, migration and angiogenesis [100]. HIF-1 expression has been negatively associated with response to chemotherapy in oesophageal squamous cell carcinomas [101]. However, a recent article investigating HIF-1 α

expression has observed a positive correlation between expression and initial response to chemo radiotherapy [102].

c-erb-B1 & B2: c-erb-B1 & B2 are proto oncogenes that code for the epidermal growth factor receptor. mRNA expression levels of c-erb-B1 & B2 have been examined in patients with oesophageal adenocarcinoma receiving neo adjuvant chemotherapy [103]. Levels of expression of c-erbB-2, but not c-erbB-1 mRNA, in pre-treatment biopsies were predictive of minor histopathologic response to neoadjuvant radiochemotherapy.

Metallothionein: Metallothionein is a family of cysteine-rich low molecular weight proteins. Reduced levels of metallothionein, a heavy metal chelator that binds to and inactivates cisplatin have been associated with a significantly increased response rate and importantly patient survival [65].

Caldesmon: Caldesmon is a protein that is encoded by the CALD1 gene. It is a calmodulin binding protein and inhibits the ATPase activity of myosin in smooth muscle. Langer et al. noted that the expression of caldesmon gene was higher in responders compared to non-responders to chemotherapy in patients with oesophageal adenocarcinoma [84].

Glutathione S-transferase: Glutathione S-transferases are enzymes involved in the detoxification of platinating agents. Glutathione S-transferase Π and P- Glycoprotein were associated with a poor response in oesophageal tumour biopsy material from 118 patients who were being treated with concurrent cisplatin and 5-FU [66].

1.6.2 Drawback of genomics and transcriptomics

A significant drawback in most of these studies has been reliance on the genome for accurate response prediction. This is because besides expression, transcription and translation would always have to follow for genome based data to be fully reliable as a marker of response to chemotherapy [104]. Moreover, genomics and transcriptomics focus on a single marker or a set of markers targeting a particular pathway. It is now clear that cancer is a result of a multitude of genetic and epigenetic alterations. Prediction of response to chemotherapy would also therefore be dictated by a combination of the changes that these alterations produce rather than individual genes or gene products.

The failure to find a clinically useful marker or set of markers based on the genome has led to much of the current research being based on proteomics; the study of the proteins finally produced by these processes. Although much work has been done on other cancers, studies on oesophageal cancer utilising proteomics for response prediction are scant.

One of the first articles utilising proteomics for response prediction in oesophageal cancer was based on SELDI (Surface enhanced laser desorption ionisation)[105]. This study concluded that there were subtle but definite differences in serum proteomic profile between responders and non-responders to chemoradiotherapy. Although initially this technique gained momentum, it has recently been criticised due to the lack of identification of proteins and high level of peaks produced that are much higher than for known biomarkers. Another drawback is the suppression of signals from the low abundance peptides by the high abundance peptides due to ion suppression [106]. Other studies have been published since utilising proteomics for response prediction [107, 108]. However, as yet no clinically

applicable proteomic profile exists that identifies a group of patients who might respond to a particular type of treatment in a neo adjuvant setting.

1.6.3 Functional imaging:

Positron emission tomography (PET) with the glucose analogue 18-fluorodeoxyglucose (18 FDG), may have a role in the prediction of tumour response during the early phase of chemotherapy [109]. The Metabolic response evaluation for Individualisation of neoadjuvant Chemotherapy in oesophageal and oesophago-gastric adenocarcinoma (MUNICON) study evaluated the role of 18 FDG-PET for response prediction in patients with locally advanced adenocarcinoma of the oesophagus and oesophago-gastric junction who were receiving neoadjuvant chemotherapy [109]. Patients received two weeks of induction platinum and fluorouracil-based chemotherapy. A decrease of 35% or more in the tumour glucose standardised uptake value (SUV) was defined as metabolic response, a surrogate marker of tumour response. The authors concluded that there was a survival benefit in responders compared to non responders, predicted by 18 FDG-PET. Moreover, some correlation was noted between metabolic and pathological responders. The authors found major histological remissions (<10% residual tumour) in 29 of 50 metabolic responders, but no histological response in metabolic non-responders. The median event-free survival was 29.7 months in metabolic responders and 14.1 months in non-responders.

The current practice for imaging in oesophago-gastric malignancies includes a CT scan of the chest, abdomen and pelvis at the time of diagnosis followed by 18 FDG-PET. Endoscopic ultrasound is used specifically to confirm local staging of tumour.

1.6.4 Non-Functional imaging:

Computerised tomography, magnetic resonance imaging, endoscopic ultrasonography and upper gastrointestinal endoscopy have all been used for non-functional imaging to predict response to neoadjuvant chemotherapy. A recent study by Schneider et al. concluded that response evaluation by endoscopy, rebiopsy, and endoscopic ultrasound did not accurately predict histopathologic regression after neoadjuvant chemoradiation for oesophageal cancer [110]. Similarly, clinical response evaluation using EUS or CT was shown to be highly inaccurate in predicting response to neoadjuvant chemotherapy.

1.6.5 Clinicopathological factors:

A variety of clinicopathological factors have been used to predict response of oesophageal cancer to chemoradiotherapy. Kogo et al. concluded that nutritional status, T stage, M stage, and alkaline phosphatase were significant factors that contributed to the response of oesophageal carcinoma to chemoradiotherapy [111]. On the other hand, a study from Dublin concluded that smaller tumour length was predictive of a greater response to chemotherapy and radiation therapy [112]. No single item or combination of items has yet been shown to have sufficient predictive accuracy to be of value in clinical practice.

1.7 Metabolomics

Metabolomics is defined as “the measurement of metabolite concentrations and fluxes and secretion in cells and tissues in which there is a direct connection between the genetic activity, protein activity and the metabolic activity itself” [113]. It is the study of global metabolite profiles in cells, tissues, and organisms.

It is believed that changes in the metabolome are the ultimate answer of an organism to genetic alterations, disease, or environmental influences. Since the small molecule composition is studied in metabolomics, it can safely be regarded as the end point of the “omics” cascade [114]. Unlike genes and proteins, which are “upstream” entities whose expression predicts cell functioning; metabolites reflect actual cellular conditions at the time of sampling. The metabolome is therefore most predictive of phenotype [115, 116].

The focus of metabolomics is on complete metabolite profiles in a sample, rather than one or a few metabolites and associated pathways. Consequently, the comprehensive and quantitative study of metabolites (metabolomics) is a desirable tool for either diagnosing disease or studying treatment response. In the context of oesophageal cancer patients and in particular adenocarcinoma, where a precursor lesion exists, this diagnostic potential could extend to the identification of the metaplastic and dysplastic states as well as correlations with specific stages of disease. It is expected that metabolomics will give even more reliable results when combined with specific proteomic signatures involving proteins with known functions.

There are two complementary approaches used for metabolomic investigations – metabolic profiling and metabolic fingerprinting. In metabolic profiling, quantitative analytical methods are developed for metabolites in a pathway or for a class of compounds. This approach produces independent information that can be interpreted in terms of known biochemical pathways and physiological interactions. In metabolic fingerprinting the intention is not to identify each observed compound but to compare patterns or fingerprints of metabolites that change in response to disease or toxin exposure [117].

Metabolic profiles are typically generated with high-throughput nuclear magnetic resonance (NMR) spectroscopy, direct infusion electrospray mass spectrometry (ESI-MS) and gas chromatography mass spectrometry (GC-MS).

1.7.1 Nuclear Magnetic Resonance Spectroscopy

NMR spectroscopy was discovered independently by Nobel laureates Edward Purcell and Felix Bloch. Two independent groups, working in s laboratories on opposite coasts of the USA, discovered NMR almost simultaneously (Bloch, Hansen, and Packard at Stanford University [118]; Purcell, Torrey, and Pound at Harvard [119]).

Nuclear magnetic resonance is an effect whereby nuclei in a magnetic field absorb and re-emit electromagnetic energy. Each nucleus has one or more protons and neutrons (except the hydrogen nucleus ^1H , which only contains a single proton), both of which have the intrinsic quantum property of spin. Inside an oriented magnetic field, the spin of the nuclei can either be oriented parallel or anti-parallel with the external magnetic field. The energy absorbed or emitted by the nuclei is at a specific resonance frequency, specific for each nucleus. In each molecule, due to differences in the electronic surroundings, each proton resonates at a slightly different frequency, called the chemical shift. This enables the identification of various compounds in complex biological mixtures.

The use of NMR spectroscopy to detect metabolites in unmodified biological samples was first reported by Seeley et al. in 1974 [120]. Ten years later, Nicholson showed that proton NMR spectroscopy could be used to diagnose diabetes mellitus [121]. He subsequently

pioneered the application of multivariate pattern recognition methods to NMR spectroscopic data that form the foundation of metabolomics analysis in NMR [122].

During the last 10 years one dimensional (1D) ^1H -NMR spectroscopy has become a standard analytical tool in biomedical metabolomics. However due to the chemical complexity of biological samples, the amount of overlap in 1D- ^1H -NMR spectra is quite substantial. In order to unambiguously assign substances in crowded regions of the NMR spectra two dimensional (2D) -NMR methods, e.g. 2D J-resolved (J resolved spectroscopy can be used to acquire “proton decoupled” 1D NMR spectra to reduce spectral congestion) [123] or 2D ^1H , ^{13}C -HSQC (**h**eteronuclear **s**ingle **q**uantum **c**oherence) spectroscopy, are becoming increasingly used for biological samples as better software and spectrometer hardware have been developed.

The work for this thesis was carried out at the Henry Wellcome Building for biomolecular NMR spectroscopy (HWB-NMR) at the University of Birmingham. The HWB-NMR is a UK national NMR facility. It provides academic and industrial users with open access to seven NMR spectrometers, most equipped with cryogenic probes, a high throughput autosampler and mass spectrometer. The majority of the data for this thesis were acquired on a 600 MHz UltraShield plus Bruker magnet with a 4-channel Bruker Avance III console (Figure 5) using a low volume cryogenically cooled probe (30 μl sample volume).



Figure 5 600 MHz UltraShield plus Bruker magnet

1.7.2 Basics of NMR

Any rotating object possesses angular momentum. This can be described as the rotational analogue of the linear momentum. A spin is a type of angular momentum. It is a fundamental property of electron and nucleus. The magnetic moment of a nucleus arises from this integral property of spin.

When a sample is placed inside a magnetic field, the individual spins precess (precession is the rotation of the spins around the main axis (vertical) of the external magnetic field) around the magnetic field. Once in a magnetic field, there are only 2 directions in which the individual spins can align – parallel or anti parallel to the magnetic field. It is important to note that a nucleus that has its spin aligned with the external field will have a lower energy than when it has its spin aligned in the opposite direction to the field. However, the difference in energy state of these two systems is very small. Thus it is conceivable that only a small amount of energy could flip a spin from the parallel to an anti parallel orientation.

The distribution of spins between the parallel and anti-parallel level is given by the Boltzmann distribution [124], hence at 0 K, all spins would orient in the parallel direction in presence of an oriented external magnetic field. However, at higher temperatures; the energy that is generated from Brownian motion is enough to flip these spins into an anti parallel orientation. It has to be understood that at equilibrium magnetisation, the energy gap in between the two energy levels is very small (eg. at room temperature, only 1 in 10,000 spins will be parallel in excess to equal distribution). The net magnetisation of the sample is parallel to the external magnetic field. However, a spectrum cannot be recorded in this state of equilibrium.

When radio frequency is applied at 90° to the external magnetic field, the spins start precessing around the axis on which the RF field is applied. For a simple 1D NMR experiment the radio frequency would be turned off when the angle between the external magnetic field and the sample magnetisation reaches 90° . Once in the transverse plane, the spins will start precessing (i.e. the macroscopic magnetisation vector rotates around the z axis

which coincides with the direction of the external magnetic field) and will relax towards the equilibrium magnetisation over time.

These precessing spins produce a time dependent magnetic field that then induces a time dependent electric field. This electric field then induces a current in the receiver coil which is recorded as a free induction decay (FID). This is then Fourier transformed to produce the final spectrum.

1.7.3 Cancer metabolism

The subject of cancer metabolism has been a topic of much research and debate over the last few decades. Although numerous pathways have already been described, key mechanisms are yet to be elucidated to complete the understanding of tumour metabolism. Listed below are some of the important effects which have improved our understanding of cancer metabolism.

1.7.3.1 The Warburg effect

Described by Warburg et al. in 1924, 'the Warburg effect' continues to be a pivotal theory in the understanding of tumour metabolism [125]. This effect described the observation that cancer cells predominantly produced energy by non-oxidative breakdown of glucose to pyruvate and then to lactate, as compared to healthy cells which primarily produce energy from pyruvate through tricarboxylic acid cycle and oxidative phosphorylation (respiration). Warburg identified the ratio of glycolysis to respiration as being one of the main differences between healthy and cancerous cells. This observation came to be known as 'the Warburg effect'. These mechanisms adapt the cancer cells to hypoxic conditions and thus account for their increased tendency for survival inside solid tumours.

1.7.3.2 The role of cancer genes in metabolic regulation

Cells employ a variety of mechanisms to adapt metabolism to specific physiological states. “The metabolic requirements of each cell type are determined by their tissue function and environment” [126]. Thus metabolic regulation can be described as the process by which cells control the chemical processes necessary for life. For example, numerous factors play a role in determining the fate of glucose in cancer cells – ‘the Warburg effect’.

One of most studied cancer genes is the p53 oncogene. p53 interjects at many points in both glycolysis and oxidative phosphorylation. One of the ways that p53 functions is to slow down glycolysis and promote oxidative phosphorylation. It thus provides a mechanism of blocking tumorigenesis and ‘the Warburg effect’ [127].

1.7.3.3 The role of metabolic reprogramming in promoting tumorigenesis

Broadly speaking, metabolic reprogramming refers to the altered metabolism in cancer cells that enables it to meet the increased anabolic requirements of a growing and dividing cell [128]. Thus altered metabolism is now considered to be a core hallmark of cancer.

The role of Hypoxia inducible transcription factor-1 is central to the understanding of metabolic regulation and metabolic reprogramming. During conditions of hypoxia, HIF-1 α helps to restore oxygen homeostasis by inducing glycolysis, erythropoiesis and angiogenesis[129]. HIF1 α activation in different cell types can either promote or repress tumorigenesis[130].

1.7.4 The role of metabolomics in the study of tumour metabolism

One of the main goals within cancer metabolomics is to develop fast and reliable methods for characterising disease non-invasively [131]. Metabolomics can be used for diagnosing cancer states directly in body fluids, through facilitating fast screening or by applying it to histopathological samples in order to classify different tumours using techniques such as magic angle spinning (MAS)-NMR [132] (Magic angle spinning NMR spectroscopy is a technique that can be used to acquire NMR spectra of intact tissue samples). Furthermore, it can be applied to solid and liquid samples *in vivo* or *in vitro*.

There is good evidence to support the use of metabolomics in cancer. Metabolomic strategies have been used to detect bladder cancer based on urinalysis [133]. Metabolomics has also been used to direct treatment plans where profiles reflect prostate cancer pathologic stage and aggressiveness, conventionally determined by histopathology only after prostatectomy [134]. More recently, the metabolomic alterations of prostate cancer progression have been characterised and sarcosine identified as a potentially important metabolic intermediary of cancer cell invasion and aggressive behavior [135].

Metabolomics has also been used to study drug resistance and metabolic therapeutic targets. Merz et al. have reviewed the possible strategies for the use of nuclear magnetic resonance-based metabolomics in detecting drug resistance in cancer [136]. NMR has been employed to study the response to chloroethylnitrosourea in melanoma and pulmonary carcinoma [137]. The authors of that study concluded that metabolomics of tumour response to an anticancer agent might identify metabolic pathways of drug efficacy and adaptation to treatment.

1.7.4.1 Common NMR detectable changes associated with malignancy

There is a plethora of studies describing the various metabolic alterations noted in blood, tissue and urine using NMR metabolomics. Listed below are some of the commonly described metabolites.

Alanine: Levels of this metabolite are increased in tissue hypoxia. It has been documented in hepatomas, astrocytomas, gliomas, meningiomas and dysembryoplastic neuroepithelial tumours.

Choline containing metabolites: These include choline, phosphocholine, phosphatidylcholine and glycerophosphocholine. They are key constituents of cell membranes. Their levels change during apoptosis and necrosis. They have been widely documented in brain tumours, sarcomas, prostate cancer and hepatoma hepatomas [138-141].

Glycine: Glycine is an amino acid and an essential precursor for *de novo* purine synthesis. The levels of glycine are decreased following the disruption of the HIF-1 α signalling pathway [142].

Lactate: Lactate is an end product of glycolysis. It increases during hypoxia and ischaemia. It has been associated with a large number of tumours[143].

Nucleotides: These are used to manufacture DNA and RNA. They are also key metabolic intermediates in fatty-acid and glycogen metabolism.

Sarcosine: Although only recently described in prostate cancer, sarcosine is a potentially important metabolic intermediary and an important predictor of cancer cell invasion and aggressive behavior in this disease[135].

Taurine: Taurine is important in osmoregulation and volume regulation. It is increased in squamous-cell carcinoma[144], prostate cancer and liver metastasis[145].

1.7.4.2 NMR in metabolomics There are several advantages of using ^1H NMR spectroscopy to acquire metabolite levels in metabolomics. It is a relatively rapid process with uncomplicated sample preparation methods. It is capable of observing all high abundance metabolites that contain non-exchangeable protons. It does not require any chromatographic separation or ionization of the metabolites prior to data acquisition in the spectrometer. The data obtained from ^1H NMR spectroscopy can be used for quantitative analysis. Moreover, it is robust and reproducible and with high throughput, is well suited to large studies on human samples. Finally, although the instrumentation is quite expensive, the costs for consumables and materials are low making this an attractive proposition for large biofluid studies.

The main disadvantage of using ^1H NMR spectroscopy for metabolomics is poor sensitivity. As a result, the observation is limited to approximately 100 metabolites which comprise less than 10% of an organism's metabolome. Another shortcoming of (1D) ^1H NMR spectroscopy is that there is a lot of overlap of resonances. As a result the ability to identify and distinguish these metabolites is limited in the crowded regions of the spectrum.

1.7.4.3 Metabolomics in oesophageal cancer

A few studies that have explored the role of metabolomics in the context of oesophageal cancer. Zhang et al. investigated the role of serum metabolic profiles derived from the combination of high performance liquid chromatography-mass spectrometry (LC-MS) and NMR [146]. This study presented results from 67 patients with AC. They also included a small number of patients with Barrett's oesophagus and high grade dysplasia. The authors identified 12 candidate metabolites that differentiated significantly between patients with cancer and healthy controls. Similarly tissue metabolomics employing GC-MS has also been attempted with the aim to identify candidate biomarkers in oesophageal carcinoma [147]. Hasim et al. performed plasma and urine metabolic profiling to identify metabolic signatures in 108 patients with SCC [148]. Another study from the same region in China has investigated ^1H NMR in human plasma to identify differences between metabolite concentrations between different ethnic groups [149]. A similar approach has also been employed in gastric carcinoma. Cai et al. used a combination of metabolomics and proteomics to investigate glucose metabolism in 65 patients with gastric cardia cancer [150].

Researchers at Imperial College London reported the results of MAS-NMR of intact tissue in thirty five patients with oesophageal adenocarcinoma and matched controls [151]. Profiles identified by these authors support the hypothesis of field change in the oesophagus even in the non-Barrett's segments of patients with AC.

Below is table of some of the recent metabolic studies which have aimed to evaluate various metabolites in oesophageal carcinogenesis.

Metabolic change	Year of publication	Title (reference)
lactic acid, valine, leucine/isoleucine, methionine, carnitine, tyrosine, tryptophan, 5-hydroxytryptophan, myristic acid, margaric acid, linolenic acid, linoleic acid, pyroglutamic acid, glutamine, b-hydroxybutyrate, citrate, lysine, creatinine, glucose, N-acetylated protein, proline, histidine, alanine, glutamate	2012	Esophageal Cancer Metabolite Biomarkers Detected by LC-MS and NMR Methods[146]
dimethylamine, a-glucose, b-glucose, citric acid, Leucine, alanine, isoleucine, valine, glycoprotein, lactate, acetone, acetate, choline, isobutyrate, unsaturated lipid, VLDL, LDL, 1-methylhistidine, Mannitol, glutamate, c-propalanine, phenylalanine, acetate, allantoin, pyruvate, tyrosine, b-glucose, guinolate, N-acetylcysteine, valine, dihydrothymine, hippurate, methylguanidine, 1-methylnicotin-amide, Citric acid	2012	Revealing the metabonomic variation of EC using 1H-NMR spectroscopy and its association with the clinicopathological characteristics[148]
phosphocholine to glutamate ratio in histologically-normal tissue	2010	Metabolic profiling detects field effects in non-dysplastic tissue from esophageal cancer patients[151]
Glutamine, β -hydroxybutyrate, Citrate, Lysine, Creatinine, α -glucose	2010	Metabolomics study of esophageal adenocarcinoma[152]
l-Valine, Naphthalene, l-Butanamine, l-Altrose, d-Galactofuranoside, Pyrimidine, Aminoquinoline, l-Tyrosine, Isoleucine, Purine, Serine, Phosphoric acid, Myo-inositol, Arabinose, Arabinofuranoside, l-Asparagine, Tetradecanoic acid, l-Alanine, Hexadecanoic acid, Bisethane	2009	Metabolomic study for diagnostic model of oesophageal cancer using gas chromatography/mass spectrometry[147]

Table 2 Recent metabolic studies in oesophageal carcinoma

Although NMR metabolomics continues to grow rapidly, its use to identify metabolites characterizing the pre-neoplastic state, different stages of disease or in the prediction of response to neoadjuvant chemotherapy in oesophageal adenocarcinomas has not been fully elucidated.

AIMS

The aims of this study were to prospectively evaluate the role of plasma and tissue profiles as:

- biomarkers for the identification of oesophago-gastric malignancy
- indicators of unstable Barrett's epithelium
- predictors of response to neoadjuvant chemotherapy

These goals would be achieved by using a combination of approaches.

1. NMR metabolomics of plasma and tissue
2. MS metabolomics of plasma and tissue
3. MALDI proteomics of plasma and tissue (manuscript in appendix)
4. Tissue gene expression profiling

This thesis concentrates on NMR metabolomics in plasma and tissue. Tissue MS metabolomics and gene expression profiling were used as confirmatory modalities as potentially useful molecules were disclosed. These other techniques are highlighted within the relevant sections of the results chapter.

METHODS

2.1 Ethical considerations

2.1.1 Ethical approval

Ethical approval was obtained from South Birmingham Research Ethics Committee for this study on the 16th May, 2008 (REC reference number - 08/H1207/3). To further perform proteomics, immunohistochemistry, genomics and transcriptomics on the collected specimens, a substantial amendment to the ethical approval was successfully obtained on 18th November, 2009.

2.1.2 University Hospital Birmingham sponsorship

A research project authentication for this project was obtained from University Hospital Birmingham on the 28th May, 2008 (Project reference – RRK 3425).

2.2 Patient Recruitment

2.2.1 Study duration

- Patients presenting to University Hospitals Birmingham between May 2009 and March 2010 as specified below.

2.2.2 Inclusion criteria

- All patients presenting with gastro-oesophageal malignancy or high grade dysplasia in Barrett's oesophagus, discussed by the oesophago-gastric multi-disciplinary team (MDT) of the pan-Birmingham Cancer Network.
- Selected patients undergoing upper GI endoscopy for benign disease (controls).
- Selected patients with non-dysplastic Barrett's oesophagus.
- Healthy volunteers.

2.2.3 Exclusion Criteria

- Patients unable to give valid consent.
- Patients refusing to take part in the study.
- Medically unwell or terminally ill patients where the collection of blood and tissue was thought inappropriate.

Sample collection

Sample collection included blood and tissue samples as specified below. Five healthy volunteers provided blood only.

2.3 Sample collection for blood

2.3.1. Time Intervals

2.3.1.1. Patients

Longitudinal blood sampling was carried out for each patient with cancer. Samples were collected at five time points.

- At diagnosis, immediately before the patient underwent staging laparoscopy. This served as the pre-chemotherapy sample.
- At the completion of chemotherapy before the patient was admitted for resectional surgery.
- After the induction of anaesthesia, but before surgery had commenced.
- Within six weeks of the surgery either at the time of, or shortly after discharge from the hospital.
- More than six weeks following surgery.

For patients who did not receive chemotherapy, the second blood sample was not collected unless the time gap between the first sample and resectional surgery was more than six weeks.

Patients undergoing palliative treatment had one sample collected at the time of contact.

2.3.1.2. Controls and patients with non-dysplastic Barrett's

These subjects were recruited at the time of endoscopy. One venous sample was collected and processed in a similar fashion.

2.3.1.3 Healthy volunteer controls

Three blood samples were collected from each volunteer. Samples were collected at random times of the day on three different days.

2.3.2. Pre-processing

6 ml of blood was collected by venepuncture into lithium heparin tubes. Lithium heparin tubes were selected for the $^1\text{H-NMR}$ analysis in order to avoid background signals from ethylenediaminetetraacetic acid (EDTA) which is used as an anticoagulant in most laboratories. These tubes were immediately placed on ice and processed within four hours. Times to centrifugation and final storage of samples were noted. Samples were centrifuged at 4°C at 200 relative centrifugal force (RCF) in a pre-cooled centrifuge. Plasma was then collected and divided into five aliquots; $700\ \mu\text{L} \times 2$, $300\ \mu\text{L} \times 2$ and a final aliquot made up of whatever was left, usually between $300\ \mu\text{L}$ to $600\ \mu\text{L}$. Samples were stored at -80°C until analysis. It has been previously published that differences between individuals are far greater than variation from any other experimental factor. Moreover, these changes can be reduced by placing the specimens on ice[153]. Nonetheless, all attempts were made to process and freeze all plasma samples within four hours of collection so as to minimise any changes in the metabolic profile.

2.3.3. Processing for NMR analysis

The aliquots of plasma were removed from -80°C storage and left to thaw at room temperature. From preliminary observations it was noticed that the plasma still had some ice crystals at 30 minutes but was fully thawed at 90 minutes. Therefore, a thaw time of one hour was used in all experiments.

The next step was ultrafiltration of the specimen to remove the proteins from plasma. This was achieved using filters (Nanosep 3K OMEGA; Pall Corporation, Ann Arbor, MI). These centrifugal filters were washed several times with 0.5 ml water at 4000 RCF at a temperature

of 36°C to remove glycerol from the filter membrane until no NMR signal was observed in the filtrate. The filters were subsequently kept wet at 4°C to avoid damage to the filter membrane.

A series of preliminary experiments were carried out to optimise conditions that could be standardised. These experiments and their results are described very briefly here followed by a complete description of the final methodology used.

2.3.3.1 Experiments to ascertain wash cycles

Typically eight washing cycles were required to remove glycerol from the filters. To optimise this, multiple Nanosep filters were washed using the technique described and filtrates were obtained at the 2nd, 4th, 6th, 7th and 8th wash were stored at -80 °C. These were later thawed and NMR spectra obtained to look for signals. The signals thus obtained confirmed that six wash cycles removed most traces of glycerol. Increased cycles showed additional impurities considered to be likely breakdown products from the membrane.

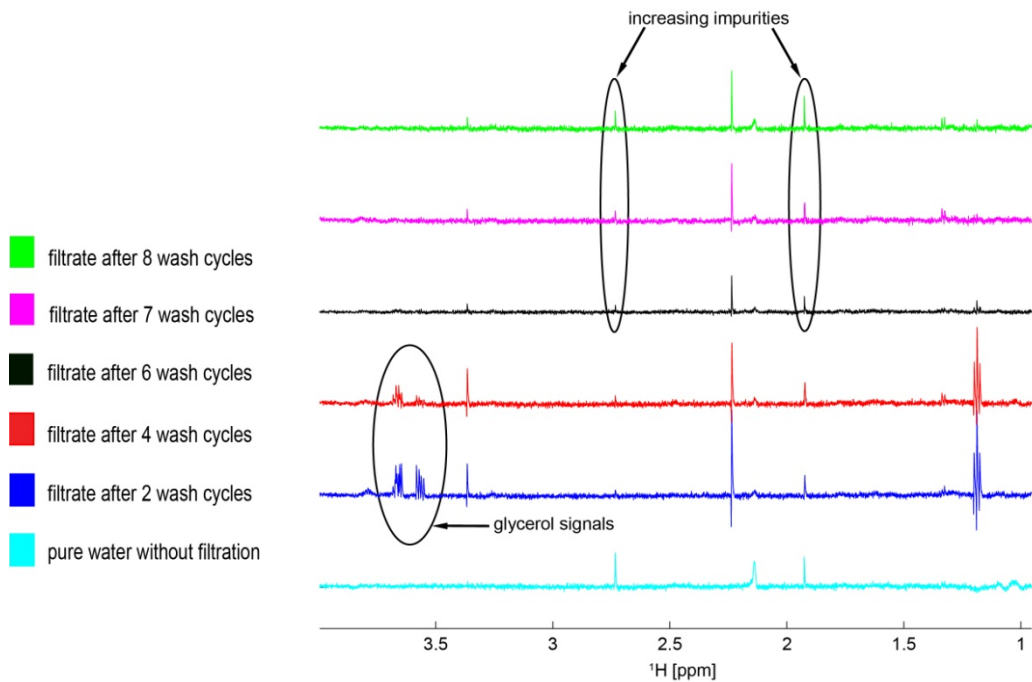


Figure 6 NMR spectra after various wash cycles

2.3.3.2 Experiments to ascertain filtration times and volumes for plasma

A number of experiments were conducted so as to optimise the:

- Sample volume for filtration
- Duration of filtration
- RCF of the centrifuge

All these experiments were conducted in a pre-cooled centrifuge maintained at 4°C .

Experiment 1

Two $700\ \mu\text{L}$ plasma aliquots were thawed and subjected to ultrafiltration, 10,000 RCF at 4°C .

After two hours, only $125\ \mu\text{L}$ of ultrafiltrate was obtained per specimen. At five hours, just

under 200 μL of ultrafiltrate was obtained. After 18 hours, the final volume of the ultrafiltrate was 275-315 μL .

Experiment 2

A 700 μL plasma aliquot was centrifuged at 10,000 RCF at 4°C for 10 minutes, designed to precipitate the proteins to the bottom of the Eppendorf vial. 600 μL of supernatant was then collected and filtered. At one hour, the volume of ultrafiltrate was 120 μL . At two hours 150 μL , at four hours between 190-200 μL and finally, at 6 hours 225-230 μL of ultrafiltrate was produced.

Experiment 3

Since the performance of filters dropped exponentially with time (as seen in the previous experiments), the 700 μL aliquot was divided into two equal parts of 350 μL each to expedite the process. At one hour, the volume of the ultrafiltrate was 110 μL , at two hours 150 μL , at four hours between 170-200 μL and finally at six hours 205-230 μL of ultrafiltrate was produced.

Experiment 4

The 700 μL aliquot of plasma was divided into three parts of 233 μL each and then filtered. At two hours, the volume of the ultrafiltrate was between 110-125 μL , at four hours, it was 150 μL and after six hours the volume was between 140-170 μL .

Experiment 5

To achieve an optimum volume of ultrafiltrate (350 μL from 700 μL plasma) in a reasonable time, the 700 μL aliquot of plasma was divided into three parts and filtered at an increased

speed of 12000 RCF for 3 hours. The resultant ultrafiltrate volume of each part was between 100-160 μL .

The final protocol for filtration of plasma consisted of filtration of 300 μL of plasma at 12,000 RCF for 3 hours. This produced a reliable volume of more than 100 μL ultrafiltrate for all samples. During these optimization experiments, it was noticed that the rate of filtration were similar for a majority of the samples. However, no attempts were made to record filtration times of individual samples or perform any statistics on the rates of filtration. No spectra were acquired for unfiltered plasma samples. Due to a background of broad NMR peaks from macromolecules, spectra from unfiltered plasma are usually acquired using a spectral technique called CPMG spectroscopy which specifically filters out those broad signals. However, this would lead to T2 editing of signal intensities. Filtered plasma samples don't contain proteins and therefore NMR spectra can be acquired using NOESY presat. However, some metabolites might be non-specifically bound to proteins and as a result get retained as part of the filtration process. Proteins together with water form a firm gel so that all the soluble particles might not get filtered and are thus lost. Compared to all other extraction methods, however, (acetonitrile, methanol chloroform), it is reproducible, protein removal is much better and the highest metabolite concentrations are achieved [154].

2.3.3.3 Experiments to ascertain buffer and TMSP concentration

Sodium phosphate was used as the buffer to maintain a pH of 7 to minimize inter-sample chemical shift variations in the metabolite spectra. Experiments were performed with buffer concentrations of 20 mM, 50 mM, 100 mM and no buffer. The most reproducible results were obtained using 100 mM sodium phosphate buffer. Reproducibility was assessed by

visual inspection of the NMR spectra. No statistical tests were performed to analyse the degree of overlap between the individual peaks. TMSP (trimethylsilyl) propionate-2,2,3,3-d₄ ; Cambridge Isotope Laboratories) was used to provide a reference for the spectra. Using a similar design as was used to optimize the buffer concentration, the optimal concentration for the TMSP was determined to be 500 μ M. These concentrations were therefore used in all experiments.

2.3.3.4 Experiments to ascertain tube diameters

Plasma ultrafiltrates were mixed with 100 mM sodium phosphate buffer (pH 7), 500 μ M TMSP and 5% D₂O (D₂O (99.9% pure; GOSS Scientific Instruments Ltd, Essex, UK) to obtain the final solution.

D₂O was added as frequency reference to counterbalance short term magnetic field disturbances and to compensate for long term magnetic field drift both of which would contribute to broader resonance lines and reduce the resolution of the NMR spectra. 0.1% sodium azide was added to prevent bacterial growth in the samples. A plasma sample from a healthy volunteer was filtered and then mixed with this solution. The resulting sample was then divided into multiple aliquots. These samples were analysed in 5 mm and 1.7 mm cryogenically cooled probes. The 5mm probe was used for both the 3 mm and 5 mm NMR tubes (Figure 7). Since the peak resolution and sensitivity was highest for the 1.7 mm tube, a repeat NMR spectrum was obtained the following day for another aliquot to access the reproducibility of this experimental setup. This additional acquisition would firstly ascertain the stability of the sample if left at room temperature and secondly access the additional variability that would be introduced by the sample preparation.

The best peak resolution and sensitivity were obtained using the 1.7mm tube in the 1.7mm cryoprobe with the Bruker 600 spectrometer as shown below. These spectra were adjusted to have a similar signal to noise ratio so that the differences seen were not due to an upscaling effect.

Most likely the improved sensitivity comes from the special coil design of the 1.7 mm probe which leads to a very high Q factor of the probe. Also, the dynamic range of this probe is possibly larger due to the very small volume that needs to be shimmed. The superiority of the shim also means that T2' relaxation (apparent transverse relaxation due to B0 field inhomogeneities) is minimised leading to sharper lines hence increasing resolution.

NMR tubes used were ordered from the manufacturer's webpage in batches of 96 tubes (part no. 112272). The probe specification at installation using the standard sucrose sample was signal: noise ratio of 234: 1. The resolution was 34% (splitting of the anomeric proton) and water hump was 24.0/29.4 Hz.

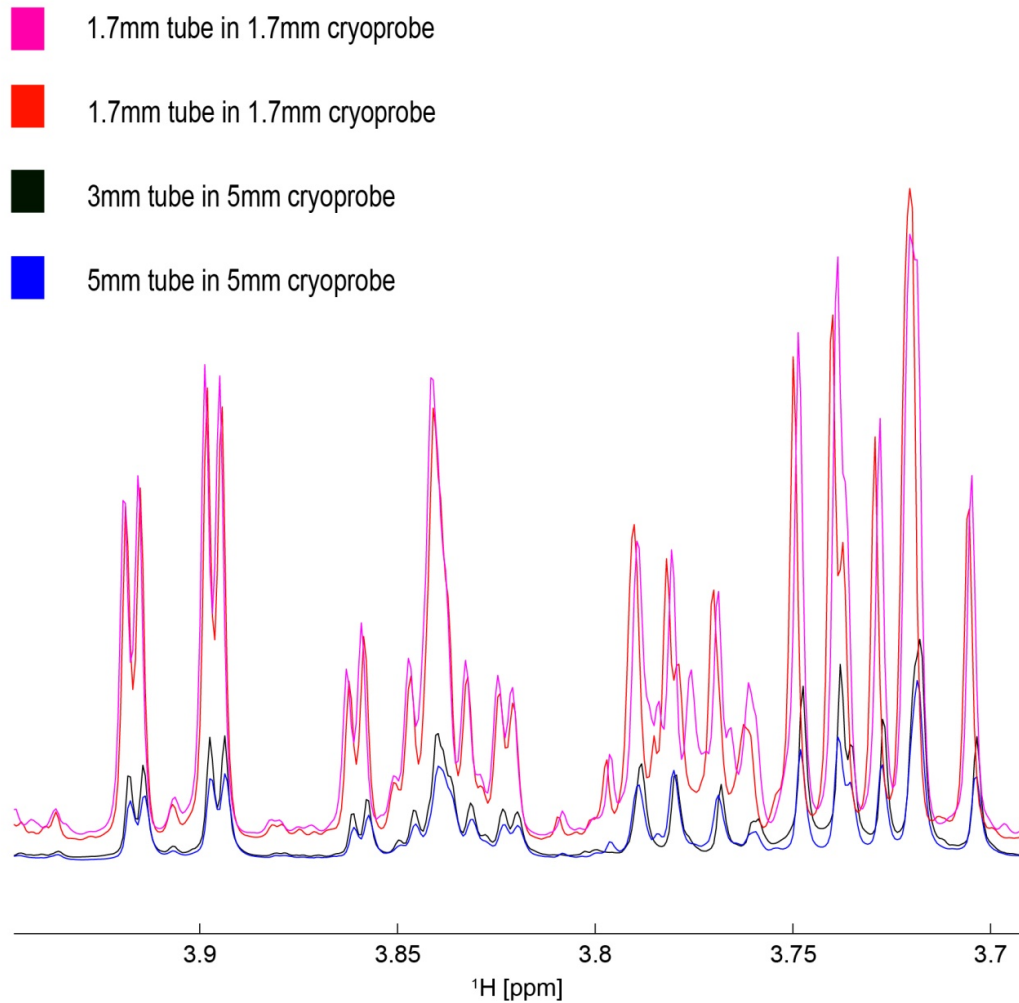


Figure 7 NMR spectra from varying tube diameters and probes

These specifications were used for all the plasma and tissue NMR experiments.

2.4 Sample collection for tissue

2.4.1. Time intervals

2.4.1.1. Patients with oesophago-gastric malignancies

Two sets of tissue samples were obtained from each patient.

1. The first sample was collected at the time of staging endoscopy carried out under general anaesthetic immediately prior to staging laparoscopy. Three to four biopsies

were collected both from tumour and normal mucosa. For oesophageal SCC and Siewert Types 1 and 2 AC, control normal mucosa was the squamous mucosa at least 5cm proximal to the beginning of the tumour. For Siewert Type 3 tumours, control normal mucosa was mucosa from the body of the stomach at least 5cm distal to the distal margin of the tumour. Finally, for distal and body gastric cancers, control normal mucosa was the columnar mucosa from the body or upper stomach at least 5cm proximal to the beginning of the tumour.

2. The second sample was collected immediately after resectional surgery. As soon as the specimen was obtained, it was transported fresh to the histopathology department. A consultant histopathologist with a special interest in oesophago-gastric cancer was pre informed about its arrival to avoid delays in processing the specimen. Sections were obtained in a standard way. Four sections of cancer tissue (each weighing approximately 60 mg) were taken from the specimen. If any Barrett's mucosa was visualised, four additional sections were taken from this tissue. Four sections of control normal mucosa (each weighing approximately 60 mg) were collected from the sites as described for the staging endoscopies.

2.4.1.2. Patients with non-dysplastic Barrett's

All these patients had three to four biopsies of Barrett's mucosa collected at the time of endoscopy (in addition to quadrantic biopsies within a local Barrett's surveillance programme). These adjacent sections of mucosa were sent for histopathology. At the same time three to four biopsies of normal oesophageal squamous mucosa at least 5 cm proximal to the Barrett's mucosa were also collected.

2.4.1.3. Patients with known high grade dysplastic Barrett's

These patients had three to four biopsies of high grade dysplasia collected at the time of endoscopy along with histologically confirmed adjacent sections of mucosa. At the same time three to four biopsies of normal oesophageal squamous mucosa at least 5cm proximal to the Barrett's segment were also collected.

2.4.1.4. Other patients

This group comprised of patients with a diagnosis of Gastro Intestinal Stromal Tumours (GIST). All these patients had three to four tumour biopsies collected at the time of endoscopy along with control mucosa. The control mucosa was the normal oesophageal squamous mucosa in the case on oesophageal or junctional GIST and the gastric mucosa in the case of gastric GIST.

2.4.1.5. Controls

All control patients had three to four biopsies of endoscopically normal oesophageal squamous mucosa collected at the time of endoscopy.

2.4.2. Sample aliquots

Endoscopic biopsies were collected in Eppendorf vials. All biopsies from the cancer tissue were placed in a single pot. Normal mucosa was collected in a separate container. If additional tissues from a visible Barrett's segment were collected, these were placed in separate Eppendorf vials and labelled by distance of the endoscope from the incisor teeth.

Each tissue section collected from the resection specimen was placed in a separate Eppendorf vial and labelled appropriately.

2.4.3. Sample transport and storage

All tissue Eppendorf vials were placed on ice and then transported to a -80°C freezer. This strategy of slow freezing was based on general principles regarding tissue viability and less formation of intra-cellular ice [155-157] when cooling occurs at around 1°C/min. While this can be further minimized by the addition of a cryoprotectant (such as glycerol or DMSO [158]), NMR interference from cryoprotectants meant that they were not used.

2.4.4. Measures to create comparable samples.

All resectional specimens were obtained by a consultant histopathologist. Transport, examination of the specimens, selection of the biopsy sites and specimen procurement took up to 40 minutes. Following this, the specimens were transported in ice and stored on a -80°C freezer. This additional step took a maximum of 10 minutes. In addition, there was a warm ischaemia time that the tissues were likely to have experienced at the time of resection. This was estimated to be between 10 and 30 minutes depending on the type of resection.

To minimise bias and maximise comparability between operative and endoscopic biopsies, the latter were kept on ice for one hour before they were transferred to a -80°C freezer.

2.4.5. Experiments to optimize a protocol for tissue freezing

Pilot experiments using surplus tissue obtained at the time of resectional surgery were carried out to see what differences existed in NMR spectra between slow and rapidly frozen tissues. Sections of tissue were halved. One set of samples were snap-frozen (Snap freezing is the process by which samples are lowered to temperatures below -70°C very rapidly. We used liquid nitrogen to achieve this in our optimisation experiments) and the other placed on ice for 10 minutes before both were transferred to a -80°C freezer. They were subsequently extracted and analysed. There were no appreciable differences in the spectra obtained from these paired tissues. Subsequently, on performing statistical analysis (PCA – principal component analysis), these tissues separated according to the clinic-pathologic factors (type of tissue) rather than the method of extraction. Subsequently, all resectional tissues were therefore immediately placed on ice for transport before being stored at -80°C .

2.4.6. Extraction of tissue

Methanol chloroform extraction originally described by Bligh and Dwyer was chosen as the extraction method to prepare samples for NMR data acquisition [159]. This was preferred over using tissue samples directly (magic angle spinning - MAS) on the basis that:

1. Methanol chloroform extraction results in 3 fractions from each tissue –a top polar phase that contains the metabolites, a middle protein phase and a bottom non polar phase where most of the lipids accumulate. As a result, each of these parts can be used separately to perform various analyses on the same tissue biopsy. On the contrary, although MAS does not result in destruction of the tissue, repeated freeze-thaw cycles coupled with high spinning speeds (4kHz) damage the structural integrity of the tissues, making them unsuitable for further analysis.

2. Methanol/chloroform/water extraction performs better than single organic solvent extractions as far as yield and reproducibility of the hydrophilic metabolites as well as recovery of the hydrophobic metabolites is concerned [160].

The technique of methanol chloroform tissue extraction for use in nuclear magnetic resonance (NMR) spectroscopy- and mass spectrometry (MS)-based metabolomics has been previously optimised by Wu et al. [160]. Tissues were first prepared for homogenisation with a Precellys®-24 ceramic bead-based homogeniser (Stretton Scientific Ltd., UK). All solvents (methanol, chloroform and water) were kept on ice at 4°C. 8 µl/mg of methanol and 2.5 µl/mg of water was added to each Precellys tube (larger volumes of solvents were used for tissue masses more than 15 mg. This was subsequently compensated for at the time of reconstitution of the sample for analysis). Tubes were placed in the Precellys 24 homogeniser for two 10s bursts at 6400 rpm. The homogenised mixture was pipetted into a clean 1.8ml glass vial using a Pasteur pipette. 8µl/mg of chloroform and 4 µl/mg of water were subsequently added to each vial. The vials were vortexed at full power for 30s each and left on ice for 10 mins. They were then centrifuged at 1800 g (3000 rpm) at 4°C for 10 mins.

This resulted in the formation of three separate layers. The polar fraction was divided into 3 aliquots (25 µL x 2 and 400 µL) and dried in a centrifugal evaporator (SpeedVac®) along with the protein fraction and stored at -80°C. The non-polar extracts were collected in glass vials, left in solution and frozen on the basis that that long term storage of dried lipids can result in denaturation [161].

2.4.7 Reconstitution of the polar extracts for NMR analysis

Dried polar extracts were reconstituted using a solution of 100mM sodium phosphate buffer (pH 7), 500 μ M TMSP, 5% D₂O and 0.1% sodium azide. The adjusted weight of each tissue in the polar aliquots was calculated (adjusted weight = original weight * polar aliquot volume/ total volume of polar extract). This weight was then diluted by a factor of five to produce a minimum volume of 40 μ L to suffice for preparation of the sample for NMR. For very small volumes, a higher dilution factor was used. The additional dilution was compensated for during the acquisition of the NMR spectra by increasing the number of acquired transients. Thus a minimum of 512 transients and a maximum for 8192 transients were acquired for the tissue to accommodate for discrepancies in weights.

2.5 NMR data acquisition

The majority of the data were acquired on a 600 MHz UltraShield plus Bruker magnet with a 4-channel Bruker Avance III console using a low volume cryogenically cooled probe (30 μ l sample volume). This spectrometer was also equipped with a sampleJet autosampler thus enabling high throughput for large studies. During storage in the sample changer, samples were maintained at 6°C prior to analysis. Before the samples were inserted into the magnet they were equilibrated for 2 minutes at a temperature of 15°C. The probe was then automatically tuned and matched for each sample, followed by automatic shimming (shimming is a procedure to make the magnetic field as homogenous as possible across the sample) and automated pulse calibration (pulse calibration is the determination of the length of the 90° pulse for a given RF field strength) for each sample [162]. Plasma samples were acquired using 256 transients. Prior to acquisition, 16 steady state scans were acquired for each spectrum. The spectral width was set to 7288 Hz for all spectra. The water resonance

was suppressed using the NOESY presat [163] pulse program which employs saturation during the 4 second interscan relaxation delay as well as during a 10 ms NOESY mixing time. A total of 32768 data points was acquired leading to an acquisition time of 2.25s.

Hadamard 2D-TOCSY experiments were performed on a 800 MHz Oxford Instruments magnet equipped with a 4-channel Varian INOVA console. This spectrometer is equipped with a HCN 5mm z-PFG cryogenic probe with enhanced ^{13}C and ^1H sensitivity. Hadamard spectroscopy is a fast method for the acquisition of multidimensional NMR spectra where the indirect dimensions are acquired in the frequency domain rather than the time domain in conventional multidimensional NMR spectroscopy by using polychromatic selective pulses. All desired frequencies are irradiated at the same time, but the phases of the different frequencies are encoded in a Hadamard matrix. As a consequence each frequency in the indirect dimension contributes to every NMR acquisition and is deconvoluted by multiplying the 1D-NMR spectra with a Hadamard matrix [164].

2.6 Data processing

Nuclear magnetic resonance data were processed using NMRLab [165] and MetaboLab [166] in the MATLAB (The Math Works, Inc., Natick, MA) programming environment.

FIDs were apodised using an exponential window function with 0.3 Hz line broadening and zero filled to 32768 data points prior to Fourier transformation. NMR spectra were automatically phase corrected using baseline properties close to the TMSP signal and outer baseline regions [166]. All spectra were automatically referenced to the TMSP resonance (0.0 ppm) of the first spectrum.

NMR spectra were then aligned to the TMSP signal and spline baseline correction was performed. Water and TMSP signals were then excluded. Total spectral area scaling was performed after exclusion of water and TMSP signals to remove differences due to sample concentration. The NMR spectra were then realigned using a cross correlation algorithm as implemented in NMRLab software. A generalised log transformation was applied to enhance small signals in the spectrum [80]. This glog transformation was performed using the following equation:

$$y = \log \left(\alpha (x - x_0) + \sqrt{(\alpha (x - x_0))^2 + \lambda} \right)$$

The parameters used were: $\lambda=10^{-7}$, $x_0=0.005$ and $\alpha=1$.

The spectra were bucketed to a bin width of 0.003ppm 41.465 x 10⁻³ppm (8 data points per bin). Data were subsequently exported as a PLS dataset.

2.7 Statistical analysis

Multivariable statistical analyses were performed in PLS-Toolbox (Version 5.2; Eigenvector Research, Manson, WA). This software takes its name from the Partial Least Squares (PLS) regression method; a supervised multivariate analysis that is used in many regression applications [71]. Further statistics were performed on the data set using the statistics toolbox in MATLAB. These included the Mann Whitney U test (non-parametric equivalent of unpaired t test), Chi square test and Spearman correlation to examine the relationships between variables.

Unsupervised principal component analysis (PCA) and supervised Partial least squares discriminant analysis (PLS-DA) were performed for each of the models. The loadings were

further improved by performing an orthogonal PLS-DA. Once the data had been imported into PLS toolbox, the x block variables (spectra) were pre-processed using mean centring. No pre-processing was performed for the y block variables (class vector). The Venetian blind algorithm was used for cross validation unless specified otherwise.

2.7.1 PCA

PCA (Principal Component Analysis) reduces the dimensionality of the data to just a few principal components that account for a large amount of the total variance between all of the NMR spectra. The results are presented in terms of scores and loadings plots. A scores plot summarises the similarities and differences between each of the NMR spectra. Each data point on the scores plot represents one sample. Thus the distance between any two data points indicates the degree of similarity or dissimilarity between those two samples.

To perform a principal component analysis, the data has to be mean centred. This means, that for each value of the x axis (ppm value of the bucketed data in case of NMR spectra) the mean value is determined from all samples and is then removed from all samples. This procedure is then repeated for each binned data point in the data set. This produces a data set whose mean is zero. The covariance matrix is then calculated. Since the covariance matrix is square, it can be diagonalised and the eigenvectors and eigenvalues for this matrix are then calculated. An eigenvector can be defined as a non-zero vector that, after being multiplied by the matrix, remains parallel to the original vector. The eigenvalue is the factor by which the eigenvector is scaled when multiplied by the matrix. During a principal component analysis, the eigenvectors are ordered with respect to their eigenvalues in descending order, so that the first principal component belongs to the eigenvector with the largest eigenvalue. Each

principal component is a weighted linear combination of all signal intensities at their respective chemical shifts. This information can be visualized in a loadings plot. Thus if two groups of samples are separated by the first principal component, then the loadings plot for this principal component is an expression of the signals that are producing this metabolic difference [167]. The final data is then prepared by keeping only the eigenvectors of interest. The eigenvectors describing the separation between different groups don't need to belong to the first principal component as the first principal component can contain variations coming from biological noise (e.g. blood plasma samples from a heterogenous patient group with differences in their fasting status).

2.7.2 PLS-DA

Partial Least Squares Discriminant Analysis (PLS-DA) is a supervised method used to improve the separation between groups of observations. For this analysis, the data analysis algorithm is provided with information on which sample belongs to which class. It then rotates the principal component in a way that a maximum separation between the classes is obtained. However, because of this additional information fed into the computer algorithm, the resulting model has to be verified by a cross validation procedure (e.g. venetian blinds (2.7.4.1) or leave one out (2.7.4.2))

At the end a discriminant analysis is performed which gives an estimate how much the different groups overlap and which can be used when using the established model to analyse unknown samples to ascertain the group of the unknown sample. In general the separation between the classes is better when using PLS-DA compared to PCA, however one needs to be cautious to not over-fitting the data and not introducing a bias by wrong class assignments.

Quite often the first two latent variables (LV, the equivalents to principal components of PCA) contribute to the maximum class separation. As a result the loading vectors can be unclear and it can be complicated to extract metabolites which separate the different classes from them.

2.7.3 OPLS-DA

Orthogonal Partial Least Squares Discriminant Analysis overcomes this problem by rotating the LV's of PLS-DA in a way that the sample separation becomes orthogonal and the first latent variable is sufficient to produce the separation seen on two latent variables in PLS-DA. In this way OPLS-DA is an extension combining the strengths of PLS-DA and Soft independent modeling of class analogy classification [168]. In terms of results prediction, OPLS-DA is identical to PLS-DA modeling. The primary benefit of OPLS-DA lies in the ease of interpretation, especially in the multi-class case. This is achieved by the separate modeling of predictive and class-related variation in the x-matrix through the identification of y-orthogonal variation. Although there no predictive performance advantage of OPLS-DA over PLS-DA, its interpretation is much more superior.

2.7.4 Cross Validation

Cross validation is a technique to assess the generalisability of the results generated as a result of the analysis. An ideal cross validation would consist of a training set where the results are obtained and multiple validation sets to validate those results. This can be performed statistically by employing various algorithms. The aim of all of these techniques is to use part of the dataset for training and other data points for validation. Cross-validation was performed by applying the “Venetian blind” algorithm when the total sample size for the

model was greater than 20. For smaller samples sizes, the “leave one out” algorithm was used.

2.7.4.1 Venetian Blind algorithm

For the venetian blind algorithm, each test set is determined by selecting every ‘n’th object in the data set, starting at objects numbered 1 through n. The number of splits/ datasets is equal to the square root of the total number of objects [169].

2.7.4.2 Leave one out algorithm

Leave one out algorithm is more conservative than the Venetian blind algorithm and as a result reserved for datasets with a sample size of less than 20. Here, each single object in the data set is used as a test set [169]. Thus the process is repeated n times till all of the observations have been used once as the validation set.

2.7.5 ROC curve

A ROC (Receiver Operating Characteristic) curve is a graphical plot of the sensitivity vs. 1-specificity. The best possible prediction method yields a point in the upper left corner of the ROC space, representing 100% sensitivity and 100% specificity. A completely random guess creates a point along a diagonal line (the so-called line of no-discrimination from the left bottom to the top right corner). Visual inspection of the scores plot and the area under the ROC curve was used to determine the strength of a model.

ROC curves were calculated using `plsroc` matlab function provided by the `pls` toolbox. These were generated using internal cross validation (2.7.4.1, 2.7.4.2).

Once a good model had been obtained (a ROC score of more than 0.7 if possible), peaks contributing significantly to the loadings were integrated. This was performed by centering each of the peaks in question individually and then integrating the points. Univariate analysis was then performed.

2.8 Assignment of peaks

The loadings obtained from the various models were exported as a Bruker format file to enable viewing in Chenomx for the purposes of peak assignment. Chenomx NMR Suite software (Professional edition, version 5, Chenomx, Edmonton, AB, Canada) is a software package capable of identifying and quantifying individual compounds based on their respective signature spectra. Once a provisional assignment had been made for the peaks with the largest contribution in the loadings, these peaks were assigned for the NMR spectra using Chenomx.

Once a list of the identifiable peaks for all the models had been prepared, the spectra were interrogated for those peaks. Differences in loadings that were not visually recognised as spectral differences were discarded. Metabolites that behaved in a consistent fashion across most models were selected for further analysis. The resultant metabolites from tissue and plasma were then cross referenced to obtain a list of metabolites that were synchronously elevated or reduced in tissue or plasma. Selection of metabolites of interest has been further explained in section 3.6.

An HSQC (Heteronuclear single-quantum correlation spectroscopy) 2D spectrum was obtained for a pooled tissue sample to enable assignment of metabolites in two dimensions using Amix (v. 3.7, Bruker Biospin). Similar to Chenomx, Amix is a software package capable of identifying and quantifying individual compounds based on their respective signature spectra. We used the Amix software to characterise the metabolites visualised in the HSQC spectra. Subsequently, more HSQC spectra were acquired to correctly characterise the metabolites of interest. The advantage of an HSQC spectrum is that it adds additional information by combining the ^1H and ^{13}C chemical shifts.

In a 2D-HSQC spectrum every proton bound ^{13}C nucleus gives rise to one signal in the spectrum. But instead of one chemical shift axis due to the multidimensional nature of the spectrum, there are now two chemical shift axes, one showing the chemical shift of the proton (typically between 0 and 10 ppm at the proton frequency of 600MHz) and the indirect axis showing the chemical shift of the directly bound ^{13}C nucleus (typically recorded to cover between 0 and 160ppm at the carbon frequency of 150MHz). Due to the independence of the proton and ^{13}C chemical shifts overlapping peaks in the 1D-NMR spectrum can often be resolved when spread over two dimensions.

2.9 Statistical total correlation spectroscopy (STOCSY)

STOCSY identifies highly correlated peak intensities in a series of spectra. This can lead to identification of peaks from the same molecule and hence aid molecule identification [170]. Although correlations are usually large within the same molecule, STOCSY aids correlation to other molecules. More importantly it can help to identify functionally correlated metabolites and thus aid in a pathway based approach. Identification of lower or even

negative correlations can lead to identification of substances in the same metabolic pathway whose concentrations are interdependent or under some common regulatory mechanism.

2.10 Assessment of response to chemotherapy

Assessment of response was made using two different techniques depending on whether the patients were receiving neoadjuvant chemotherapy followed by a potentially curative resection or only palliative chemotherapy.

For patients undergoing neoadjuvant chemotherapy, assessment of response was made after histopathological assessment of the resected specimen using Mandard criteria [171]. For palliative patients, this was assessed using radiological RECIST criteria [172].

2.10.1 Histopathological assessment

This was made by assessment of the Tumour Regression Grade (TRG) in the resected histopathological specimen as described by Mandard et al. [171].

Grade 1 (complete regression) – complete absence of histologically identifiable residual cancer and fibrosis extending through the different layers of the oesophageal wall, with or without granuloma.

Grade 2 – presence of rare residual cancer cells scattered through the fibrosis.

Grade 3 – increase in the number of residual cancer cells, but fibrosis still predominating.

Grade 4 – residual cancer outgrowing fibrosis.

Grade 5 – absence of regressive changes.

2.10.2 Radiological assessment

This was performed using a combination of contrast enhanced CT (CECT) and with additional CT-PET or MRI as deemed necessary on clinical grounds. RECIST (Response Evaluation Criteria In Solid Tumours) criteria described by the task force formulated by European Organization for Research and Treatment of Cancer (EORTC), the National Cancer Institute [172] of the United States, and the National Cancer Institute of Canada Clinical Trials Group were used.

Patients selected for palliative chemotherapy by the MDT underwent spiral/multi-slice CT, with oral contrast or water including chest, abdomen (pelvis optional) at baseline and within two weeks of completion of chemotherapy (Maximum slice width 5mm, IV contrast/venous phase). Baseline lesions were categorized as measurable (lesions that can be accurately measured in at least one dimension (longest diameter to be recorded) as ≥ 10 mm with spiral CT scan or non-measurable (all other lesions, including small lesions <10 mm with spiral CT scan]). Serial measurements of target lesions were made following the detailed RECIST recommendations.

Thus all patients whose response was classified according to the RECIST criteria in this study underwent a CT scan of the chest, abdomen and pelvis at the time of diagnosis and within two weeks of completion of chemotherapy

Evaluation of target lesions.

Complete response – the disappearance of all target lesions.

Partial response – at least a 30% decrease in the sum of the longest diameter of target lesions, taking as reference the baseline sum longest diameter.

Progressive disease – at least a 20% increase in the sum of the longest diameter of target lesions, taking as reference the smallest sum longest diameter recorded since the treatment started or the appearance of one or more new lesions.

Stable disease – neither sufficient shrinkage to qualify for partial response nor sufficient increase to qualify for progressive disease, taking as reference the smallest sum longest diameter since the treatment started.

Evaluation of non target lesions.

Complete response – the disappearance of all nontarget lesions

Incomplete response/stable disease – the persistence of one or more non target lesion(s)

Progressive disease – the appearance of one or more new lesions and/or unequivocal progression of existing nontarget lesions.

2.10.3 Calculation of overall response

In both Mandard and RECIST, the various response grades were collapsed into two categories to increase the numbers of samples in each group and identify major differences that characterised any degree of response

Mandard stage was therefore classified as responders and non responders, where responders consisted of patients with TRG 1,2,3 and non responders consisted of patients with TRG 4,5.

For RECIST staging, patients were classified as complete responders, partial responders and non responders. Complete and partial responders were then grouped together as responders.

2.11 Statistical modelling

Samples were divided into different comparator groups to address the various aims of the study. These are described below.

2.11.1 Plasma modelling

1. Controls vs. gastro-oesophageal adenocarcinoma

Plasma samples from control patients were compared with pre-treatment (samples from patients undergoing neo adjuvant treatment) samples, pre-surgery (patients only undergoing resection) samples from patients with resectable gastro-oesophageal adenocarcinoma and pre-treatment plasma samples from patients with advanced gastro-oesophageal adenocarcinoma undergoing palliative chemotherapy.

The aim of this model was to see if it was possible to discriminate between plasma of patients with cancer and those without and evaluate profiles in the plasma of cancer patients which could be potentially used as biomarkers.

2. Non-dysplastic Barrett's vs. oesophageal adenocarcinoma types 1,2

Plasma samples from patients with non dysplastic Barrett's oesophagus were compared with pre-treatment (for patients undergoing neo adjuvant treatment) samples, pre surgery (patients only undergoing resection) samples and pre-treatment plasma samples from patients with advanced oesophageal adenocarcinoma (types 1,2) undergoing palliative chemotherapy.

The aim of this model was specifically examine the differences between plasma profiles of patients with pre neoplastic disease i.e. non-dysplastic Barrett's vs. patients with frank malignancy. Success of this model could enable us to develop plasma markers of neoplastic progression.

3. Overall response

Pre chemotherapy plasma from responders (patients with TRG 1-3 or response on RECIST) was compared with non responders (patients with TRG 4-5 or no response on RECIST). Only patients with oesophageal adenocarcinoma types 1,2 were included in this analysis.

The aim of this model was to identify profiles in plasma that would enable prediction of a sub-group of patients who were more likely to respond to chemotherapy.

4. Stage on N (Table 1)

For this model, only plasma samples from patients not receiving chemotherapy were considered. Pre-surgery plasma samples and samples from patients undergoing palliative treatment without chemotherapy were thus included in the analysis. Patients with adenocarcinoma (oesophageal, gastric, distal gastric) were included. In the operated patients, N stage was determined from histopathology of the resected specimen. For patients undergoing palliative treatment, the highest N stage recorded for any investigation was considered. Patients were classified as node negative (N0) or node positive (N1).

The aim of this model was to enable identification of profiles in plasma that could diagnose locally advanced disease. It would also serve as a validation for any potential biomarkers that are identified for cancer since the candidate biomarker should increase with increasing burden of disease.

5. *Stage on T* (Table 1)

For this model, only plasma samples from patients not receiving chemotherapy were considered. Pre-surgery plasma samples and samples from patients undergoing palliative treatment without chemotherapy in patients with adenocarcinoma (oesophageal, gastric, distal gastric) were included.

T stage was determined from histopathology of the resected specimen or in patients undergoing palliative treatment, the highest T stage recorded for any investigation was considered. Patients were then classified as having T1 or T2 disease; or T3 or T4 disease to separate tumours confined within the wall of the organ from those with full-thickness involvement.

The aim of this model was to enable identification of profiles in plasma that could diagnose locally advanced disease. It would also serve as a validation for any potential biomarkers that are identified for cancer since the candidate biomarker should increase with increasing burden of disease.

6. 'Bacon and egg' model

Plasma samples at 3 time points from the 5 healthy volunteer controls were divided into 5 groups (one group per individual) to access the intra individual variation versus the inter-individual variation between subjects. This model was named 'bacon and egg' since the metabolomic profile of an individual changes due to various environmental influences like fasting, type of food, or medications. The aim of this was to provide proof of principle that NMR analysis could distinguish between any two healthy individuals and that metabolomic changes in blood during chemotherapy in a patient were not merely experimental variations.

2.11.2 Tissue modelling

1. Normal squamous mucosa vs. normal gastric columnar mucosa

Tissue biopsies of normal oesophageal squamous mucosa from control patients and from the normal squamous mucosa of patients with oesophageal SCC or Oesophageal AC (types 1,2) were compared with normal columnar tissue biopsies of gastric mucosa from patients with junctional AC (type 3) and patients with body or distal gastric adenocarcinoma. The aim of this model was to demonstrate the ability of NMR in differentiating between two normal tissue types before attempts were made in differentiating between normal and cancer mucosa.

2. Normal squamous mucosa vs. oesophageal adenocarcinoma type 1,2

Paired normal oesophageal squamous mucosa biopsies were compared with biopsies from adenocarcinoma in patients with Oesophageal AC (types 1,2) (both pre- and post-treatment).

The aim of this model was to identify profiles in cancer mucosa that were different from normal mucosa and thus evaluate their role as a potential biomarker. Differing metabolite profiles would also help gaining an insight into the differing metabolism in these tissues.

3. Normal squamous mucosa vs. Barrett's mucosa in the presence of a cancer vs. oesophageal adenocarcinoma types 1,2

Samples from those patients with oesophageal adenocarcinoma (types 1,2) who also had morphologically identified Barrett's were included in this analysis. Three comparative groups were therefore created. This included patients both pre and post treatment.

The aim of this model was to validate the differences that were seen in model 2 and evaluate if there were sequential differences in the candidate biomarkers in these three tissues.

4. Non dysplastic Barrett's vs. Barrett's mucosa in the presence of a cancer

Tissue samples of Barrett's mucosa from patients who were undergoing surveillance with no histologic evidence of dysplasia were compared with Barrett's mucosa from patients with evidence of oesophageal adenocarcinoma type 1,2 adjacent to the Barrett's mucosa.

The aim of this model was identify tissue profiles that would be altered in dysplasia and thus enable development of biomarkers that could potentially identify a group of patients with non-dysplastic Barrett's who were more likely to progress to dysplasia or carcinoma.

5. Overall response

Pre-chemotherapy cancer tissue biopsies from responders (patients with TRG 1-3 or response on RECIST) were compared with non responders (patients with TRG 4-5 or no response on RECIST). Only patients with oesophageal adenocarcinoma type 1,2 were included in this analysis.

The aim of this model was to identify profiles in cancer tissue that would enable prediction of a sub-group of patients who were more likely to respond to chemotherapy.

RESULTS

3.1 Demographics

258 participants were recruited. The breakdown was as follows.

Name of Group	Number of participants
Oesophago-gastric malignancy	137
Benign non dysplastic Barrett's oesophagus	9
High grade dysplasia of the oesophagus	4
Gastro intestinal stromal tumours	2
Controls patients with symptomatic GORD or dyspepsia	101
Healthy volunteer controls	5

Table 3 Distribution of participants recruited for the study

3.1.1 Patients with oesophago-gastric malignancy

137 patients had oesophago-gastric malignancy. The mean age of these patients was 66 years (range 31-87 years). 123 of these patients were Caucasian, seven were Asian and seven were Afro-Caribbean. More than 75% were males (105 vs. 32). 103 of these patients were deemed fit for curative treatment and had a curable stage while 34 were treated with a palliative intent (these patients were either unfit or had a stage that was deemed incurable). Further breakdown of these patients is as follows.

Oesophago-gastric malignancy	
Oesophageal AC (type 1,2)	71
Oesophageal AC (type 3)	12
Body/ distal gastric AC	33
Oesophageal SCC	21
Total	137

Table 4 Distribution of patients according to type of cancer

The stage specific breakdown of these patients is as follows (this radiologic stage and represents the stage at the completion of their pre-op tests)

Stage	Number of patients
Tx N0 M0	3
T1/2 N0 M0	14
T1/2 N1 M0	7
T3/4 Any N M0	89
Any T Any N M1	23
Staging not available	1

Table 5 Stage specific breakdown of patients

Of the 137 patients, 48 did not receive chemo/ radiotherapy; 3 patients received radiotherapy only and 86 patients received chemotherapy.

The breakdown of the various chemotherapeutic agents used is as follows:

Chemotherapy regime	Number of patients
CF	35
ECF	3
ECX	35
ECX (with bevacizumab/ oxiplatin/ radiotherapy)	4
EOX	5
MIC	2
Agent not known	2

Table 6 Breakdown of patients according to type of chemotherapy received

CF – Cisplatinum, 5-Fluorouracil

ECF – Epirubicin, Cisplatinum, 5-Fluorouracil

ECX – Epirubicin, Cisplatinum, Xeloda (Capecitabine)

EOX – Epirubicin, Oxaliplatin, Xeloda (Capecitabine)

MIC – Mitomycin, Ifosfamide and Cisplatinum

3.1.2 Patients with Non dysplastic Barrett’s oesophagus

Nine patients had non dysplastic Barrett’s oesophagus and were recruited from a surveillance endoscopy programme. Their mean age was 57 years (range 39-69 years). There were eight males, all were Caucasian.

3.1.3 Patients with high grade dysplasia of the oesophagus

Three patients with high grade dysplasia had columnar HGD and one patient had squamous HGD. Their mean age was 67 years (range 58-80 years). Three were males and all were Caucasian.

3.1.4 Controls patients with GORD symptoms or dyspepsia

101 control patients were recruited from endoscopy clinics. These patients had presented with symptoms suggestive of GORD or dyspepsia, had not taken a proton pump inhibitor for two weeks and had endoscopically normal appearances. Their mean age was 60 years (range 23-94 years). Nearly half of these patients were males (n=48), 89% were Caucasians, 7% Asian, 3% Afro-Caribbean and one patient was mixed race.

3.1.5 Comparison of patients with oesophago-gastric malignancy vs. controls

There was a statistically significant difference in the age distribution between the two groups (p=0.001; Mann Whitney U test). There was also a statistically significant difference in the distribution of sex between the two groups (p<0.001; Chi square test). There was no difference in the distribution of ethnicity between the two groups (p=0.77; df = 2; Chi square test).

24 patients of 137 patients with cancer did not have any pre existing co morbidities compared with 29 of 101 patients in the Control group. 13 patients with cancer were not taking any regular medications compared with 20 patients in the Control group.

The mean co morbid conditions in the cancer group were 1.93 ± 1.12 (range 1 – 6). The mean number of medications was 3.96 ± 2.26 (range 1 – 9). The commonest co morbid condition was hypertension (n=35) followed by diabetes (n=14). The most common medication in this group was proton pump inhibitors.

The mean co morbid conditions in the control group were 2.24 ± 1.74 (range 1 – 10). The mean number of medications was 3.26 ± 2.9 (range 1 – 15). Similar to the oesophago-gastric group, the commonest co morbid condition was hypertension (n=24) followed by diabetes (n=10). The most common medication again was proton pump inhibitors.

There was no statistically significant difference between the number of co morbid conditions in between the two groups ($p= 0.597$; Mann Whitney U test). However, not surprisingly, the oesophago-gastric group were taking more medications ($p= 0.008$; Mann Whitney U test).

3.2 Quality control

3.2.1 Plasma samples

The blood samples were placed on ice immediately following collection. The mean time for transfer of blood samples on ice from patient to centrifuge was 98.4 ± 55 (range 9 – 249) minutes. 67.1% of the samples were processed within 2 hours of obtaining them. The total mean time including transfer, preparation of plasma to storage in a -80°C freezer was 118.4 ± 56.7 (range 26 – 271) minutes.

3.2.2 Endoscopic biopsies

All endoscopic biopsies were collected in Eppendorf vials and immediately placed on ice. The mean time from taking the biopsy to be placed on ice was 1.1 ± 11 (range 0 – 130) minutes. The mean time from taking the biopsy to a definitive storage in a -80°C freezer was 65.9 ± 47.4 (range 5 – 233) minutes. 72.5% of the samples reached definitive storage within 90 minutes. The mean weight of the endoscopic biopsies was 13.5 mg (range 5.1 – 18 mg).

3.2.3 Resectional tissue

The mean time from obtaining the tissue in theatre, transport to the histopathology laboratory, obtaining and placing the specimens on ice was 22.1 ± 11.4 (range 6 – 62) minutes. The mean total time from obtaining the specimen to storage in a -80°C freezer was 34.1 ± 11.7 (range 17 – 76) minutes. The mean weight of the resectional biopsies was 45.3 mg (range 14.2 – 53 mg).

No attempts were made to elucidate any metabolic differences between the endoscopic and resectional biopsies. All attempts were made to equilibrate for differences in time to freezing (section 2.4.4) and the sample sizes (section 2.4.7). Based on the various analyses performed in this study, it is unlikely that there were any systematic differences in resectional and endoscopic biopsies.

3.3 NMR plasma results

Spectra were obtained for all 391 plasma samples. 9 spectra were excluded from the analysis due to a poor quality of the spectrum. As a result, the final tissue analysis was performed on 383 spectra.

Model 1. Controls vs. gastro-oesophageal adenocarcinoma

A total of 165 samples were entered into this model. Of these, 97 were from control patients and 68 were from patients with gastro-oesophageal adenocarcinoma.

11.09% of the variability was explained by the first latent variable. Latent variables are variables that are not observed but are mathematically calculated from the data (Page 79).

The use of two first latent variables was suggested by the cross validation, accounting for 21.85% of the variability. To reduce the number of latent variables and to align the scores along the latent variables, orthogonal PLS-DA was then performed (Figure 9). Good discrimination was obtained using the first one latent variable with an area under the curve of 0.8008 on performing a ROC analysis.

Loadings obtained on the first latent variable were then exported to a Bruker format to enable display on the Chenomx software. A list of peaks was thus produced which were discriminatory on the first latent variable (Figure 10).

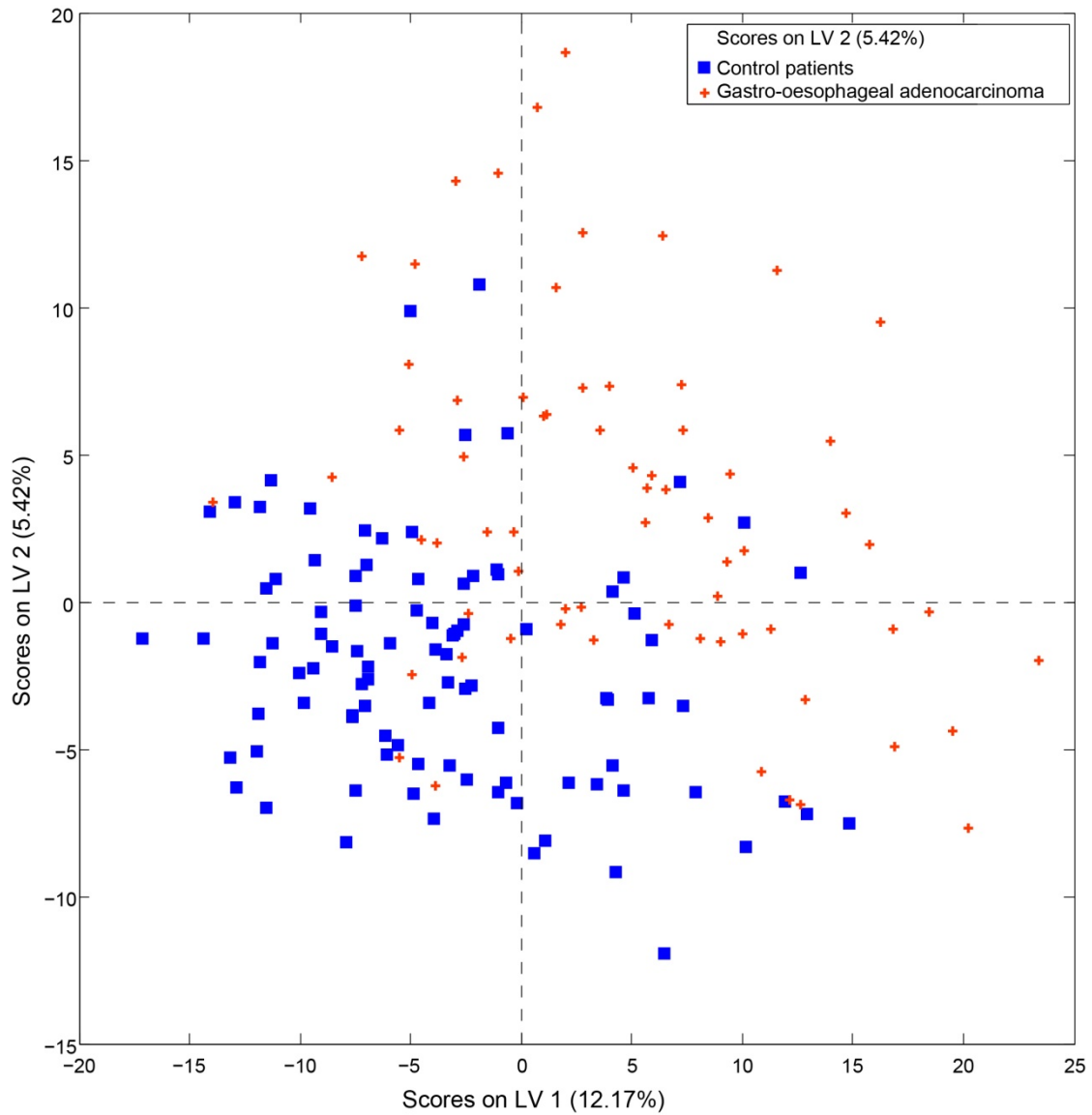


Figure 8 PLS-DA Model 1 plasma

Crosses indicate patients with gastro-oesophageal adenocarcinoma and squares indicate control patients (patients with GORD symptoms or dyspepsia).

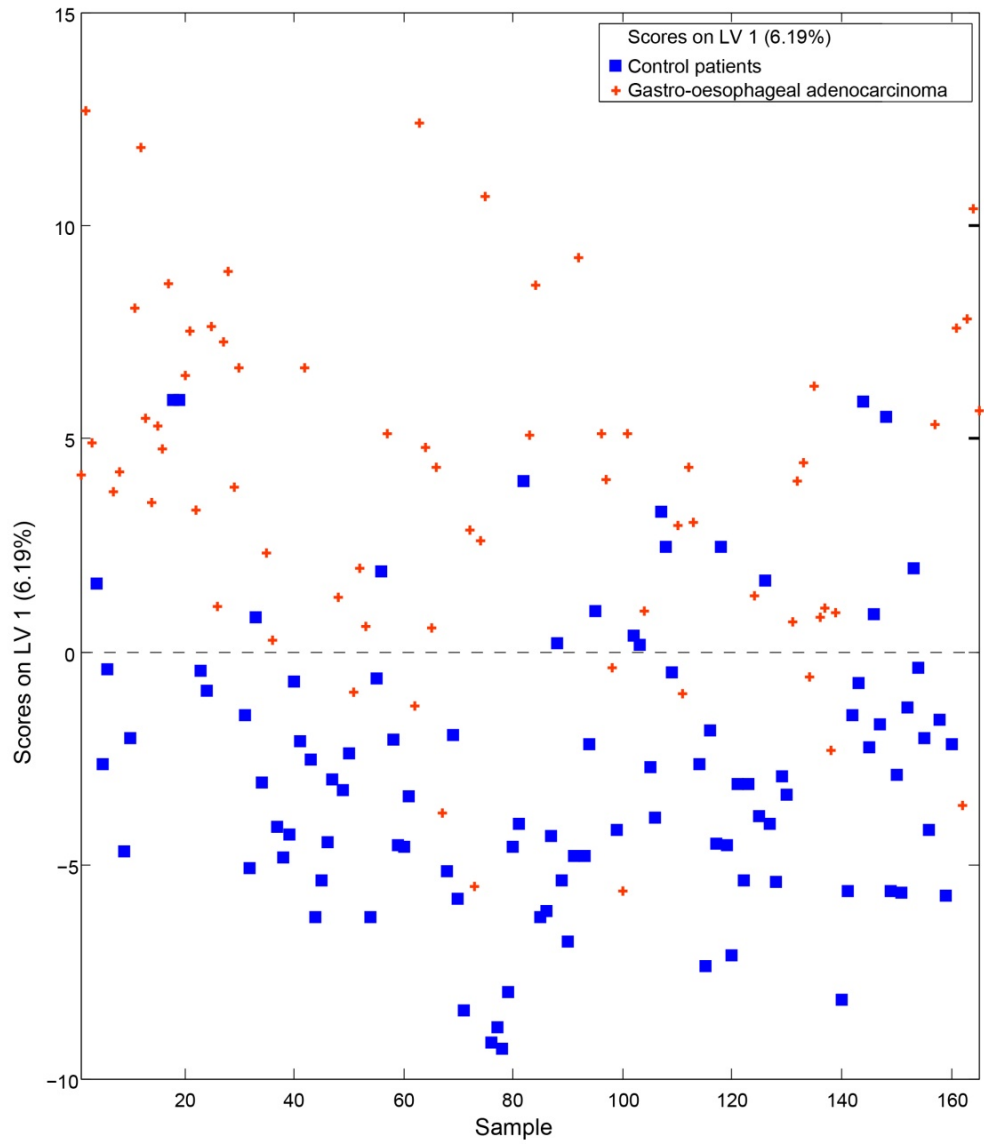


Figure 9 OPLS-DA Model 1 Plasma

Crosses indicate patients with gastro-oesophageal adenocarcinoma and squares indicate control patients (patients with GORD symptoms or dyspepsia).

PATIENTS WITH GASTRO-OESOPHAGEAL ADENOCARCINOMA

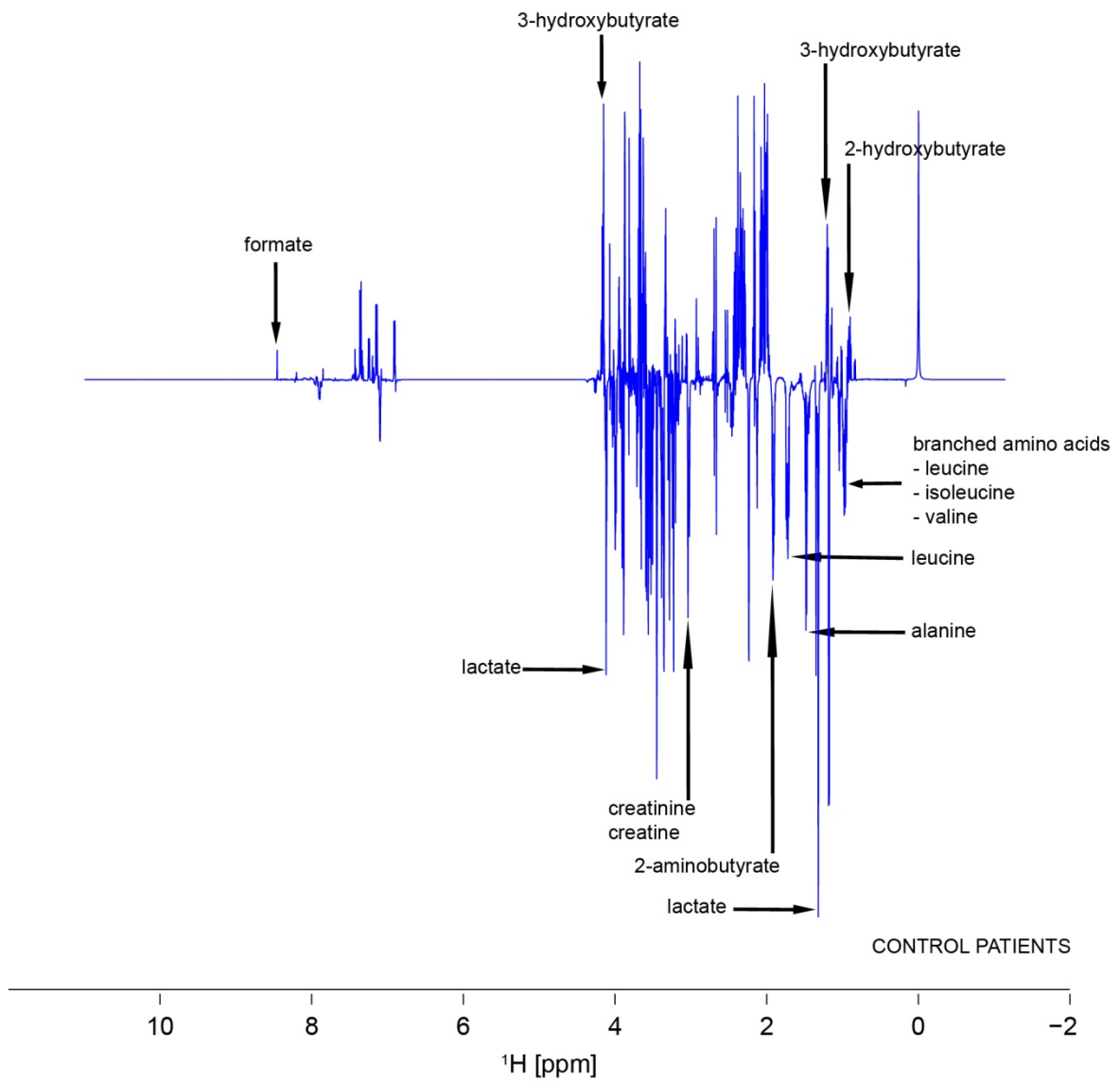


Figure 10 Loadings plot for LV1 Model 1 Plasma obtained from OPLS-DA

Model 2. Non-dysplastic Barrett's vs. oesophageal adenocarcinoma type 1,2

A total of 49 samples were entered into this model. Of these, 10 were from patients with non-dysplastic Barrett's oesophagus and 39 were from patients with oesophageal adenocarcinoma type 1,2.

8.22% of the variability was explained by the first latent variable. The use of two first latent variables was suggested by the cross validation, accounting for 13.4% of the variability. To reduce the number of latent variables and to align the scores along the latent variables, orthogonal PLS-DA was then performed (Figure 11). Use of two latent variables accounting for a total of 13.4% of the variability was suggested by the cross validation. Poor discrimination was obtained using the first latent variable with an area under the curve of 0.5051 on performing a ROC analysis.

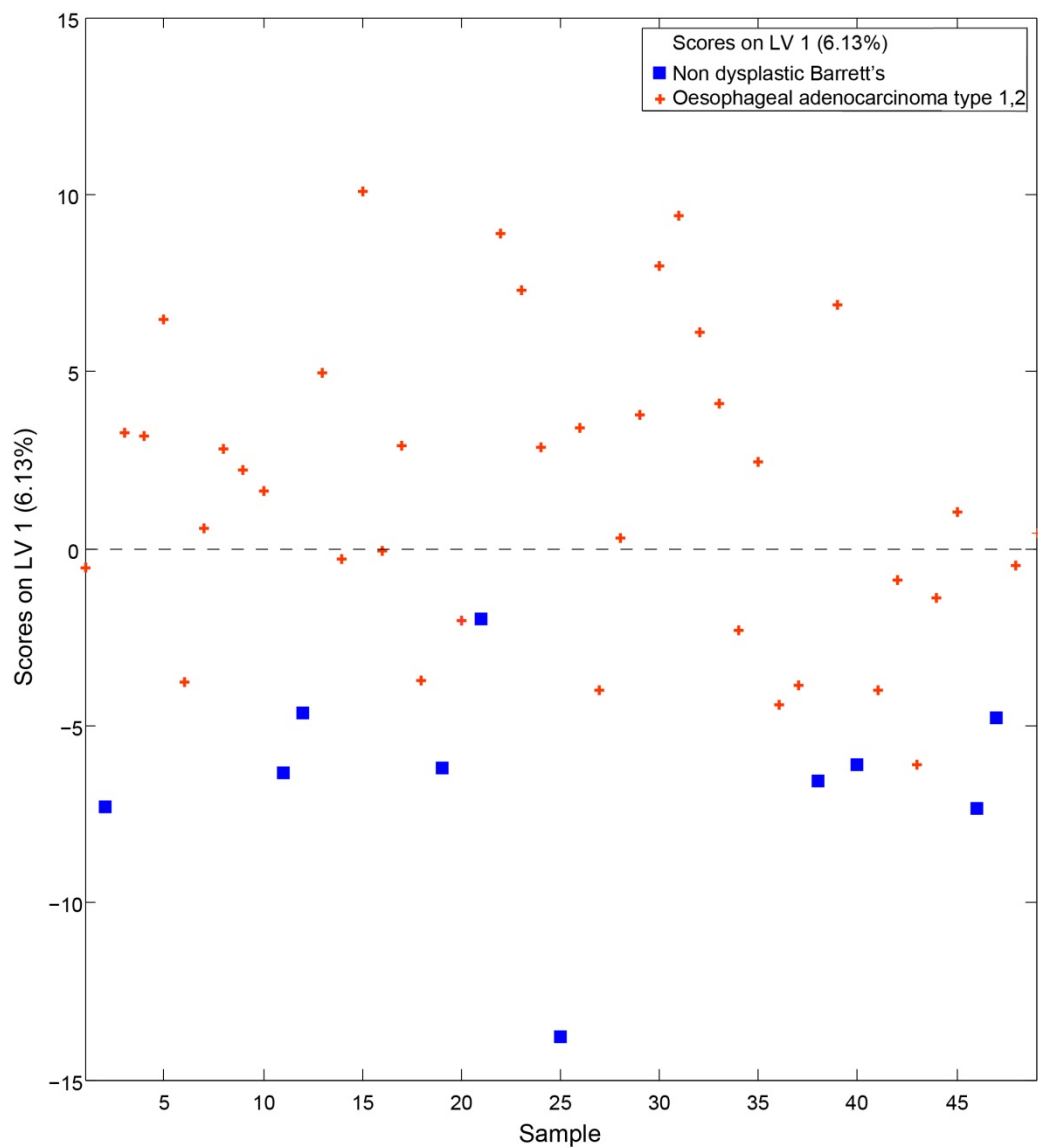


Figure 11 OPLS-DA Model 2 Plasma

Crosses indicate patients with oesophageal adenocarcinoma type 1,2 and squares indicate patients with non dysplastic Barrett's oesophagus.

Model 3. Overall response

A total of 24 samples were entered into this model. Of these, 8 were plasma samples from responders and the remainder from non responders. As explained earlier, this model compared pre chemotherapy plasma from responders (patients with TRG 1-3 or response on RECIST) against non responders (patients with TRG 4-5 or no response on RECIST). There was very good concordance between response evaluation on Mandard criteria and RECIST staging. Only one patient differed with regards to response using the two approaches. In that case, the Mandard grade was used to classify the patient was used since it is regarded as the gold standard for accessing response.

16.44% of the variability was explained by the first latent variable. The use of only the first latent variable was suggested by the cross validation (Figure 12). Good discrimination was obtained using the first one latent variable with an area under the curve of 0.7031 on performing a ROC analysis.

The loadings obtained on the first latent variable were then exported to a Bruker format to enable display on the Chenomx software. A list of peaks was thus produced which were discriminatory on the first latent variable (Figure 13).

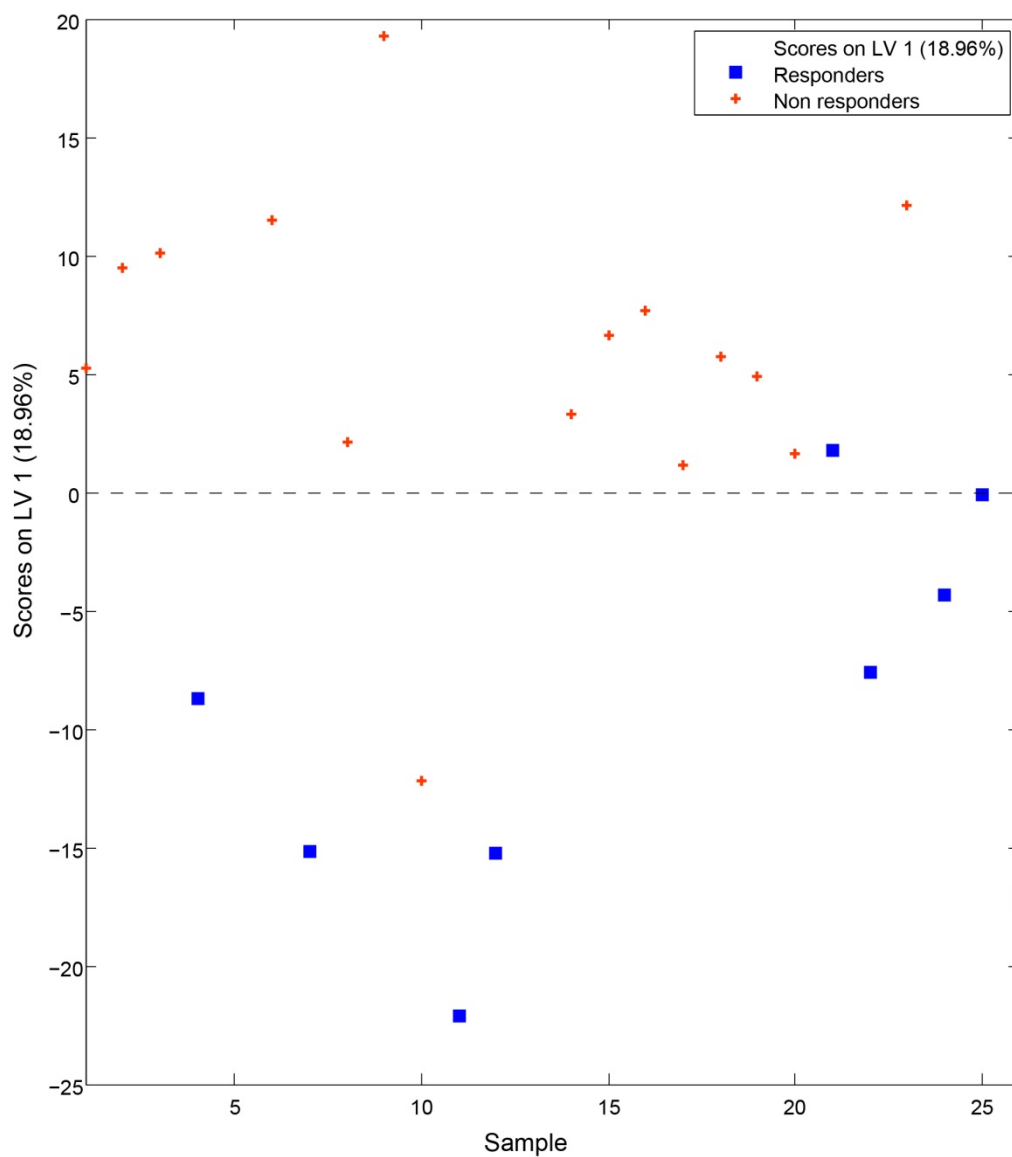


Figure 12 PLS-DA Model 3 Plasma

Crosses indicate non responders (patients with TRG 4-5 or no response on RECIST) and squares indicate responders (patients with TRG 1-3 or response on RECIST).

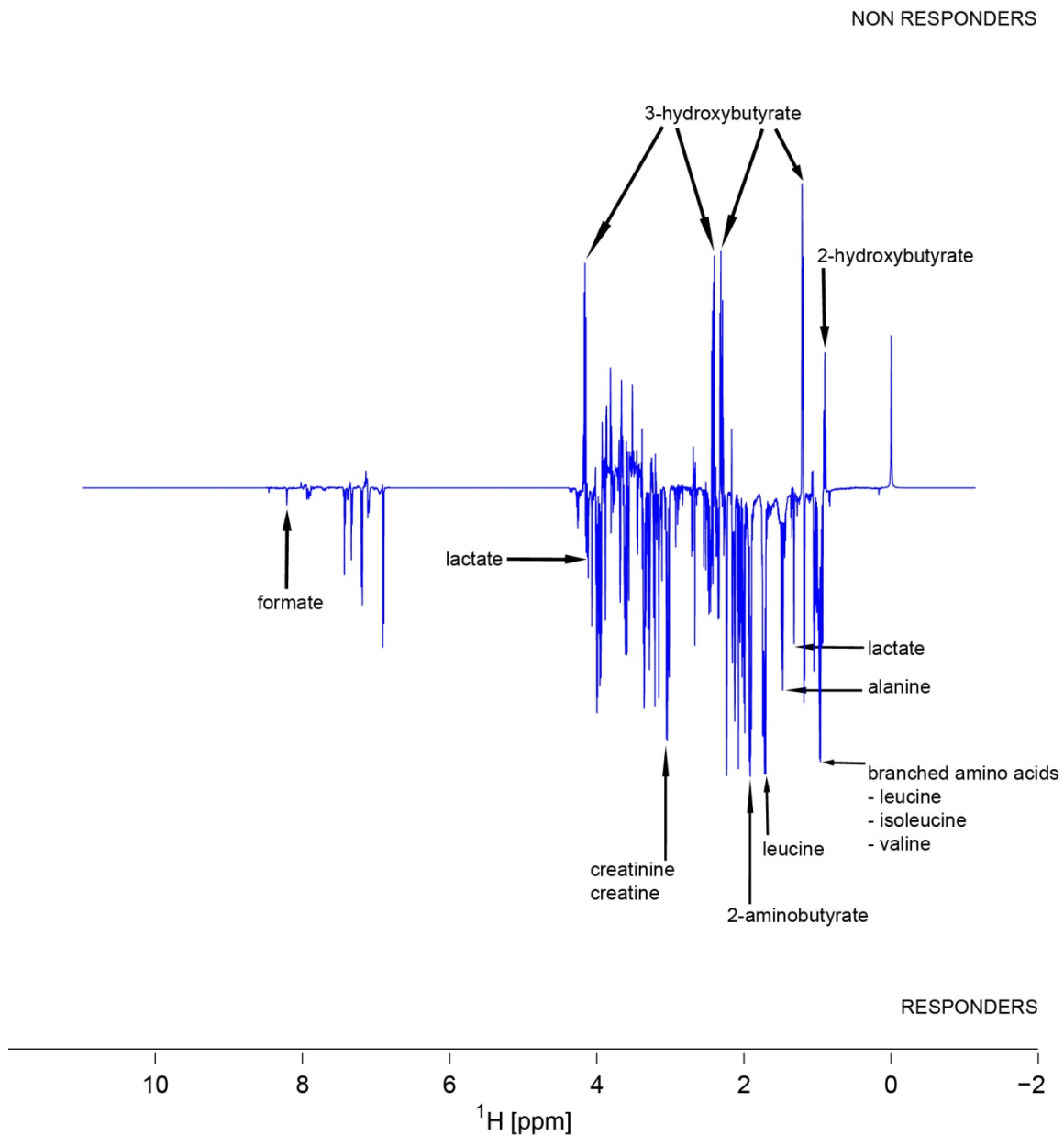


Figure 13 Loadings plot for LV1 Model 3 Plasma

Model 4. Stage on N

A total of 23 samples were entered into this model. Of these, 9 were plasma samples from patients who had nodal stage of N0 and remainder had nodal status N1.

26.01% of the variability was explained by the first latent variable. The use of only the first latent variable was suggested by the cross validation (Figure 14). Good discrimination was obtained using the first latent variable with an area under the curve of 0.8413 on performing a ROC analysis.

The loadings obtained on the first latent variable were then exported to a Bruker format to enable display on the Chenomx software. A list of peaks was thus produced which were discriminatory on the first latent variable (Figure 15).

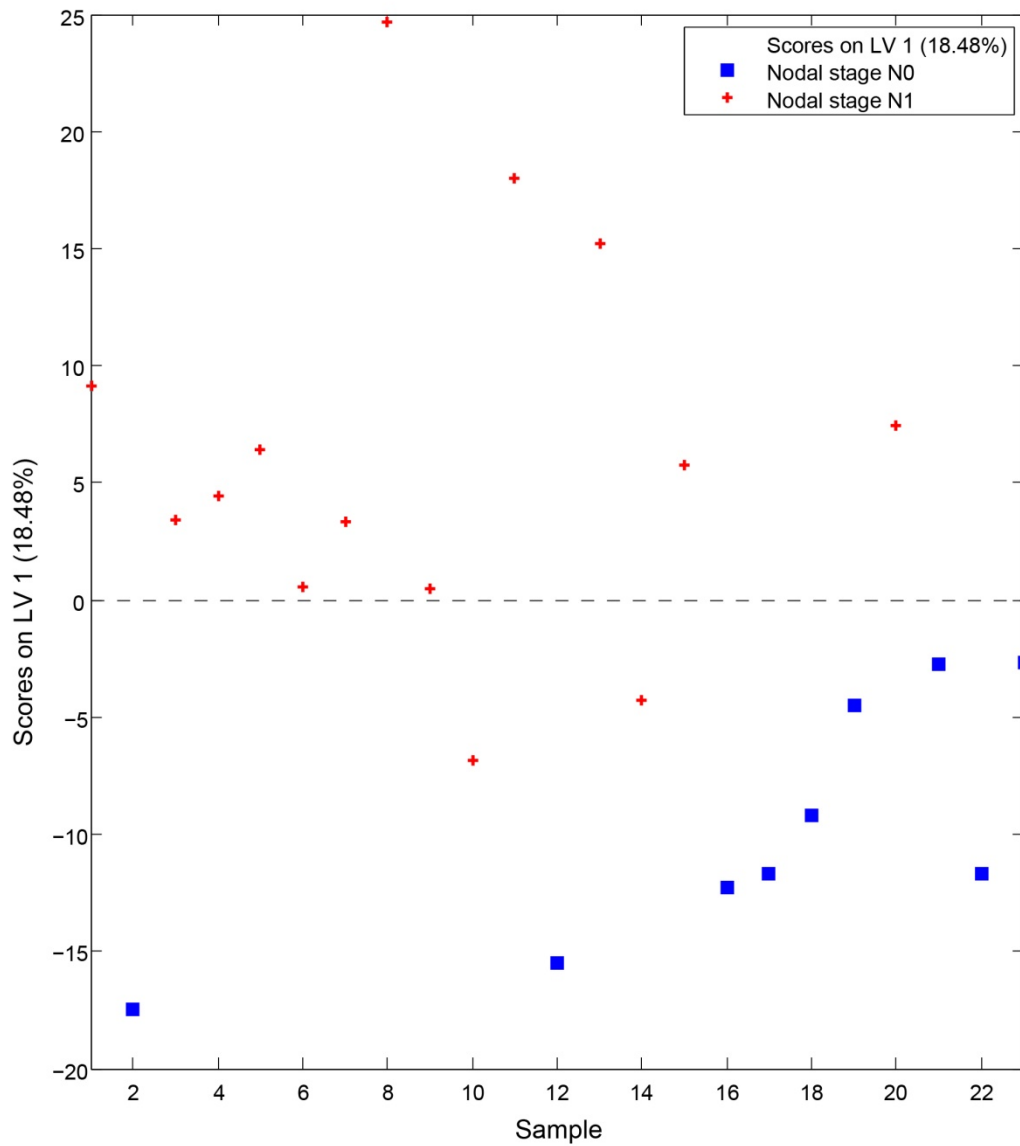


Figure 14 PLS-DA Model 4 Plasma

Crosses indicate patients with nodal stage N0 (node negative) and squares indicate patients with nodal stage N1 (node positive).

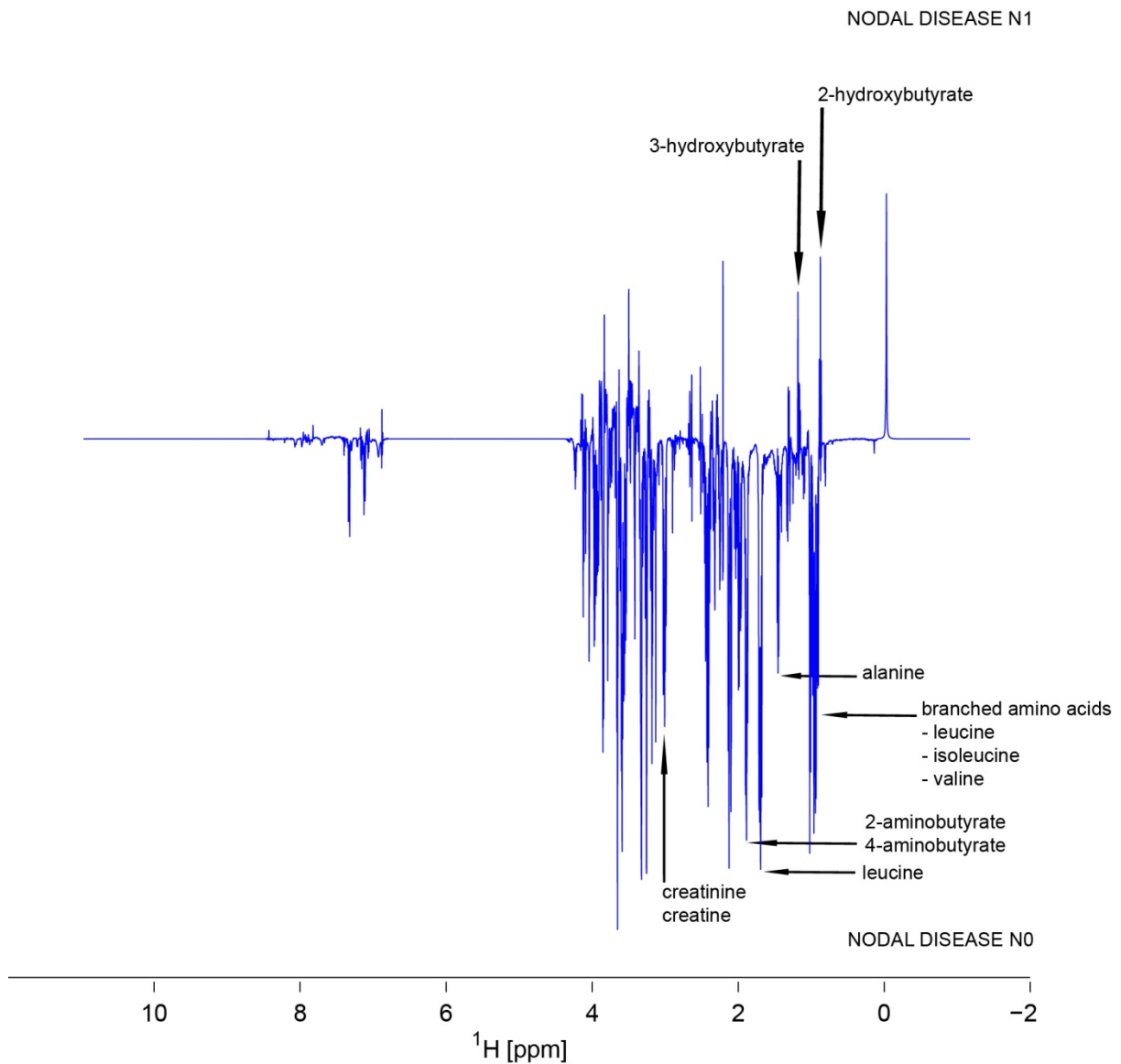


Figure 15 Loadings plot for LV1 Model 4 Plasma

Model 5. Stage on T

A total of 23 samples were entered into this model. Of these, 11 were plasma samples from patients who had T1 or T2 tumours and remainder had nodal status T3 or T4 tumours.

30.53% of the variability was explained by the first latent variable. The use of only the first latent variable was suggested by the cross validation (Figure 16). Good discrimination was

obtained using the first latent variable with an area under the curve of 0.8182 on performing a ROC analysis.

The loadings obtained on the first latent variable were then exported to a Bruker format to enable display on the Chenomx software. A list of peaks was thus produced which were discriminatory on the first latent variable (Figure 17).

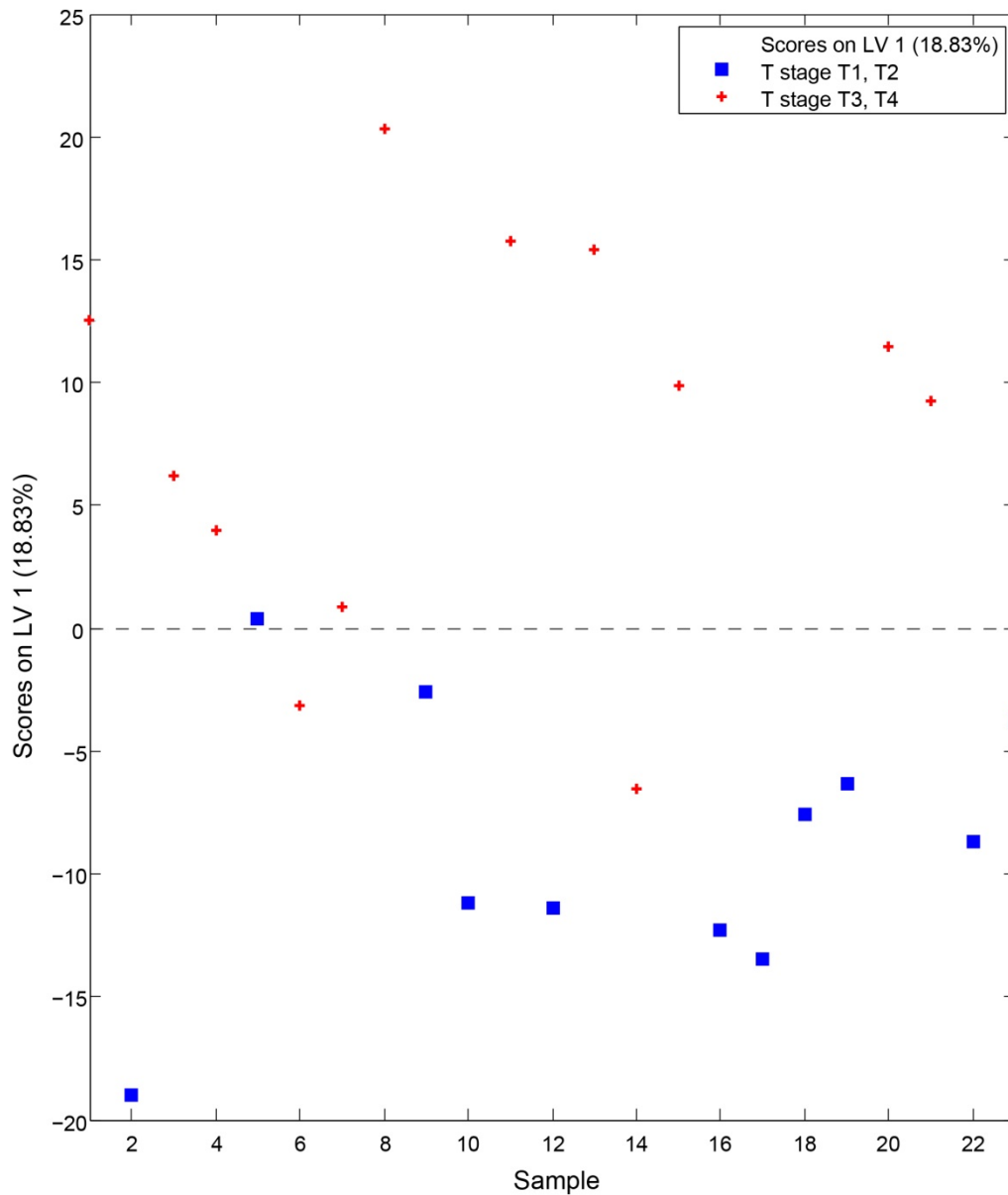


Figure 16 PLS-DA Model 5 Plasma

Crosses indicate patients with T stage 1 or 2 and squares indicate patients with T stage 3 or 4.

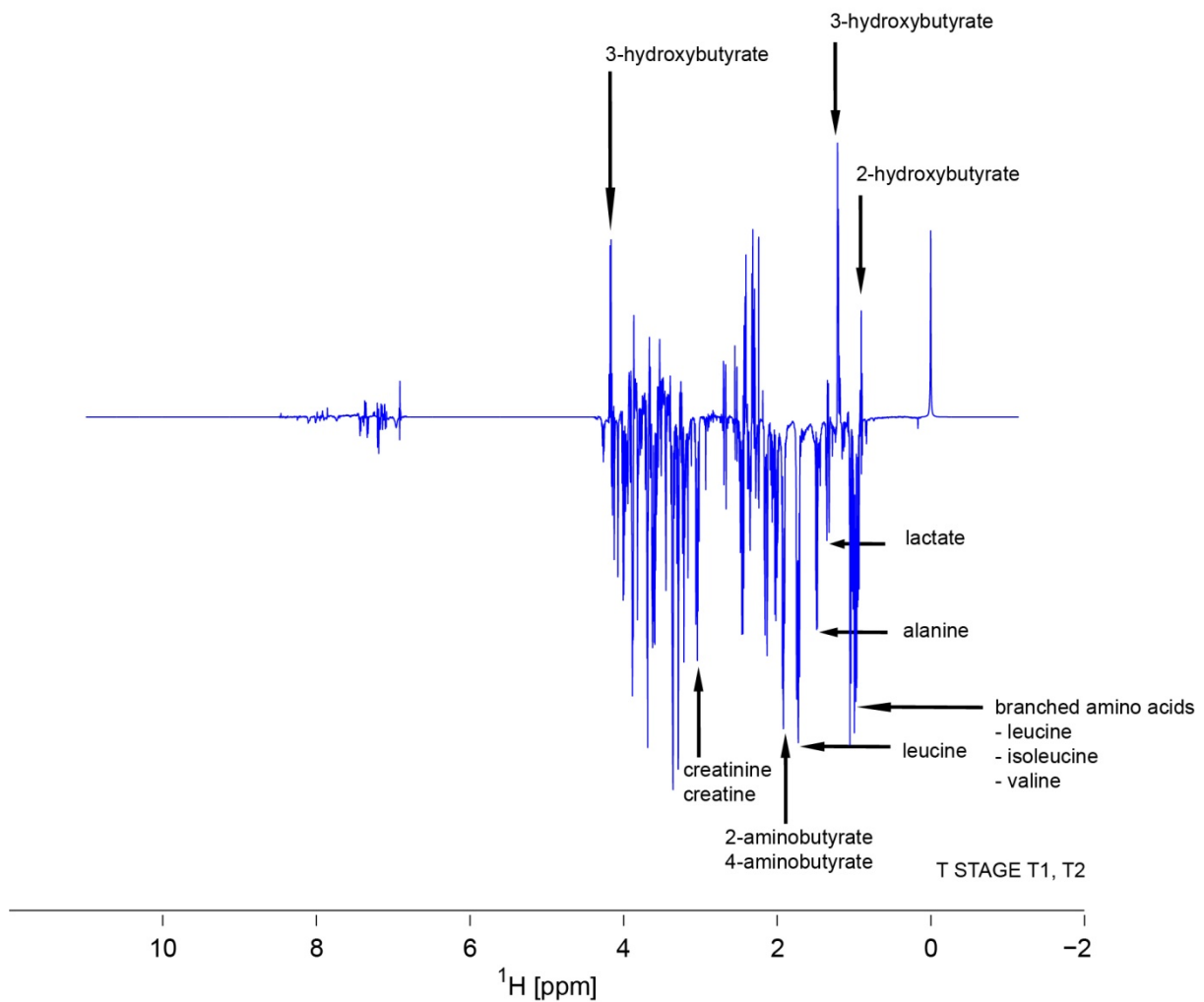


Figure 17 Loadings plot for LV1 Model 5 Plasma

Model 6. 'Bacon and egg' model

14 samples were entered into the model (one sample was excluded due to sub standard quality of spectrum).

The 'leave one out' algorithm was used for cross validation. 12.37% of the variability was explained by the first latent variable. The use of first four latent variables was suggested by

the cross validation, accounting for 69.5% of the variability. However, visually, good separation was obtained the first three latent variables was achieved (Figure 18). Area under the curve for the five groups was 0.6364, 0.9697, 0.9091, 1 and 0.7273.

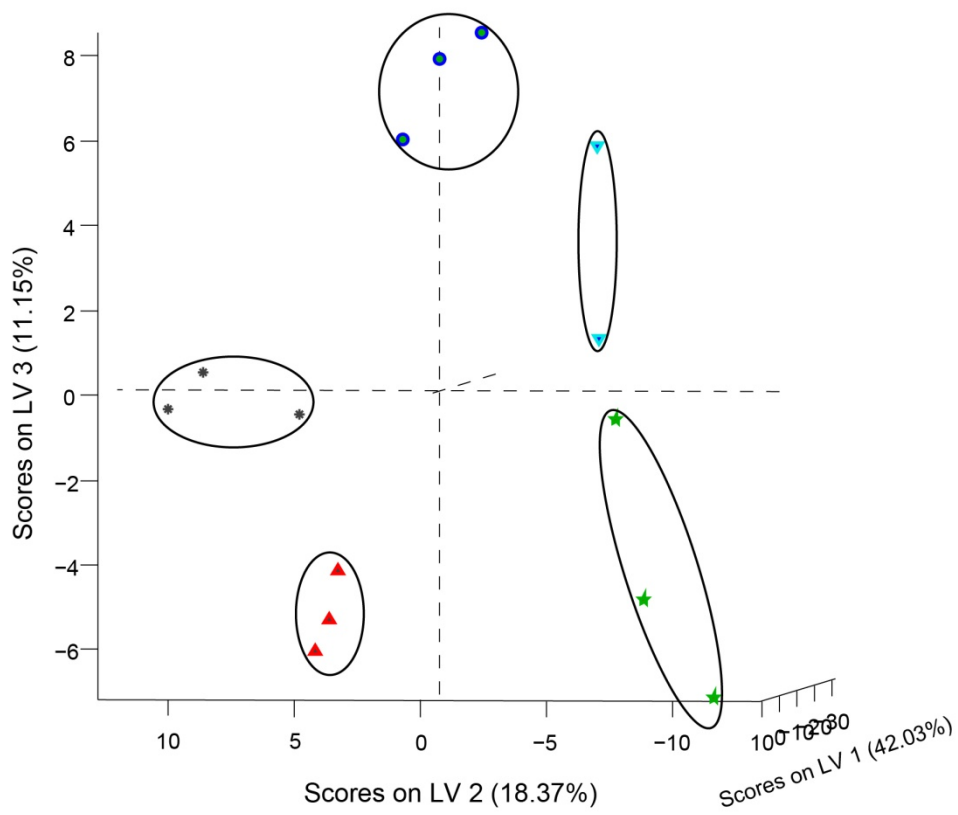


Figure 18 PLS-DA Model 6 Plasma (LV1 vs. LV2 vs. LV3).

The sample cluster for each volunteer has been highlighted with a solid circle.

3.4 NMR tissue results

Spectra were obtained for all 333 tissues. 4 spectra were excluded from the analysis due to a poor quality of the spectrum. As a result, the final tissue analysis was performed on 329 spectra.

Model 1. Normal squamous mucosa vs. normal gastric columnar mucosa

A total of 174 samples were entered into this model. Of these, 136 were tissue biopsies from normal squamous mucosa and the remainder were normal columnar mucosa biopsies.

21.32% of the variability was explained by the first latent variable. The use of two first latent variable was suggested by the cross validation, accounting for 24.22% of the variability (Figure 19). To reduce the number of latent variables and to align the scores along the latent variables, orthogonal PLS-DA was then performed (Figure 20). Use of 2 latent variables accounting for a total of 24.54% of the variability was suggested by the cross validation. Good discrimination was obtained using the first one latent variable with an area under the curve of 0.9478 on performing a ROC analysis.

A number of metabolites were noticed to be significantly different in between the two classes on the loadings. On comparison of the spectra at the chemical shift for those metabolites, these differences were visually confirmed in the processed spectra without glog transformation (Figure 21, Figure 22).

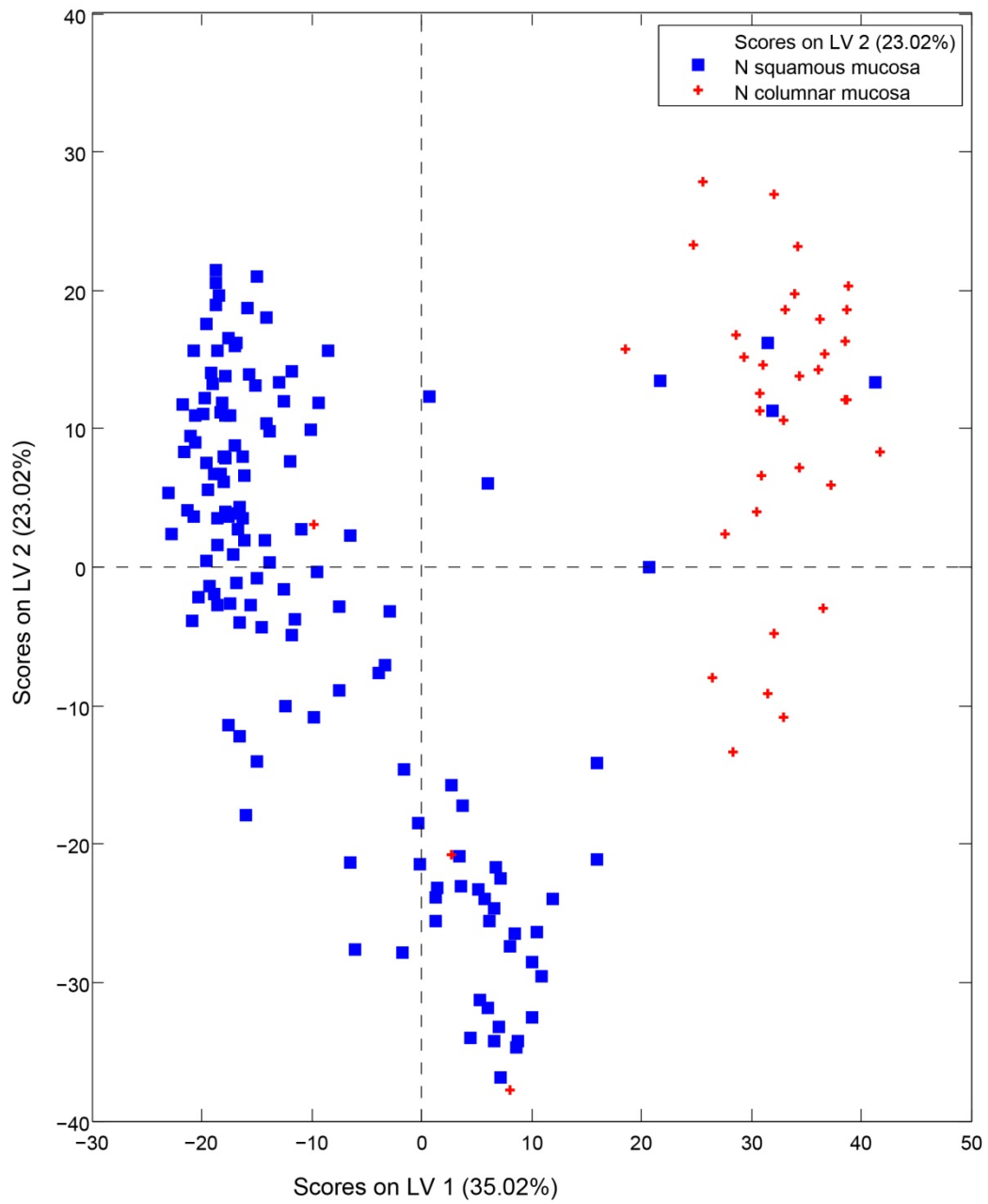


Figure 19 PLS-DA Model 1 Tissue (LV1 vs. LV2)

Crosses indicate tissue biopsies from normal columnar mucosa and squares indicate biopsies from normal squamous mucosa.

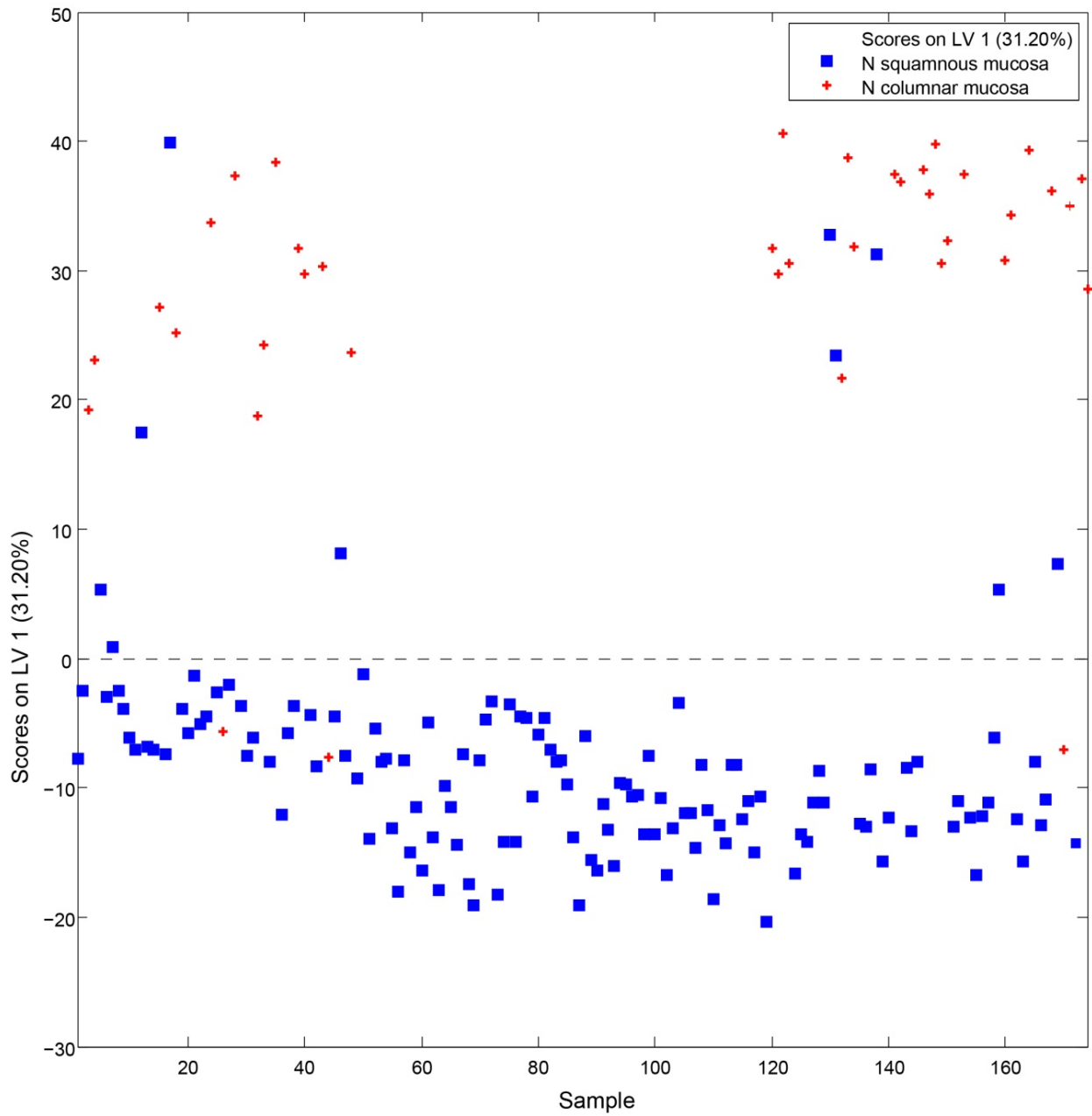


Figure 20 OPLS-DA Model 1 Tissue

Crosses indicate tissue biopsies from normal columnar mucosa and squares indicate biopsies from normal squamous mucosa.

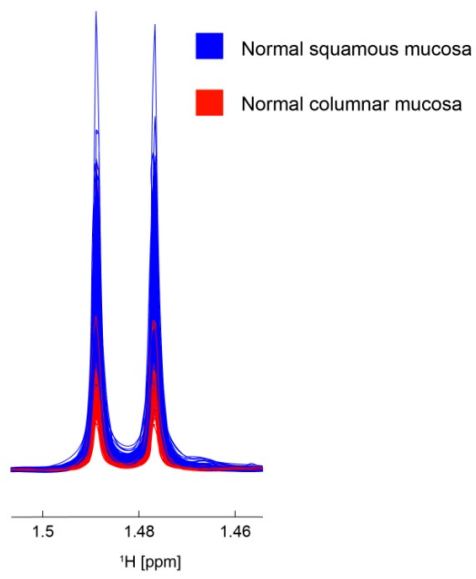


Figure 21 Levels of alanine in normal squamous tissue and normal columnar tissue on Model 1 Tissue

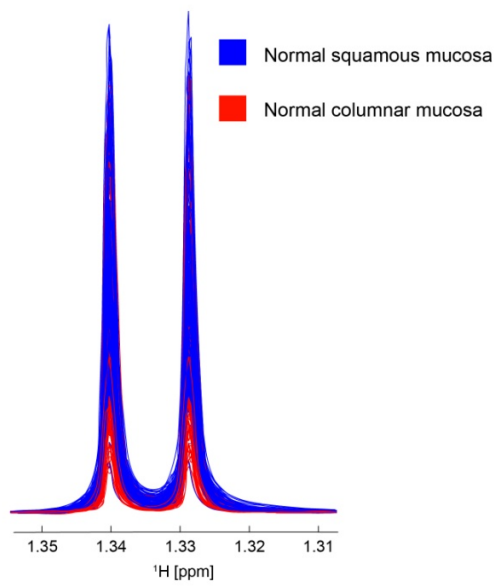


Figure 22 Level of lactate in normal squamous tissue and normal columnar tissue on Model 1 Tissue

(These were figures were for illustration purposes only and as such no attempts were made to draw out any inferences from the differing levels of these metabolites).

Model 2. Normal squamous mucosa vs. oesophageal adenocarcinoma type 1,2

A total of 116 samples were entered into this model. Of these, 59 were tissue biopsies from normal squamous mucosa and the remainder were biopsies from the cancer mucosa.

29.75% of the variability was explained by the first latent variable. The use of only the first latent variable was suggested by the cross validation (Figure 23). Good discrimination was obtained on the scores plot with an area under the curve of 0.9176 on performing a ROC analysis.

The loadings obtained on the first latent variable were then exported to a Bruker format to enable display on the Chenomx software. A list of peaks was thus produced which were discriminatory on the first latent variable (Figure 24).

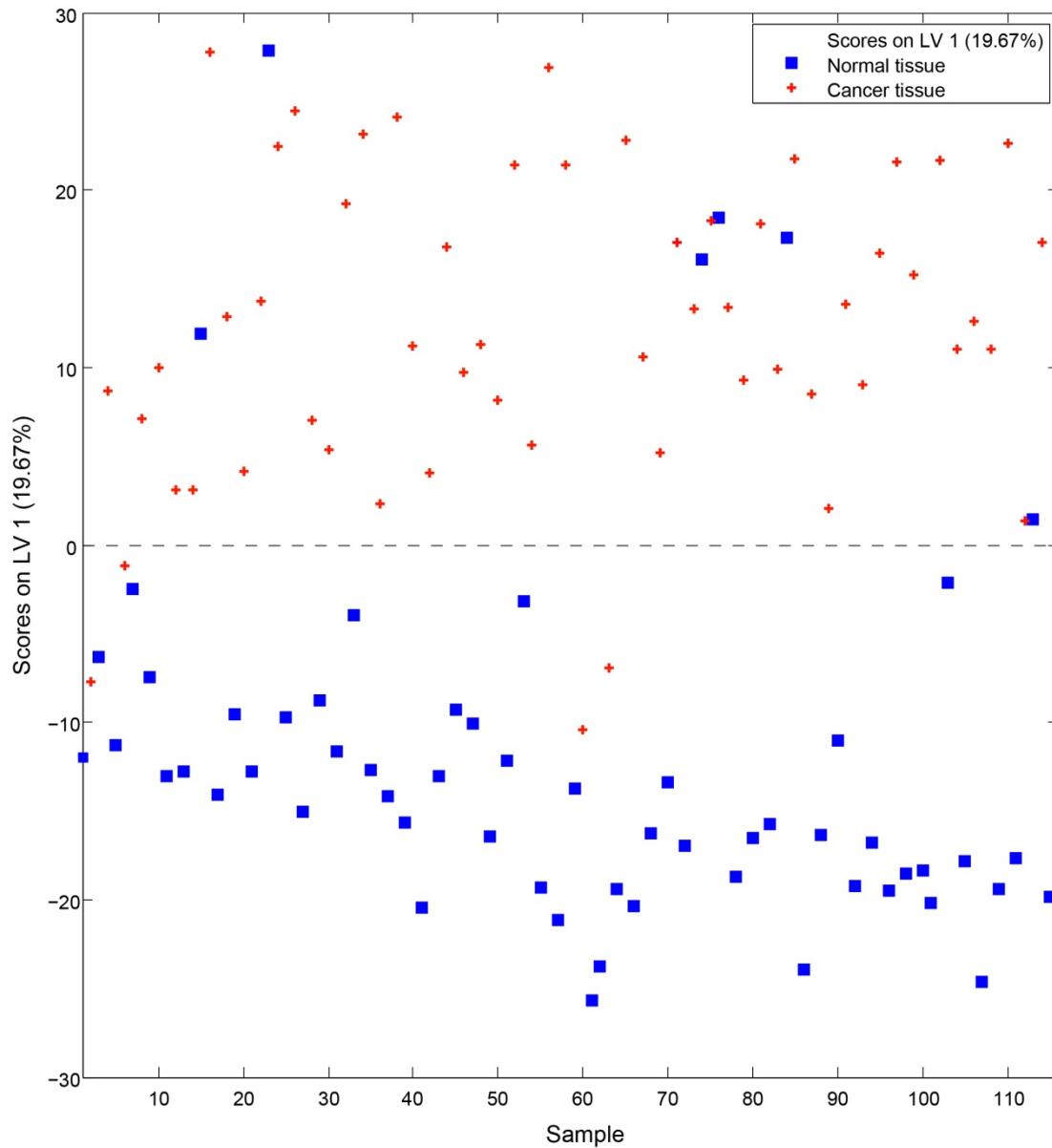


Figure 23 PLS-DA Model 2 Tissue

Crosses indicate tissue biopsies from normal squamous mucosa and squares indicate biopsies from cancer mucosa in patients with oesophageal adenocarcinoma type 1,2.

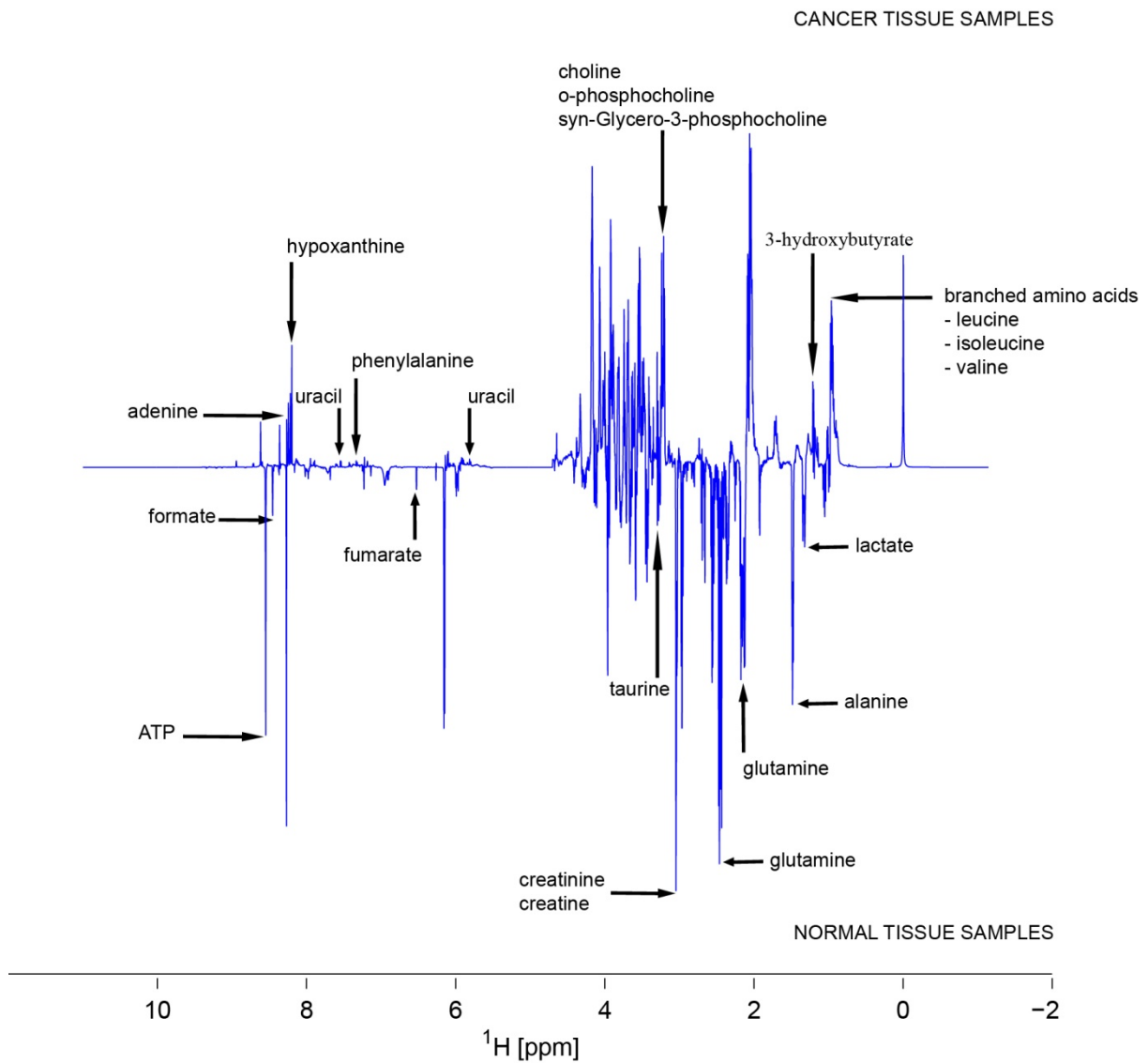


Figure 24 Loadings plot for LV1 Model 2 Tissue

Model 3. Normal squamous mucosa vs. Barrett's mucosa in the presence of a cancer vs. oesophageal adenocarcinoma type 1,2

A total of 32 samples were entered into this model. Of these, 11 were tissue biopsies from normal squamous mucosa, 11 were tissue biopsies from morphologically identified Barrett's mucosa and the remaining 10 spectra were from biopsies of the cancer mucosa. Only 10

samples were available for the third class as one spectrum had been excluded in the beginning due to substandard spectral quality.

PLS-DA was performed in the PLS toolbox. 28.44% of the variability was explained by the first latent variable. The use of three latent variables was suggested by the cross validation, predicting a total variability of 51.39%. On examination of the scores plot, only lv1 and lv2 were important in discriminating between the 3 classes. As a result, only 2 latent variables accounting for a total of 49.07% of the variability were used for this model (Figure 25). The scores plot thus obtained differentiated between normal squamous mucosa and Barrett's/cancer mucosa on lv1 and between Barrett's mucosa and cancerous mucosa on lv2. The ROC value for the prediction of normal squamous mucosa was 1. The ROC values for the prediction of Barrett's mucosa and cancerous mucosa were 0.7013 and 0.6955 respectively.

For the identification of metabolites discriminating in between these three classes, two sub-models were created comparing normal squamous mucosa vs. Barrett's mucosa and Barrett's mucosa vs. cancerous mucosa. The comparison between normal squamous mucosa and cancerous mucosa has already been made in model 2.

For the submodel comparing normal squamous mucosa vs. Barrett's mucosa, cross validated PLS-DA suggested the use of two latent variables accounting for a total variability of 45.18%. To reduce the number of latent variables and to align the scores along the latent variables, orthogonal PLS-DA was then performed. Use of 2 latent variables accounting for a total of 45.18% of the variability was suggested by the cross validation. Good discrimination was obtained using the first one latent variable with an area under the curve of 1 on performing a ROC analysis.

For the submodel comparing Barrett's mucosa vs. cancerous mucosa, cross validated PLS-DA suggested the use of two latent variables accounting for a total variability of 37.08%. To reduce the number of latent variables and to align the scores along the latent variables, orthogonal PLS-DA was then performed. Use of 2 latent variables accounting for a total of 37.08% of the variability was suggested by the cross validation. Good discrimination was obtained using the first one latent variable with an area under the curve of 0.7636 on performing a ROC analysis.

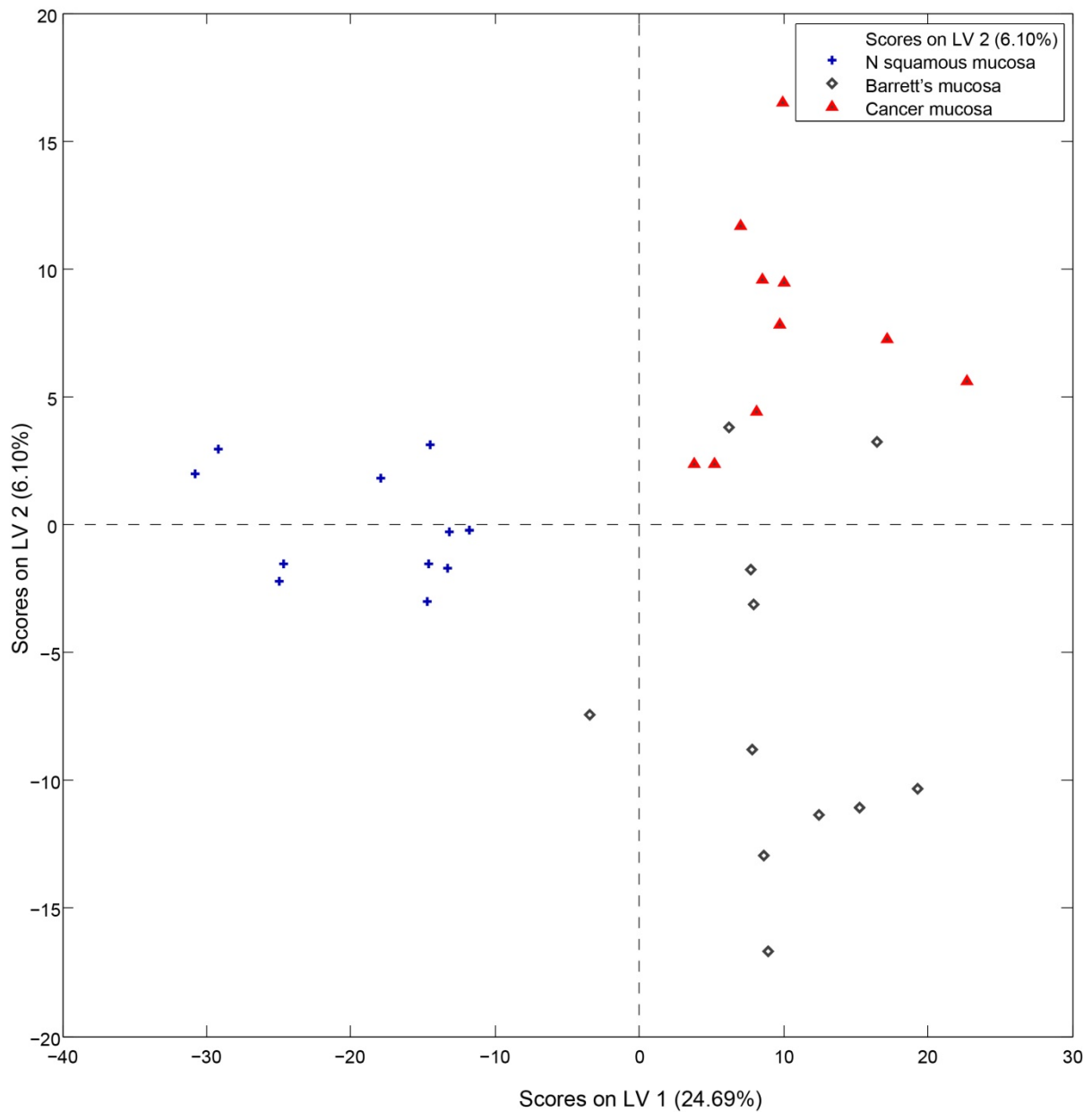


Figure 25 PLS-DA Model 3 Tissue (LV1 vs. LV2)

Crosses indicate tissue biopsies from normal squamous mucosa, triangles indicate biopsies from Barrett's mucosa and squares indicate biopsies from cancer mucosa in patients with oesophageal adenocarcinoma type 1,2.

Model 4. Non dysplastic Barrett's vs. Barrett's mucosa in the presence of a cancer

A total of 20 samples were entered into this model. Of these, 7 were tissue biopsies from non dysplastic Barrett's mucosa and 13 biopsies were of the Barrett's mucosa from patients who had oesophageal adenocarcinoma type 1,2.

The 'leave one out' algorithm was used for cross validation. 29.21% of the variability was explained by the first latent variable. The use of only the three latent variables was suggested by the cross validation accounting for a total variability of 43.09% (Figure 26). To reduce the number of latent variables and to align the scores along the latent variables, orthogonal PLS-DA was then performed. Good discrimination was obtained on the scores plot on lv1 with an area under the curve of 0.9121 on performing a ROC analysis.

The loadings obtained on the first latent variable were then exported to a Bruker format to enable display on the Chenomx software. A list of peaks was thus produced which were discriminatory on the first latent variable (Figure 27).

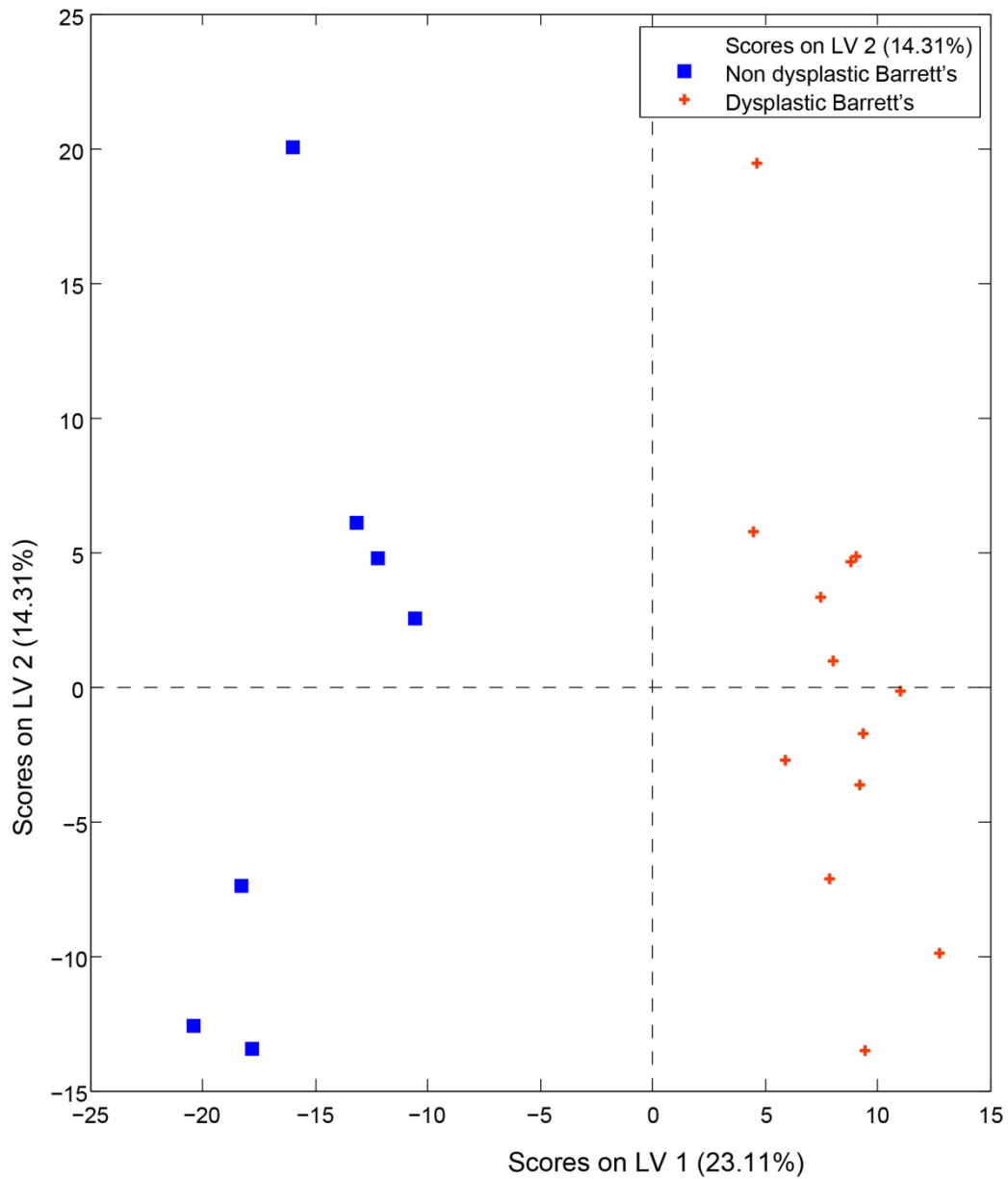


Figure 26 PLS-DA Model 4 Tissue (LV1 vs. LV2)

Crosses indicate tissue biopsies from non dysplastic Barrett's mucosa in patients undergoing surveillance endoscopy for Barrett's oesophagus and squares indicate biopsies Barrett's mucosa in patients with oesophageal adenocarcinoma type 1,2.

The following peaks were considered discriminatory for the two classes.

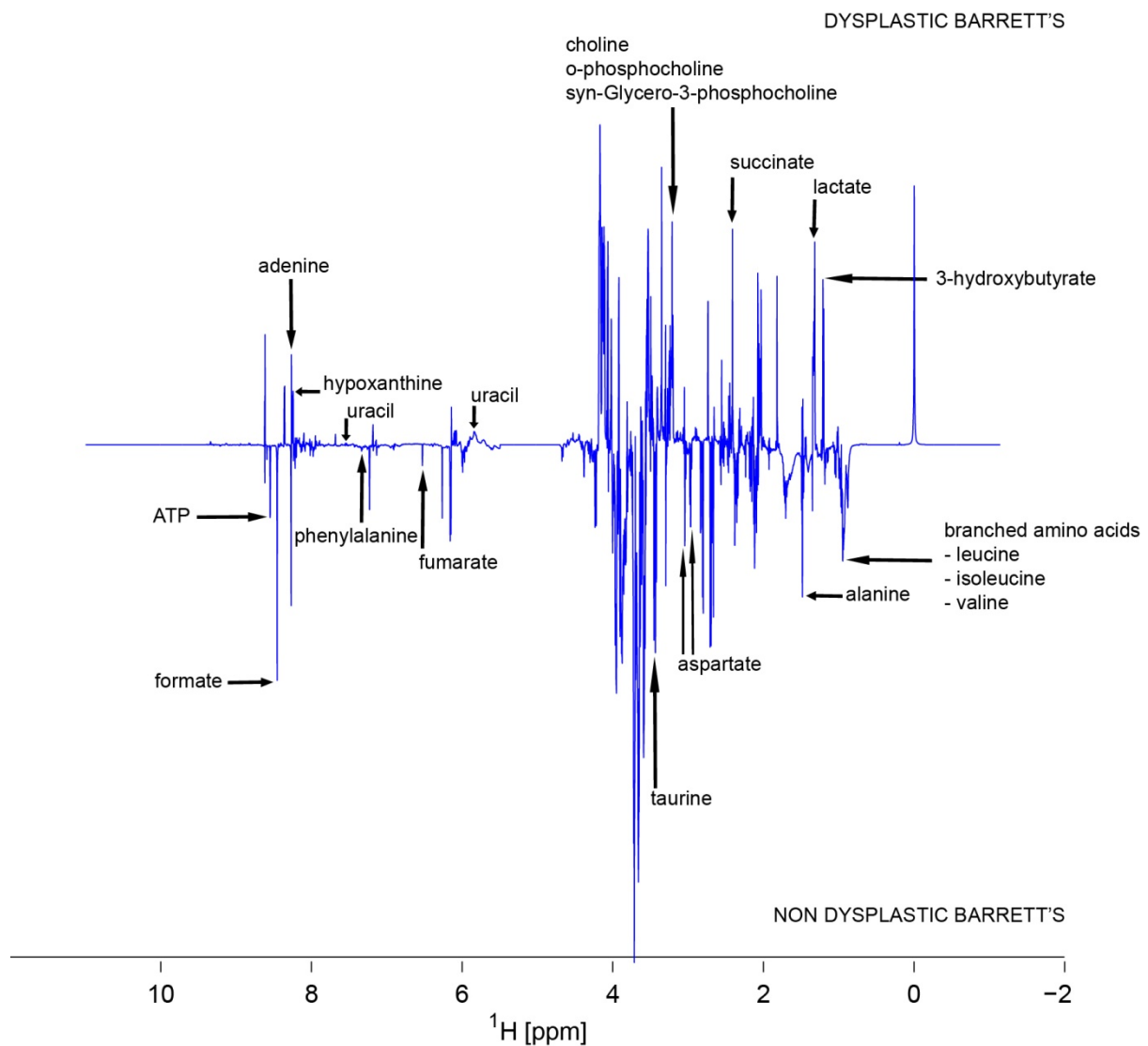


Figure 27 Loadings plot for LV1 Model 4 Tissue

Model 5. Overall response

A total of 25 samples were entered into this model. Of these, 12 were tissue biopsies from cancerous mucosa in patients who eventually responded to neo-adjuvant chemotherapy and 13 tissue biopsies were from cancerous mucosa in patients who did not respond to neo-adjuvant chemotherapy.

22.01% of the variability was explained by the first latent variable. The use of only the first latent variable was suggested by the cross validation (Figure 28). Good discrimination was obtained on the scores plot with an area under the curve of 0.6987 on performing a ROC analysis.

The loadings obtained on the first latent variable were then exported to a Bruker format to enable display on the Chenomx software. A list of peaks was thus produced which were discriminatory on the first latent variable (Figure 29).

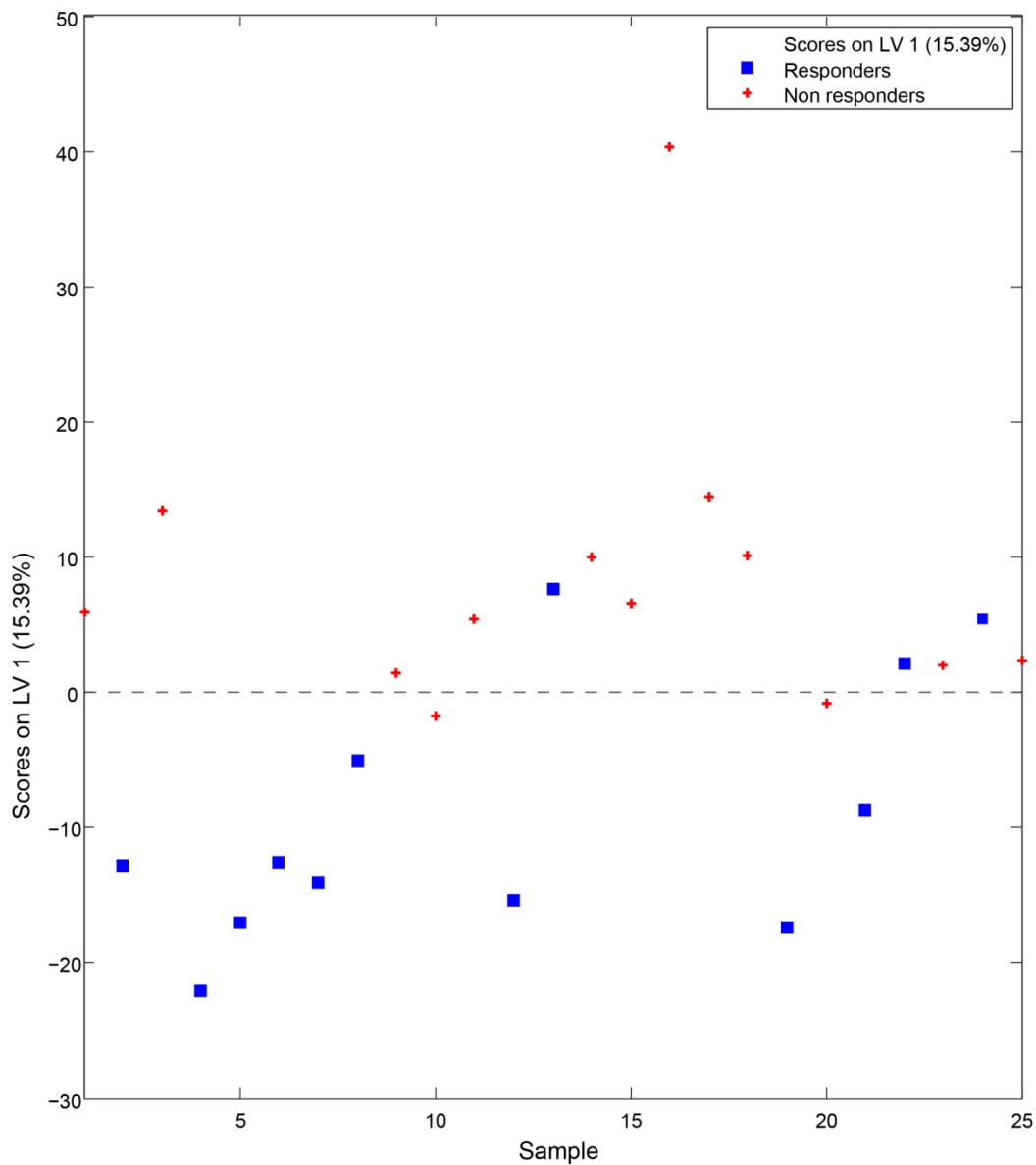


Figure 28 PLS-DA Model 5 Tissue

Crosses indicate non responders (patients with TRG 4-5 or no response on RECIST) and squares indicate responders (patients with TRG 1-3 or response on RECIST).

The following peaks were considered discriminatory for the two classes.

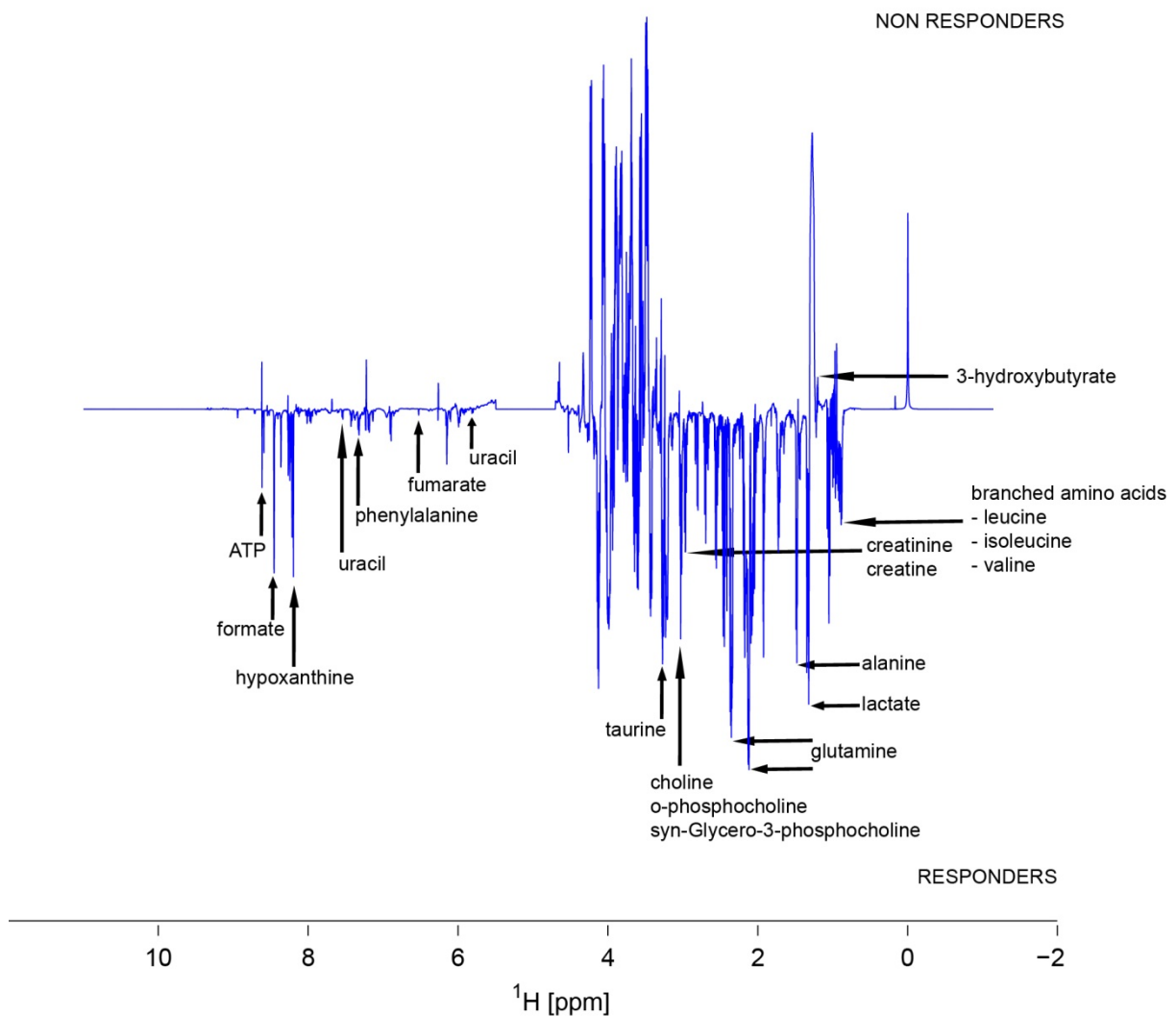


Figure 29 Loadings plot for LV1 Model 5 Tissue

3.5 Univariate analysis of metabolites

Univariate analysis was performed for all metabolites that were identified using the Chenomx software. Univariate analysis was performed using non-parametric tests (Mann Whitney U test) on the integrals of the individual metabolites. The first step before performing the integration for any peak was to align that individual peak. Following this the limit of integration was defined to include the entire peak except if there was overlap with a

neighbouring signal in which case the minimum between the two peaks was used as a boundary for integration. For metabolites with peaks at several chemical shifts, the resonance at the chemical shift with least overlap with other peaks was selected.

3.5.1 Results of univariate analysis in plasma (tabulated results in appendix)

On univariate analysis of the integration of metabolites, the largest numbers of statistically differing metabolites were seen in Model 1. Four metabolites were significant in model 4 followed by three metabolites each in model 2 and model 3. However there was no metabolite that was consistently significant in models 2,3 and 4. Nine metabolites were statistically significant in model 5 on univariate analysis. Since model 6 only compared plasma samples at 3 time points from the 5 healthy volunteer controls, no attempts were made to identify any metabolites for univariate analysis.

3.5.2 Results from tissue (tabulated results in appendix)

On univariate analysis of the integration of metabolites, the largest numbers of statistically differing metabolites were seen in Model 1. Since model 1 had only been constructed to demonstrate the ability of NMR in differentiating between two normal tissue types, no attempts were made to explore these differences any further.

In model 2 of tissue, again a large number of metabolites were statistically significant. Model 3 of tissue compared three different types of tissue and thus a non parametric analysis was not performed. Five metabolites were statistically significant in model 4 followed by only one metabolite in model 5 on univariate analysis.

3.6 Selection of metabolites of interest

Selection of metabolites for further discussion was made on the basis the results of the multivariate analysis (PLS-DA) followed by the statistical significance on univariate analysis. These differences were then confirmed by visual inspection of overlaid spectra (without g log transformation) for the various models.

Inspection of the loadings plots for the various models in plasma analysis revealed that 3-hydroxybutyrate was elevated in plasma from cancer patients (Model 1 plasma). It was higher in non responders (Model 3 plasma), node positive disease (Model 4 plasma) and full thickness tumours (Model 5 plasma) compared to responders, node negative and early local disease. When cross referenced with the univariate analysis, the level of 3-hydroxybutyrate was indeed higher in plasma from cancer patients ($p < 0.05$; Mann Whitney U test; Model 1). Increased levels of 3-hydroxybutyrate were also noticed in cancer mucosa as compared to paired normal control mucosa (Model 2 tissue). These differences were further confirmed on visual inspection of the spectra (Figure 43, Figure 44, Figure 45, Figure 46).

No other consistent differences were obtained from plasma based on multivariate analysis. Similarly, none of the metabolites were statistically significant in all the models on univariate analysis.

Inspection of the loadings plots for tissue revealed that hypoxanthine was higher in cancer mucosa as compared to normal mucosa (Model 2 tissue). In model 3 it was noticed that levels of hypoxanthine in Barrett's mucosa associated with cancer were in between those of normal mucosa and cancer mucosa. This difference was also noted on univariate analysis for model 2

($p < 0.0001$; Mann Whitney U test). These differences were eventually confirmed on inspection of the spectra (Figure 31, Figure 32).

In model 2, both choline containing metabolites and valine were significant on multivariate and univariate analysis. Similarly, in model 4 choline containing metabolites were noticed on multivariate and univariate analysis. None of the other metabolites were consistently seen both on multivariate and univariate analysis and confirmed on inspection of the spectra.

STOCSY was also performed for most of the models in tissue to identify any significant correlations or anti-correlations between metabolites. This has been further discussed in section 3.7.3.

3.7 Differences in metabolite levels for plasma and tissue

3.7.1 Hypoxanthine

Hypoxanthine was elevated in biopsies from adenocarcinoma in patients with oesophageal AC (type 1,2) (both pre and post treatment) compared with paired normal oesophageal squamous mucosa in Tissue model 2. This difference was first observed on the loadings. On comparison of the spectra at the chemical shift for hypoxanthine, these differences could be visually appreciated in the processed spectra without glog transformation (Figure 31). To confirm this result an NMR spectrum was acquired for a tissue sample which had high levels of hypoxanthine before and after it had been spiked to 100 mM exogenous hypoxanthine (Figure 30).

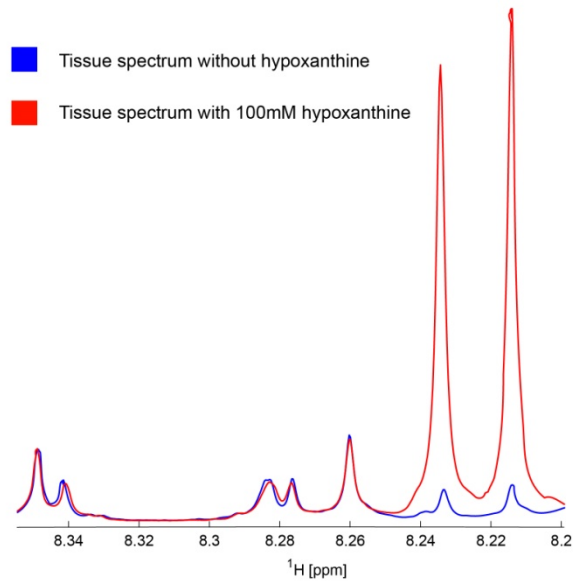


Figure 30 NMR spectra of a tissue homogenate with and without a hypoxanthine spike (100 mM)

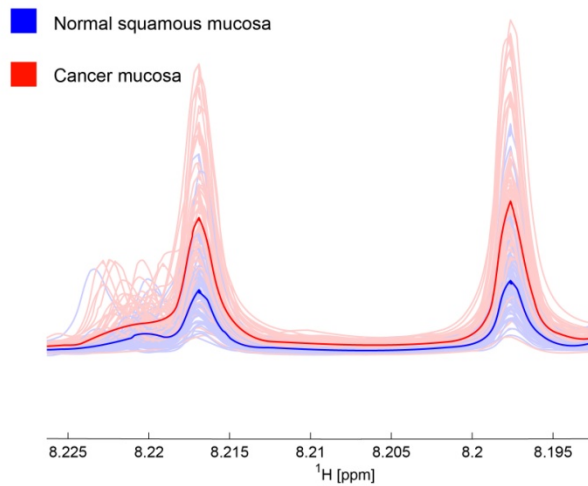


Figure 31 Level of hypoxanthine in normal squamous tissue and paired cancer mucosa (model 2).

The faded lines indicate individual spectra while the dark line indicates the mean spectrum for that class.

These differences were further examined by analysing the difference in the hypoxanthine levels in spectra from normal squamous mucosa and Barrett's mucosa in the presence of the spectrum of the cancer mucosa from the same patient. Levels of hypoxanthine in Barrett's mucosa were confirmed to lie in between those for normal squamous mucosa and cancer mucosa.

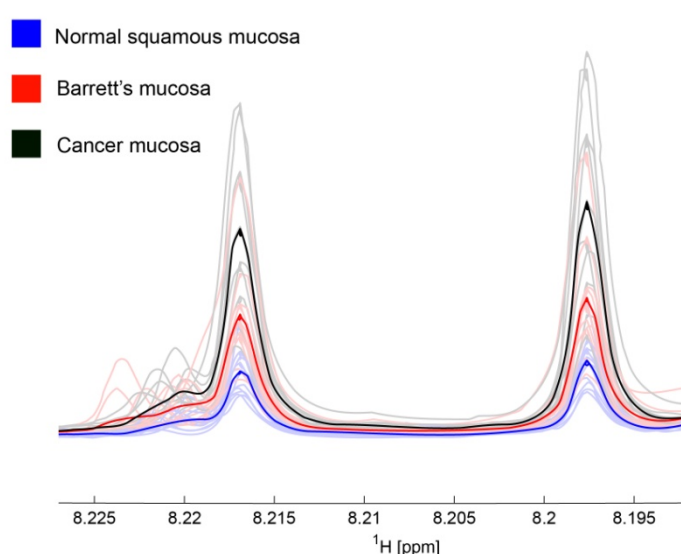


Figure 32 Levels of hypoxanthine in normal squamous tissue, paired Barrett's and cancer mucosa (model 3)

Elevated levels of hypoxanthine were observed in pre treatment biopsies of cancer mucosa from responders compared to non responders (model 5) on the loadings plot. These differences were also seen the spectra (Figure 33), although not as pronounced as the previous two models.

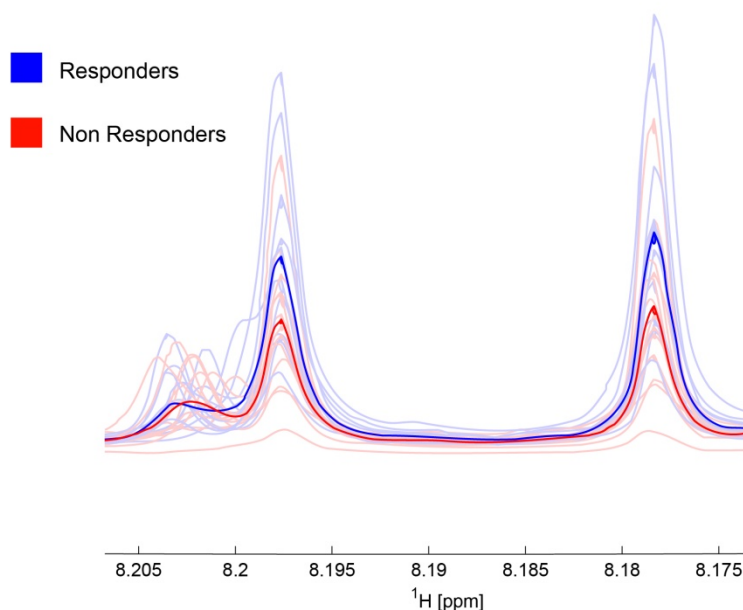


Figure 33 Level of hypoxanthine in pre chemotherapy cancer mucosa from responders and non responders (model 5).

The levels of hypoxanthine in plasma were very low. As a result an analysis of the differences between the various groups could not be performed.

To confirm the findings seen on NMR, further experiments were performed as described below.

3.7.1.1 Hypoxanthine levels in tissue (MS metabolomics)

Metabolomics Profiling with ESI was carried out using a maXis™ ultra-high resolution Q-TOF mass spectrometer coupled to HPLC separation. HPLC was carried out using a Dionex UltiMate™ 3000 (Thermo Scientific) which consists of a capillary pump, binary pump, and

autosampler whereby sample was maintained at 4°C in a thermostated autosampler before injection of 2 µl on to a capillary reversed-phase column with dimensions 300- m ID 150-mm length. The flow rate was set to 0.4 ml/min with solvent A composed of water: 0.1% formic acid and solvent B composed of acetonitrile: 0.1% formic acid in positive ion mode. For negative ion mode data, 5 mM ammonium acetate was substituted for the formic acid in solvents A and B. The sample was eluted initially with Solvent A for 7 minutes and then with a gradient climbing towards 100% B over 4.25 minutes which was then held for a further 3.75 minutes. Sodium formate was incorporated was injected as an external calibrant.

To reduce systematic errors associated with instrumental drift, samples were run in a randomly selected order. Data were collected in ESI mode in separate runs operated in full scan mode with ranges set from 50 to 600 m/z. Capillary voltage was 4,800 V with a scan rate of 0.5 scan per second; the nebulizer pressure was set 0.4 Bar, with a dry gas temperature of 4 L/min. The datasets were automatically recalibrated and all relevant features were extracted in the profile analysis 2.0 (Bruker Daltonics) processing software. Data was bucketed to 1 min/0.3 Mz ranges before normalization to total sum of buckets. A Principal Component Analysis (PCA) of the processed data was then generated. Putative identification of metabolites was possible using accurate HMDB database [173, 174] and subsequently confirmed where possible by MS/MS fragmentation. Fragmentation patterns were compared not just to HMDB database but also to published fragmentation data as generated by Lu et al. [175].

Hypoxanthine was elevated in biopsies from adenocarcinoma in patients with oesophageal ADC (type 1,2) (both pre and post treatment) compared with paired normal oesophageal squamous mucosa in Tissue model 2 (Figure 34).

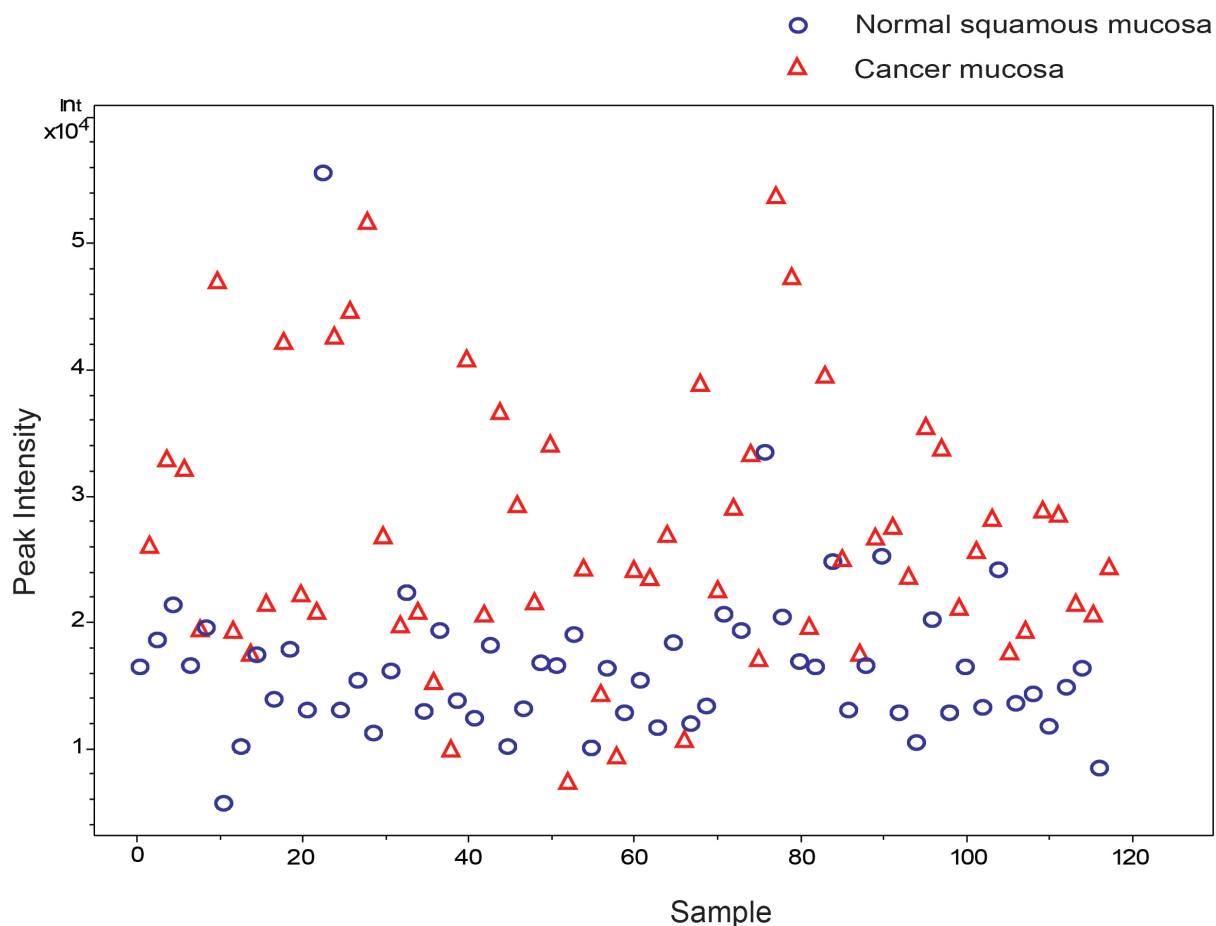


Figure 34 Level of hypoxanthine in normal squamous tissue and paired cancer mucosa (model 2) on MS metabolomics

Circles indicate tissue biopsies from normal squamous mucosa and triangles indicate biopsies from cancer mucosa in patients with oesophageal adenocarcinoma type 1,2.

Much similar to the results from NMR, the level of hypoxanthine in Barrett's mucosa in the presence of a cancer was thus confirmed to be in between those for normal squamous mucosa and cancer mucosa (Figure 35).

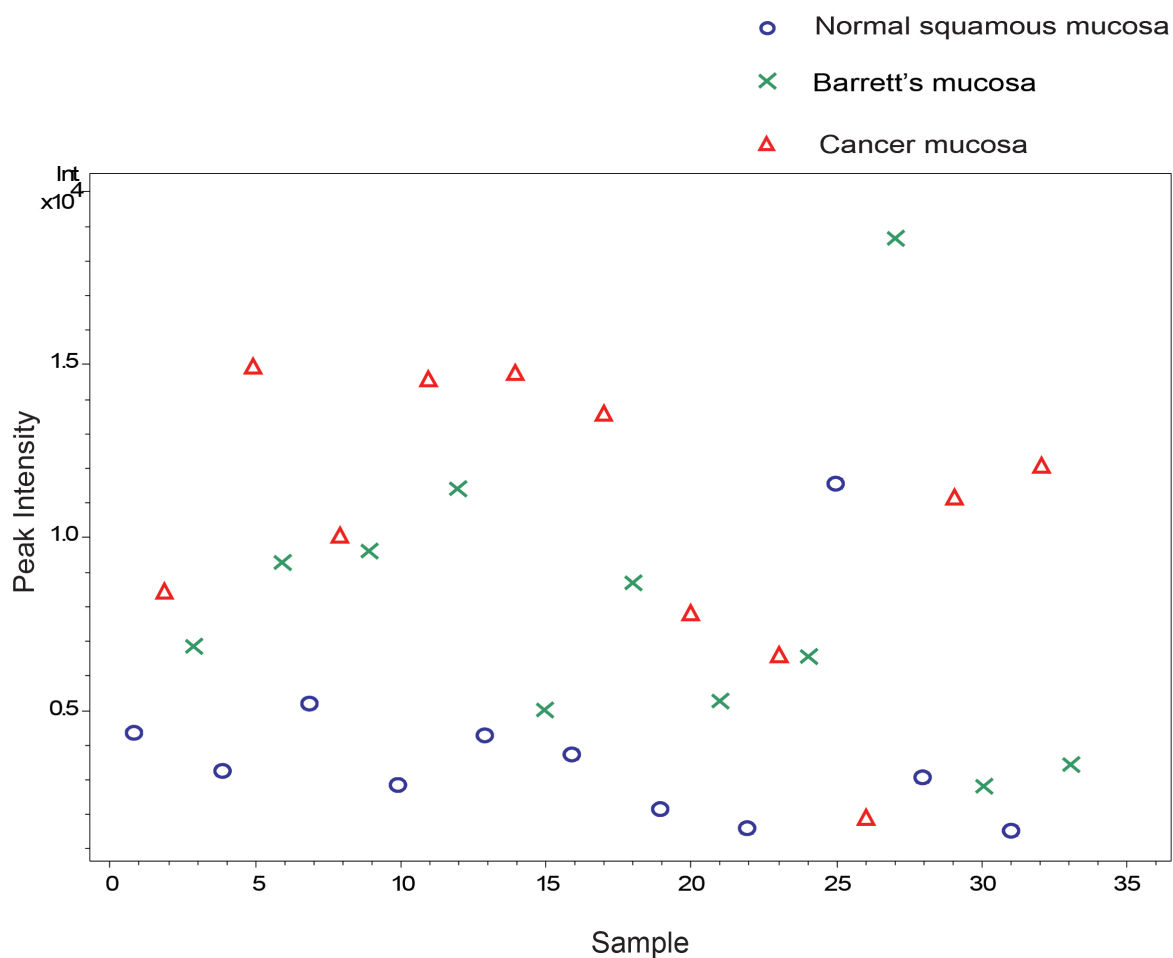


Figure 35 Levels of hypoxanthine in normal squamous tissue, paired Barrett's and cancer mucosa (model 3) on MS metabolomics

Circles indicate tissue biopsies from normal squamous mucosa, crosses indicate biopsies from Barrett's mucosa and triangles indicate biopsies from cancer mucosa in patients with oesophageal adenocarcinoma type 1,2.

3.7.1.2 Hypoxanthine phosphoribosyl transferase activity

Total cellular RNA was extracted using TRIZOL (Invitrogen). Frozen biopsies were homogenised directly in the reagent and further processed following the supplier's instructions. The resulting total RNA was then further purified on RNeasy Mini columns

(Qiagen) according to the supplied protocol. RNA quality was checked on an Agilent Bioanalyser and only RNA with a RNA integrity number (RIN) of 6.0 or more was used.

200 ng of this total RNA was worked up following the manufacturers' procedures using an Ambion WT Expression kit then fragmented and labelled using an Affymetrix WT Terminal Labelling Kit.

Labelled RNA was hybridised to Affymetrix Human Gene 1.0 ST arrays followed by washing and staining on an Affymetrix FS450 fluidics station. Arrays were scanned using an Affymetrix Scanner 3000 7G. Affymetrix Command Console was used for instrument control and data acquisition. All procedures were according to standard Affymetrix protocols.

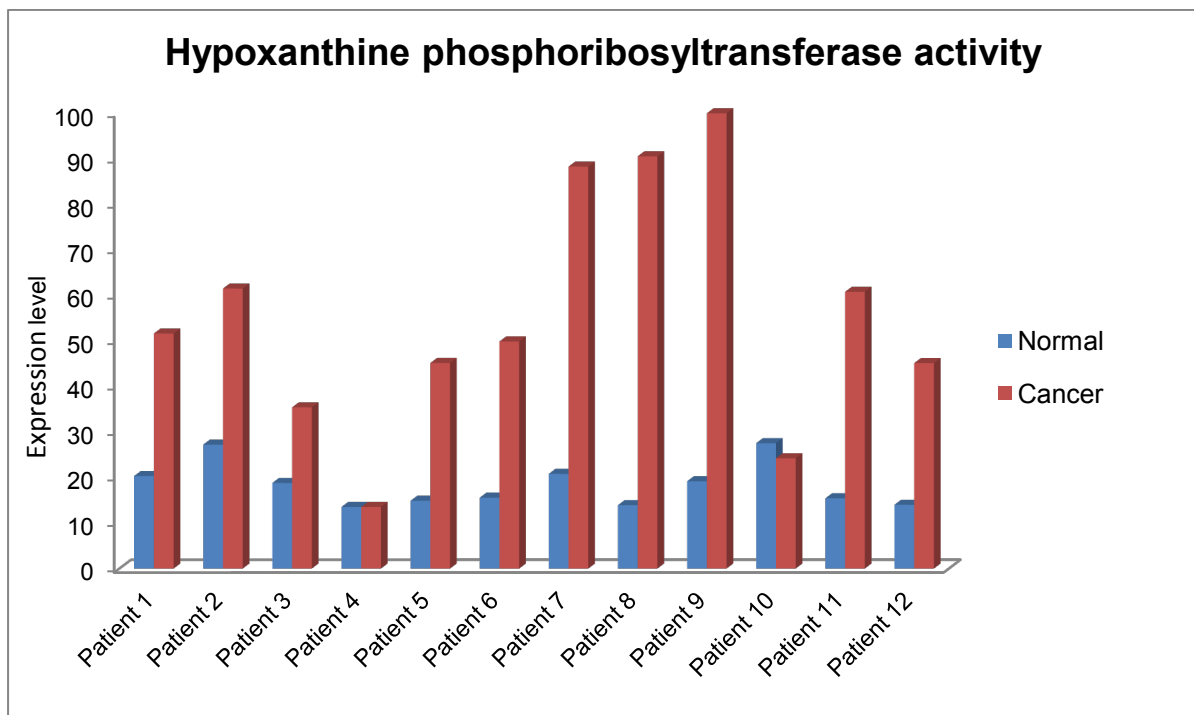


Figure 36 Hx-PRTase activity as indicated by gene expression analysis (Affymetrix) for normal squamous mucosa and paired cancer mucosa. Patient number represents the anonymised biopsy tag.

It was seen the hypoxanthine phosphoribosyltransferase activity was higher in cancer mucosa compared to the adjacent normal mucosa (Figure 36). This supports the observation of higher levels of hypoxanthine in cancer tissues seen in metabolomics.

Furthermore, a similar pattern to that seen in hypoxanthine in tissue was again observed in a those patients who had the trio of normal, Barrett's and cancer mucosa (Figure 37).

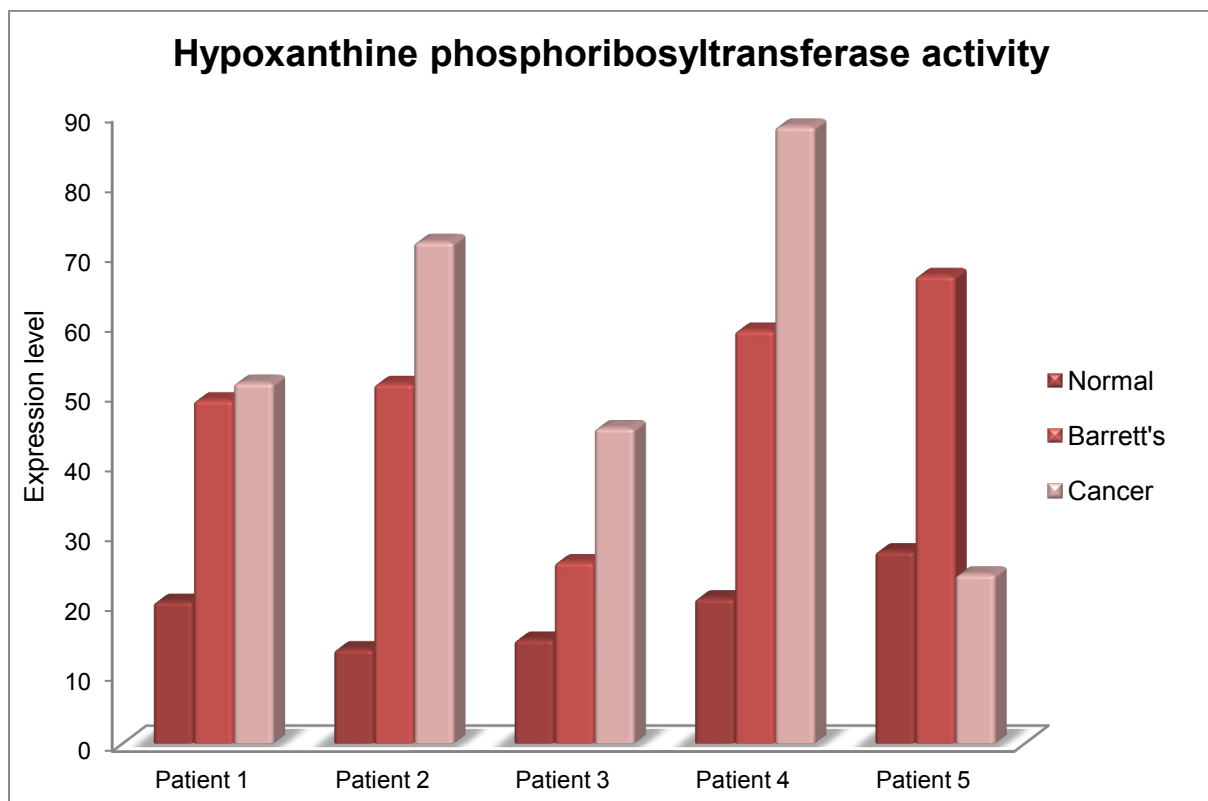


Figure 37 Hx-PRTase activity as indicated by gene expression analysis (Affymetrix) for normal squamous mucosa, and paired Barrett's and cancer mucosa

3.7.2 3-hydroxybutyrate

3-hydroxybutyrate was elevated in biopsies from adenocarcinoma in patients with Oesophageal ADC (type 1,2) (both pre and post treatment) compared to paired normal oesophageal squamous mucosa biopsies in Tissue model 2. This difference was first observed

on the loadings. On comparison of the spectra at the chemical shift for 3-hydroxybutyrate, these differences could be visually appreciated in the processed spectra without glog transformation (Figure 41).

To confirm the presence of 3-hydroxybutyrate in the samples, a 2D Hadamard $^1\text{H},^1\text{H}$ -TOCSY-NMR spectrum was obtained on 3-hydroxybutyrate (chemical shift 1.22 ppm) (Figure 38). The selective pulses used had Gaussian shape using a selection bandwidth of 16 Hz. The spectra used longitudinal encoding and a DIPSI2 mixing sequence of 0, 70 and 120 ms for the TOCSY transfer [176]. 256 transients were acquired for 7 selected frequencies.

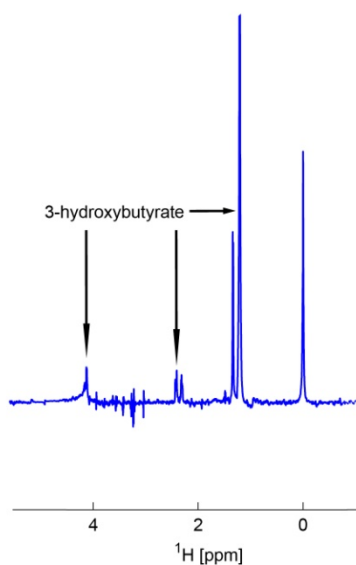


Figure 38 2D Hadamard $^1\text{H},^1\text{H}$ -TOCSY-NMR spectrum on a tissue homogenate with suspected high level of 3-hydroxybutyrate

The doublet at 1.2ppm was selected for the Hadamard and the magnetisation was transferred using TOCSY to the quartet at 2.3ppm and the doublet at 4.15ppm.

Further confirmation of the presence of 3-hydroxybutyrate was obtained by acquiring an NMR spectrum for a tissue sample which had high levels of 3-hydroxybutyrate before and after it had been spiked to 500 μM exogenous 3-hydroxybutyrate (Figure 39, Figure 40).

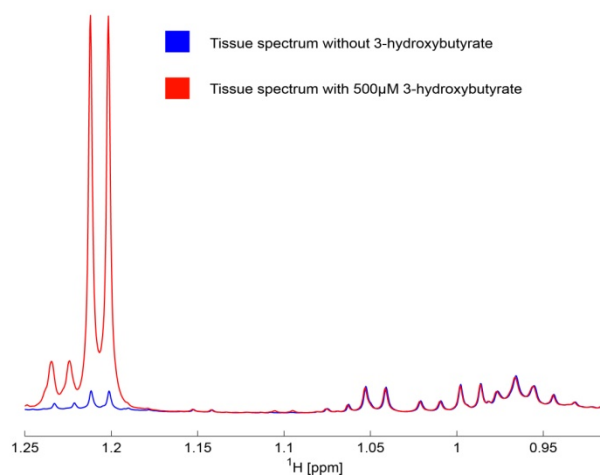


Figure 39 NMR spectra of a tissue homogenate with and without a 3-hydroxybutyrate spike (500 μM)

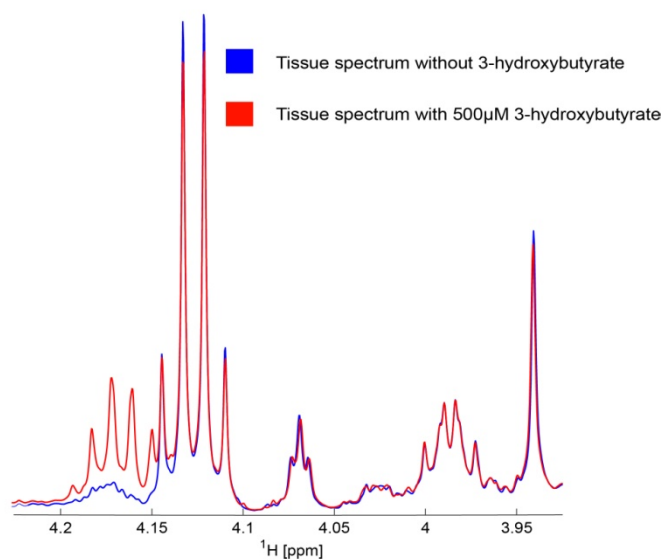


Figure 40 NMR spectra of a tissue homogenate with and without a 3-hydroxybutyrate spike (500 μM)

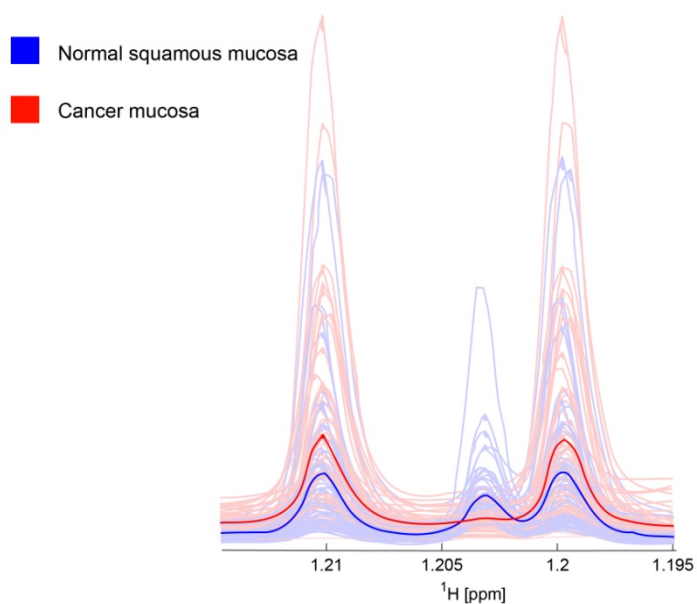


Figure 41 Level of 3-hydroxybutyrate in normal squamous tissue and paired cancer mucosa on Model 2 Tissue

The difference in the levels of 3-hydroxybutyrate for tissue models 3, 4 and 5 was not visualised on the spectra.

3-hydroxybutyrate was elevated in pre treatment plasma samples from patients with oesophageal adenocarcinoma (type 1,2) compared with plasma from control patients in model 2. This difference was first observed on the loadings. On comparison of the spectra at the chemical shift for 3-hydroxybutyrate, these differences could be visually appreciated in the processed spectra without glog transformation (Figure 42, Figure 43).

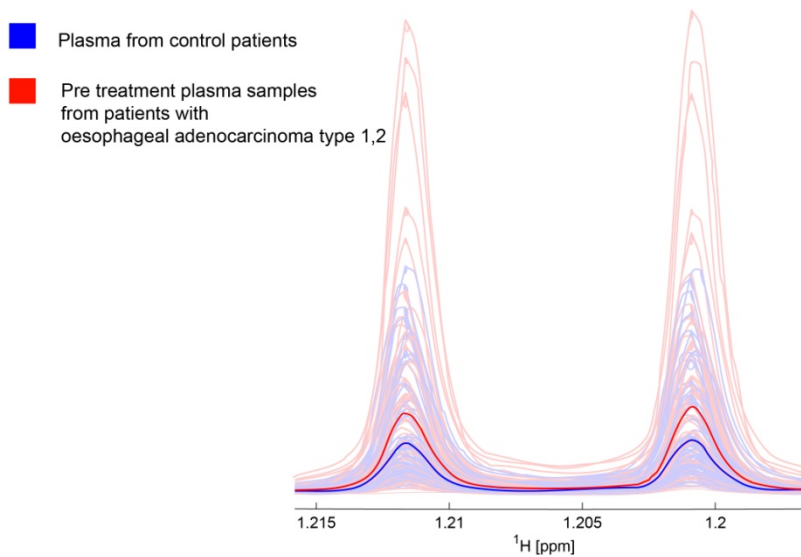


Figure 42 Level of 3-hydroxybutyrate in plasma from control patients and pre treatment plasma from patients with cancer Model 1 Plasma

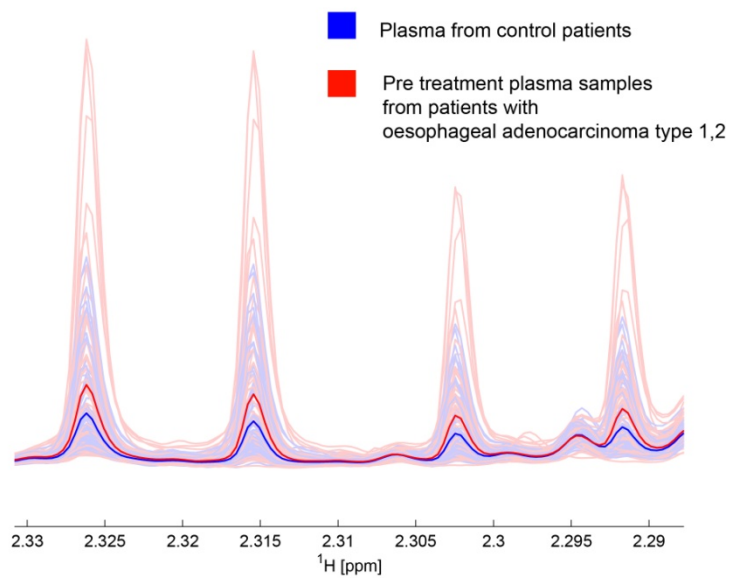


Figure 43 Level of 3-hydroxybutyrate in plasma from control patients and pre treatment plasma from patients with cancer Model 1 Plasma

Similarly, elevated levels of 3-hydroxybutyrate were noticed for pre treatment plasma samples from non responders versus pre treatment plasma samples from responders (model 3) (Figure 44). On analysing the plasma samples longitudinally, the levels for 3-hydroxybutyrate were higher following treatment for both responders and non responders. 3-hydroxybutyrate was also elevated in plasma from patients with nodal disease N1 vs. plasma from patients with nodal disease N0 (model 4) (Figure 45) and plasma from patients with T stage T3, T4 vs. plasma from patients with T stage T1, T2 (model 5) (Figure 46).

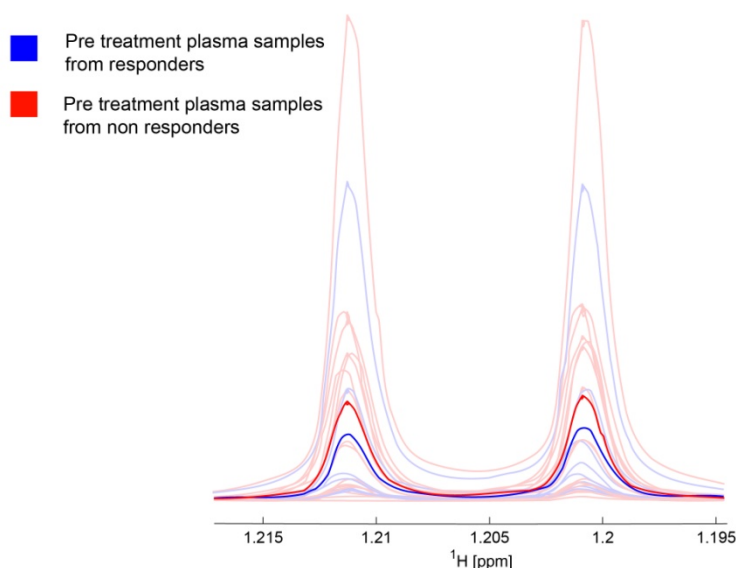


Figure 44 Level of 3-hydroxybutyrate in pre treatment plasma samples from responders and non-responders Model 3 Plasma

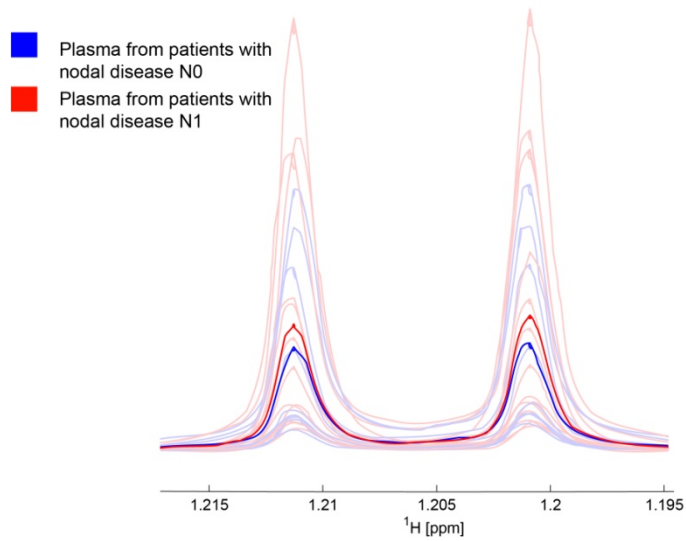


Figure 45 Level of 3-hydroxybutyrate in pre surgery plasma samples from patients not receiving neoadjuvant chemotherapy and plasma samples from patients undergoing palliative treatment without chemotherapy on Model 4 Plasma

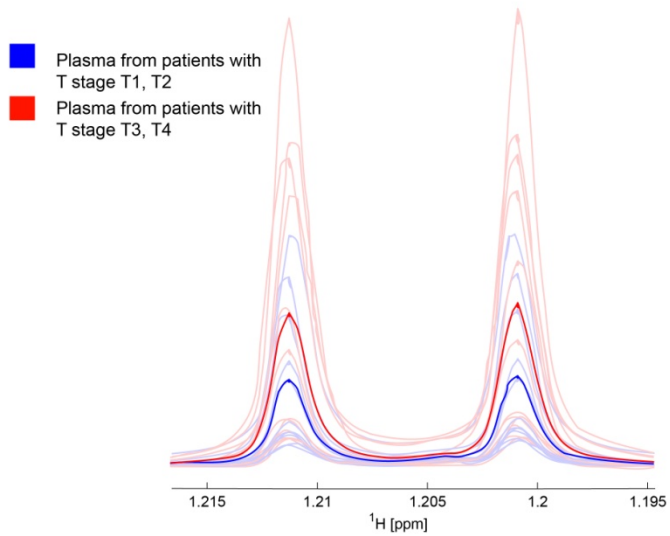


Figure 46 Level of 3-hydroxybutyrate in pre surgery plasma samples from patients not receiving neoadjuvant chemotherapy and plasma samples from patients undergoing palliative treatment without chemotherapy on Model 5 Plasma

3.7.3 Succinate and fumarate

In most tissue models a positive correlation was seen between succinate and fumarate levels. However, for model 4 (dysplastic Barrett's vs. non dysplastic Barrett's), a reversed correlation was noticed between. To further confirm this result an NMR spectrum was acquired for a tissue sample before and after it had been spiked to 500 μM exogenous succinate and fumarate on two separate occasions (Figure 47, Figure 48).

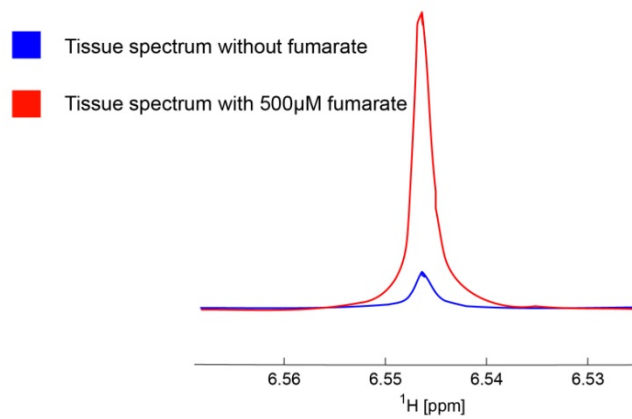


Figure 47 NMR spectra of a tissue homogenate with and without a fumarate spike (500 μM)

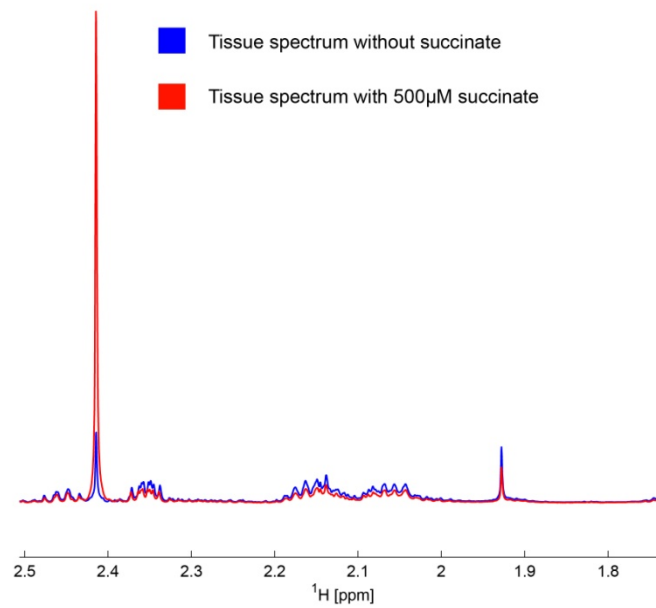


Figure 48 NMR spectra of a tissue homogenate with and without a succinate spike (500 μM)

A STOCSY was then performed on each of the classes in this model. It was noticed that although for non dysplastic Barrett's there was a positive correlation between succinate and fumarate (0.6615) (Figure 49); this correlation was negative for dysplastic Barrett's (-0.4594) (Figure 50). These results were further confirmed on performing a Spearman correlation on the integrals of these metabolites.

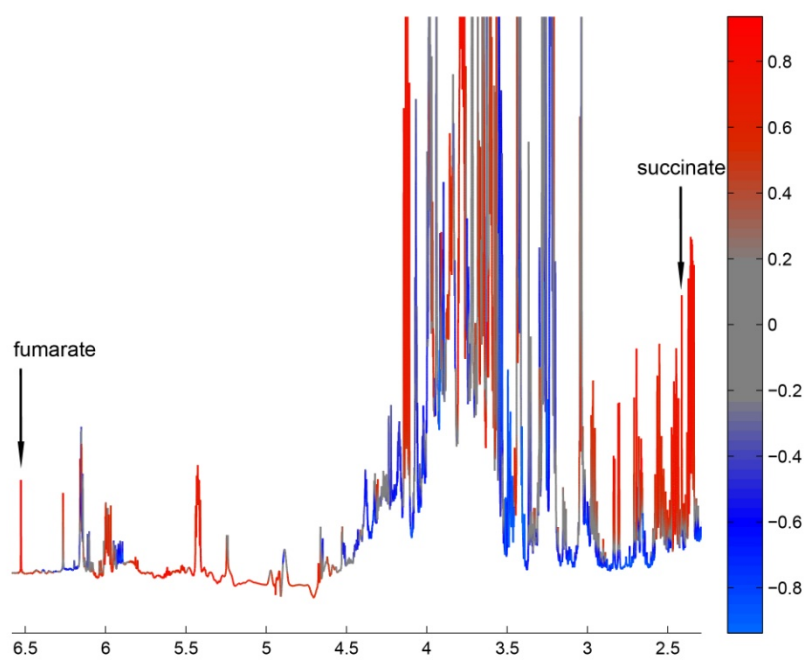


Figure 49 STOCSY on non dysplastic Barrett's tissue samples on Model 4 Tissue

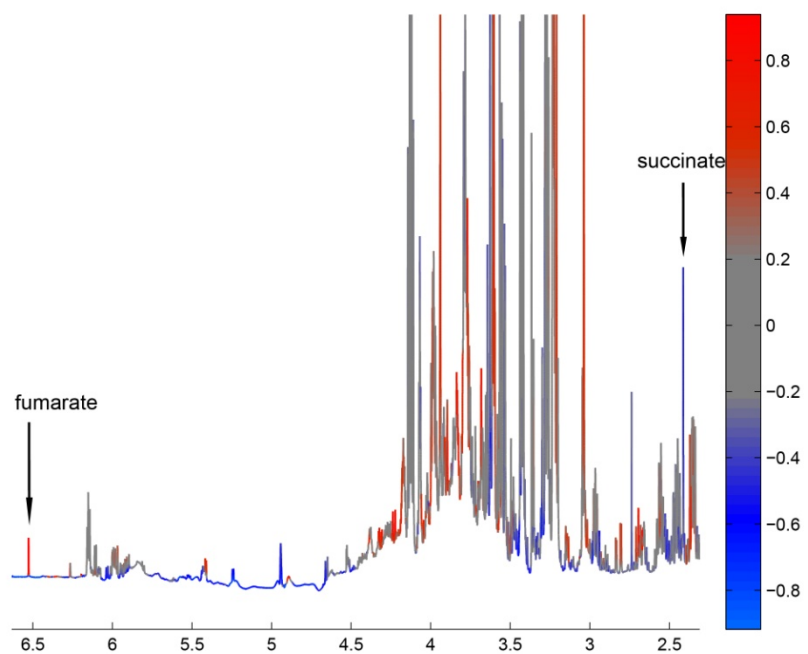


Figure 50 STOCSY on dysplastic Barrett's tissue samples on Model 4 Tissue

Following this observation, STOCSY was performed on the three subclasses in model 3 for tissue (normal squamous mucosa vs. dysplastic Barrett's mucosa vs. cancer mucosa). Similar results were obtained as for model 4. There was no correlation between succinate and fumarate for normal squamous mucosa (0.1368) (Figure 51) and cancer mucosa (-0.1325) (Figure 53). However, this correlation was stronger and negative for the dysplastic Barrett's mucosa (-0.4678) (Figure 52).

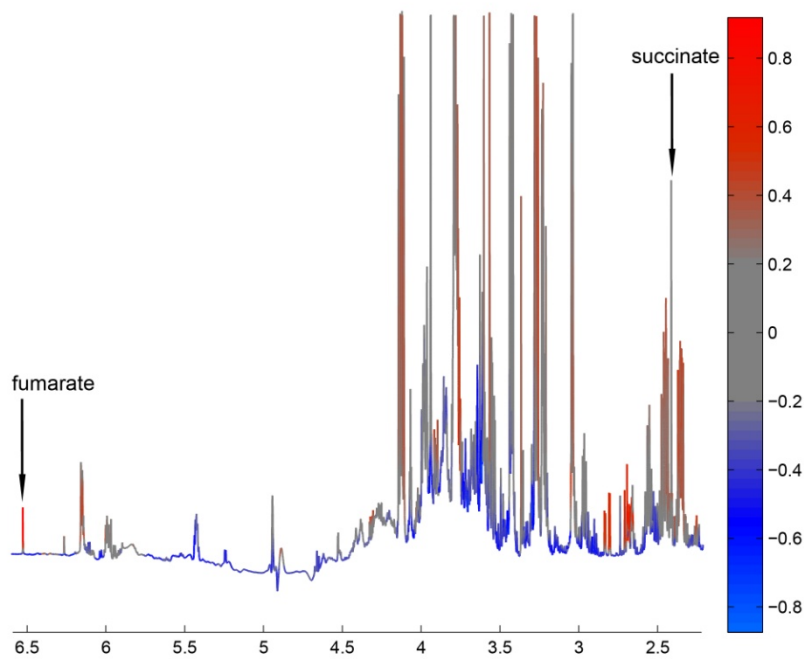


Figure 51 STOCSY on Normal squamous mucosa on Model 3 Tissue

A positive correlation is indicated on the STOCY in red; no correlation in grey and negative correlation with blue.

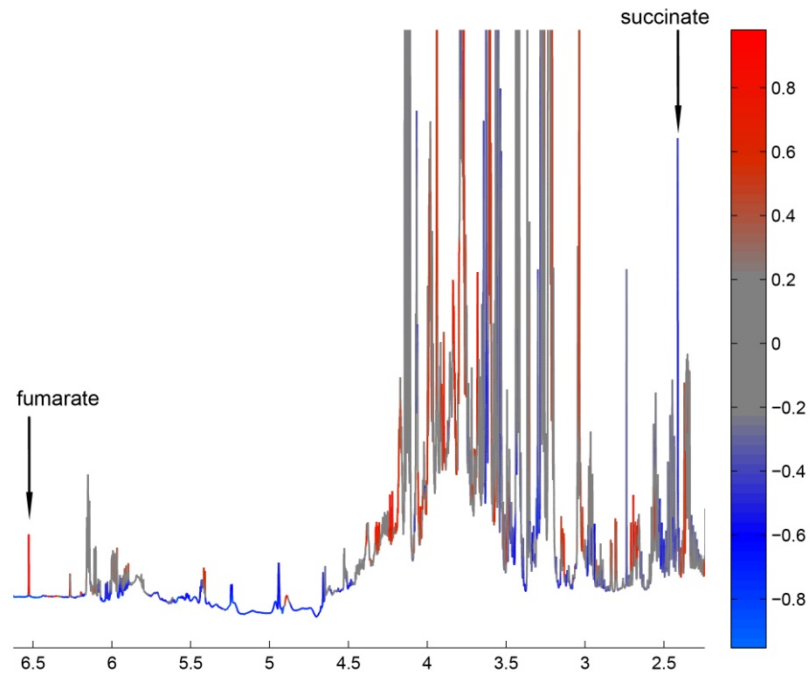


Figure 52 STOCSY on dysplastic Barrett's tissue samples on Model 3 Tissue

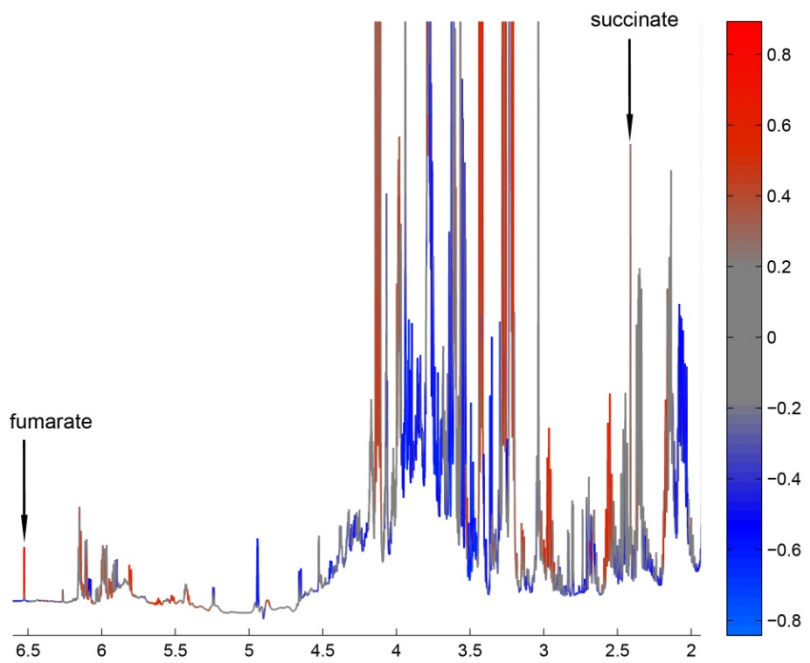


Figure 53 STOCSY on cancer tissue samples on Model 3 Tissue

3.7.4 Resonance at 2.737 ppm (Metabolite X)

An unassigned resonance at 2.737 ppm was observed to be highly elevated in dysplastic Barrett's mucosa in Tissue model 3. The mean intensity of this peak in the paired normal squamous mucosa and cancer mucosa was much lower than for the dysplastic Barrett's mucosa (Figure 54).

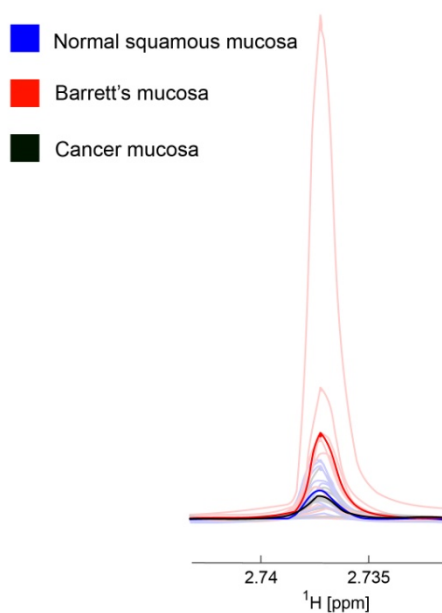


Figure 54 Level of Metabolite X in normal squamous tissue, paired Barrett's and cancer mucosa on Model 3 Tissue

Following this observation, this peak was further examined in Tissue model 4, which compared Non dysplastic Barrett's mucosa from patients undergoing Barrett's surveillance to patients with dysplastic Barrett's mucosa (patients who had Barrett's mucosa associated with an adenocarcinoma). As in model 3, the mean intensity of the peak at 2.737 ppm was much higher in dysplastic Barrett's mucosa compared to non-dysplastic Barrett's mucosa (Figure 55).

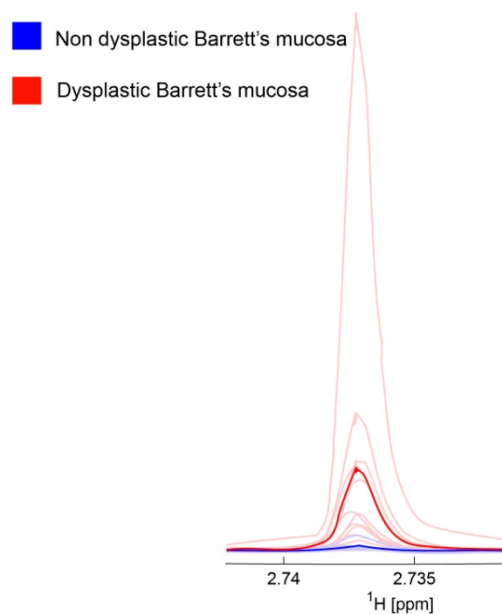


Figure 55 Level of Metabolite X in non dysplastic and dysplastic Barrett's mucosa on Model 4 Tissue

The only peak matching the resonance of this peak in Chenomx was sarcosine, but this was confirmed not to be the case as the second peak for sarcosine at 3.6 ppm was not present in these spectra. This peak could not be assigned to a specific substance from public or commercially available databases.

Following this a 2D ^{13}C -HSQC was obtained to ascertain the carbon shift for this metabolite. It was confirmed to be ^1H 2.737 ppm and ^{13}C as 41.34 ppm (Figure 56).

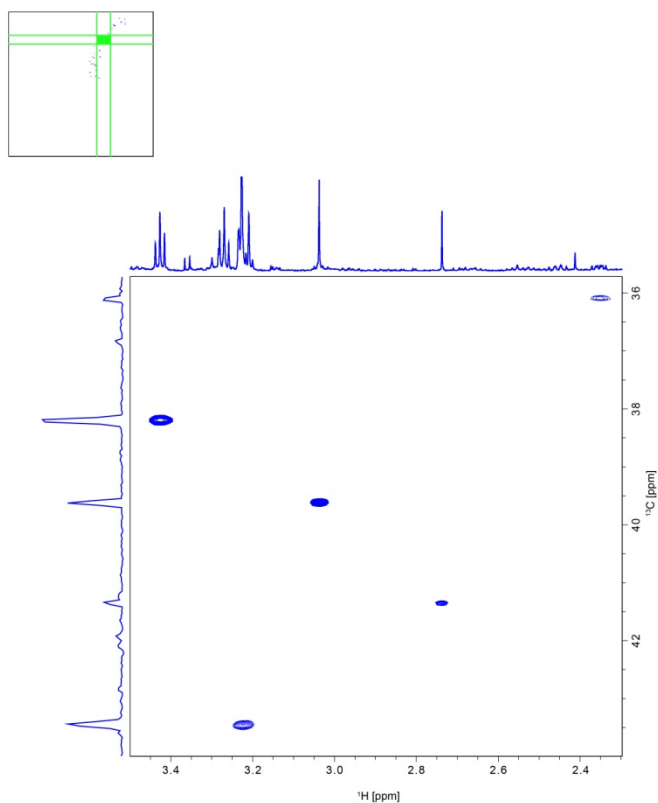


Figure 56 2D ^{13}C -HSQC on a tissue sample with high concentration of Metabolite X

The proton and carbon shifts for this molecule were determined as ^1H 2.737 ppm and ^{13}C 41.34 ppm respectively.

For further exploration of this molecule a homonuclear 2D- ^1H , ^1H -TOCSY NMR spectrum was acquired. In a TOCSY pulse sequence magnetisation is transferred between different proton nuclei of the same molecule, which will lead to cross peaks in between atoms connected by a scalar coupling in the 2D spectrum. By investigating columns or rows of this spectrum all proton resonances belonging to one molecule can be identified.

The 2D TOCSY spectrum was acquired at a field strength of 600.13 MHz. 16 transients were acquired for each FID after acquiring 16 steady state scans at the beginning of the 2D-NMR experiment. A total of 2048 data points for the direct and 256 data points for the indirect time

domain were acquired. The spectral width was set to 7211 Hz (12 ppm) for both dimensions. The inter-scan relaxation delay was set to 2s. A hard pulse power of 25 kHz was used while the DIPSI-2 sequence was executed at a B_1 field strength of 6250 Hz for a mixing time of 60 ms.

A detailed inspection of the 2D-TOCSY spectrum did not reveal any further resonances belonging to the ^1H resonance at 2.737 ppm (Figure 57).

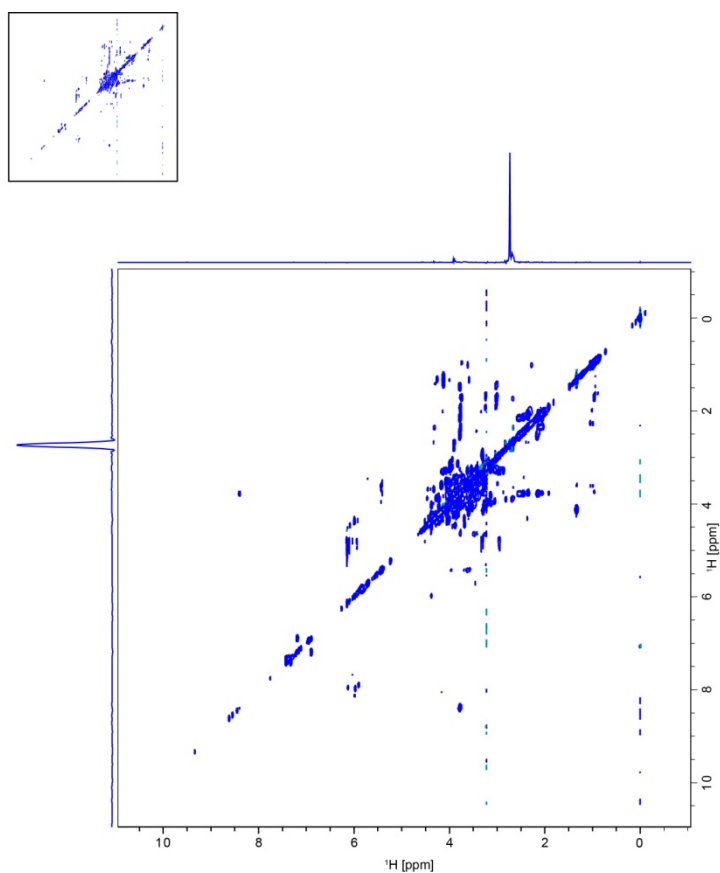


Figure 57 Homonuclear 2D- ^1H , ^1H -TOCSY NMR spectrum with high concentration of Metabolite X

To exclude contamination following methanol chloroform extraction, a 1D spectrum was obtained from tissues extracted using phosphate buffer solution and extraction buffer. The peak was again visualized at 2.737 ppm, confirming the presence of this metabolite in tissue.

This peak was also present in all plasma samples at 2.738 ppm (Figure 58).

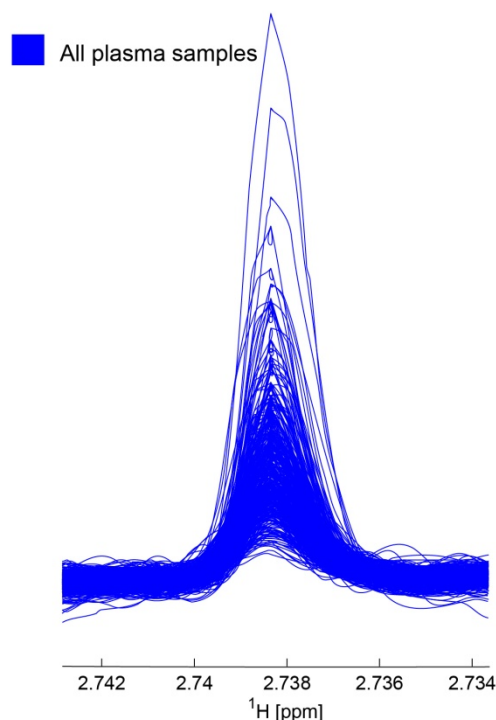


Figure 58 Level of Metabolite X in all plasma samples

3.7.5 Unassigned resonance at 3.72 ppm (Metabolite Y)

A peak at 3.72 ppm was observed to be highly elevated in non dysplastic Barrett's mucosa in Tissue model 4 (Figure 59). The mean intensity of this peak in the dysplastic Barrett's mucosa was much lower. Once again, an assignment for this peak could not be obtained by searching the available databases.

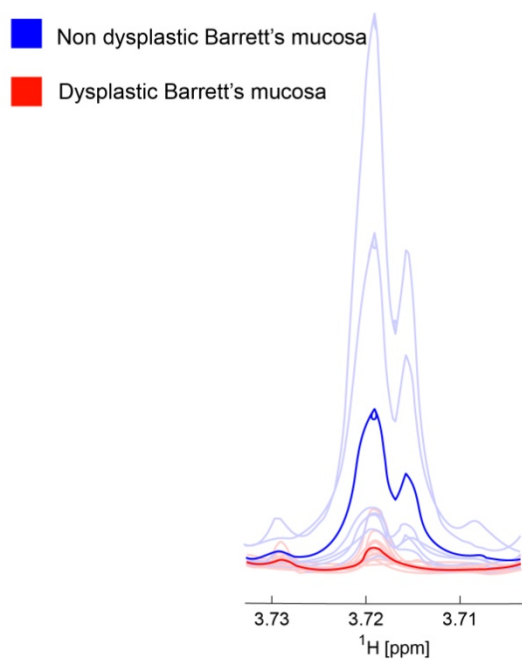


Figure 59 Level of Metabolite Y in non dysplastic and dysplastic Barrett's mucosa on Model 4 Tissue

Following this a 2D ^1H , ^{13}C -HSQC NMR spectrum with a very large number of data points for the indirect dimension was obtained in order to ascertain the carbon shift for this metabolite with very high precision. It was confirmed to be ^1H 3.72 ppm and ^{13}C as 72.3 ppm (Figure 60).

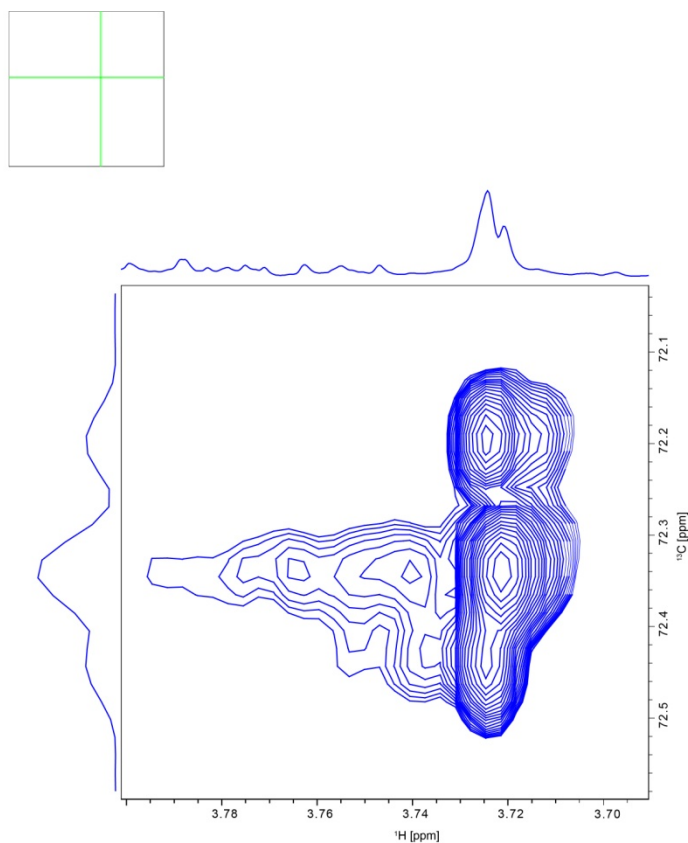


Figure 60 2D ^1H , ^{13}C -HSQC NMR of a tissue sample with high concentration of Metabolite Y. The proton and carbon shifts for this molecule were determined as ^1H 3.72 ppm and ^{13}C 72.3 ppm respectively.

For further exploration of this molecule a homonuclear 2D- ^1H , ^1H -TOCSY NMR spectrum was acquired. However, a detailed inspection of the 2D-TOCSY spectrum didn't reveal any further resonances belonging to the ^1H resonance at 3.72 ppm (Figure 61).

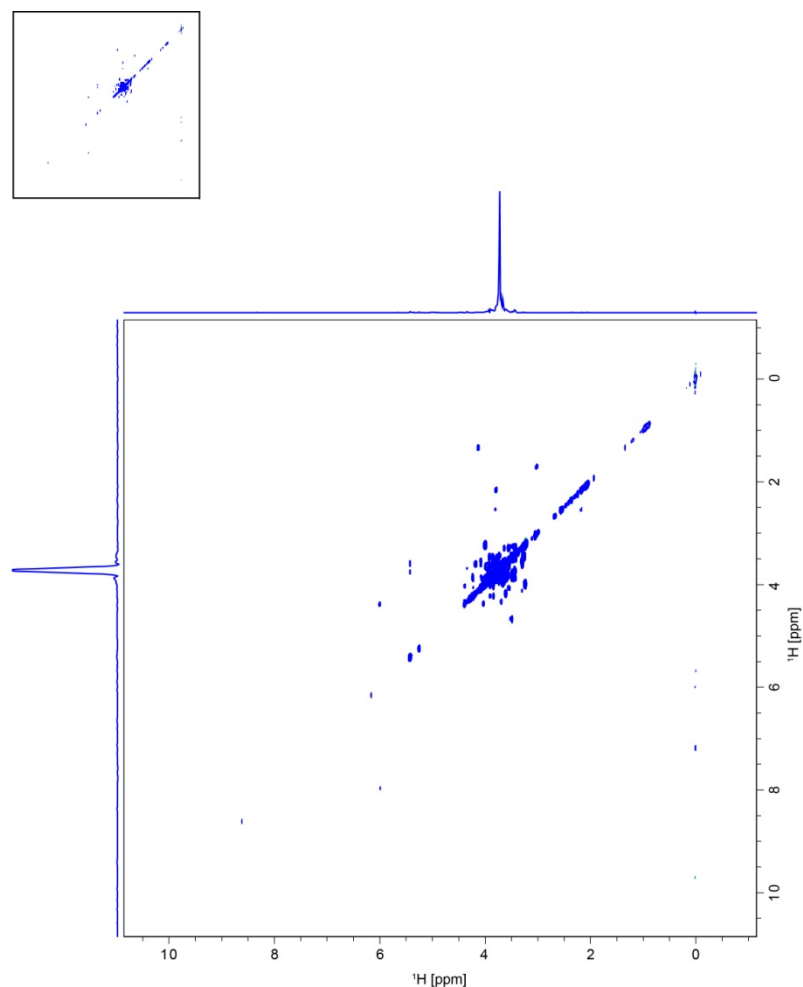


Figure 61 Homonuclear 2D- ^1H , ^1H -TOCSY NMR spectrum with high concentration of Metabolite Y

Due to lack of an identity for this metabolite, it was again postulated that this might be the result of contamination during the methanol chloroform extraction. While considered unlikely on the basis that the quantity of metabolite Y should have been proportional to the weight of the tissue extracted (as the methanol and chloroform were added in proportion to the weight), and this was not the case, to completely exclude this as possibility, a 2D ^{13}C -HSQC was obtained from tissue extracted using phosphate buffer solution. The resulting spectrum was overlaid with the high resolution 2D ^1H , ^{13}C -HSQC spectrum that was acquired earlier (Figure 62). The overlay confirmed the presence of this metabolite at the same

resonance in the tissue extracted using phosphate buffer solution. It was concluded that this was a metabolite found in the tissue, although it could not be further defined.

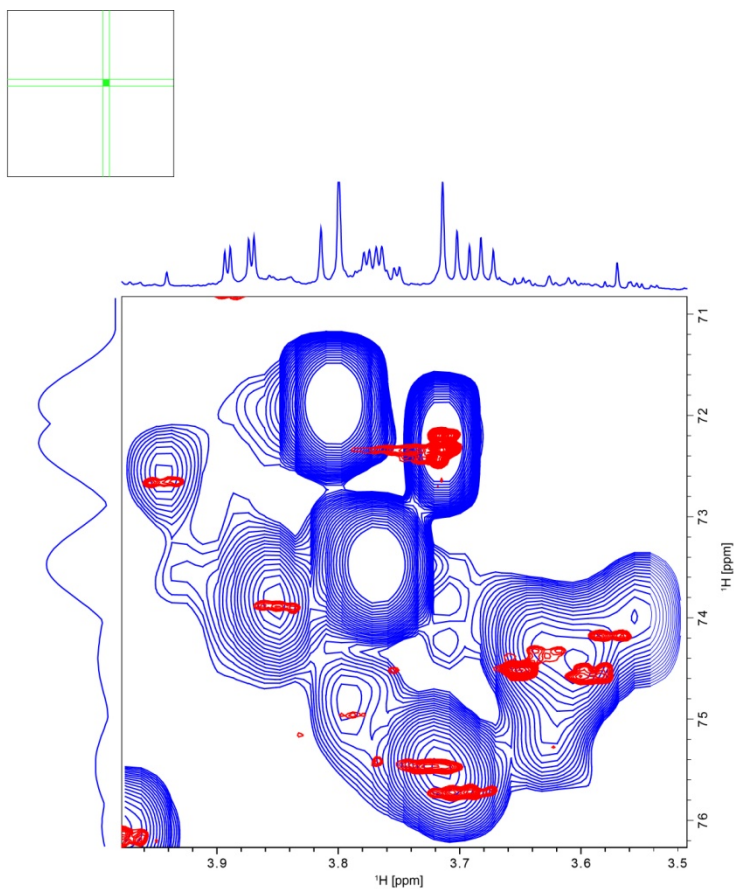


Figure 62 Overlay 2D ^1H , ^{13}C -HSQC

2D ^{13}C -HSQC was obtained from tissue extracted using phosphate buffer solution (represented in red) overlaid with ^1H , ^{13}C -HSQC NMR of a tissue sample with high concentration of Metabolite Y (represented in blue).

DISCUSSION

Numerous biomarkers that identify disease, cancer stage and prognosis have been described in the last 20 years. Some of these reflect exciting discoveries at the genome level. A few are currently used in standard clinical practice. These include CA 19.9 and CA 125 for diagnosis of pancreatic and ovarian malignancies, prostate specific antigen for diagnosis, stage and prognostication in prostate cancer and carcino-embryonic antigen (CEA) for monitoring colonic cancer as a means of identifying recurrence [177].

There have been major advances in treatments tailored to a specific predictor or gene signature. Markers have been described that can predict how a disease might respond to a particular treatment. In breast cancer, human epidermal growth factor receptor 2 (Her-2) overexpression predicts response to trastuzumab, the monoclonal antibody that blocks this receptor [178] and oestrogen receptor positivity predicts tamoxifen response [179]. In chronic myeloid leukaemia, a breakpoint cluster region–Abelson murine leukaemia oncogene (BCR–ABL) translocation predicts response to imatinib mesylate [180]. Similarly for colonic cancer, mutations in KRAS predict response to epidermal growth factor receptor (EGFR) specific antibody therapy [181]. In lung cancer EGFR kinase domain mutations predict response to erlotinib or gefitinib) [182] and in brain tumours EGFR mutations in the extracellular domain dictate response EGFR inhibitors [183]. Similar predictors that can be used to direct treatment for oesophageal adenocarcinoma have yet to be described.

Despite these advances, genomic and more recently proteomic technologies, have failed to provide satisfactory information describing the aetiology, pathogenesis and outcome for many conditions. Oesophageal adenocarcinoma has received relatively little attention,

relative to its importance as a cause of cancer death in the UK. The aim of the present study was to see if plasma and tissue metabolomics could shed any light on various aspects of this disease, its development from its precursor condition Barrett's oesophagus and subsequent treatment.

During this study, a number of metabolites were seen to be statistically significant on multivariate (PLS-DA) analysis or univariate (integrations). 3-hydroxybutyrate was significant both in plasma (multivariate and univariate) and tissue and has been discussed in a subsequent section. Other interesting metabolites identified in plasma included formate, glycerophosphocholine, lysine, pyruvate and valine.

Formate has a distinctive chemical shift so preliminary identification was easy. However, it is only a singlet and therefore there was no definite assignment using 1D NMR spectra only. The only way to be certain was perform spiking experiments; however these were limited only to a few metabolites due to paucity of sample volumes. Lysine and valine are essential amino acids and as such differences could have been due to differences in protein degradation or transport processes into the cell and therefore changes wouldn't necessarily be metabolism related. The levels of pyruvate again can depend on actual nutritional state of person. Measurements of nutritional state were not performed for any of the patients in this study so it would be difficult to comment on the levels of pyruvate.

Hypoxanthine was noticed to be significant in tissue and has been discussed subsequently. After exclusion of model 1 (since it was not a clinically relevant model), only lactate and choline containing metabolites were significant in more than one model (two models each).

Lactate was statistically different in tissue models 2 and 4 on univariate analysis. A higher level was seen in normal tissue as compared to cancer mucosa (model 2) and in dysplastic Barrett's as compared to non-dysplastic Barrett's. It is difficult in the context of this study to comment on the differences in the levels of lactate. This is because of factors like variability from the time from biopsy to extraction and the warm ischaemia of the tissues, especially for the resectional specimens. During the warm ischaemia and to a lesser extent during the cold ischaemia, glycolysis is carrying on and thus levels of lactate may not accurately represent the presampling conditions. Lactate increases rapidly during hypoxia and ischaemia. Thus poorly vascularized tumours have a low intracellular pH as a result of increased lactate production. Increased rates of lactate production have been associated with a variety of neoplasms [143].

Choline containing metabolites were statistically different in models 2 and 4 of tissue. In model 2, a higher level of choline was seen in cancer mucosa as compared to normal mucosa and in dysplastic Barrett's as compared to non-dysplastic Barrett's in model 4. The term choline containing metabolites refers to choline, phosphocholine, phosphatidylcholine and glycerophosphocholine. These are key constituents of cell membranes. Their levels are known to change during apoptosis and necrosis.

Choline containing metabolites have been previously identified in numerous studies. Phospholipid metabolism has been investigated in breast cancer cells during exposure to the antimetabolic drugs paclitaxel, vincristine, colchicine, nocodazole, methotrexate and doxorubicin using ^{31}P NMR spectroscopy [184]. Phosphocholine to glutamate ratio has been shown to show the presence of oesophageal cancer in histologically-normal tissue [151].

Choline and glycerophosphocholine have been identified in childhood brain tumours using both in vivo magnetic resonance spectroscopy (MRS) and ex vivo ^1H HR-MAS [185].

Thus the current project identified a number of metabolites that were either increased or reduced in a diseased state. Before making any conclusions about their use in clinical practice, the metabolism of the consistently observed metabolites needs to be discussed, so that any potential role in cancer can be appreciated.

4.1 Hypoxanthine

An elevated level of hypoxanthine was observed in cancer mucosa compared to control normal squamous mucosa from the same patients (Figure 31). More importantly, when a trio of samples were compared from patients with oesophageal adenocarcinoma who also had biopsies of their corresponding Barrett's mucosa and normal squamous mucosa; the levels were lowest in the control mucosa and highest in the cancer mucosa (Figure 32). The findings of NMR were confirmed by similar observations from MS metabolomics of these samples. This finding was further supported by gene expression profiling of a limited number of tissues. These tissues were part of the larger sample group that was used for the NMR experiments.

4.1.1 Hypoxanthine and its role in purine salvage

Purine nucleotides are essential components of any cell comprising not just the raw material for the synthesis of DNA but also acting as vital cofactors for many different enzymatic reactions responsible for cell proliferation. Purine biosynthesis proceeds along two known

routes. These include *de novo* synthesis and recycling of endogenous or exogenous purines through a salvage pathway (Figure 63).

The *de novo* pathway for purine nucleotide synthesis leads to the formation of inosine 5'-monophosphate (IMP) in ten metabolic steps. Hydrolysis of ATP is required to drive several reactions in this pathway. Overall, the *de novo* pathway for purine nucleotide synthesis is expensive in terms of moles of ATP utilized per mole of IMP synthesized.

The salvage pathway involves the housekeeping protein hypoxanthine-guanine phosphoribosyl transferase (Hx-PRTase) which catalyses the addition of phosphoribosyl pyrophosphate to guanine or hypoxanthine to form guanosine monophosphate and inosine monophosphate respectively. In the absence of this pathway, hypoxanthine would proceed to form the waste product uric acid, through the formation of xanthine [186]. This is the congenital metabolic abnormality seen in Lesch-Nyhan syndrome where free purines (hypoxanthine and guanine) are oxidized by xanthine oxidase to uric acid which is sparingly soluble and causes gout [187].

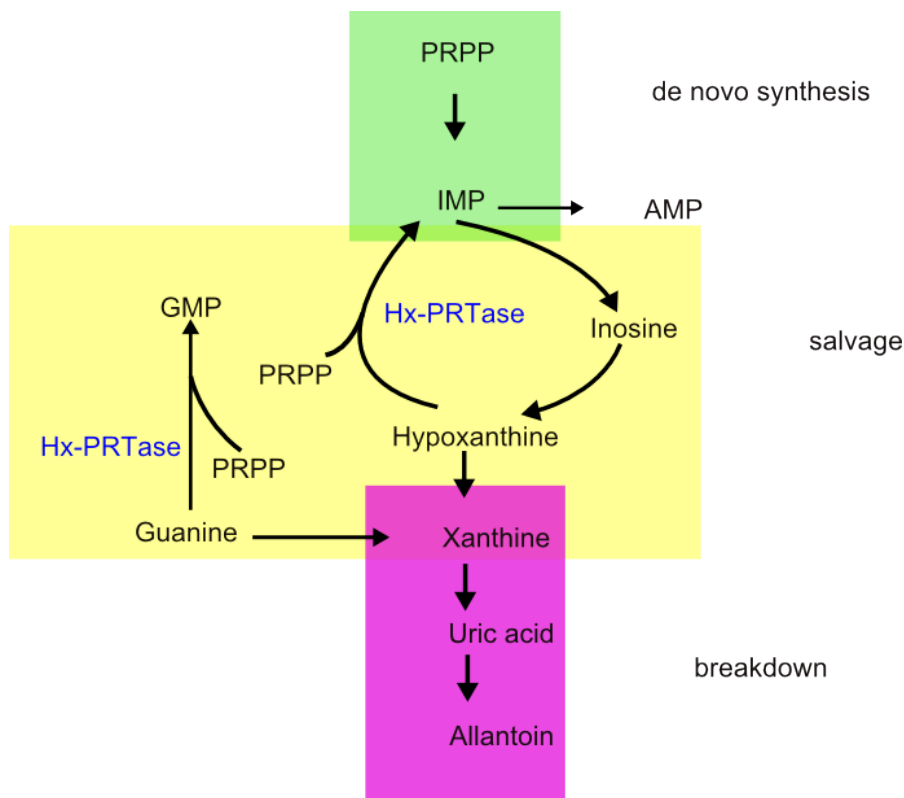


Figure 63 The purine Salvage pathway of purine synthesis

This pathway involves the utilization of the housekeeping protein hypoxanthine-guanine phosphoribosyl transferase (Hx-PRTase) which catalyses the addition of phosphoribosyl pyrophosphate to guanine or hypoxanthine to form guanosine and inosine respectively.

The salvage pathways are used to recover bases and nucleosides that are formed during degradation of RNA and DNA, offsetting the potential waste of a vital resource. One of the other roles of purine salvage is that of enabling ingested purines or those synthesized in one tissue to be made available to other tissues [188]. Given its importance, it is not surprising that the purine salvage pathway has been implicated in human cancer development [189]. In order to cope with rapid cell replication tumour cells use the more efficient purine salvage pathway for energy production and nucleic acid synthesis [190].

One important aspect of the salvage pathway would appear to lie in its ability to confer resistance to inhibitors of *de novo* nucleotide biosynthesis by salvage of extracellular nucleotides and nucleosides [191]. In a study by Natsumeda et al., it was noted that the activities of salvage enzymes of hypoxanthine and adenine (adenine phosphoribosyltransferase) were between 2 and 32 fold higher than that of amidophosphoribosyltransferase (a strictly *de novo* enzyme) in hepatomas, regenerating and differentiating livers [192]. It has long been known that inhibition of *de novo* synthesis leads to increased accumulation of substrates of the salvage pathway [193, 194]. The ability of cells to overcome the cytotoxicity of these metabolites also appears to increase in parallel with malignancy [195]. One study suggested an important role for the salvage pathways of purine and pyrimidine biosynthesis in the increased resistance of the more tumourigenic cell lines [195]. In addition, circumvention of the inhibition of *de novo* pathway by an efficient salvage process may also confer a survival advantage to the cells by reducing or abolishing the effects of an anti metabolite [196]. The greater capacity of the purine salvage pathway than the *de novo* pathway, along with further rises in its activity in response to the drugs targeted against the *de novo* pathway highlights its likely importance [197]. Inhibition of purine nucleoside and base salvage could thus increase the anti proliferative effects of an antipurine chemotherapeutic agent.

4.1.2 Activity of enzymes and metabolites of the salvage pathway in various cancers

An increased level of hypoxanthine in plasma and a reduced level in urine has been previously demonstrated in patients with gastric and colonic carcinomas [198]. Recent metabolic profiling in colorectal cancer reveals the purine salvage pathway substitutes *de novo* synthesis in the progression of the disease [190] while earlier work by Rubie et al. has

demonstrated the overexpression of the Hx-PRTase gene in colorectal and other tumours [199].

In plasma from children with acute lymphoblastic leukaemia or non Hodgkin lymphoma, hypoxanthine levels have been reported to be higher than in healthy controls and these levels decreased after methotrexate administration [200]. An increased level of hypoxanthine in the urine has been noticed in mesothelioma transplanted nude mice. Moreover, the level of this metabolite was reduced following response to chemotherapy [201].

On the other hand, a reduced level of urinary hypoxanthine was reported by Yoo et al. in patients with non Hodgkin lymphoma. They reasoned that the level of hypoxanthine might be decreased due to consumption by tumour cells [202].

Higher levels of hypoxanthine-guanine phosphoribosyltransferase activity have been documented in tumours compared to peritumoural tissues [203]. Similarly, increased levels of adenosine deaminase and xanthine oxidase have been noticed in cancerous tissues compared to adjacent non-malignant tissues in human colorectal cancer [204]. A similar trend has been noticed in bladder cancer where xanthine oxidase activity is increased in patients with papillary and multiple tumours compared to the tumour free group. Adenosine deaminase activity was increased in patients with multiple and invasive tumours compared to patients with single and superficial tumours [205]. Elevated levels of purine salvage pathway enzymes have also been reported in human osteosarcoma [206].

4.1.3 Cancer drugs acting on purine metabolism

5-FU belongs to a class of drugs known as anti metabolites. Chemotherapeutic antimetabolites are used to target key enzymes in the *de novo* purine and pyrimidine pathways [191]. The original hypothesis for the use of these drugs was that rapidly proliferating cells, i.e. tumour cells, would be more sensitive to these agents than normally dividing cells. However, it is now accepted that both acquired and inherent resistance to these drugs is more common in cancer cells compared to normal cells.

The efficacy of 5-FU is limited by a lack of response achieving response rates of only 10-20% when used as a single agent [207, 208]. Attempts at biomodulation of 5-FU to improve its efficacy led to the observation that an excess of intracellular folate was necessary for the optimal inhibition of thymidylate synthetase and for an increased cytotoxic effect of fluorinated pyrimidines [209]. This observation led to the first clinical trial of 5-FU in combination with folinic acid in 1982 [210]. A subsequent meta-analysis confirmed that the response rate following this combination was statistically higher than after 5-FU alone [211]. Methotrexate augments the actions of 5-FU by inhibiting dihydrofolate reductase and decreasing the folate pool required for pyrimidine biosynthesis [212]. A study by Fernandes et al. revealed a 25 fold increase in the inhibition of soft agar colony formation of murine tumour cells when methotrexate preceded 5-FU [213].

Over the years, it has become increasingly obvious that in order to attain reliable response rates for anti-metabolites, drugs need to target not only against the key enzymes of *de novo* pathways but also the salvage pathways that can otherwise circumvent the inhibition of a *de novo* pathway [191, 195, 214, 215].

Dipyridamole is a reversible competitive nucleoside transport inhibitor. During experiments by Kinsella and Haran [195], it was noticed that dipyridamole could enhance 5-FU cytotoxicity by inhibiting thymidine salvage in cells in which the DNA-directed effects of 5-FU predominated [209]. This was subsequently confirmed in human colon carcinoma cell lines in which inhibition of TS has been shown to be growth limiting at relatively low concentrations of 5-FU [216, 217]. Potentiation of the effect of 5-FU by dipyridamole has been shown in human colon cancer cell lines [218] where its addition increased toxicity of 5-FU 3-fold. It was suggested that dipyridamole enhanced 5-FU toxicity by blocking salvage of thymidine.

Encouraged by these results, Budd et al. conducted a phase 1 trial to evaluate the combination of dipyridamole, 5-FU and folinic acid patients with advanced refractory malignancy. The authors reported objective tumour responses in five of 13 patients with breast cancer, and concluded that phase 2 trials of this combination were justified [219]. However, the results of a subsequent phase 2 trial were disappointing [220].

Most studies have mainly focussed on the inhibition of pyrimidine salvage by dipyridamole although a small number of studies have investigated the role of dipyridamole in the inhibition of purine salvage. Turner et al., looked at a novel antifolate, lometrexol (5,10-dideazatetrahydrofolate) that inhibits *de novo* purine biosynthesis. The authors noticed that co-incubation of lometrexol with hypoxanthine abolished its cytotoxicity. The addition of dipyridamole to this prevented hypoxanthine rescue and as a result, growth was inhibited by the combination of lometrexol, dipyridamole and hypoxanthine [221].

Chen et al., in a study to elucidate the role of dipyridamole induced methotrexate toxicity in an ovarian carcinoma cell line, concluded that dipyridamole potentiated the activity of methotrexate by inhibiting the salvage of hypoxanthine, and to a lesser extent, that of thymidine [222]. Thus there is some evidence to support the inhibition of hypoxanthine salvage by dipyridamole.

However, even if the redeployment of existing inhibitors of the salvage pathway is unsuccessful, this research provides good evidence for further work in this direction. Effective inhibitors of a salvage pathway that works in epithelial tumours would represent a useful alternative to current chemotherapeutic regimens.

4.2 Succinate and fumarate

Fumarate was elevated in non dysplastic Barrett's mucosa and succinate elevated in dysplastic Barrett's mucosa. This finding was further investigated by performing a STOCSY on each of the classes in this model (Tissue model 4). This technique allows identification of highly correlated peak intensities. It was noticed that although for non dysplastic Barrett's there was a positive correlation between succinate and fumarate (0.6615); this correlation was negative for dysplastic Barrett's mucosa (-0.4594) (Figure 49; Figure 50).

To further examine this finding, a STOCSY was performed on the more complex model 3 for tissue (normal squamous mucosa vs. Barrett's mucosa in the presence of cancer vs. cancer mucosa) on each of the three subclasses. Similar results were obtained as for model 4. There was no correlation between succinate and fumarate for normal squamous mucosa (0.1368)

and cancer mucosa (-0.1325). However, this correlation was stronger and negative for dysplastic Barrett's mucosa (-0.4678) (Figure 51; Figure 52; Figure 53).

4.2.1 Succinate and its role in carcinogenesis.

Succinate plays an important biochemical role within the energy generating mitochondria as a component of the citric acid cycle and its capability of donating electrons to the electron transport chain by the reaction: succinate + FAD → fumarate + FADH₂. This is catalysed by complex II of the mitochondrial Electron Transport Chain, also called Succinate Dehydrogenase (SDH). In recent years, it has also been implicated in carcinogenesis.

SDH is a housekeeping gene with a key bioenergetic role. However mutations in the gene encoding for SDH can cause cancer: mutations in subunits B, C or D of SDH specifically can lead to the development of human paraganglioma (HPGL) or pheochromocytoma [223-225].

Paragangliomas are typically benign tumours derived from neuronal ectoderm cells along the sympathetic or parasympathetic nervous systems [226]. In 2000, Baysal et al. discovered that the gene mutated in a particular HPGL syndrome associated with the 11q23locus (PGL1) was in fact SDHD (succinate-ubiquinone oxidoreductase subunit D) [223]. Following this initial discovery, it did not take long to identify the genes of two other HPGL-associated loci, PGL4 (1p36) and PGL3 (1q21), to be SDHB (succinate-ubiquinone oxidoreductase subunit B) and SDHC (succinate-ubiquinone oxidoreductase subunit C), respectively [224, 225].

Mutations in the SDH genes are associated not only with familial syndromes but are also observed in sporadic paraganglioma and in pheochromocytoma, a subtype of paraganglioma

derived from catecholamine-secreting chromaffin cells, usually in the adrenal medulla [227]. The observation that loss of function of the SDH complex is mostly associated with paraganglioma, regardless of the SDH subunit involved, suggests that tumorigenesis because of these mutations stems from a common biochemical pathway. This is supported by the observation that mutations in either SDHB or SDHD result in the disintegration of the SDH complex and a complete loss of SDH enzymatic activity [228-230]

A biochemical explanation of how SDH functions as a tumour suppressor was put forward in 2005 by Selak et al. who demonstrated how succinate that accumulates as a result of SDH inhibition, inhibits HIF- α prolyl hydroxylases in the cytosol [227]. This would in turn lead to the stabilization and activation of the important transcription factor, HIF-1 α which would activate glycolysis [231].

A recent study examined the expression of SDH in colorectal cancer and analyzed the relationship among its expression, clinicopathological characteristics and prognosis. It also analyzed the relationship between SDH and HIF-1 α . Some 336 colorectal tissue cores were examined using tissue microarray analysis by immunohistochemical analysis. It was noted that expression levels of SDHB in colorectal cancer were reduced compared with normal mucosa adjacent to the primary tumour. However there were no significant differences in the expression level of SDHA, SDHC and SDHD in colorectal cancer and normal mucosa. Only expression levels of the subunit B were reduced in the cancer mucosa. The authors did find a close association between SDHB expression and tumour differentiation grade [232].

A recent report using 2-D DIGE and MS with the pH range of 4–7 found that in colon cancer some proteins such as succinate dehydrogenase subunit A, were down-regulated [233].

4.2.2 Succinate and fumarate in the Tricarboxylic acid cycle (TCA)

In the TCA cycle, succinate is oxidized to fumarate by succinate dehydrogenase. Fumarate is then hydrated to form L-malate by fumarase. The final reaction in the TCA cycle is catalyzed by malate dehydrogenase, converting L-malate to oxaloacetate. Thus the concentrations of succinate and fumarate are proportional assuming the activity of SDH is normal.

4.2.3 Further research into SDH

In this study, a negative correlation was noticed between succinate and fumarate in the pre-neoplastic tissue which was not apparent in normal tissue or frankly neoplastic tissue. This observation may be important as it may indicate dysfunction of SDH as previously noted in other neoplastic tissues.

If this finding can be confirmed in future studies, it may be a useful tool in the risk stratification of patients with Barrett's oesophagus. Quantification of succinate and fumarate in these tissues might enable prediction of an identifiable biochemical response that exists in the absence of histologic change. That this change might reflect an unstable epithelium, seems an attractive hypothesis, which in turn might lead to the identification of a metabolic marker in non-dysplastic Barrett's patients capable of identifying the high risk group likely to progress to adenocarcinoma.

4.3 3-hydroxybutyrate

In the current study, the level of 3-HB was increased in cancer mucosa compared to the adjacent normal mucosa. This difference although visualized on inspection of paired spectra

(Figure 41), was much more apparent on the loadings plot (Figure 24). This observation was confirmed by obtaining a 2D Hadamard $^1\text{H}, ^1\text{H}$ -TOCSY-NMR spectrum for 3-HB and further by selective spiking of samples with high levels of 3-hydroxybutyrate with exogenous 3-HB. An elevated level of 3-HB was also noticed in the pre treatment plasma samples from patients with oesophageal adenocarcinoma (type 1,2) compared to plasma from control patients. To add to this, elevated levels of 3-HB were noticed for pre treatment plasma samples from non responders vs. pre treatment plasma samples from responders, supporting other observations that 3-HB might indeed be a marker of aggressive disease. 3- HB levels were also noted to be higher in plasma from patients with node positive disease compared to those with node negative disease and in plasma from patients with the more advanced T stages (T3, T4 vs. T1, T2). It is unlikely that these differences were due to a difference in the fasting status of the patients as all patients had fasted overnight at the time of tissue sampling (during endoscopy or during surgery) and most plasma sampling was performed at the same time.

Both advanced stage and non-response to chemotherapy are associated with poor prognosis. While measuring 3-HB levels in the former situation may be of limited value in decision-making, it might have a role in assessing disease response and this seems worthy of prospective evaluation.

4.3.1 Metabolism of 3-hydroxybutyrate

3-hydroxybutyrate (3-HB) is one of the two main ketone bodies (along with aceto-acetate) that represent the end product of beta-oxidation of fatty acids. Beta-oxidation allows the production of vital acetyl CoA and provides a route whereby fatty acids can be utilized to provide energy via the TCA cycle (Figure 64).

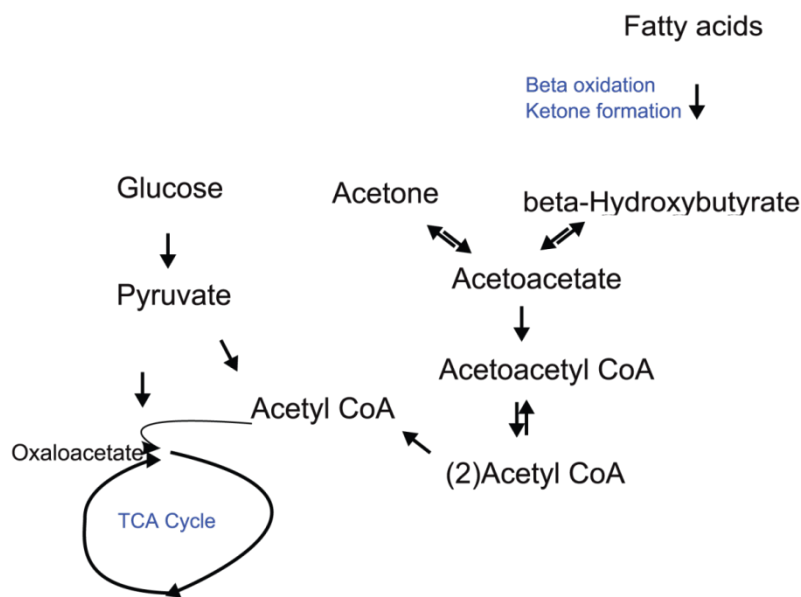


Figure 64 Metabolism of 3-hydroxybutyrate

3-Hydroxybutyrate, a ketone formed as a break down product of fatty acid beta oxidation can reform acetyl groups for use in the Krebs cycle. This proceeds via the formation of acetoacetate.

Although acetyl groups that are not metabolized in the TCA cycle will ultimately form 3-HB (as well as acetoacetate and acetone), the reverse process is possible within the cell. At a systemic level, 3 HB is mostly synthesized in the liver from acetyl-CoA after beta oxidation of fatty acids and can be used as an energy source by other tissue such as the brain when blood glucose is low. It is both secreted and taken up by the same monocarboxylate transporters (MCTs). After uptake by MCTs, it can re-enter the TCA cycle as acetyl-CoA and undergo oxidative metabolism, resulting in the production of high levels of ATP. High levels of this metabolite are seen in patients with diabetic ketoacidosis and alcoholic ketoacidosis.

Ketone bodies can also be produced from some amino acids (leucine, isoleucine, lysine, phenylalanine, tyrosine and tryptophan).

4.3.2 Role of 3-HB and ketone bodies in carcinogenesis

Numerous reports have implicated ketone bodies in carcinogenesis. Elevated levels of 3-HB have been detected in the serum of patients with colorectal malignancy [234]. Tiziani et al. observed elevated levels of 2- and 3-HB in patients with late stage head and neck cancer compared to early stage disease [235]. On the other hand, lower levels of 3-hydroxybutyrate have been reported from serum of patients with pancreatic cancer compared to healthy controls [236].

Recently Bonuccelli *et al.* provided conclusive evidence that ketone bodies and lactate fuel tumour growth and metastasis [237]. The administration of 3-HB in a xenograft model increased tumour growth 2.5-fold, without any measurable increases in tumour vascularization/ angiogenesis. 3-HB can also act as a chemo-attractant, stimulating the migration of epithelial cancer cells [237]. It has been suggested that 3-HB might be useful as a marker to identify high-risk cancer patients at diagnosis, for treatment stratification and/or for evaluating therapeutic efficacy during anticancer therapy [238].

The view that 3-hydroxybutyrate may be fuelling cancer is in part supported by the finding of increased breast cancer risk in a cohort of Mexican women who obtained a high percentage of calories from carbohydrate but not from fat [239].

Levels of 3-HB are however, profoundly affected by starvation. Blood glucose and insulin concentrations fall acutely during the first three days of fasting followed by a rise in the concentration of free fatty acids and ketone bodies that continues to increase and does not reach a plateau for more than two weeks [240]. Plasma levels of ketone bodies, rise significantly during starvation as a result of accelerated catabolism of fatty acids [241]. All tissue samples and most of the plasma samples in this study had been collected from patients who had fasted overnight. This fasting was probably further compounded by long term starvation in patients with advanced gastro-oesophageal malignancy. It would thus be difficult to completely eliminate starvation as one of the possible causes for the increased levels of 3-HB in cancer mucosa. However, since starvation should equally effect both types of tissues (i.e normal mucosa and cancer mucosa), it would be unreasonable to completely ascribe these findings to starvation. Furthermore, it would be difficult to ascertain from the results of this study if the 3-HB was consumed or produced by the cancer cells.

4.4 Comparison of results to proteomic data [242]

The aims of the proteomics part of the study were similar to that of metabolomic analysis. Models were constructed in a similar fashion. During proteomic experiments it was noticed that normal oesophageal, normal gastric tissue and tumour tissues generated distinctly different MALDI spectra. MALDI spectra of polypeptides and lipids discriminated between oesophageal adenocarcinoma and Barrett's and normal oesophagus, and between gastric cancer and normal stomach. However, the MALDI approach profiles the most abundant lipids (structural lipids) and low molecular weight proteins to generate a 'tissue fingerprint' and therefore does not provide in-depth biological information. Thus, although some

comparisons can be made between the two studies in terms of how different tissue types are, there is little direct overlap in terms of disease mechanism.

Firstly, the construction of the models was successful i.e. models which differentiated well on NMR metabolomics also differentiated well on MALDI proteomics. The primary method of extraction for tissues i.e. methanol chloroform extraction, worked well for both the analyses although tissues for proteomics were further processed before being submitted for analysis. However, this is where the commonalities between the two modalities end. Since both the studies were conducted synchronously, no attempts were made to specifically look for markers in proteomics that could identify involvement of particular pathways in light of the metabolomics results. Although this may be possible in future in-depth proteomic studies, what this study has demonstrated with great conviction is that the plasma and tissue processing protocols that we had developed were adequate to identify differences in between various types of histological tissues. The next step from here would be a combined proteomics/ metabolomics study specifically looking for pathways that were shown to be involved in this study.

4.5 NMR metabolomics in biomarker discovery

The human genome project which was completed in 2003 identified approximately 23,000 genes. “The post-genomic era was heralded by a greater awareness of functional genomic technologies. There was also a greater availability of technologies for global transcriptional and proteomic profiling” [243]. This paved the way for numerous biomarker studies utilizing genomics, transcriptomics and proteomics. One of the main disadvantages of this approach is that not all genes are under transcriptional control. Thus the information obtained from functional genomics is limited, especially due to post-transcriptional and post-translational modifications [104]. The possibilities with proteomics continue to be limited as the proteome of an organism remains an immense technical challenge. “There is thus an increased need to further define the phenotype resultant from a genetic modification to understand how the transcriptional or proteomic network may conspire to alter the expected phenotype” (Julian L. Griffin in *Metabolic profiles to define the genome: can we hear the phenotypes?*) [243].

The metabolome is therefore most predictive of phenotype [115, 116]. Comprehensive and quantitative study of metabolites, or metabolomics, is best placed for diagnosing disease and to evaluate the role of novel treatment strategies. Metabolic profiles can be acquired using technologies like nuclear magnetic resonance (NMR) spectroscopy, direct infusion electrospray mass spectrometry (ESI-MS) and gas chromatography mass spectrometry (GC-MS).

4.5.1 Strengths of the study

One of the main challenges in this study was to test the feasibility of conducting a large biomarker profiling study using blood and tissue. Although, blood (plasma or serum) has

been previously used for biomarker profiling in metabolomics; this is probably the largest patient series examining tissue profiles utilising NMR.

The first step towards achieving this goal was to optimise a tissue extraction protocol that could yield high quality specimens not only for NMR metabolomics, but also MS metabolomics and proteomics. It was also important that the variability in the mass of individual tissue specimens was accounted for to avoid differences due to the size of the biopsy. Protocols were successfully developed to achieve this.

Once such protocols had been established, the next challenge was to optimise a method of tissue transport and storage that was not only reproducible but also feasible. Although, most studies in the past have utilised snap frozen tissues, we instead chose to utilise the concept of slow freezing for this study. This firstly helped us to equalise the warm ischaemia time of post resectional specimens to endoscopically obtained biopsies. More importantly it enabled us to formulate a protocol that was practical and obviated the use of liquid nitrogen. Thus this protocol could be used in facilities where the availability of liquid nitrogen is limited or the restrictions on its use limit large studies. However, it has to be conceded that the results of this study may reflect the profiles from our tissue extraction protocols only and might not be generalisable to other protocols.

4.5.2 Advantages and disadvantages of using NMR for metabolomics

NMR was used in the present study to acquire metabolite profiles in this study. Although one of the disadvantages of NMR over MS is its limited sensitivity; ease of sample preparation, reproducibility and quantitativity of NMR are unsurpassed. NMR data were acquired for 724

samples. The acquisition time for some of these samples extended to 16 hours with a total period of NMR experiments spanning three months. Instrument reproducibility was thus important for such a large study. Although MS metabolomics was also used as part of this study, it was used as a validation tool rather than in the discovery phase.

Though most conditions can be controlled, there are still obstacles that had to be overcome with NMR. While spectral variation due to temperature changes can be avoided by stringent control of sample temperature, controlling spectral shifts due to varying pH is much more difficult as even really small pH variations will lead to visible shifts in NMR spectra. These small pH dependent variations in chemical shift were further reduced by adding several data points together into single bins. A disadvantage of this processing technique is that it can lead to artifacts due to signals potentially belonging to two adjacent bins. A manual inspection was therefore necessary, compressing several bins into a single bin if necessary to avoid these artifacts.

4.5.3 Advantages and disadvantages of using metabolomics for tissue profiling

Metabolomics is the most downstream of all the 'omic' sciences so it should explain most of the variations in the phenotype. However, one of the disadvantages of using metabolomics is that it only represents a snapshot of the metabolic profile. As a result it fails to indicate the processes or pathways that are dysregulated that might be causing these effects. Moreover, an increased quantity of a metabolite may indicate overproduction or underusage, a dilemma that metabolomics fails to address. Some of these weaknesses can be compensated for by using a combination of approaches that may indicate the pathways of interest, although this may not always be possible.

4.6 Future studies

This study has identified a large number of metabolic changes in oesophageal adenocarcinoma. Although, the findings from this study are quite substantial; it probably forms only the first step towards the successful discovery and validation of a biomarker. A variety of studies need to be performed before any concrete conclusions can be drawn out.

One of the future studies would consist of a validation study on a separate cohort of patients examining the metabolites of interest. Other studies would include enzyme based assays for specific metabolites validate and estimate accurate concentrations of these metabolites. Cell based studies would help further elucidate the proposed pathways for these effects. They would also allow testing of inhibitors of these pathways (e.g. dipyrimadole) in cell lines treated with various chemotherapeutic regimens. A population based cross sectional study would enable quantification of normal levels of these metabolites. One of the final steps would then be to produce and validate a diagnostic test assessing for the diseased state.

Another direction for future studies could be exploring modalities such as in vivo MRS and ex vivo ^1H HR-MAS. Both of these techniques have shown good promise in the last decade. On the subject of oesophageal cancer, ^1H magic angle spinning – nuclear magnetic resonance spectroscopy has been recently utilised to generate metabolic profiles of tumour tissue, proximal histologically normal mucosa from cancer patients and proximal histologically normal mucosa from a control group [151]. The authors of this study were able to identify metabolites in tissue that could identify the presence of oesophageal cancer. Thus a combination of these techniques is likely to yield further data towards the understanding of oesophageal carcinogenesis. In vivo MRS, although has been used for some malignancies

(primarily brain tumors) [185], it's use in oesophageal cancer has not yet been documented .

One of the greatest advantages of this tool is that it obviates the need for tissue biopsies.

However, the oesophagus and stomach and quite accessible to endoscopy and biopsy continues to be the mainstay of diagnosis. Perhaps further use of this technology would be seen in the coming years for lesions that are hard to biopsy.

CONCLUSION

Some important milestones were achieved during this study. A tissue extraction protocol was optimised that could yield high quality specimens not only for NMR metabolomics, but also MS metabolomics and proteomics. Moreover, this protocol was developed without the need for liquid nitrogen, thus adding to the simplicity of the protocol.

Using NMR metabolomics, it was possible to differentiate successfully between two normal tissue types from a large number of patients with gastro oesophageal malignancy. This was a necessary first step since before commenting on differences in between cancer and normal. It was important to explore the capability of NMR metabolomics in doing the same with normal tissue types. Besides this, NMR metabolomics was also able to distinguish between normal, pre-neoplastic stages and cancer.

This study identified alterations in a metabolite (hypoxanthine) that may point towards the possibility of identifying a cohort of patients with Barrett's oesophagus who were at a high risk of malignant transformation. This is quite important for Barrett's surveillance programmes and may eventually reduce the need for repeated endoscopies and biopsies in a sub group of patients. However, these conclusions have to be guarded since the number of patients with non dysplastic Barrett's and Barrett's in the presence of cancer were limited. Moreover, a successful validation of this hypothesis would require longitudinal follow up of patients with Barrett's oesophagus and this was beyond the scope of the present study.

3-hydroxybutyrate was identified as a marker in tissue and plasma that may indicate advanced or unresectable disease. The place for such markers in the current staging of

oesophago-gastric malignancies needs to be established following their successful validation. This study also identified a potential dysregulation of succinate dehydrogenase and emphasised its importance in oesophageal carcinogenesis. However, these results were obtained from a very small cohort of patients and further work is required to explain and validate the significance of such changes.

The natural progression from this study would be a validation study followed by cell based studies to actually understand the pathways involved. A successful conclusion of such studies may pave the way for new biomarkers and treatments in the management of gastro-oesophageal malignancy.

REFERENCES

1. Ferlay, J., et al., *Estimates of worldwide burden of cancer in 2008: GLOBOCAN 2008*. Int J Cancer. **127**(12): p. 2893-917.
2. <http://info.cancerresearchuk.org/cancerstats/types/oesophagus/incidence/#source25>. Cancer Research UK.
3. Hennessy, T.P.J. and A. Cuschieri, *Surgery of the oesophagus*. 2nd ed. ed1992, Oxford: Butterworth-Heinemann. 356p.
4. Jaskiewicz, K., W.F. Marasas, and F.E. van der Walt, *Oesophageal and other main cancer patterns in four districts of Transkei, 1981-1984*. S Afr Med J, 1987. **72**(1): p. 27-30.
5. Weston, A.P., et al., *p53 protein overexpression in low grade dysplasia (LGD) in Barrett's esophagus: immunohistochemical marker predictive of progression*. Am J Gastroenterol, 2001. **96**(5): p. 1355-62.
6. Kamangar, F., et al., *Esophageal cancer in Northeastern Iran: a review*. Arch Iran Med, 2007. **10**(1): p. 70-82.
7. Launoy, G., et al., *Oesophageal cancer in France: potential importance of hot alcoholic drinks*. Int J Cancer, 1997. **71**(6): p. 917-23.
8. Robert, V., et al., *High frequency in esophageal cancers of p53 alterations inactivating the regulation of genes involved in cell cycle and apoptosis*. Carcinogenesis, 2000. **21**(4): p. 563-5.
9. Williams, N.S., C.J. Bulstrode, and P.R. O'Connell, *Bailey and Love's Short Practice of Surgery*. 25 ed2008: A Hodder Arnold Publication.
10. Devesa, S.S., W.J. Blot, and J.F. Fraumeni, Jr., *Changing patterns in the incidence of esophageal and gastric carcinoma in the United States*. Cancer, 1998. **83**(10): p. 2049-53.
11. http://www.wcrf-uk.org/audience/media/press_release.php?recid=167.
12. <http://info.cancerresearchuk.org/cancerstats/types/oesophagus/incidence/>. Cancer Research UK.
13. Barrett, N.R., *Chronic peptic ulcer of the oesophagus and 'oesophagitis'*. Br J Surg, 1950. **38**(150): p. 175-82.
14. Carrie, A., *Adenocarcinoma of the upper end of the oesophagus arising from ectopic gastric epithelium*. Br J Surg, 1950. **37**(148): p. 474.
15. Fearon, E.R. and B. Vogelstein, *A genetic model for colorectal tumorigenesis*. Cell, 1990. **61**(5): p. 759-67.
16. Jankowski, J., *Gene expression in Barrett's mucosa: acute and chronic adaptive responses in the oesophagus*. Gut, 1993. **34**(12): p. 1649-50.
17. Jankowski, J., et al., *Proliferating cell nuclear antigen in oesophageal diseases; correlation with transforming growth factor alpha expression*. Gut, 1992. **33**(5): p. 587-91.
18. Jankowski, J.A., et al., *Molecular evolution of the metaplasia-dysplasia-adenocarcinoma sequence in the esophagus*. Am J Pathol, 1999. **154**(4): p. 965-73.
19. Jankowski, J.A. and N.A. Wright, *Epithelial stem cells in gastrointestinal morphogenesis, adaptation and carcinogenesis*. Semin Cell Biol, 1992. **3**(6): p. 445-56.
20. Theisen, J., et al., *Chronology of the Barrett's metaplasia-dysplasia-carcinoma sequence*. Dis Esophagus, 2004. **17**(1): p. 67-70.
21. Rothery, G.A., et al., *Histological and histochemical changes in the columnar lined (Barrett's) oesophagus*. Gut, 1986. **27**(9): p. 1062-8.

22. Younes, M., et al., *p53 Protein accumulation is a specific marker of malignant potential in Barrett's metaplasia*. Dig Dis Sci, 1997. **42**(4): p. 697-701.
23. Casson, A.G., et al., *Cyclin D1 polymorphism (G870A) and risk for esophageal adenocarcinoma*. Cancer, 2005. **104**(4): p. 730-9.
24. Reid, B.J., et al., *Predictors of progression to cancer in Barrett's esophagus: baseline histology and flow cytometry identify low- and high-risk patient subsets*. Am J Gastroenterol, 2000. **95**(7): p. 1669-76.
25. Rabinovitch, P.S., et al., *Predictors of progression in Barrett's esophagus III: baseline flow cytometric variables*. Am J Gastroenterol, 2001. **96**(11): p. 3071-83.
26. Winters, C., Jr., et al., *Barrett's esophagus. A prevalent, occult complication of gastroesophageal reflux disease*. Gastroenterology, 1987. **92**(1): p. 118-24.
27. Provenzale, D., et al., *A guide for surveillance of patients with Barrett's esophagus*. Am J Gastroenterol, 1994. **89**(5): p. 670-80.
28. Sontag, S.J., et al., *Barrett's, low grade dysplasia and fear; yearly endoscopy is not justified: Surveillance every 2-3 years detects all cancers early*. Gastroenterology, 1999(G1381): p. 116.
29. Hameeteman, W., et al., *Barrett's esophagus: development of dysplasia and adenocarcinoma*. Gastroenterology, 1989. **96**(5 Pt 1): p. 1249-56.
30. Schnell, T.G., et al., *Long-term nonsurgical management of Barrett's esophagus with high-grade dysplasia*. Gastroenterology, 2001. **120**(7): p. 1607-19.
31. *Guidelines for the diagnosis and management of Barrett's columnar-lined oesophagus*.
32. Shaheen, N.J., et al., *Is there publication bias in the reporting of cancer risk in Barrett's esophagus?* Gastroenterology, 2000. **119**(2): p. 333-8.
33. Wijnhoven, B.P., et al., *Adenocarcinomas of the distal oesophagus and gastric cardia are one clinical entity*. Rotterdam Oesophageal Tumour Study Group. Br J Surg, 1999. **86**(4): p. 529-35.
34. Rudiger Siewert, J., et al., *Adenocarcinoma of the esophagogastric junction: results of surgical therapy based on anatomical/topographic classification in 1,002 consecutive patients*. Ann Surg, 2000. **232**(3): p. 353-61.
35. von Rahden, B.H., et al., *Lymphatic vessel invasion as a prognostic factor in patients with primary resected adenocarcinomas of the esophagogastric junction*. J Clin Oncol, 2005. **23**(4): p. 874-9.
36. Aikou, T. and H. Shimazu, *Difference in main lymphatic pathways from the lower esophagus and gastric cardia*. Jpn J Surg, 1989. **19**(3): p. 290-5.
37. Hosch, S.B., et al., *Esophageal cancer: the mode of lymphatic tumor cell spread and its prognostic significance*. J Clin Oncol, 2001. **19**(7): p. 1970-5.
38. *Office for National Statistics*.
39. Greene, F.L., *AJCC cancer staging manual*. 6th ed. / editors: Frederick L. Greene ... [et al.] ed2002, New York ; London: Springer. xiv, 421 p.
40. Sobin, L.H., M.K. Gospodarowicz, and C. Wittekind, *TNM classification of malignant tumours*. 7th ed. ed, Oxford: Wiley-Blackwell. xx, 309 p.
41. Killinger, W.A., Jr., et al., *Stage II esophageal carcinoma: the significance of T and N*. J Thorac Cardiovasc Surg, 1996. **111**(5): p. 935-40.
42. Altorki, N. and D. Skinner, *Should en bloc esophagectomy be the standard of care for esophageal carcinoma?* Ann Surg, 2001. **234**(5): p. 581-7.
43. Nigro, J.J., et al., *Node status in transmural esophageal adenocarcinoma and outcome after en bloc esophagectomy*. J Thorac Cardiovasc Surg, 1999. **117**(5): p. 960-8.

44. Ellis, F.H., Jr., et al., *Esophagogastrectomy for carcinoma of the esophagus and cardia: a comparison of findings and results after standard resection in three consecutive eight-year intervals with improved staging criteria*. J Thorac Cardiovasc Surg, 1997. **113**(5): p. 836-46; discussion 846-8.
45. Malthaner, R.A., S. Collin, and D. Fenlon, *Preoperative chemotherapy for resectable thoracic esophageal cancer*. Cochrane Database Syst Rev, 2006. **3**: p. CD001556.
46. *Surgical resection with or without preoperative chemotherapy in oesophageal cancer: a randomised controlled trial*. Lancet, 2002. **359**(9319): p. 1727-33.
47. Cunningham, D., et al., *Perioperative chemotherapy versus surgery alone for resectable gastroesophageal cancer*. N Engl J Med, 2006. **355**(1): p. 11-20.
48. Arnott, S.J., et al., *Preoperative radiotherapy in esophageal carcinoma: a meta-analysis using individual patient data (Oesophageal Cancer Collaborative Group)*. Int J Radiat Oncol Biol Phys, 1998. **41**(3): p. 579-83.
49. Walsh, T.N., et al., *A comparison of multimodal therapy and surgery for esophageal adenocarcinoma*. N Engl J Med, 1996. **335**(7): p. 462-7.
50. Fiorica, F., et al., *Preoperative chemoradiotherapy for oesophageal cancer: a systematic review and meta-analysis*. Gut, 2004. **53**(7): p. 925-30.
51. Gaast, A.V., et al., *Effect of preoperative concurrent chemoradiotherapy on survival of patients with resectable esophageal or esophagogastric junction cancer: Results from a multicenter randomized phase III study*. Journal of Clinical Oncology, 2010. **28**(15s).
52. Levard, H., et al., *5-Fluorouracil and cisplatin as palliative treatment of advanced oesophageal squamous cell carcinoma. A multicentre randomised controlled trial. The French Associations for Surgical Research*. Eur J Surg, 1998. **164**(11): p. 849-57.
53. Nagashima, F., et al., *Biological markers as a predictor for response and prognosis of unresectable gastric cancer patients treated with irinotecan and cisplatin*. Jpn J Clin Oncol, 2005. **35**(12): p. 714-9.
54. Teniere, P., et al., *Postoperative radiation therapy does not increase survival after curative resection for squamous cell carcinoma of the middle and lower esophagus as shown by a multicenter controlled trial. French University Association for Surgical Research*. Surg Gynecol Obstet, 1991. **173**(2): p. 123-30.
55. Zieren, H.U., et al., *Adjuvant postoperative radiation therapy after curative resection of squamous cell carcinoma of the thoracic esophagus: a prospective randomized study*. World J Surg, 1995. **19**(3): p. 444-9.
56. Fok, M., et al., *Postoperative radiotherapy for carcinoma of the esophagus: a prospective, randomized controlled study*. Surgery, 1993. **113**(2): p. 138-47.
57. Forshaw, M.J., J.A. Gossage, and R.C. Mason, *Neoadjuvant chemotherapy for oesophageal cancer: the need for accurate response prediction and evaluation*. Surgeon, 2005. **3**(6): p. 373-82, 422.
58. Geh, J.I., A.M. Crellin, and R. Glynne-Jones, *Preoperative (neoadjuvant) chemoradiotherapy in oesophageal cancer*. Br J Surg, 2001. **88**(3): p. 338-56.
59. Evans, W.E. and M.V. Relling, *Pharmacogenomics: translating functional genomics into rational therapeutics*. Science, 1999. **286**(5439): p. 487-91.
60. Heidelberger, C., et al., *Fluorinated pyrimidines, a new class of tumour-inhibitory compounds*. Nature, 1957. **179**(4561): p. 663-6.
61. Wu, X., et al., *Genetic variations in radiation and chemotherapy drug action pathways predict clinical outcomes in esophageal cancer*. J Clin Oncol, 2006. **24**(23): p. 3789-98.

62. Sarbia, M., et al., *The prognostic significance of genetic polymorphisms (Methylenetetrahydrofolate Reductase C677T, Methionine Synthase A2756G, Thymidilate Synthase tandem repeat polymorphism) in multimodally treated oesophageal squamous cell carcinoma.* Br J Cancer, 2006. **94**(2): p. 203-7.
63. Joshi, M.B., et al., *High gene expression of TSI, GSTP1, and ERCC1 are risk factors for survival in patients treated with trimodality therapy for esophageal cancer.* Clin Cancer Res, 2005. **11**(6): p. 2215-21.
64. Saeki, H., et al., *Role of dihydropyrimidine dehydrogenase activity in patients with esophageal cancer.* Anticancer Res, 2002. **22**(6B): p. 3789-92.
65. Hishikawa, Y., et al., *Overexpression of metallothionein correlates with chemoresistance to cisplatin and prognosis in esophageal cancer.* Oncology, 1997. **54**(4): p. 342-7.
66. Harpole, D.H., Jr., et al., *The prognostic value of molecular marker analysis in patients treated with trimodality therapy for esophageal cancer.* Clin Cancer Res, 2001. **7**(3): p. 562-9.
67. Liao, Z., et al., *Polymorphism at the 3'-UTR of the thymidylate synthase gene: a potential predictor for outcomes in Caucasian patients with esophageal adenocarcinoma treated with preoperative chemoradiation.* Int J Radiat Oncol Biol Phys, 2006. **64**(3): p. 700-8.
68. Lu, J.W., et al., *Polymorphism in the 3'-untranslated region of the thymidylate synthase gene and sensitivity of stomach cancer to fluoropyrimidine-based chemotherapy.* J Hum Genet, 2006. **51**(3): p. 155-60.
69. Goekkurt, E., et al., *Polymorphisms of glutathione S-transferases (GST) and thymidylate synthase (TS)--novel predictors for response and survival in gastric cancer patients.* Br J Cancer, 2006. **94**(2): p. 281-6.
70. Langer, R., et al., *Comparison of pretherapeutic and posttherapeutic expression levels of chemotherapy-associated genes in adenocarcinomas of the esophagus treated by 5-fluorouracil- and cisplatin-based neoadjuvant chemotherapy.* Am J Clin Pathol, 2007. **128**(2): p. 191-7.
71. Metzger, R., et al., *ERCC1 mRNA levels complement thymidylate synthase mRNA levels in predicting response and survival for gastric cancer patients receiving combination cisplatin and fluorouracil chemotherapy.* J Clin Oncol, 1998. **16**(1): p. 309-16.
72. Lenz, H.J., et al., *Thymidylate synthase mRNA level in adenocarcinoma of the stomach: a predictor for primary tumor response and overall survival.* J Clin Oncol, 1996. **14**(1): p. 176-82.
73. Ichikawa, W., et al., *Simple combinations of 5-FU pathway genes predict the outcome of metastatic gastric cancer patients treated by S-1.* Int J Cancer, 2006. **119**(8): p. 1927-33.
74. Schneider, S., et al., *Downregulation of TS, DPD, ERCC1, GST-Pi, EGFR, and HER2 gene expression after neoadjuvant three-modality treatment in patients with esophageal cancer.* J Am Coll Surg, 2005. **200**(3): p. 336-44.
75. Kato, J., et al., *Expression of survivin in esophageal cancer: correlation with the prognosis and response to chemotherapy.* Int J Cancer, 2001. **95**(2): p. 92-5.
76. Peyrone, M., *Ueber die Einwirkung des Ammoniaks auf Platinchlorür.* Justus Liebigs Annalen der Chemie, 1844. **51**(1): p. 1-29.
77. Rabik, C.A. and M.E. Dolan, *Molecular mechanisms of resistance and toxicity associated with platinating agents.* Cancer Treat Rev, 2007. **33**(1): p. 9-23.

78. Masuda, H., T. Tanaka, and U. Takahama, *Cisplatin generates superoxide anion by interaction with DNA in a cell-free system*. *Biochem Biophys Res Commun*, 1994. **203**(2): p. 1175-80.
79. Gillet, L.C. and O.D. Scharer, *Molecular mechanisms of mammalian global genome nucleotide excision repair*. *Chem Rev*, 2006. **106**(2): p. 253-76.
80. Fareed, K.R., et al., *Biomarkers of response to therapy in oesophago-gastric cancer*. *Gut*, 2009. **58**(1): p. 127-43.
81. Madhusudan, S. and I.D. Hickson, *DNA repair inhibition: a selective tumour targeting strategy*. *Trends Mol Med*, 2005. **11**(11): p. 503-11.
82. Hegde, M.L., T.K. Hazra, and S. Mitra, *Early steps in the DNA base excision/single-strand interruption repair pathway in mammalian cells*. *Cell Res*, 2008. **18**(1): p. 27-47.
83. Zarate, R.N., et al., *Xeroderma pigmentosum group D 751 polymorphism as a predictive factor in resected gastric cancer treated with chemo-radiotherapy*. *World J Gastroenterol*, 2006. **12**(37): p. 6032-6.
84. Langer, R., et al., *Association of pretherapeutic expression of chemotherapy-related genes with response to neoadjuvant chemotherapy in Barrett carcinoma*. *Clin Cancer Res*, 2005. **11**(20): p. 7462-9.
85. Warnecke-Eberz, U., et al., *High specificity of quantitative excision repair cross-complementing 1 messenger RNA expression for prediction of minor histopathological response to neoadjuvant radiochemotherapy in esophageal cancer*. *Clin Cancer Res*, 2004. **10**(11): p. 3794-9.
86. Wei, J., et al., *ERCC1 mRNA levels and survival of advanced gastric cancer patients treated with a modified FOLFOX regimen*. *Br J Cancer*, 2008. **98**(8): p. 1398-402.
87. Grabowski, P., et al., *Prognostic value of nuclear survivin expression in oesophageal squamous cell carcinoma*. *Br J Cancer*, 2003. **88**(1): p. 115-9.
88. Nakamura, M., et al., *Survivin as a predictor of cis-diamminedichloroplatinum sensitivity in gastric cancer patients*. *Cancer Sci*, 2004. **95**(1): p. 44-51.
89. Vallbohmer, D., et al., *Survivin, a potential biomarker in the development of Barrett's adenocarcinoma*. *Surgery*, 2005. **138**(4): p. 701-6; discussion 706-7.
90. Sarbia, M., et al., *Expression of Bax, a pro-apoptotic member of the Bcl-2 family, in esophageal squamous cell carcinoma*. *Int J Cancer*, 1997. **73**(4): p. 508-13.
91. Kang, S.Y., et al., *Low expression of Bax predicts poor prognosis in patients with locally advanced esophageal cancer treated with definitive chemoradiotherapy*. *Clin Cancer Res*, 2007. **13**(14): p. 4146-53.
92. Zimmermann, K.C., et al., *Cyclooxygenase-2 expression in human esophageal carcinoma*. *Cancer Res*, 1999. **59**(1): p. 198-204.
93. Boku, N., et al., *Biological markers as a predictor for response and prognosis of unresectable gastric cancer patients treated with 5-fluorouracil and cis-platinum*. *Clin Cancer Res*, 1998. **4**(6): p. 1469-74.
94. Cascinu, S., et al., *Expression of p53 protein and resistance to preoperative chemotherapy in locally advanced gastric carcinoma*. *Cancer*, 1998. **83**(9): p. 1917-22.
95. Nakata, B., et al., *p53 protein overexpression as a predictor of the response to chemotherapy in gastric cancer*. *Surg Today*, 1998. **28**(6): p. 595-8.
96. Okumura, H., et al., *The predictive value of p53, p53R2, and p21 for the effect of chemoradiation therapy on oesophageal squamous cell carcinoma*. *Br J Cancer*, 2005. **92**(2): p. 284-9.

97. Sarbia, M., et al., *The predictive value of molecular markers (p53, EGFR, ATM, CHK2) in multimodally treated squamous cell carcinoma of the oesophagus*. Br J Cancer, 2007. **97**(10): p. 1404-8.
98. Akamatsu, M., et al., *c-erbB-2 oncoprotein expression related to chemoradioresistance in esophageal squamous cell carcinoma*. Int J Radiat Oncol Biol Phys, 2003. **57**(5): p. 1323-7.
99. Izzo, J.G., et al., *Association of activated transcription factor nuclear factor kappaB with chemoradiation resistance and poor outcome in esophageal carcinoma*. J Clin Oncol, 2006. **24**(5): p. 748-54.
100. Harris, A.L., *Hypoxia--a key regulatory factor in tumour growth*. Nat Rev Cancer, 2002. **2**(1): p. 38-47.
101. Sohda, M., et al., *Pretreatment evaluation of combined HIF-1alpha, p53 and p21 expression is a useful and sensitive indicator of response to radiation and chemotherapy in esophageal cancer*. Int J Cancer, 2004. **110**(6): p. 838-44.
102. Ogawa, K., et al., *Clinical significance of HIF-1alpha expression in patients with esophageal cancer treated with concurrent chemoradiotherapy*. Anticancer Res. **31**(6): p. 2351-9.
103. Miyazono, F., et al., *Quantitative c-erbB-2 but not c-erbB-1 mRNA expression is a promising marker to predict minor histopathologic response to neoadjuvant radiochemotherapy in oesophageal cancer*. Br J Cancer, 2004. **91**(4): p. 666-72.
104. Thongboonkerd, V., *Genomics, proteomics and integrative "omics" in hypertension research*. Curr Opin Nephrol Hypertens, 2005. **14**(2): p. 133-9.
105. Hayashida, Y., et al., *Possible prediction of chemoradiosensitivity of esophageal cancer by serum protein profiling*. Clin Cancer Res, 2005. **11**(22): p. 8042-7.
106. Alaoui-Jamali, M.A. and Y.J. Xu, *Proteomic technology for biomarker profiling in cancer: an update*. J Zhejiang Univ Sci B, 2006. **7**(6): p. 411-20.
107. Langer, R., et al., *Protein expression profiling in esophageal adenocarcinoma patients indicates association of heat-shock protein 27 expression and chemotherapy response*. Clin Cancer Res, 2008. **14**(24): p. 8279-87.
108. Maher, S.G., et al., *Serum proteomic profiling reveals that pretreatment complement protein levels are predictive of esophageal cancer patient response to neoadjuvant chemoradiation*. Ann Surg. **254**(5): p. 809-16; discussion 816-7.
109. Lordick, F., et al., *PET to assess early metabolic response and to guide treatment of adenocarcinoma of the oesophagogastric junction: the MUNICON phase II trial*. Lancet Oncol, 2007. **8**(9): p. 797-805.
110. Schneider, P.M., et al., *Response evaluation by endoscopy, rebiopsy, and endoscopic ultrasound does not accurately predict histopathologic regression after neoadjuvant chemoradiation for esophageal cancer*. Ann Surg, 2008. **248**(6): p. 902-8.
111. Kogo, M., et al., *Scoring system for predicting response to chemoradiotherapy, including 5-Fluorouracil and platinum, for patients with esophageal cancer*. Dig Dis Sci, 2008. **53**(9): p. 2415-21.
112. MacGuill, M., et al., *Clinicopathologic factors predicting complete pathological response to neoadjuvant chemoradiotherapy in esophageal cancer*. Dis Esophagus, 2006. **19**(4): p. 273-6.
113. Nicholson, J.K. and I.D. Wilson, *Opinion: understanding 'global' systems biology: metabolomics and the continuum of metabolism*. Nat Rev Drug Discov, 2003. **2**(8): p. 668-76.
114. Schmidt, C., *Metabolomics takes its place as latest up-and-coming "omic" science*. J Natl Cancer Inst, 2004. **96**(10): p. 732-4.

115. Fiehn, O., *Metabolomics--the link between genotypes and phenotypes*. Plant Mol Biol, 2002. **48**(1-2): p. 155-71.
116. Weckwerth, W., *Metabolomics in systems biology*. Annu Rev Plant Biol, 2003. **54**: p. 669-89.
117. Dettmer, K. and B.D. Hammock, *Metabolomics--a new exciting field within the "omics" sciences*. Environ Health Perspect, 2004. **112**(7): p. A396-7.
118. Bloch, F., W.W. Hansen, and M. Packard, *The Nuclear Induction Experiment*. Physical Review, 1946. **70**: p. 474-485.
119. Purcell, E.M., H.C. Torrey, and R.V. Pound, *Resonance Absorption by Nuclear Magnetic Moments in a Solid*. Physical Review, 1946. **69**: p. 37-38.
120. Hoult, D.I., et al., *Observation of tissue metabolites using ³¹P nuclear magnetic resonance*. Nature, 1974. **252**(5481): p. 285-7.
121. Nicholson, J.K., et al., *Proton-nuclear-magnetic-resonance studies of serum, plasma and urine from fasting normal and diabetic subjects*. Biochem J, 1984. **217**(2): p. 365-75.
122. Holmes, E., et al., *Development of a model for classification of toxin-induced lesions using ¹H NMR spectroscopy of urine combined with pattern recognition*. NMR Biomed, 1998. **11**(4-5): p. 235-44.
123. Ludwig, C. and M.R. Viant, *Two-dimensional J-resolved NMR spectroscopy: review of a key methodology in the metabolomics toolbox*. Phytochem Anal. **21**(1): p. 22-32.
124. Levitt, M.H., *Spin dynamics : basics of nuclear magnetic resonance* 2001, Chichester: John Wiley & Sons.
125. Warburg, O., F. Wind, and E. Negelein, *Über den Stoffwechsel von Tumoren im Körper*. Klinische Wochenschrift, 1926. **5**(19): p. 829-832.
126. Metallo, Christian M. and Matthew G. Vander Heiden, *Understanding Metabolic Regulation and Its Influence on Cell Physiology*. Molecular cell, 2013. **49**(3): p. 388-398.
127. Puzio-Kuter, A.M., *The Role of p53 in Metabolic Regulation*. Genes Cancer, 2011. **2**(4): p. 385-91.
128. Ward, Patrick S. and Craig B. Thompson, *Metabolic Reprogramming: A Cancer Hallmark Even Warburg Did Not Anticipate*. Cancer Cell, 2012. **21**(3): p. 297-308.
129. Carmeliet, P., et al., *Role of HIF-1alpha in hypoxia-mediated apoptosis, cell proliferation and tumour angiogenesis*. Nature, 1998. **394**(6692): p. 485-90.
130. Chiavarina, B., et al., *HIF1-alpha functions as a tumor promoter in cancer associated fibroblasts, and as a tumor suppressor in breast cancer cells: Autophagy drives compartment-specific oncogenesis*. Cell Cycle, 2010. **9**(17): p. 3534-51.
131. Madsen, R., T. Lundstedt, and J. Trygg, *Chemometrics in metabolomics--a review in human disease diagnosis*. Anal Chim Acta. **659**(1-2): p. 23-33.
132. Moestue, S., et al., *HR MAS MR spectroscopy in metabolic characterization of cancer*. Curr Top Med Chem. **11**(1): p. 2-26.
133. Issaq, H.J., et al., *Detection of bladder cancer in human urine by metabolomic profiling using high performance liquid chromatography/mass spectrometry*. J Urol, 2008. **179**(6): p. 2422-6.
134. Cheng, L.L., et al., *Metabolic characterization of human prostate cancer with tissue magnetic resonance spectroscopy*. Cancer Res, 2005. **65**(8): p. 3030-4.
135. Sreekumar, A., et al., *Metabolomic profiles delineate potential role for sarcosine in prostate cancer progression*. Nature, 2009. **457**(7231): p. 910-4.

136. Merz, A.L. and N.J. Serkova, *Use of nuclear magnetic resonance-based metabolomics in detecting drug resistance in cancer*. *Biomark Med*, 2009. **3**(3): p. 289-306.
137. Morvan, D. and A. Demidem, *Metabolomics by proton nuclear magnetic resonance spectroscopy of the response to chloroethylnitrosourea reveals drug efficacy and tumor adaptive metabolic pathways*. *Cancer Res*, 2007. **67**(5): p. 2150-9.
138. Cheng, L.L., et al., *Enhanced resolution of proton NMR spectra of malignant lymph nodes using magic-angle spinning*. *Magn Reson Med*, 1996. **36**(5): p. 653-8.
139. Chen, J.H., et al., *Biochemical analysis using high-resolution magic angle spinning NMR spectroscopy distinguishes lipoma-like well-differentiated liposarcoma from normal fat*. *J Am Chem Soc*, 2001. **123**(37): p. 9200-1.
140. Millis, K., et al., *Classification of human liposarcoma and lipoma using ex vivo proton NMR spectroscopy*. *Magn Reson Med*, 1999. **41**(2): p. 257-67.
141. Tomlins, A.M., et al., *High resolution 1H NMR spectroscopic studies on dynamic biochemical processes in incubated human seminal fluid samples*. *Biochim Biophys Acta*, 1998. **1379**(3): p. 367-80.
142. Griffiths, J.R. and M. Stubbs, *Opportunities for studying cancer by metabolomics: preliminary observations on tumors deficient in hypoxia-inducible factor 1*. *Adv Enzyme Regul*, 2003. **43**: p. 67-76.
143. Preul, M.C., et al., *Accurate, noninvasive diagnosis of human brain tumors by using proton magnetic resonance spectroscopy*. *Nat Med*, 1996. **2**(3): p. 323-5.
144. El-Sayed, S., et al., *An ex vivo study exploring the diagnostic potential of 1H magnetic resonance spectroscopy in squamous cell carcinoma of the head and neck region*. *Head Neck*, 2002. **24**(8): p. 766-72.
145. Moreno, A., et al., *1H MRS markers of tumour growth in intrasplenic tumours and liver metastasis induced by injection of HT-29 cells in nude mice spleen*. *NMR Biomed*, 1998. **11**(3): p. 93-106.
146. Zhang, J., et al., *Esophageal cancer metabolite biomarkers detected by LC-MS and NMR methods*. *PLoS One*, 2012. **7**(1): p. e30181.
147. Wu, H., et al., *Metabolomic study for diagnostic model of oesophageal cancer using gas chromatography/mass spectrometry*. *J Chromatogr B Analyt Technol Biomed Life Sci*, 2009. **877**(27): p. 3111-7.
148. Hasim, A., et al., *Revealing the metabolomic variation of EC using (1)H-NMR spectroscopy and its association with the clinicopathological characteristics*. *Mol Biol Rep*, 2012. **39**(9): p. 8955-64.
149. Ayxiam, H., et al., *[Metabolomic variation of esophageal cancer within different ethnic groups in Xinjiang, China]*. *Zhonghua Yu Fang Yi Xue Za Zhi*, 2009. **43**(7): p. 591-6.
150. Cai, Z., et al., *A combined proteomics and metabolomics profiling of gastric cardia cancer reveals characteristic dysregulations in glucose metabolism*. *Mol Cell Proteomics*, 2010. **9**(12): p. 2617-28.
151. Yakoub, D., et al., *Metabolic profiling detects field effects in nondysplastic tissue from esophageal cancer patients*. *Cancer Res*, 2010. **70**(22): p. 9129-36.
152. Zhang, J., et al., *Metabolomics study of esophageal adenocarcinoma*. *J Thorac Cardiovasc Surg*, 2011. **141**(2): p. 469-75, 475 e1-4.
153. Teahan, O., et al., *Impact of analytical bias in metabolomic studies of human blood serum and plasma*. *Anal Chem*, 2006. **78**(13): p. 4307-18.
154. Tiziani, S., et al., *Optimized metabolite extraction from blood serum for 1H nuclear magnetic resonance spectroscopy*. *Anal Biochem*, 2008. **377**(1): p. 16-23.

155. Pegg, D.E., *Principles of cryopreservation*. Methods Mol Biol, 2007. **368**: p. 39-57.
156. Mazur, P., *Physical factors implicated in the death of microorganisms at subzero temperatures*. Ann N Y Acad Sci, 1960. **85**: p. 610-29.
157. Mazur, P., *Cryobiology: the freezing of biological systems*. Science, 1970. **168**(3934): p. 939-49.
158. Kneteman, N.M., et al., *Long-term cryogenic storage of purified adult human islets of Langerhans*. Diabetes, 1989. **38**(3): p. 386-96.
159. Bligh, E.G. and W.J. Dyer, *A rapid method of total lipid extraction and purification*. Can J Biochem Physiol, 1959. **37**(8): p. 911-7.
160. Wu, H., et al., *High-throughput tissue extraction protocol for NMR- and MS-based metabolomics*. Anal Biochem, 2008. **372**(2): p. 204-12.
161. Christie, W.W., *Advances in lipid methodology* 1993, Dundee: Oily Press. 335p.
162. Wu, P.S. and G. Otting, *Rapid pulse length determination in high-resolution NMR*. J Magn Reson, 2005. **176**(1): p. 115-9.
163. Kumar, A., R.R. Ernst, and K. Wuthrich, *A two-dimensional nuclear Overhauser enhancement (2D NOE) experiment for the elucidation of complete proton-proton cross-relaxation networks in biological macromolecules*. Biochem Biophys Res Commun, 1980. **95**(1): p. 1-6.
164. Kupce, E. and R. Freeman, *Frequency-domain Hadamard spectroscopy*. J Magn Reson, 2003. **162**(1): p. 158-65.
165. Gunther, U.L., C. Ludwig, and H. Ruterjans, *NMRLAB-Advanced NMR data processing in matlab*. J Magn Reson, 2000. **145**(2): p. 201-8.
166. Ludwig, C. and U.L. Gunther, *MetaboLab--advanced NMR data processing and analysis for metabolomics*. BMC Bioinformatics. **12**: p. 366.
167. Griffiths, W.J., *Metabolomics, metabonomics and metabolite profiling* 2008, Cambridge: RSC Publishing. xi, 323 p.
168. Bylesjö, M., et al., *OPLS discriminant analysis: combining the strengths of PLS-DA and SIMCA classification*. Journal of Chemometrics. **20**(8-10): p. 341-351.
169. ; Available from: <http://wiki.eigenvector.com/index.php?title=Crossval>.
170. Sasic, S., A. Muszynski, and Y. Ozaki, *A New Possibility of the Generalized Two-Dimensional Correlation Spectroscopy. I. Sample-Sample Correlation Spectroscopy*. The journal of physical chemistry, 2000. **104**(27): p. 6380-6387.
171. Mandard, A.M., et al., *Pathologic assessment of tumor regression after preoperative chemoradiotherapy of esophageal carcinoma. Clinicopathologic correlations*. Cancer, 1994. **73**(11): p. 2680-6.
172. Therasse, P., et al., *New guidelines to evaluate the response to treatment in solid tumors. European Organization for Research and Treatment of Cancer, National Cancer Institute of the United States, National Cancer Institute of Canada*. J Natl Cancer Inst, 2000. **92**(3): p. 205-16.
173. Wishart, D.S., et al., *HMDB: a knowledgebase for the human metabolome*. Nucleic Acids Res, 2009. **37**(Database issue): p. D603-10.
174. Wishart, D.S., et al., *HMDB: the Human Metabolome Database*. Nucleic Acids Res, 2007. **35**(Database issue): p. D521-6.
175. Lu, W., E. Kimball, and J.D. Rabinowitz, *A high-performance liquid chromatography-tandem mass spectrometry method for quantitation of nitrogen-containing intracellular metabolites*. J Am Soc Mass Spectrom, 2006. **17**(1): p. 37-50.
176. Freeman, R. and E. Kupce, *New methods for fast multidimensional NMR*. J Biomol NMR, 2003. **27**(2): p. 101-13.

177. Ludwig, J.A. and J.N. Weinstein, *Biomarkers in cancer staging, prognosis and treatment selection*. Nat Rev Cancer, 2005. **5**(11): p. 845-56.
178. Kostler, W.J., et al., *Monitoring of serum Her-2/neu predicts response and progression-free survival to trastuzumab-based treatment in patients with metastatic breast cancer*. Clin Cancer Res, 2004. **10**(5): p. 1618-24.
179. Fisher, B., et al., *Tamoxifen in treatment of intraductal breast cancer: National Surgical Adjuvant Breast and Bowel Project B-24 randomised controlled trial*. Lancet, 1999. **353**(9169): p. 1993-2000.
180. Jaffe, E.S., *Pathology and genetics of tumours of haematopoietic and lymphoid tissues* 2001, Lyon: IARC Press ; Oxford : Oxford University Press [distributor]. 351 p.
181. Sullivan, K.M. and P.S. Kozuch, *Impact of KRAS Mutations on Management of Colorectal Carcinoma*. Patholog Res Int. **2011**: p. 219309.
182. Ladanyi, M. and W. Pao, *Lung adenocarcinoma: guiding EGFR-targeted therapy and beyond*. Mod Pathol, 2008. **21 Suppl 2**: p. S16-22.
183. Lee, J.C., et al., *Epidermal growth factor receptor activation in glioblastoma through novel missense mutations in the extracellular domain*. PLoS Med, 2006. **3**(12): p. e485.
184. Sterin, M., et al., *Levels of phospholipid metabolites in breast cancer cells treated with antimetabolic drugs: a 31P-magnetic resonance spectroscopy study*. Cancer Res, 2001. **61**(20): p. 7536-43.
185. Wilson, M., et al., *A quantitative comparison of metabolite signals as detected by in vivo MRS with ex vivo 1H HR-MAS for childhood brain tumours*. NMR Biomed, 2009. **22**(2): p. 213-9.
186. Harrison, R., *Structure and function of xanthine oxidoreductase: where are we now?* Free Radic Biol Med, 2002. **33**(6): p. 774-97.
187. Salway, J.G., *Metabolism at a glance*. 3rd ed. ed2004, Malden, Mass. ; Oxford: Blackwell. 125 p.
188. Murray, A.W., *The biological significance of purine salvage*. Annu Rev Biochem, 1971. **40**: p. 811-26.
189. Sanfilippo, O., et al., *Relationship between the levels of purine salvage pathway enzymes and clinical/biological aggressiveness of human colon carcinoma*. Cancer Biochem Biophys, 1994. **14**(1): p. 57-66.
190. Ong, E.S., et al., *Metabolic profiling in colorectal cancer reveals signature metabolic shifts during tumorigenesis*. Mol Cell Proteomics.
191. Weber, G., *Biochemical strategy of cancer cells and the design of chemotherapy: G. H. A. Clowes Memorial Lecture*. Cancer Res, 1983. **43**(8): p. 3466-92.
192. Natsumeda, Y., et al., *Enzymic capacities of purine de Novo and salvage pathways for nucleotide synthesis in normal and neoplastic tissues*. Cancer Res, 1984. **44**(6): p. 2475-9.
193. Plagemann, P.G., R. Marz, and R.M. Wohlhueter, *Transport and metabolism of deoxycytidine and 1-beta-D-arabinofuranosylcytosine into cultured Novikoff rat hepatoma cells, relationship to phosphorylation, and regulation of triphosphate synthesis*. Cancer Res, 1978. **38**(4): p. 978-89.
194. Cadman, E. and C. Benz, *Uridine and cytidine metabolism following inhibition of de novo pyrimidine synthesis by pyrazofurin*. Biochim Biophys Acta, 1980. **609**(3): p. 372-82.
195. Kinsella, A.R. and M.S. Haran, *Decreasing sensitivity to cytotoxic agents parallels increasing tumorigenicity in human fibroblasts*. Cancer Res, 1991. **51**(7): p. 1855-9.

196. Marshman, E., et al., *Dipyridamole potentiates antipurine antifolate activity in the presence of hypoxanthine in tumor cells but not in normal tissues in vitro*. Clin Cancer Res, 1998. **4**(11): p. 2895-902.
197. Natsumeda, Y., et al., *Significance of purine salvage in circumventing the action of antimetabolites in rat hepatoma cells*. Cancer Res, 1989. **49**(1): p. 88-92.
198. Vannoni, D., et al., [*Purine metabolism in human tumors*]. Medicina (Firenze), 1989. **9**(1): p. 51-4.
199. Rubie, C., et al., *Housekeeping gene variability in normal and cancerous colorectal, pancreatic, esophageal, gastric and hepatic tissues*. Mol Cell Probes, 2005. **19**(2): p. 101-9.
200. Hashimoto, H., et al., *Effect of high-dose methotrexate on plasma hypoxanthine and uridine levels in patients with acute leukemia or non-Hodgkin lymphoma in childhood*. Leukemia, 1992. **6**(11): p. 1199-202.
201. Buhl, L., et al., *Urinary hypoxanthine and pseudouridine as indicators of tumor development in mesothelioma-transplanted nude mice*. Cancer Res, 1985. **45**(3): p. 1159-62.
202. Yoo, B.C., et al., *Identification of hypoxanthine as a urine marker for non-Hodgkin lymphoma by low-mass-ion profiling*. BMC Cancer. **10**: p. 55.
203. Camici, M., et al., *Purine salvage enzyme activities in normal and neoplastic human tissues*. Cancer Biochem Biophys, 1990. **11**(3): p. 201-9.
204. Ozturk, H.S., et al., *Activities of the enzymes participating in purine and free-radical metabolism in cancerous human colorectal tissues*. Cancer Biochem Biophys, 1998. **16**(1-2): p. 157-68.
205. Gulec, M., et al., *Adenosine deaminase and xanthine oxidase activities in bladder washing fluid from patients with bladder cancer: a preliminary study*. Clin Biochem, 2003. **36**(3): p. 193-6.
206. Meyer, W.H., et al., *Hypoxanthine:guanine phosphoribosyltransferase activity in xenografts of human osteosarcoma*. Cancer Res, 1986. **46**(10): p. 4896-9.
207. Grem, J.L. and P.H. Fischer, *Enhancement of 5-fluorouracil's anticancer activity by dipyridamole*. Pharmacol Ther, 1989. **40**(3): p. 349-71.
208. Sotos, G.A., L. Grogan, and C.J. Allegra, *Preclinical and clinical aspects of biomodulation of 5-fluorouracil*. Cancer Treat Rev, 1994. **20**(1): p. 11-49.
209. Kinsella, A.R., D. Smith, and M. Pickard, *Resistance to chemotherapeutic antimetabolites: a function of salvage pathway involvement and cellular response to DNA damage*. Br J Cancer, 1997. **75**(7): p. 935-45.
210. Machover, D., et al., *Treatment of advanced colorectal and gastric adenocarcinomas with 5-FU combined with high-dose folinic acid: a pilot study*. Cancer Treat Rep, 1982. **66**(10): p. 1803-7.
211. *Modulation of fluorouracil by leucovorin in patients with advanced colorectal cancer: evidence in terms of response rate. Advanced Colorectal Cancer Meta-Analysis Project*. J Clin Oncol, 1992. **10**(6): p. 896-903.
212. Thomas, D.M. and J.R. Zalberg, *5-fluorouracil: a pharmacological paradigm in the use of cytotoxics*. Clin Exp Pharmacol Physiol, 1998. **25**(11): p. 887-95.
213. Fernandes, D.J. and J.R. Bertino, *5-fluorouracil-methotrexate synergy: enhancement of 5-fluorodeoxyridylate binding to thymidylate synthase by dihydropteroylpolyglutamates*. Proc Natl Acad Sci U S A, 1980. **77**(10): p. 5663-7.
214. Fox, M., J.M. Boyle, and A.R. Kinsella, *Nucleoside salvage and resistance to antimetabolite anticancer agents*. Br J Cancer, 1991. **64**(3): p. 428-36.

215. Weber, G. and N. Prajda, *Targeted and non-targeted actions of anti-cancer drugs*. Adv Enzyme Regul, 1994. **34**: p. 71-89.
216. Schwartz, J., et al., *Dipyridamole potentiation of FUDR activity against human colon cancer in vitro and in patients*. Proc Am Soc Chem Oncol, 1987. **6**: p. 83.
217. Miller, E.M., J.F. Wilson, and P.H. Fischer, *Folinic acid alters the mechanism by which dipyridamole increases the toxicity of fluorouracil in human colon cancer cells*. Proc Am Assoc Cancer Res, 1987. **28**: p. 326.
218. Grem, J.L. and P.H. Fischer, *Augmentation of 5-fluorouracil cytotoxicity in human colon cancer cells by dipyridamole*. Cancer Res, 1985. **45**(7): p. 2967-72.
219. Budd, G.T., et al., *Phase I trial of dipyridamole with 5-fluorouracil and folinic acid*. Cancer Res, 1990. **50**(22): p. 7206-11.
220. Budd, G.T., P. Herzog, and R.M. Bukowski, *Phase I/II trial of dipyridamole, 5-fluorouracil, leukovorin, and mitoxantrone in metastatic breast cancer*. Invest New Drugs, 1994. **12**(4): p. 283-7.
221. Turner, R.N., G.W. Aherne, and N.J. Curtin, *Selective potentiation of lometrexol growth inhibition by dipyridamole through cell-specific inhibition of hypoxanthine salvage*. Br J Cancer, 1997. **76**(10): p. 1300-7.
222. Chan, T.C. and S.B. Howell, *Role of hypoxanthine and thymidine in determining methotrexate plus dipyridamole cytotoxicity*. Eur J Cancer, 1990. **26**(8): p. 907-11.
223. Baysal, B.E., et al., *Mutations in SDHD, a mitochondrial complex II gene, in hereditary paraganglioma*. Science, 2000. **287**(5454): p. 848-51.
224. Niemann, S. and U. Muller, *Mutations in SDHC cause autosomal dominant paraganglioma, type 3*. Nat Genet, 2000. **26**(3): p. 268-70.
225. Astuti, D., et al., *Gene mutations in the succinate dehydrogenase subunit SDHB cause susceptibility to familial pheochromocytoma and to familial paraganglioma*. Am J Hum Genet, 2001. **69**(1): p. 49-54.
226. Dahia, P.L., *Evolving concepts in pheochromocytoma and paraganglioma*. Curr Opin Oncol, 2006. **18**(1): p. 1-8.
227. Selak, M.A., et al., *Succinate links TCA cycle dysfunction to oncogenesis by inhibiting HIF-alpha prolyl hydroxylase*. Cancer Cell, 2005. **7**(1): p. 77-85.
228. Gimenez-Roqueplo, A.P., et al., *The R22X mutation of the SDHD gene in hereditary paraganglioma abolishes the enzymatic activity of complex II in the mitochondrial respiratory chain and activates the hypoxia pathway*. Am J Hum Genet, 2001. **69**(6): p. 1186-97.
229. Gimenez-Roqueplo, A.P., et al., *Functional consequences of a SDHB gene mutation in an apparently sporadic pheochromocytoma*. J Clin Endocrinol Metab, 2002. **87**(10): p. 4771-4.
230. Douwes Dekker, P.B., et al., *SDHD mutations in head and neck paragangliomas result in destabilization of complex II in the mitochondrial respiratory chain with loss of enzymatic activity and abnormal mitochondrial morphology*. J Pathol, 2003. **201**(3): p. 480-6.
231. Maxwell, P.H., *The HIF pathway in cancer*. Semin Cell Dev Biol, 2005. **16**(4-5): p. 523-30.
232. *Expression and Clinical Significance of Succinate Dehydrogenase complex of mitochondria in colorectal cancer*, 2011.
233. Friedman, D.B., et al., *Proteome analysis of human colon cancer by two-dimensional difference gel electrophoresis and mass spectrometry*. Proteomics, 2004. **4**(3): p. 793-811.

234. Ma, Y.L., et al., [*Study on specific metabonomic profiling of serum from colorectal cancer patients by gas chromatography-mass spectrometry*]. *Zhonghua Wei Chang Wai Ke Za Zhi*, 2009. **12**(4): p. 386-90.
235. Tiziani, S., V. Lopes, and U.L. Gunther, *Early stage diagnosis of oral cancer using ¹H NMR-based metabolomics*. *Neoplasia*, 2009. **11**(3): p. 269-76, 4p following 269.
236. Ouyang, D., et al., *Metabolomic Profiling of Serum from Human Pancreatic Cancer Patients Using (¹H) NMR Spectroscopy and Principal Component Analysis*. *Appl Biochem Biotechnol*.
237. Bonuccelli, G., et al., *Ketones and lactate "fuel" tumor growth and metastasis: Evidence that epithelial cancer cells use oxidative mitochondrial metabolism*. *Cell Cycle*. **9**(17): p. 3506-14.
238. Pavlides, S., et al., *The autophagic tumor stroma model of cancer: Role of oxidative stress and ketone production in fueling tumor cell metabolism*. *Cell Cycle*. **9**(17): p. 3485-505.
239. Romieu, I., et al., *Carbohydrates and the risk of breast cancer among Mexican women*. *Cancer Epidemiol Biomarkers Prev*, 2004. **13**(8): p. 1283-9.
240. Owen, O.E., et al., *Liver and kidney metabolism during prolonged starvation*. *J Clin Invest*, 1969. **48**(3): p. 574-83.
241. Girard, J., et al., *Adaptations of glucose and fatty acid metabolism during perinatal period and suckling-weaning transition*. *Physiol Rev*, 1992. **72**(2): p. 507-62.
242. Singhal, R., et al., *MALDI profiles of proteins and lipids for the rapid characterisation of upper GI-tract cancers*. *J Proteomics*, 2013. **80C**: p. 207-215.
243. Griffin, J.L., *Metabolic profiles to define the genome: can we hear the phenotypes?* *Philos Trans R Soc Lond B Biol Sci*, 2004. **359**(1446): p. 857-71.

APPENDIX

Metabolite integrations for plasma and tissue

Ethical approval

Substantial amendment to ethical approval

UHB sponsorship letter

Protocol

Patient information sheet

Patient consent form

Data collection proforma – patients

Volunteer control information sheet

Volunteer control consent form

Data collection proforma – controls

Manuscript: MALDI profiles of proteins and lipids for the rapid characterisation of upper GI-tract cancers

Metabolite	Mean	Std. Deviation
2-aminobutyrate	.024353	.0071546
2-hydroxy iso valerate	.006647	.0074908
2-hydroxybutyrate	.008692	.0064992
3-hydroxybutyrate	.011039	.1270739
Acetate	.042426	.0445935
Acetoacetate	.067231	.1093225
Acetone	.087114	.1311031
Acetyl amino acid	.015647	.0054581
Alanine	.378017	.1138357
Choline	.010403	.0053265
Citrate	.057453	.0236251
Creatine	.020796	.0174333
Creatine phosphate	.011646	.0038897
Creatinine	.063032	.0220004
Dimethylglycine	.006198	.0032916
Ethanol	.017162	.0511004
Formate	.003991	.0023409
Glutamate	.037824	.0126958
Glutamine	.114068	.0348504
Glutathione	.001007	.0126733
Glycerol	.028757	.0120554
G-phosphocholine	-.015137	.0182915
Hypoxanthine	.000384	.0005470
Isoleucine	.047963	.0156006
Isopropanol	.015552	.1035024
Keto iso valerate	.009650	.0033401
Lactate	1.770996	.6719760
Leucine	.192808	.0576260
Lysine	.258454	.0615606
O-phosphocholine	.017204	.0068388
Phenylalanine	.029661	.0073930
Pyruvate	.033200	.0256216
Threonine	.020343	.0063527
Tyrosine	.032894	.0111381
Valine	.223737	.0565852

Metabolite integrations for plasma

Metabolite	p value (Mann Whitney U test)
Formate	0.00005106440632984040
Pyruvate	0.00006400452968875750
Hypoxanthine	0.00018893424196922500
Dimethylglycine	0.00039802607111595400
Acetyl amino acid	0.00584657806660471000
3-hydroxybutyrate	0.00847444991898300000
Isopropanol	0.01105007819702430000
Ethanol	0.01290584831592470000
Glutamate	0.01768895824647080000

Significant metabolites in model 1 plasma

Metabolite	p value (Mann Whitney U test)
Formate	0.01168524053145980000
Glutathione	0.01610264007719110000
Pyruvate	0.04858648391825310000

Significant metabolites in model 2 plasma

Metabolite	p value (Mann Whitney U test)
Isoleucine	0.02343481218857220000
Dimethylglycine	0.03443122146081490000
Tyrosine	0.03729508449041750000

Significant metabolites in model 3 plasma

Metabolite	p value (Mann Whitney U test)
G-phosphocholine	0.00556404350217377000
Valine	0.02334220201289080000
Creatinine	0.03220968567371050000
Lysine	0.03763531378731430000

Significant metabolites in model 4 plasma

Metabolite	p value (Mann Whitney U test)
G-phosphocholine	0.00675510459297715000
Threonine	0.00811802832829044000
O-phosphocholine	0.00974012240527190000
Valine	0.01382302382037670000
Lysine	0.01382302382037670000
Leucine	0.01382302382037670000
Glycerol	0.01638235277370590000
Dimethylglycine	0.02277472785404030000
Keto iso valerate	0.04867667180111600000

Significant metabolites in model 5 plasma

Metabolite	Mean	Std. Deviation
4-hydroxy phenyl lactate	.018215	.0345528
Acetate	.119616	.0820797
α -keto iso valerate	.005753	.0127742
Alanine	.286643	.1306737
AMP	.004013	.0037977
Aspartate	.006169	.0034534
ATP	.025864	.0149452
Choline	.084977	.0457011
Creatine	.199382	.0850647
Creatinine	.025959	.0301362
Formate	.058906	.0587258
Fumarate	.004351	.0021874
Glucose	.005892	.0048112
Glutamate	.222381	.0715619
Glutamine	.148623	.0739374
Glutathione	.022378	.0105691
Glycogen	.030431	.0430747
G-phosphocholine	.164114	.1554231
Hydroxy iso valerate	.000207	.0001928
Hypoxanthine	.008627	.0061983
Inosine	.008277	.0063262
Inositol	.095442	.0435443
Iso leucine	.004962	.0025601
Lactate	2.031453	.9644534
Leucine	.017673	.0093018
O-phosphocholine	.300370	.2682802
Phenylalanine	.009980	.0047249
Succinate	.031898	.0287288
Taurine	.085309	.0322215
Tyrosine	.010881	.0058323
Uracil	.000889	.0010912
Valine	.019401	.0071317

Metabolite integrations for tissue

Metabolite	p value (Mann Whitney U test)
G-phosphocholine	0.0000000000000000783
O-phosphocholine	0.00000000000000003487
Glutamine	0.00000000000000025264
Alanine	0.00000000000000404783
Creatinine	0.00000000000000894615
Choline	0.0000000000008294786
Glycogen	0.0000000000454229413
Glutathione	0.0000000000796944585
ATP	0.0000000003448514800
Valine	0.0000000006757361607
Glutamate	0.0000000029092553732
Acetate	0.0000000135033067310
Hypoxanthine	0.0000001114204629791
Inosine	0.0000003231716628324
Glucose	0.00000034593623024716
Creatine	0.00000096180980364916
Taurine	0.00000575888759804659
Fumarate	0.00002171090580425370
Phenylalanine	0.00002176838237348080
Lactate	0.00008104621804410970
AMP	0.00010601210048534400
Inositol	0.00011034186855826800
Aspartate	0.00025810564781414200
Tyrosine	0.00304201600067409000
α -keto iso valerate	0.00401715346647147000
4-hydroxy phenyl lactate	0.01152722517356030000

Significant metabolites in model 1 tissue

Metabolite	p value (Mann Whitney U test)
Glutamine	0.0000000000007739282
ATP	0.0000000000050670429
Alanine	0.0000000000443959995
Creatine	0.0000000001706646402
Creatinine	0.0000000003485538814
Hypoxanthine	0.0000000009798046121
Choline	0.0000000089376757203
Uracil	0.000000026376364523
Fumarate	0.0000000292720659715
O-phosphocholine	0.0000000399947185098
G-phosphocholine	0.0000028492311608275
Glutathione	0.0000958354679895991
Glycogen	0.00002221336919832280
Inosine	0.00002634051216311610
Acetate	0.00286219695558342000
Taurine	0.00836440680389192000
Valine	0.01006364892583440000
Glutamate	0.01006810993498070000
Glucose	0.01273950619676460000
Iso leucine	0.03143098977002870000
Leucine	0.03992567174334220000
Lactate	0.04074856500688650000

Significant metabolites in model 2 tissue

Metabolite	p value (Mann Whitney U test)
Succinate	0.00625929392305007000
O-phosphocholine	0.02391934824795000000
Lactate	0.02931834791715420000
Inositol	0.03573443118569690000
Aspartate	0.04307557946267690000

Significant metabolites in model 4 tissue

Metabolite	p value (Mann Whitney U test)
Tyrosine	0.04125988432522410000

Significant metabolites in model 5 tissue

National Research Ethics Service

South Birmingham Research Ethics Committee

Osprey House
Albert Street
Redditch
Worcestershire B97 4DE
Rosa.Downing@westmidlands.nhs.uk

Telephone: 01527 587575
Facsimile: 01527 587503

16 May 2008

Professor Derek Alderson
Barling Professor of Surgery
University Hospitals Birmingham
Academic Department of Surgery
Room 29, 4th Floor
Queen Elizabeth Hospital
B15 2TH

Dear Professor Alderson

Full title of study: Metabolomics in prediction of response to neoadjuvant chemotherapy in oesophageal and gastric cancer
REC reference number: 08/H1207/3

Thank you for your letter, responding to the Committee's request for further information on the above research and submitting revised documentation] subject to the conditions specified below.

The further information has been considered on behalf of the Committee by the Chair.

Confirmation of ethical opinion

On behalf of the Committee, I am pleased to confirm a favourable ethical opinion for the above research on the basis described in the application form, protocol and supporting documentation as revised.

Ethical review of research sites

The Committee has designated this study as exempt from site-specific assessment (SSA). There is no requirement for [other] Local Research Ethics Committees to be informed or for site-specific assessment to be carried out at each site.

Conditions of the favourable opinion

The favourable opinion is subject to the following conditions being met prior to the start of the study.

Management permission or approval must be obtained from each host organisation prior to the start of the study at the site concerned.

Management permission at NHS sites ("R&D approval") should be obtained from the relevant care organisation(s) in accordance with NHS research governance arrangements.

Guidance on applying for NHS permission is available in the Integrated Research Application System or at <http://www.rdforum.nhs.uk>.

Approved documents

The final list of documents reviewed and approved by the Committee is as follows:

<i>Document</i>	<i>Version</i>	<i>Date</i>
Application	5.5	
Application	5.5	
Investigator CV		
Protocol	2	15 April 2008
Covering Letter		
Covering Letter		05 November 2007
GP/Consultant Information Sheets	1	23 September 2007
GP/Consultant Information Sheets	1	23 September 2007
Participant Information Sheet: Volunteer Controls	1	23 September 2007
Participant Information Sheet: Controls	2	15 April 2008
Participant Information Sheet: PIS	2	15 April 2008
Participant Consent Form: Volunteer Controls	1	23 September 2007
Participant Consent Form	1	23 September 2007
Response to Request for Further Information		

Statement of compliance

The Committee is constituted in accordance with the Governance Arrangements for Research Ethics Committees (July 2001) and complies fully with the Standard Operating Procedures for Research Ethics Committees in the UK.

After ethical review

Now that you have completed the application process please visit the National Research Ethics Website > After Review

You are invited to give your view of the service that you have received from the National Research Ethics Service and the application procedure. If you wish to make your views known please use the feedback form available on the website.

The attached document "After ethical review – guidance for researchers" gives detailed guidance on reporting requirements for studies with a favourable opinion, including:

- Notifying substantial amendments
- Progress and safety reports
- Notifying the end of the study

The NRES website also provides guidance on these topics, which is updated in the light of changes in reporting requirements or procedures.

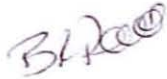
We would also like to inform you that we consult regularly with stakeholders to improve our service. If you would like to join our Reference Group please email referencegroup@nres.npsa.nhs.uk.

08/H1207/3

Please quote this number on all correspondence

With the Committee's best wishes for the success of this project

Yours sincerely



 **Mr R K Vohra**
Chair

Email: Rosa.Downing@westmidlands.nhs.uk

Enclosures: "After ethical review – guidance for researchers"

Copy to: Dr Chris Counsell, Research and Development Manager, Research and Development Office, 4th Floor, Nuffield House, Queen Elizabeth Hospital, Edgbaston, Birmingham, B15 2TH



National Research Ethics Service

South Birmingham Research Ethics Committee

Osprey House
Albert Street
Redditch
Worcestershire B97 4DE
Rosa.Downing@westmidlands.nhs.uk
Tel: 01527 587575
Fax: 01527 587503

Chairman: Dr S Bowman
Administrator: Mrs Rosa Downing

Date: 23 December 2009

Professor Derek Alderson
Barling Professor of Surgery
University Hospitals Birmingham
Academic Department of Surgery
Room 29, 4th Floor
Queen Elizabeth Hospital
Birmingham
B15 2TH

Dear Professor Alderson

Study title: Metabolomics in prediction of response to neoadjuvant chemotherapy in oesophageal and gastric cancer
REC reference: 08/H1207/3
Amendment number: AM01
Amendment date: 18 November 2009

The above amendment was reviewed by the Sub-Committee in correspondence.

Ethical opinion

The members of the Committee taking part in the review gave a favourable ethical opinion of the amendment on the basis described in the notice of amendment form and supporting documentation.

Approved documents

The documents reviewed and approved at the meeting were:

Document	Version	Date
Protocol	3	20 November 2009
Notice of Substantial Amendment (non-CTIMPs)	AM01	18 November 2009

Membership of the Committee

The members of the Committee who took part in the review are listed on the attached sheet.

R&D approval

All investigators and research collaborators in the NHS should notify the R&D office for the relevant NHS care organisation of this amendment and check whether it affects R&D approval of the research.

Statement of compliance

The Committee is constituted in accordance with the Governance Arrangements for Research Ethics Committees (July 2001) and complies fully with the Standard Operating Procedures for Research Ethics Committees in the UK.

08/H1207/3:

Please quote this number on all correspondence

Yours sincerely



Mrs Rosa Downing
Committee Co-ordinator

Enclosures: List of names and professions of members who took part in the review

Copy to: Dr Christopher Counsell, University Hospital Birmingham

Research Project AuthorisationProject reference: **RRK 3425**

Local REC reference:

Main REC reference: 08/H1207/3

Professor D Alderson
Academic Department of Surgery
Room 29, 4th Floor
Queen Elizabeth Hospital
B15 2TH

28 May 2008

Dear Professor Alderson

Metabolomics in predictor of response to neoadjuvant chemotherapy in oesophageal and gastric cancer

Thank you for submitting details of your proposed research project, which I am happy to authorise on behalf of University Hospital Birmingham. The following document versions were reviewed:

Protocol - version: Version 2 dated 15/04/08

Participant information sheet (main) - version: Version 2 dated 15/04/08

Participant consent form (main) - version: Version 2 dated 15/04/08

Sponsorship

University Hospital Birmingham NHS Trust has agreed to act as sponsor for this study. Note, however, that initially this only applies to patients recruited from this Trust. To enrol other centres into the study a copy of this letter must be sent to the relevant NHS R&D Office who should contact the UHB R&D Office

Indemnity arrangements.

Researchers who hold substantive or honorary contracts with University Hospital Birmingham (UHBT) will be covered against claims of negligence by patients of UHBT under the Clinical Negligence Scheme for Trusts (CNST). This scheme does not cover 'no fault' compensation and the Trust is precluded from taking out separate insurance to cover this. Any patient or volunteer taking part in the study is entitled to know that if they suffered injury as a result of participating in the study they would first have to prove negligence in a court of law before they could gain compensation.

If the study involves patients of any other Trust or healthcare organisation, you will need to confirm the indemnity arrangements with that organisation.

Reporting Adverse Events

If this study involves an intervention in the treatment of patients then you must ensure that any serious adverse events, **regardless of whether you believe the event is related to the research or the intervention**, are reported according to the Trust's policy on reporting research-related adverse events. Note that you must also follow any Adverse Event reporting requirements stipulated by the sponsor.

A copy of the Trust policy may be obtained from the R&D office and is also available on the R&D section of the Trust's intranet and internet sites. A copy of a blank SAE form is enclosed.

Research and Development Office (UHB)

Director: Professor James Neuberger Manager: Dr Christopher Counsell
4th Floor, Nuffield House, Queen Elizabeth Hospital, Edgbaston
Birmingham B15 2TH
Tel: 0121 697 8311 Fax: 0121 697 8310 Email: R&D@uhb.nhs.uk
Website: www.uhb.nhs.uk/research

**BCRO Reception
Wellcome Trust CRF,
Queen Elizabeth Hospital
Tel Ext: 3883**

Pharmacy

If your study involves Pharmacy then you must ensure that they are ready to initiate the study before the first patients are recruited.

Drugs and Treatment outside the study

Approval for the study to commence cannot be taken to imply approval for the same form of treatment to continue beyond the end of the study, or for patients who are not part of the study. If it is likely that continuing treatment is required at the end of the study, then it is the Principal Investigator's responsibility to ensure that study participants are fully aware of the types of treatment that would be available to them.

Research Governance

You should ensure that you and your research team abide by the Trust policies on research governance. These are available from the R&D Office and on the R&D section of the Trust's intranet and internet sites (www.uhb.nhs.uk/research)

Annual Reports

The R&D Office will request information about progress with the study in 6 months, 12 months and annually thereafter. Approval for this study may be withdrawn if you do not complete and return reports when requested.

Study Files

You must set up and maintain a study file containing the essential documents needed to facilitate a full audit of the conduct of the study. The minimum requirements for the content and layout of the study file are set out in the enclosed documents. This file may be audited at short notice by the R&D Office, the sponsor, or regulatory authorities.

Accrual Records

It is essential that you maintain up-to-date and accurate records of recruitment and participation in your study. You will be asked to provide these figures as part of the annual reporting and on request at other times during the year. For non-industry sponsored studies the Trust is likely to be required to report accrual data to the Department of Health and the UKCRN. You should keep an anonymised record, with dates, of patients approached, consented, screened, recruited, completed, and dropped out as appropriate.

Duration

It is expected that the study will begin at University Hospital Birmingham within 12 months of Trust authorisation. If there is a long delay in starting the study, the Trust may consider withdrawing authorisation for the study. Unless explicitly withdrawn, Trust approval lasts for as long as the study has valid ethics committee and regulatory approval. You must apply for an extension to the ethics approval if the study is to continue longer than stated in the original ethics application.

Protocol Amendments

Trust approval will usually automatically cover minor protocol amendments. Details of all substantial amendments must be sent to the R&D Office together with copies of the ethics approval and/or regulatory approval for the amendments and copies of any revised documents. The R&D office will acknowledge all amendments. A substantial amendment is defined by NRES (the National Research Ethics Service) and covers any change that could affect the safety, conduct or the resource implications of the study.

Archiving

For studies designated as a Clinical Trial of an Investigational Medicinal Product (CTIMP), it is a **legal** requirement to retain essential documents for at least **5 years** after the declared end of the study. The sponsor or regulatory authorities may insist on a longer retention period for a particular study. For all other types of study there are no statutory requirements but generally accepted good practice guidelines recommend that documents are retained for at least 5 years. Documents must be archived in a way such that they can be readily accessed (24 hours notice) if required for audits or regulatory purposes. The cost of archiving is borne by the Principal or Lead Investigator and should be taken into account when applying for research grants or seeking other forms of funding.

Health Records Labelling**Research and Development Office (UHB)**

Director: Professor James Neuberger Manager: Dr Christopher Counsell
4th Floor, Nuffield House, Queen Elizabeth Hospital, Edgbaston
Birmingham B15 2TH
Tel: 0121 697 8311 Fax: 0121 697 8310 Email: R&D@uhb.nhs.uk
Website: www.uhb.nhs.uk/research

BCRO Reception
Wellcome Trust CRF,
Queen Elizabeth Hospital
Tel Ext: 3883

The Health Records of study subjects are retained according to the Trust's "*Health Records Management Policy*"; for patients in research studies the retention period is 15 years after the last treatment or consultation related to the study. The Principal Investigator must ensure that all records for patients involved in a study are clearly labelled to ensure that the retention policy can be followed.

Cover for absence

If the Principal Investigator is likely to be absent and out of contact for a prolonged period (> 2 weeks), the PI must either explicitly suspend patient recruitment and patient-related activity in the study, or explicitly delegate the responsibilities of Principal Investigator to a named deputy. The PI must be satisfied that their deputy is sufficiently qualified through education, training and experience to take on the role of PI. These periods of absence and delegation must be recorded in the study file.

Yours sincerely,



Professor J Neuberger
Associate Medical Director Research and Development

Enclosed: Sample study file layout
 Adverse Event Report

Copies to: Mr Singhal
 Relevant Service Departments
 Division 2 Manager, Kevin Bolger

Research and Development Office (UHB)

Director: Professor James Neuberger Manager: Dr Christopher Counsell
4th Floor, Nuffield House, Queen Elizabeth Hospital, Edgbaston
Birmingham B15 2TH
Tel: 0121 697 8311 Fax: 0121 697 8310 Email: R&D@uhb.nhs.uk
Website: www.uhb.nhs.uk/research

BCRO Reception
Wellcome Trust CRF,
Queen Elizabeth Hospital
Tel Ext: 3883

PROTOCOL
[VERSION 2, 15th April 2008]

Metabolomic analysis of peripheral blood to predict the response to neoadjuvant chemotherapy in oesophageal and gastric cancer

Background

Oesophageal cancer is a highly aggressive malignancy with approximately 7,500 new cases diagnosed in United Kingdom every year. It is the 9th leading cause of cancer¹; and 5th leading cause of death due to cancer in the United Kingdom. More than 50% of oesophageal cancer patients present with unresectable disease, contributing to its dismal overall 5-year survival rate of between 9 and 40%, even in resectable stages.

While a meta-analysis of neoadjuvant chemotherapy trials in oesophageal cancer did not show an overall survival benefit, most studies were dominated by squamous cell cancer. The subgroup however, who respond to this treatment has been consistently shown to have a survival benefit and this was particularly evident in the largest and most recent trial conducted by the Medical Research Council which was dominated by patients with adenocarcinoma. These patients need to be identified from non responders either before, or at an early stage of this potentially toxic treatment.

Aims

We aim to prospectively evaluate the role of plasma metabolites in prediction of response to neoadjuvant chemotherapy by application of the principles of proteomics.

Inclusion Criteria

All patients considered medically fit for neoadjuvant chemotherapy and belong to one of the following groups

1. Have potentially surgically resectable disease
 - Adenocarcinoma of the oesophagus
 - Adenocarcinoma of the gastro oesophageal junction (Siewert types 1,2,or 3)
 - Gastric carcinomaand have not received any prior treatment for their cancer.
2. Are receiving palliative chemotherapy.

Exclusion Criteria

1. Patients who are considered medically unfit for chemotherapy.
2. Patients who are unable to complete their neoadjuvant therapy during the course of treatment.

Staging investigations

All patients should have a

1. Spiral/ Multi-slice CT with oral contrast or water of chest and abdomen (pelvis is optional). Maximum slice width 5mm. IV contrast/venous phase.
2. Endoscopic ultrasound (EUS) for all Type III gastro-oesophageal junctional tumours and according to local practice for other tumours. For obstructing tumours, the use of an oesophago-probe is preferable, but dilatation to facilitate complete scanning is permissible.

The results of an EUS should take precedence over other imaging modalities when staging tumour and nodes, whereas CT should take precedence when staging distal disease.

3. Diagnostic Laparoscopy with intraperitoneal wash +/- laparoscopic ultrasound.
4. PET scan for assessment of hepatic/ extra hepatic disease.
5. MRI or bone scans if clinically indicated.

Histological confirmation of diagnosis and baseline staging investigations must be reviewed by a Multidisciplinary Team (MDT).

Assessment of Response to neoadjuvant chemotherapy

Spiral/multi-slice CT, with oral contrast or water including chest, abdomen (pelvis optional) within 2 weeks of completion of chemotherapy. This is part of routine practice and is not being carried out solely for purposes of research. Maximum slice width 5mm. IV contrast/venous phase. Volumetric assessments would be made to assess the reduction in total volume of the tumour.

Final assessment of response will be made after examination of the histopathological specimen.

Recruitment

Patients who fit the inclusion criteria would be provided with the patient information sheet once they have been informed of the diagnosis. These patients would have up to 1 week to decide whether they would like to participate in the study.

At the same time healthy volunteer controls suffering with reflux disease would be recruited into the study. They would be supplied with information sheet for volunteer controls. General practitioners for both patients and controls would be subsequently informed. The recruitment process is expected to last 6 – 12 months.

Sample size calculation

For a test with a sensitivity of 80%, we want the sample size to estimate its sensitivity to within 5%. This amounts to saying that the confidence interval for sensitivity should have a width of 10% ($2 \times 5\% = 10\%$). Because 0.8 lies near the extreme of the range of sensitivity (0-1) it is better to use a confidence interval based on a score test rather than the usual Wald statistic. (Wilson (1927) discussed in Agresti and Coull, *Am. Stat.* May 1998; 52, 2 (equation 2)). For a 95% confidence interval to have a total width of 10%, we require approximately 132 patients.

Methodology

Patients will be divided into 2 groups i.e. responders and non responders based on the post chemotherapy investigations and examination of the histopathological specimen obtained after oesophagectomy.

Blood samples will be collected from all patients who fit the inclusion criteria. These samples will be divided into 'responders' and 'non responders' and will be collected at serial time intervals; before, during and after treatment with neoadjuvant chemotherapy. At the same time they will be also collected from healthy patients with benign oesophageal disease confirmed on endoscopy. These would serve as 'controls'.

Metabolomic analysis of plasma will involve -

1. Sample Collection and processing: Blood samples will be collected, placed on ice and processed within 20 minutes. They are subsequently centrifuged to remove red blood cells. Plasma samples will be deproteinized by filtration or addition of acetonitrile, followed by centrifugation and replacement of solvent to yield 600 μL ultrafiltrate/sample in

90% H_2O /10% D_2O for NMR analysis. (The D_2O is added for frequency locking during the acquisition of the NMR spectrum) Pooled samples will be used in the first instance i.e. the ultrafiltrate from responders is pooled and compared with the pooled ultrafiltrate from non responders. This should identify major areas of difference. Tissues will either be analysed by MAS-NMR (magic angle spinning) to reduce the line widths in the spectrum or by extracting tissue samples using a MEOH/EtOH mixture followed by lyophilisation.

2. NMR fingerprinting: The ultrafiltrate will be analyzed by 600 and 800 MHz spectrometers using cryogenically cooled probes. 1D spectra or 2D *J*-resolved spectra will be recorded to identify changes in metabolite concentrations. Spectra will be processed using software written by researchers at HWB-NMR in Birmingham, PLS-toolbox for PCA/PLS and the Chenomx software for signal identification. Relevant metabolites will be identified from loadings plots in PCA or PLS analysis.

3. Validation: Once resonances are identified, we will confirm the identity of signals by adding metabolites to the sample. An enhanced peak confirms the metabolite initially identified using the reference software. To identify unknown metabolites 2D COSY and HSQC spectra will be recorded.

PATIENT INFORMATION SHEET
[VERSION 2, 15th April 2008]

Metabolomic analysis of peripheral blood to predict the response to neoadjuvant chemotherapy in oesophageal and gastric cancer

Invitation

You are being invited to take part in a research study. Before you decide whether to take part it is important for you to understand why the research is being done and what it will involve. Please take time to read the following information carefully and discuss it with friends, relatives and your GP if you wish. Ask us if there is anything that is not clear or if you would like more information. Take time to decide whether or not you wish to take part.

Your hospital doctor will have explained that you have developed cancer of the oesophagus (the tube leading from your throat to your stomach) or stomach. As you know the treatment of these cancers may involve chemotherapy, radiotherapy and surgery. We are currently investigating the best way to identify patients who would respond to chemotherapy so as to tailor treatment for individual patients and reduce the potential for side effects. We would like to invite you to take part in a research study being conducted by the University Hospital Birmingham Upper Gastrointestinal surgery unit.

Why have I been chosen?

You have been chosen for this study because you have cancer of the oesophagus/ stomach of a type considered suitable for chemotherapy (drug treatment).

Why is the research being done?

Recent research has shown that only a proportion of patients are likely to respond to chemotherapy. Our aim is potentially separate responders from non responders preferably at an early stage of this treatment to avoid unnecessary chemotherapy and its side effects.

Do I have to take part?

No. Taking part in the study is entirely voluntary. If you decide not to take part this will not affect your relationship with your doctor in any way or the treatment you are offered in the future. When you have read this information sheet and the consent form, we would encourage you to discuss the study with others if you wish, to help you decide whether to take part. No effective treatment will be withheld if you take part in this research.

At any time you may withdraw your consent without giving a reason and without affecting your future care, but data on your progress will continue to be collected unless you specifically request this to stop. If you do not wish to take part in this study, you will be offered whatever treatment your hospital doctor thinks is best for you.

What will happen to me if I take part?

This research does not alter the treatment you receive in the hospital in any way. You will continue to receive the treatment that was best suited for your type of cancer. We will take blood samples coinciding with the times of your routine blood tests. We will also analyse tiny pieces of samples (about the size of a pin head) from the oesophagus/ stomach removed at the time of endoscopy and surgery. We will not take any samples that will interfere with how the Doctors treat you. We will not ask the Surgeons to take any extra tissue for us and the surgery would be the same whether you take part or not.

How is the research done?

We intend to use state of the art metabolomic analysis (an investigation into the activity of cancer cells) to identify predictors of response from your blood and tissue specimens.

Who is organising and funding the research?

Professor Derek Alderson is the overall lead of the research group. The research will be funded in part with the funds available with the Upper Gastrointestinal surgery unit at the University Hospitals Birmingham Foundation trust and other government funding bodies.

What do I have to do?

If you agree to take part in the study there is nothing extra that you need to do.

What medical tests are involved?

None over and above that were initially planned for your treatment.

What are the side effects of any treatment received when taking part?

There are no additional side effects or complications beyond those associated with the standard treatment.

What are the possible disadvantages and risks of taking part?

As we are not undertaking additional procedures there are no disadvantages to taking part.

What are the possible benefits of taking part?

There is no intended benefit to you personally from taking part in this study. The information we get from this study will help us to treat future patients with cancer of the oesophagus/ stomach better.

What if something goes wrong?

As we only take blood samples and tissue samples during endoscopy and from the oesophagus/ gastric that has been surgically removed, no risks are anticipated from your participation in the study.

Will my taking part in this study be kept confidential?

If you consent to take part in the research any of your medical records may be inspected by the professionals involved in the research. Your details however are anonymous and any tissue or data from the study will be anonymous. It will not be possible to trace these back to you.

All information which is collected about you during the course of the research will be kept strictly confidential.

Any information about you which leaves the hospital will have your name and address removed so that you cannot be recognised from it.

What will happen to the results of the research study?

The results of the study will be published in a suitable medical journal. Patients taking part will not be identified in any published report. You will be able to obtain a summary of the findings from patient support groups, or your study doctor.

How many patients would be required for the study?

Although it is difficult to predict exact numbers before preliminary results of the study are available, we estimate not more than 150 participants would be required. The recruitment process is expected to last 6 – 12 months.

Who has reviewed the study?

The South Birmingham Ethics Committee and the University Hospital Birmingham Research and Development Committee have reviewed and approved this study.

Contact for Further Information

If you have any concerns or further questions about the study you can telephone Dr Rishi Singhal on 0121 627 2276, University of Birmingham. If you have any concerns about the study and wish to contact someone independent, you may telephone the Research and Development office at the Queen Elizabeth hospital.

You will be provided with a copy of this form for your records.

PATIENT CONSENT FORM
[VERSION 2, 15th April 2008]

Metabolomic analysis of peripheral blood to predict the response to neoadjuvant chemotherapy in oesophageal and gastric cancer

Patient Identification Number for this trial:

Name of Researcher: Mr Rishi Singhal 0121 6272276

1. I confirm that I have read and understand the patient information sheet (Version 2, 15th April 2008) for the above study and have had the opportunity to ask questions.
2. I understand that my participation is voluntary and that I am free to withdraw at any time, without giving any reason, without my medical care or legal rights being affected.
3. I understand that sections of any of my medical notes may be looked at by responsible individuals from the research group or from regulatory authorities where it is relevant to my taking part in research. I give permission for these individuals to have access to my records.
4. I agree that my GP be informed of my involvement with this research study
5. I agree to take part in the above study.

_____ Name of Patient	_____ Date	_____ Signature
_____ Name of Person taking consent (if different from researcher)	_____ Date	_____ Signature
_____ Researcher	_____ Date	_____ Signature

1 for patient; 1 for researcher; 1 to be kept with hospital notes

GP LETTER
[VERSION 2, 15th April 2008]

Metabolomic analysis of peripheral blood to predict the response to neoadjuvant chemotherapy in oesophageal and gastric cancer

Dear Dr _____

Your Patient: _____ (DOB: ____ / ____ / ____)

has been found to have oesophageal/ gastric cancer. This patient has kindly agreed to take part in a research aimed to identify predictors of response to neoadjuvant chemotherapy in oesophageal/ gastric cancer. The participation in this research would not in any way alter the treatment appropriate for the type of cancer.

Please find enclosed a copy of the patient information sheet for this trial. You will be kept up to date with your patient's progress but if you have any concerns or questions regarding this study please contact the responsible physician:

Professor/Mr _____ at University Hospital Birmingham Foundation Trust

Tel: _____

Metabolomics in prediction of response to neoadjuvant chemotherapy in patients with oesophageal adenocarcinoma

Data collection proforma – Rishi Singhal

Date:

Hospital Number:

Study Number:

Patient name:

Sex:

Weight:

Height:

BMI:

Ethnicity:

Caucasian

Asian

Chinese

Other

Contact No.:

Smoking status:

Non smoker

Ex smoker

Smoker

Alcohol status:

Non drinker

Mild drinker

Moderate

Severe

--

Cancer

Oesophageal/Gastric

Adeno/Squamous

Siewert type

OGD location: Distance -

Length -

Staging

TNM

EUS

Date:

CT

	Date	Findings	
1 st CT			
2 nd CT			

PET

	Date	Findings	
1 st PET			
2 nd PET			

Staging laparoscopy

	Date	Findings	
1 st staging lap			
2 nd staging lap			

Histopathology

Date:

TRG:

Chemotherapy

5FU/ ECX/ ECX+B

	Start	End	Complete (Y/N)	Complications
Cycle 1				
Cycle 2				
Cycle 3				

Dates

Date of diagnosis:

Date of Chemotherapy start:

Date of Chemotherapy finish:

Date of Surgery:

Date of Discharge:

Medical Comorbidities

Drug History

Blood sample collection

	Sample No.	Date	Sample time	Fasting status	Time in centrifuge	Time in freezer
1 st sample						
2 nd sample						
3 rd sample						

Tissue sample collection

	Sample No.	Date	Sample time	Fasting status	Time in freezer	Number of specis
1 st sample						
2 nd sample						
3 rd sample						

INFORMATION SHEET FOR VOLUNTEER CONTROLS
[VERSION 2, 15th April 2008]

Metabolomic analysis of peripheral blood to predict the response to neoadjuvant chemotherapy in oesophageal and gastric cancer

Invitation

You are being invited to take part in a research study. The first thing we would like to inform you is that you do not have the disease that we are investigating (ie Oesophageal or gastric cancer). Before you decide whether to take part it is important for you to understand why the research is being done and what it will involve. Please take time to read the following information carefully and discuss it with friends, relatives and your GP if you wish. Ask us if there is anything that is not clear or if you would like more information. Take time to decide whether or not you wish to take part.

Why have I been chosen?

Although you do not have the disease we are investigating, we require a number of patients with other conditions to act as a control for our experiments. Your participation will help us to standardize our research and obtain meaningful results.

Why is the research being done?

Recent research has shown that only a proportion of patients with cancer of the oesophagus/ stomach are likely to respond to chemotherapy. Our aim is potentially separate responders from non responders preferably at an early stage of this treatment to avoid unnecessary chemotherapy and its side effects.

Do I have to take part?

No. Taking part in the study is entirely voluntary. If you decide not to take part this will not affect your relationship with your doctor in any way or the treatment you are offered in the future. When you have read this information sheet and the consent form, we would encourage you to discuss the study with others if you wish, to help you decide whether to take part. No effective treatment will be withheld if you take part in this research.

At any time you may withdraw your consent without giving a reason and without affecting your future care, but data on your progress will continue to be collected unless you specifically request this to stop. If you do not wish to take part in this study, you will be offered whatever treatment your hospital doctor thinks is best for you.

What will happen to me if I take part?

This research does not alter the treatment you receive in the hospital in any way. We will take blood samples and also analyse tiny pieces of samples (about the size of a pin head) from the oesophagus/ stomach that were removed at the time of endoscopy. We will not take any samples that will interfere with how the Doctors treat you.

How is the research done?

We intend to use state of the art metabolomic analysis (an investigation into the activity of cancer cells) to identify predictors of response from your blood and tissue specimens.

Who is organising and funding the research?

Professor Derek Alderson is the overall lead of the research group. The research will be funded in part with the funds available with the Upper Gastrointestinal surgery unit at the University Hospitals Birmingham Foundation trust and other government funding bodies.

What do I have to do?

If you agree to take part in the study there is nothing extra that you need to do.

What medical tests are involved?

None over and above that were initially planned for your treatment.

What are the side effects of any treatment received when taking part?

There are no additional side effects or complications beyond those associated with the standard treatment.

What are the possible disadvantages and risks of taking part?

As we are not undertaking additional procedures there are no disadvantages to taking part.

What are the possible benefits of taking part?

There is no intended benefit to you personally from taking part in this study. The information we get from this study will help us to treat future patients with cancer of the oesophagus/ stomach better.

What if something goes wrong?

As we only take blood samples and tissue samples during endoscopy from the oesophagus/ stomach, no risks are anticipated from your participation in the study.

Will my taking part in this study be kept confidential?

If you consent to take part in the research any of your medical records may be inspected by the professionals involved in the research. Your details however are anonymous and any tissue or data from the study will be anonymous. It will not be possible to trace these back to you.

All information which is collected about you during the course of the research will be kept strictly confidential. Any information about you which leaves the hospital will have your name and address removed so that you cannot be recognised from it.

What will happen to the results of the research study?

The results of the study will be published in a suitable medical journal. Patients taking part will not be identified in any published report. You will be able to obtain a summary of the findings from patient support groups, or your study doctor.

How many healthy volunteers would be required for the study?

Although it is difficult to predict exact numbers before preliminary results of the study are available, we estimate not more than 150 participants would be required. The recruitment process is expected to last 6 – 12 months.

Who has reviewed the study?

The South Birmingham Ethics Committee and the University Hospital Birmingham Research and Development Committee have reviewed and approved this study.

Contact for Further Information

If you have any concerns or further questions about the study you can telephone Dr Rishi Singhal on 0121 627 2276, University of Birmingham. If you have any concerns about the study and wish to contact someone independent, you may telephone the Research and Development office at the Queen Elizabeth hospital.

You will be provided with a copy of this form for your records.

VOULENTEER CONTROLS CONSENT FORM
[VERSION 2, 15th April 2008]

Metabolomic analysis of peripheral blood to predict the response to neoadjuvant chemotherapy in oesophageal and gastric cancer

Patient Identification Number for this trial:
Name of Researcher: Mr Rishi Singhal 0121 6272276

1. I confirm that I have read and understand the information sheet for volunteer controls (Version 2, 15th April 2008) for the above study and have had the opportunity to ask questions.
2. I understand that my participation is voluntary and that I am free to withdraw at any time, without giving any reason, without my medical care or legal rights being affected.
3. I understand that sections of any of my medical notes may be looked at by responsible individuals from the research group or from regulatory authorities where it is relevant to my taking part in research. I give permission for these individuals to have access to my records.
4. I agree that my GP be informed of my involvement with this research study
5. I agree to take part in the above study.

_____ Name of Patient	_____ Date	_____ Signature
_____ Name of Person taking consent (if different from researcher)	_____ Date	_____ Signature
_____ Researcher	_____ Date	_____ Signature

1 for patient; 1 for researcher; 1 to be kept with hospital notes

GP LETTER (GP information for volunteer controls)
[VERSION 2, 15th April 2008]

Metabolomic analysis of peripheral blood to predict the response to neoadjuvant
chemotherapy in oesophageal and gastric cancer

Dear Dr _____

Your Patient: _____ (DOB: ____ / ____ / ____)

has kindly agreed to take part in a research aimed to identify predictors of response to neoadjuvant chemotherapy in oesophageal/ gastric cancer. The tissue and blood specimens obtained from your patient would be used as a control in our experiments. The participation in this research would not in any way alter his/ her treatment.

Please find enclosed a copy of the patient information sheet for this trial. You will be kept up to date with your patient's progress but if you have any concerns or questions regarding this study please contact the responsible physician:

Professor/Mr _____ at University Hospital Birmingham Foundation Trust

Tel: _____

Available online at www.sciencedirect.com

SciVerse ScienceDirect

www.elsevier.com/locate/jprot

MALDI profiles of proteins and lipids for the rapid characterisation of upper GI-tract cancers

Rishi Singhal^a, John B. Carrigan^a, Wenbin Wei^a, Phillipe Tanriere^b, Rahul K. Hejmadi^b, Colm Forde^b, Christian Ludwig^a, Josephine Bunch^c, Rian L. Griffiths^c, Philip J. Johnson^a, Olga Tucker^a, Derek Alderson^a, Ulrich L. Günther^a, Douglas G. Ward^{a,*}

^aSchool of Cancer Sciences, University of Birmingham, Edgbaston, Birmingham, B15 2TT, UK

^bQueen Elizabeth Hospital, Edgbaston, Birmingham, B15 2TH, UK

^cSchool of Chemistry, University of Birmingham, Edgbaston, Birmingham, B15 2TT, UK

ARTICLE INFO

Article history:

Received 16 October 2012

Accepted 8 January 2013

Keywords:

Oesophageal adenocarcinoma

Gastric adenocarcinoma

Endoscopy

Biopsy

MALDI

HNPs 1–3

ABSTRACT

Aim: To identify a reliable MALDI ‘cancer fingerprint’ to aid in the rapid detection and characterisation of malignant upper GI-tract disease from endoscopic biopsies.

Methods: A total of 183 tissue biopsies were collected from 126 patients with or without oesophago-gastric malignancy and proteins and lipids separated by methanol/chloroform extraction. Peak intensities in the lipid and protein MALDI spectra from five types of samples (normal oesophageal mucosa from controls, normal oesophageal mucosa from patients with oesophageal adenocarcinoma, nondysplastic Barrett’s oesophagus, oesophageal adenocarcinoma, normal gastric mucosa and gastric adenocarcinoma) were compared using non-parametric statistical tests and ROC analyses.

Results: Normal oesophageal and gastric tissue generated distinct MALDI spectra characterised by higher levels of calgranulins in oesophageal tissue. MALDI spectra of polypeptides and lipids discriminated between oesophageal adenocarcinoma and Barrett’s and normal oesophagus, and between gastric cancer and normal stomach. Many down-regulations were unique to each cancer type whilst some up-regulations, most notably increased HNPs 1–3, were common.

Conclusions: MALDI spectra of small tissue biopsies generated with this straightforward method can be used to rapidly detect numerous cancer-associated biochemical changes. These can be used to identify upper GI-tract cancers regardless of tumour location.

© 2013 Elsevier B.V. All rights reserved.

1. Introduction

Oesophageal cancer is a highly aggressive malignancy with some 8000 new patients diagnosed in the United Kingdom each year, making it the ninth most common cancer and fifth most common cause of death from cancer [1]. The incidence of adenocarcinoma of the oesophagus has risen dramatically since the mid-1970s accounting for nearly three quarters of all

oesophageal cancers in most Western countries [2]. Adenocarcinoma is strongly linked to the rising incidence of gastro-oesophageal reflux disease and specifically within that condition, to the development of Barrett’s metaplasia where the normal squamous epithelium is replaced by a columnar lining. Changes in the epidemiology of oesophageal adenocarcinoma have been accompanied by changes in gastric cancer in the West. Whilst less than 10% of gastric cancers were located at or

* Corresponding author at: School of Cancer Sciences, College of Medical and Dental Sciences, University of Birmingham, Edgbaston, Birmingham, B15 2TT, UK. Tel.: +44 1214149528.

E-mail address: d.g.ward@bham.ac.uk (D.G. Ward).